2012

Predicting early-age thermal behavior of mass concrete for bridge foudnation

Jinxin Li
Iowa State University

Predicting early-age thermal behavior of mass concrete for bridge foundations

by

Jinxin Li

A thesis submitted to the graduate faculty

in partial fulfillment of the requirements for the degree of

MASTER OF SCIENCE

Major: Civil Engineering (Civil Engineering Materials)

Program of Study Committee:
KejinWang, Co-Major Professor
Charles Jahren, Co-Major Professor
Mervyn Marasinghe

Iowa State University

Ames, Iowa

2012

TABLE OF CONTENT

LIST OF FIGURES

LIST OF TABLES

ABSTRACT

Large volume concrete continues to present increasing concern in the construction of bridges. Due to the increased heat generation during massive concrete foundation construction, the concern for cracking, resulting from thermal contraction, is increased. To reduce the thermal cracking potential and ensure the safety and durability of the foundation structure, several practices are utilized, such as using low heat generating cement, proper insulation, cooling pipes and so forth.

The objectives of this research are to explore the current available early age mass concrete thermal analysis software packages and provide recommendations for mass concrete construction practices. Currently, there are several computer software packages capable of evaluating the early age development of concrete. 4C Temp&Stress, which is discussed in detail in this study, is a user friendly and flexible software package capable of analyzing mass concrete structures.

The sensitivity study results of using 4C Temp&Stress indicate that a reduced least dimension, extended for removal time, and reduced fresh placement temperature could reduce the maximum temperature and decrease cracking potential. Current insulation and formwork materials and practices are confirmed to be to a practical approach in mass concrete construction. The recommended layout and dimensions of post cooling systems will be discussed to provide the most efficiency cooling system. Besides these, other methods and strategies are investigated in case study for controlling the thermal cracking of massive concrete placements.

The findings of this study also indicate relationship between maximum temperature difference and maximum tensile stress/strength ratio at different time interval, and between the concrete maximum temperature and maximum temperature difference with the fresh placement temperature of the concrete and the depth of concrete for a specific mix design in mass concrete projects. The models allow contractors, or the Iowa Department of Transportation (Iowa DOT) to roughly estimate the thermal behavior and cracking potential.

ACKOWLEDGEMENT

I would like to thank my advisor Dr. KejinWang and Dr. Charles Jahren for their motivation, advice and guidance during my two year graduate study. I would also like to thank Dr. Mervyn Marasinghe for his patience and suggestions on statistical analysis in my thesis. I am truly grateful for the hours that they have spent advancing my knowledge. I am also indebted to Jacob Shaw and Adam Miller for exploring ConcreteWorks computer software as a comparison of 4C Temp&Stress, which is the computer tool I have studied at the beginning of my research. Working with them has made my time at Iowa State University a truly memorable experience

I also extend my thanks to the technical advisory committee for the Iowa Mass Concrete for Bridge Foundations Study including: James Nelson, Wayne Sunday, Todd Hanson, Ahmad Abu-Hawash, Chris Cromwell, Mark Dunn, and Linda Narigon. Special thanks to Kyle Riding for provided information and guidance on ConcreteWorks software and Jens Ole Frederiksen for answering operation questions on 4C Temp&Stress software. I would also express my thanks to John Gajda, Jeremy Purvis, Jason Cole, and Dan Timmons for providing field data for mass concrete construction. These supports are gratefully acknowledged

I would finally like to thank my family for their years of support, love and encouragement. My parents Wei Li and Ping Jin provide me endless support in areas related to finances, decision making, and have instilled in me great confidence.

CHAPTER 1 INTRODUCTION

The application of mass concrete increases with the increasing construction of buildings and as more bridges and dams. In the meantime, the challenges of high heat generation and problems with thermal behavior become a concern. The excessive heat of mass concrete may lead to cracking and other temperature related damage to the concrete structures such as in foundations and dams. Thermal stress developed from concrete heat development, curing period, and environmental conditions could potentially lead to structure cracking. Thermal cracking primarily develops due to volume changes when relatively large temperature differences exist between the interior and the surface of a concrete placement. When cracking occurs, repair can be very expensive and may delay project completion. In order to improve the durability of mass concrete, mix design and construction methods should be planned to properly control the temperature, especially the maximum temperature and temperature difference between the interior and the surface of the concrete.

Current mass concrete Specification DS-09047 developed by the Iowa DOT was based on the best information that the Iowa DOT staff had collected before the construction of West Bound (WB) I-80 Bridge in Council Bluffs, Iowa. Several additional items of information are available at present including temperature records for most of mass concrete placements. Recommendations based on current information are provided as a part of this study. The objectives of this research are

- To develop models regarding the heat and stress development used in available computer software packages.
- To provide recommendations for mass concrete construction of river bridge foundations or substructures by conducting a series of sensitivity and case studies.
- To provide temperature predicting models using information that is commonly available to construction projects of Iowa DOT.

Many computer programs are available to analyze early age concrete behavior such as ANSYS, ConcreteWorks and 4C Temp&Stress. ANSYS is mainly used to perform finite structural analysis, and is not focused on thermal analysis of mass concrete. In addition,

complex inputs and structural analysis knowledge are required compared to 4C Temp&Stress and ConcreteWorks. ConcreteWorks is capable of predicting the temperature development and cracking potential of mass concrete. However, the program provides limited temperature output up to 14 days and cracking potential up to 7 days. Furthermore, ConcreteWorks lacks of flexibility of creating new construction methods and editing outputs. The commercially available computer software package is used in this research is 4C Temp&Stress. Detailed advantages and disadvantages of the computer programs will be discussed in section 2.6.

Chapter 1 states the general scope and purpose of this study. Chapter 2 shows the literature review which are correlated to mass concrete, thermal and mechanical properties of concrete, and current available computer programs for mass concrete thermal cracking evaluation. Introduction of 4C Temp&Stress including assumptions, inputs, outputs and major advantages are discussed in Chapter 3. Data collection and study plan are introduced in Chapter 4. Verification of the ability of 4C Temp&Stress conducted using WB I-80 Missouri River Bridge foundation construction data is presented in Chapter 5. Chapter 6 provides the results of a series of sensitivity studies taking dimensional size of mass concrete, placement time and date, fresh placement temperature, quantity of cement, insulation material, and form removal time into consideration. After the sensitivity studies, case studies on the WB I-80 over the Missouri River Bridge and US 34 Bridge at Glenwood are discussed in Chapter 7. Maximum temperature and maximum temperature difference relationships between fresh placement temperature and depth of concrete are studied based on 4C Temp&Stress analysis results. Furthermore, case study on a current mass concrete project is provided as additional program analysis results.

At the end of the study, recommendations of the usage of the software program and construction recommendations will be provided by comparing the results from measurements and computer programs, case studies.

CHAPTER 2 LITERATURE REVIEW

2.1 Introduction

As discussed in Chapter 1, temperature development is an important factor to mass concrete thermal behavior. In order to reduce thermal cracking potential, it is important to control the temperature development of mass concrete. The generation of heat in concrete is mainly due to the cement hydration process. In this chapter, literature findings on cement hydration thermal properties and mechanical properties of concrete will be discussed. Section 2.3 describes the definition of mass concrete, the important factors affecting mass concrete thermal behavior and developmental specifications developed by the Iowa DOT. Section 2.4 describes the existing prediction models on concrete thermal behavior and cracking potential evaluation. In addition, section 2.5 states and compares current simulation computer programs related to mass concrete heat development and cracking potential prediction.

2.2 General Information

In this section, hydration of cement will be discussed first, including the process of cement heat of hydration; factors affecting cement heat of hydration, and testing methods of the hydration process. Next several thermal and mechanical properties of concrete will be defined and discussed such as coefficient of thermal expansion, elastic modulus and creep.

2.2.1 Cement Hydration

Concrete is primarily made up by cementitious material, aggregate, and water. A cementitious material is any material which reacts during hydration to give the concrete strength. There are many different types of cementitious materials used in concrete including Portland cement, slag, fly ash, and silica fume. The hydration process of cement is a series of nonreversible chemical reactions between cement and water. Early hydration has an influence on concrete plasticity and later hydration governs concrete strength.

2.2.1.1 Cement Heat of Hydration Process

Primary compounds in Portland cement include calcium aluminates and calcium silicates. Compounds have the following notation: A=Al_2O_3, C=CaO, F=Fe_2O_3, H=H_2O, M=MgO, S=SiO_2, $\underline{S}$=SO_3. Calcium aluminates include tricalcium aluminate (C_3A) and ferrite (C_4AF), calcium silicates include are alite (C_3S) and belite (C_2S). Calcium silicates induce similar hydration reaction. The principal hydration products are calcium silicate hydrate(C-S-H) and calcium hydroxide (CH). Other major products are ettringite (C-A-$\bar{S}$-H) and monosulfate. Ettringite formed when the sulfate and tricalcium aluminate are dissolved in water. Monosulfate is the result of tricalcium aluminate reacting with ettringite compounds.

A typical hydration process includes 5 stages: mixing, dormancy, hardening, cooling and densification shown in Figure 1. Stage 1 (the mixing/ dissolution stage) happens when aluminates and sulfate dissolve and react quickly. In this stage, a gel like ettringite (C-A-$\bar{S}$-H) is formed. The gel limits water's access to aluminate and slows the reaction and hence reduces the heat.

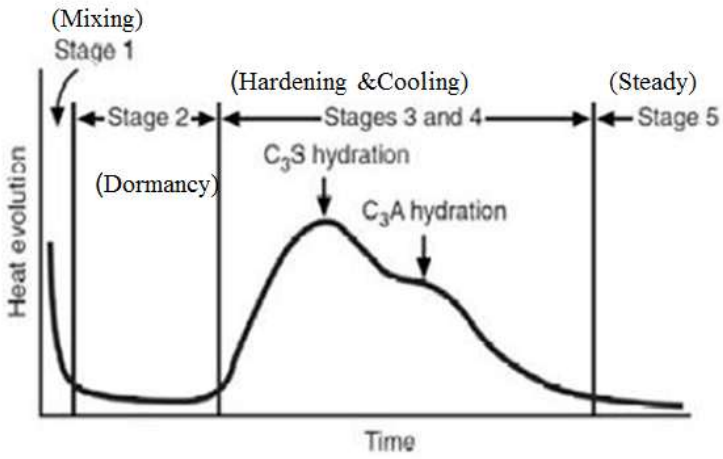

Figure 1 Stages of hydration (Kim, 2010)

Stage 2 (the dormancy/induction period) is when the gel (C-A-$\bar{S}$-H) controls aluminate reactions so that little heat is generated in concrete. Stage 2 generally occurs between 2-4 hours after concrete mixing. This stage is suitable for transporting concrete and maintaining concrete workability. During this stage, the silicates still dissolve slowly while releasing calcium ions in solution.

Hardening stage, also called acceleration period, is the third stage when alite (C_3S) and belite (C_2S) in the cement start to hydrate and release heat. Two compounds, calcium silicate hydrate(C-S-H) and calcium hydroxide (CH), are formed in this stage. Additionally, concrete releases the majority of its heat and gain its strength due to the formation of calcium silicate hydrate and calcium hydroxide. It is also important to apply the curing compound before concrete starts hardening to prevent water from evaporating, thus reducing the risk of plastic shrinkage cracking.

The cooling stage or the deceleration stage occurs right after final set. Final set is a critical point when the concrete achieves a defined stiffness. The buildup C-S-H and CH begins to limit access of water to the cement, so silicate reactions become slow. Generally, final set occurs at 10 to 13 hours after mixing for Portland cement with Supplementary cementitious materials (SCMs) added. During this stage, the heat peak is reached and the temperature begins to drop. Once these reactions are greatly slowed, the concrete begins to cool and experience strain. Mass concrete thermal cracking occurs during the cooling stage when the concrete has strength and begins to cool. When the exterior of the concrete cools much faster than the interior, stress from the contraction of the exterior relative to the interior will cause cracking.

The final stage is densification (the steady stage), which can continue for years. In this stage, hydrated cement products occupy space and reduce the rate of hydration remarkably. The hydration is completely controlled by the diffusion process, and the temperature will cool down to a steady stage.

Generally, concrete will gain approximately 50 percent of its strength during first 72 hours after mixing. Most of the strength of concrete comes from the calcium silicate hydrate (C-S-H) and the calcium hydroxide (C-H) crystals. Monosulfate does not make a significant contribution to the strength of the concrete (Kim, 2010).

2.2.1.2 Factors that Affect Cement Heat of Hydration

The rate and amount of the heat generated during hydration process is primarily influenced by cement type and SCMs. Different cement types affect heat of hydration due to various cement chemical compositions, such as C_3S and C_2S. Cement types are primarily

classified according to ASTM C 150 as eight types: Type I Normal, Type IA normal, air-entraining, Type II moderate sulfate resistance, Type IIA moderate sulfate resistance, air-entraining, Type III high early strength, Type IIIA high early strength, air-entraining, Type IV low heat of hydration, and Type V high sulfate resistance (ASTM C 150, 2005). Type I cement is general-purpose cement that can be used when no special properties are required such as pavement, floors, reinforced concrete buildings, bridges, tanks, reservoirs, pipe, masonry units, and precast concrete. Type II cement is used where resistance to sulfate attack is important. Type III cement provides high early strength. It is used for quick construction, such as cold weather, or forms that need to be removed quickly. Type IV cement is used where a minimal amount of heat generated from hydration is desired. Type V cement is generally used when concrete is exposed under severe sulfate condition. Air-entraining Portland cement (Type IA, IIA, and IIIA) contains small quantities of air-entraining material. These cements improve the concrete resistance to freezing and thawing. Furthermore, blended hydraulic cements are popular and used in all aspects of concrete now. ASTM C595 recognizes two primary classes of blended cement: Type IS -Portland blast-furnace slag cement and Type IP -Portland-pozzolan cement. Blended cement usually will perform moderate sulfate resistance, and low or moderate heat of hydration with air-entrainment. (Steven H. K., Beatrix K., and William P., 2008)

Most concrete today introduced in SCMs to improve concrete properties, such as fly ash and slag cement. In general, SCMs delay hydration process, reduce heat peak, and extend heat generation.

Fly ash is a fine residue from the combustion of ground or powered coal which is widely used as SCMs in concrete. Fly ash is classified into two types in the United States, Class F and Class C. Class F fly ash is produced by burning anthracite or bituminous coal and has low-calcium content(less than 10% CaO). Class C fly ash is produced when subbituminous coal is burned and has a high-calcium (10%-30% CaO). In mixed concrete, fly ash is used in about 50% of mixtures and different types of fly ash have different dosage recommendations. Class F fly ash is often used 15%-25% by mass of cementitious material, and Class C fly ash is used as 15-40%. Fly ash as replacement for Portland cement improves workability of the concrete due to reducing heat of hydration and shrinkage. Adding fly ash

will delay setting times, and increase ultimate strength when hydration is completed (Steven H. K., Beatrix K., and William P., 2008, p. 59).

Ground granulated blast-furnace slag (GGBFS), is another common SCM, which is also known as slag cement. GGBFS improves the workability of the concrete, and lowers the cost of concrete materials. In addition, concrete that utilizes GGBFS has a lower rate of hydration which reduces the overall rate of heat gain from hydration. The Iowa DOT limits the percentage that GGBFS may replace cement in a mass concrete mix up to 50%. The sensitivity study varies the replacement level of GGBFS from 0 - 50%.

Water to cementitious material ratio (w/c) affects heat of hydration process as well. The heat generation decreases as the w/c ratio decreases. However, if the w/c ratio is too low, complete hydration is not possible due to insufficient reaction space for hydration process. Complete hydration of cement, in general, requires a w/c about 0.4 (Sidney M., J. Francis Y., David D., 2003).

2.2.1.3 Measurements of Heat of Hydration

The heat development of concrete can be tested in lab condition or predicted by computational models. Most of hydration results are obtained under lab conditions using calorimeter tests methods to monitor heat of hydration over time. Calorimeter tests can be classified into three types: adiabatic, semi-adiabatic, and isothermal calorimetry. The adiabatic calorimeter measures the heat of hydration of samples in an insulated system with no heat gain or loss. This method gives a good estimate of a concrete temperature rise. However, high set-up costs and large sample size can be less practical than a semi-adiabatic calorimeter.

A semi-adiabatic calorimeter allows a certain amount of heat loss during testing. The temperature measured by semi-adiabatic calorimeter is typically 2-3% lower than adiabatic calorimeter results. This method is often simpler and less expansive compared to adiabatic calorimeter.

An isothermal calorimeter measures the rate of heat hydration when the specimen temperature is close to environmental temperature. Since the calorimeter is required to remain at a fixed temperature, the temperature variation in the field is not taken into account.

This method can be used for testing paste or mortar over a relatively short period. There are also many prediction models available from literature, which will be discussed in section 2.4. In mass concrete projects, the heat development is monitored by sensors embedded at different locations. Sensor type, monitor machine and sensor locations should be studied before installation. Generally contractors or consulting company provide recommendations to apply sensors. Either onsite measurements or laboratory testing is acceptable (Riding, 2007).

2.2.2 Thermal Properties &Mechanical Properties

Concrete thermal and mechanical properties are important for mass concrete thermal behavior and strength development. Understanding the effects of thermal and mechanical properties is critical to thermal control. Thermal properties of concrete are described, including heat of hydration, thermal conductivity, specific heat, and coefficient of thermal expansion. Mechanical properties such as maturity, compressive strength, tensile strength, modulus of elasticity, shrinkage, creep and Poisson's ratio are included in following section.

2.2.2.1 Thermal Properties of Concrete

The key factors for heat of hydration of cements are types and sources of cement, total cement content, environmental temperature, and admixture. Effects of cement type and SCMs have been discussed in section 2.2.1.2. The rate of the hydration reaction increases with increasing cement content and temperature during hydration. Also, the amount of exposed surface area and the ambient temperature at various exposed surfaces affect hydration of concrete.

Thermal conductivity (Btu*in/h*ft^2*°F or KJ/Kg*°C) describes the rate of heat flow through a material per unit thickness per degree of temperature difference across the thickness of the specimen. Aggregate has the highest thermal conductivity influence of any component in the concrete. The thermal conductivity is high for large density of the aggregate. The moisture content of the concrete also strongly influences the conductivity at very early ages, because water has a lower conductivity than aggregates. Furthermore, the lower w/c ratio and denser cement in high-strength concrete could result in higher thermal

conductivity. U.S. Bureau of reclamation has reported thermal conductivity values for different types of aggregates used in normal-strength concrete mixes shown in Table 1.

Table 1 Typical thermal conductivity values for concrete selected by type of aggregate (U.S. Bureau of Recalmation 1940)

Aggregate Type	Thermal Conductivity Btu*in/h*ft^2*°F (KJ/Kg*°C)
Quartzite	24(4.5)
Dolomite	22(4.2)
Limestone	18-23(2.6-3.3)
Granite	18-19(2.6-2.7)
Rhyolite	15(2.2)
Basalt	13-15(1.9-2.2)

Specific heat (Btu/lb*°F or KJ/Kg*°C) of concrete is defined as the amount of heat energy required to raise the temperature of a unit mass of a material by one degree. It is a function of the concrete composition and the type of aggregate used, but is not significantly affected by the mineralogical character of the aggregate. Higher strength concrete has higher specific heat. High moisture content of the concrete reduces the specific heat. Generally, specific heat values vary from 0.20-0.25Btu/lb*°F (ACI Committee 207, 2007).

The coefficient of thermal expansion (CTE) (1/°F or 1°/C) of concrete is one of the most important parameters in predicting stress distributions in concrete members. The CTE is defined as the change in unit length of a material in response to one degree of temperature change. There are several factors that affect the CTE including mixture proportions, water to cement ratio, aggregate type, cement type and humidity condition of the concrete. The cement paste of normal concrete usually has a higher coefficient of thermal expansion than the aggregate. But the aggregate has a dominant effect because of its large volume in concrete mix (Kejin W., Jiong H. and Zhi.G., 2008& Riding, 2007). CTE is several times higher for fresh concrete than it is for hardened concrete, and decreases sharply during the first ten hours of hydration and remains constant thereafter. It is relatively independent of age after few hours of casting up to 28 days. Due to the significant influence of the aggregates on the coefficient of thermal expansion and the large variation of this coefficient for different types of aggregate, it is important to measure the coefficient of the thermal expansion for the

particular concrete under investigation. Recommended value for Iowa use is discussed in Thermal Properties Report for CP Tech Center and shown in Table 2 (Sidney M., J. Francis Y., David D., 2003).

Table 2 Typical ranges for Iowa common aggregate CTE values

Aggregate	Coefficient of Thermal Expansion10^{-6}/°F(10^{-6}/°C)
Granite	4-5(7-9)
Basalt	3.3-4.4(6-8)
Limestone	3.3(6)
Dolomite	4-5.5(7-10)
Sandstone	6.1-6.7(11-12)
Quartzite	6.1-7.2(11-13)
Marble	2.2-4(4-7)
Concrete	4.1-7.3(7.4-13)

2.2.2.2 Mechanical Properties of Concrete

The term "maturity or equivalent age" is typically used to account for the combined effect of both time and temperature. There are two maturity methods commonly used, Nurse-Saul method and the Equivalent Age method. Nurse-Saul temperature function is used to relate both temperature and time, and was used in ConcreteWorks (Khan, 1995). The principle for estimating concrete strength using maturity concepts is described in ASTM C 1074. Maturity method is used for concrete strength prediction in this research. Temperature-time-strength relationship of a concrete mixture is developed in laboratory tests. The temperature-time factor could also be defined as the integral of the temperature history and may be calculated using equation below:

$$M(t)=\sum(T_a - T_0)\cdot \Delta T \qquad \text{Equation 1}$$

,where M(t) is the temperature-time factor at age (°C-hrs/days). T_a is the average temperature during time interval ΔT (°C), and T_0 is the datum temperature (°C).

Another maturity function is used to computer equivalent age:

$$t_e=\sum e^{-Q(\frac{1}{T_a}-\frac{1}{T_s})\Delta T} \qquad \text{Equation 2}$$

,where t_e is equivalent age at a specified temperature T_s (days or hrs), Q is activation energy divided by the gas constant (K),T_a is average temperature of concrete during time interval ΔT(K), T_s is specified temperature (K), and ΔT is time interval(days or hrs) (ASTM C1074, 2002).

Compressive strength development used maturity method is shown below (Viviani, 2005):

$$f_c(t) = a + b \cdot \log\left(\log\left(M(t)\right)\right), f_c \geq 0 \qquad \text{Equation 3}$$

,where f_c is the compressive strength development (MPa), a is a fit parameter which is usually negative(MPa), b is a fit parameter(MPa/°C/hr).

The key parameter in equivalent age equation is activation energy. The idea of "activation energy" is proposed by Svante Arrhenius in 1988. Activation energy describes the effect of temperature on the rate of strength development, which could be also measured in laboratory testing (Carino). First, determine the compressive strengths of mortar specimens which are at different constant temperatures. Next, find the value of the rate constant at each temperature by fitting a strength-age relationship. Plot the natural logarithms of the rate constants against the reciprocals of the absolute curing temperature, and best fit the equation to present the variation of the rate constant with the temperature as equation below.

$$k = Ae^{\frac{-E}{RT}} \qquad \text{Equation 4}$$

,where A is called the frequency factor, E is activation energy, and RT is gas constant. (N.J.Carine, H.S.Lew, 2011)

The modulus of elasticity of concrete is defined as the ratio of normal stress to corresponding strain for tensile or compressive stresses below the proportional limit of a material, and is normally expressed as a function of the concrete compressive strength. The ACI Code recommended the model to predict elastic modulus, and ConcreteWorks also established expression for modulus of elasticity, which will be discussed in section 2.4. In addition, the elastic modulus could be calculated from the measured stress-strain responses. The elastic modulus increases very rapidly at very early ages (Khan A.A., 1998).

Massive concrete structures need to meet strength requirements by varying the geometry and reinforcement of mass concrete. The determination of geometry and reinforcement of concrete structure is usually using 28-day compressive strength. Excessive

strength may lead to higher heat generated and increase the potential for cracking. In addition, compressive strength is affected by the curing condition. It was found that water cured condition gains higher compressive strength than sealed cured. Both the compressive strength and the modulus of elasticity of concrete increase rapidly during the first few hours due to the rapid increase reactions in the heat of hydration (Khan, 1995).

Actual tensile strength is one of the most important considerations and should be determined to correspond in time and the critical volume change. Tensile strength can be determined by three methods, the uniaxial tension test, the splitting tensile test and the modulus of rupture test (ACI Committee 207, 2007). Few references are available on the tensile strength of concrete at very early ages. The elastic modulus of the aggregates was the most important factor influencing the modulus of rupture. The tensile strength was more affected by a change in the curing conditions than the compressive strength. The modules of rupture be taken as $0.44\ f_c^{(2/3)}$ in MPa units , which was proposed by Jerome (Ge Z. , 2005).

Early-age shrinkage and swelling play an important role in the development of early-age stress. They affect the serviceability and durability of the mature concrete. Shrinkage is defined as the decrease in concrete volume in the absence of stress, and is mainly attributed to drying shrinkage due to the loss of moisture. Moisture loss can also occur during hydration due to the consumption of water, which causes a contraction of volume. An increase in temperature of hardened concrete results in a higher rate of shrinkage and a higher ultimate shrinkage strain. Additional stresses may occur due to chemical swelling, while the concrete temperature is rising. Chemical swelling can last from 10 to 20 hours and strongly depends on the types of cement. Secondary autogenous shrinkage starts after the chemical swelling process. If the rate of secondary shrinkage is high, the risk of cracking after setting increases due to the restraint tensile stresses in the concrete. The shrinkage is mainly affected by the following factors: composition of concrete, member size, member shape, curing conditions, relative humidity, and ambient temperature (Khan, 1995).

Early-age creep of concrete has an important effect in reducing stresses induced during the hydration period. Creep is defined as a continuous increase in strain under constant stress, sometimes called creep compliance, is defined as the total strain per unit stress. Creep is a complex problem, especially at very early ages. The influence of moisture

divides creep into basic creep and drying creep. Basic creep is the creep of concrete in a perfectly sealed condition. Drying creep is the additional creep caused by moisture loss under constant stress. Creep affects the serviceability and durability of concrete structures. It is influenced by the following factors: concrete composition, loading age, temperature, loading duration, moisture condition, and stress level. During the hydration process, large thermal and shrinkage gradients can cause stresses which are significantly affected by concrete creep. It is a well-established phenomenon that the creeping rate of hydrating concrete decrease with age of loading. The presence of creep during the hydration period is at very early ages, and would have an effect of reducing tensile stresses. When temperature is increasing during hydration, tensile stresses develop near the concrete surface where the temperature is lower and compressive stresses develop at the center where higher temperatures exist. During this phase the concrete has low strength, low elastic modulus and high early age creep. When the center of the concrete starts cooling down, tensile stresses caused by thermal gradients will reduce and may develop at the center of the concrete so that results in concrete volume change. During this process, high concrete strength resulting in an increased modulus of elasticity and low creep.

Lastly, poisson's ratio can be determined conveniently by direct strain measurements in uniaxial compression or can be determined dynamically using Equation 5 below:

$$v_d = \frac{E_d}{2G_d} - 1 \qquad \text{Equation 5}$$

an average passion ratio value is 0.19 for concrete mixes with 28-days.For different concrete, poisson's ratio generally falls in the range of 0.15-0.2. Very limited information is available on poison's ratio of concrete at early ages (Sidney M., J. Francis Y., David D., 2003).

2.3 Mass Concrete & Specification

Definition of mass concrete and specification in Iowa will be discussed in the following subsection. Two major concerns for mass concrete are thermal cracking and delayed ettringite formation (DEF). Since temperature is considered as a criterion to avoid the high potential of mass concrete structural failure, temperature limits regulated in Iowa development mass concrete specifications is also shown in this subsection. The factors affecting mass concrete thermal behavior are described in section 2.3.2, including

environmental effects and construction practices. Then effective thermal control methods are recommended.

2.3.1 Mass Concrete Definition & Specification

ACI defines mass concrete as "any volume of concrete with dimensions large enough to require that measures be taken to cope with generation of heat from hydration of the cement and attendant volume change to minimizing cracking" (ACICommittee207 1R, 2005). The Iowa DOT defines mass concrete as "any concrete footing with a least dimension greater than 5 feet or other concrete placements with a least dimension greater than 4 feet." Thermal behavior is the most important characteristic which differentiates mass concrete from other structural concrete. High temperature development causes damage to mass concrete by thermal cracking or/and delayed ettringite formation (DEF). Usually, DEF occurs when the internal temperature exceeds 158°F (70°C). When DEF occurs, the concrete paste usually expands and sometimes cracks the concrete with detrimental results. Thermal cracking is generally due to unexpected volume changes in mass concrete, and can lead to the tensile stress exceeding the tensile strength of concrete. Thermal cracking generally happens when large internal and external temperature differences occur. Large temperature difference results in large thermal stresses which can cause cracking of the surface. Texas DOT limits temperature difference between surface and interior should be 35°F (20°C) or less to minimize thermal cracking (Riding, 2007). The Iowa DOT also has developmental specifications on mass concrete thermal control includes maximum placement temperature should not exceed 70°F or less than 40°F; the maximum concrete temperature during the period of heat dissipation shall not exceed 160°F, and maximum temperature differential restrictions during different periods as Table 2 shown. The temperature difference limit is shown in Table 3 below, where maximum temperature difference is measured from maximum interior concrete temperature to surface sensor temperature (IowaDOT, 2010).

Table 3 Limit of maximum temperature difference in Iowa developmental specification

Hours after Placement	Maximum Temperature Differential °F(°C)
0-24	20(11.1)
24-48	30(16.7)
48-72	40(22.2)
>72	50(27.8)

Generally, temperature difference is defined as the temperature difference between maximum temperature in the concrete, and the concrete temperature at the sensor location. In a mass concrete structure, sensors are recommended to be put into three places: center of the placement, midpoint of the side surface and midpoint of the top surface. Sensors located at the surface should be installed with minimum a 2 inches concrete cover. Sometimes, sensors are installed at the corner of the placement. In some computer software packages, the temperature difference is defined as the difference between the maximum interior temperature and minimum temperature at the concrete surface.

2.3.2 Control of Thermal Behavior of Mass Concrete

In mass concrete, thermal strains and stresses are developed by volume change. The volume change is primarily from generation and dissipation by heat of cement hydration. It is important to understand mass concrete thermal behavior and control thermal development to avoid thermal cracking. The main purpose of controlling temperature of mass concrete is to reduce volume changes effectively by controlling the temperature difference in concrete. Thermal gradient is the main cause for volume change, which is defined as "the temperature change along a particular path or through a section of a structure" according to ACI code (ACI Committe 207, 2005). Thermal gradient is categorized as mass gradient and surface gradient. Mass gradient describes the temperature difference of maximum interior temperature and ambient temperature. The properties of mass concrete itself, subbase material below the mass concrete, and geometry have influence on stress and strains. Surface gradient is the result of surface concrete temperature to more stable internal temperature. Surface temperature is greatly affected by daily and annual cycled ambient temperature, which varies stresses as well. Surface cracking, so called thermal shock, usually occurs when

extreme contrast exists between ambient temperature and internal temperature. For example, thermal shock may occur when forms and insulation are removed very soon on an extremely cold day.

In order to properly control thermal behavior, it is recommended that construction limit the maximum temperature, reduce the maximum temperature difference as much as possible, support mass concrete without restraint, and relieve stress through creep. However, none of these conditions could be achieved thoroughly. To efficiently reduce maximum temperature and temperature differences, several thermal control methods are recommended, including precooling, cementitious material content control, and post cooling control. ACI 207.1R describes recommendations to reduce initial placement temperature. For instance, precooling processes use cooled aggregates to reduce the peak temperature of concrete. Using lower heat Portland cement, blended hydraulic cement, and reducing the cement content by replacing it with a slag or pozzolanic material also benefit thermal control from mix design aspect. In addition, water reducers and retarders reduce temperature rise during first 12-16 hours. However, they have little influence on total heat development after 24 hours from concrete casting. Post cooling methods, such as embedded cooling pipes, remove heat from the concrete and limit the temperature rise in the structure. Furthermore, some construction management practices protect the structure from excessive temperature difference by modifying handling, scheduling and construction procedures.

Lower heat-generating cement systems are recommended for mass concrete construction including the use of pozzolans, controlling of aggregate grading, so on and so forth (ACICommittee207 1R, 2005). Construction practices for temperature control include those such as cooling batch water or using water with ice, spraying or immersion aggregates in cool water, and applying insulation to minimize temperature differentials. Furthermore, embedded cooling pipes, as a post-cooling method, is a useful construction practice to control thermal behavior of mass concrete. (ACI Committee 207 , 2005). Detailed ACI recommendations are shown in Appendix A.

2.4 Prediction Models of Concrete Thermal Behavior & Cracking

Prediction of temperature and thermal stress development could help engineers understand mass concrete thermal behavior and reduce cracking potential. Several prediction models of cement hydration process are obtained from literature and discussed in section 2.4.1. Heat transfer model is shown in Fourier's Law equation below, which could be used to calculate temperature distributed inside the cross section.

$$k\left(\frac{\partial^2 T}{\partial x^2}+\frac{\partial^2 T}{\partial y^2}\right)+q=\rho c_p\frac{\partial T}{\partial t} \qquad \text{Equation 6}$$

,where k is thermal conductivity,(w/°C), T is temperature(°C), x,y are coordinates at a particular point in the structure, q is rate of internal heat generation(w/m^3), ρ is concrete density (Kg/m^3), c_p is specific heat of concrete(J/Kg· ℃) , and t is time (Munich, 1994). More prediction models on different concrete properties will be discussed later in this section, including compressive strength, elastic modulus, tensile strength and creep. The last section in 2.4 focuses on estimating cracking potential.

2.4.1 Heat of Cement Hydration Model

There are many temperature prediction models. Engineers and contractors need a reliable and accurate method of testing or predicting heat of hydration process. In Zhi Ge's (Ge Z. , 2005) dissertation, a hydration model considering the effect of GGBFS, is described based on the Iowa concrete database. In order to calculate the heat development, the equivalent age and prediction models are required. The nonlinear regression analysis to obtain H_{ult}, β, and τ is performed based on literature concrete data. Then the relationship among the hydration parameters and cementitious materials properties through statistical analysis is established as Equation 7 describes. Since cement is not 100% hydrated, the ultimate heat of hydration is the total heat generated during hydration process as Equation 8 and 9. Cement heat of hydration models are described below:

$$H(t)=H_{ult}\cdot\exp\left(-\left[\frac{\tau}{t_{eq}}\right]^{\beta}\right) \qquad \text{Equation 7}$$

,where, H_{ult} is ultimate heat of hydration of cementitious materials (KJ/Kg), t_{eq} is equivalent age (hrs), τ and β are hydration parameters.

$$H_{ult}=H_{total}*\alpha_u \qquad \text{Equation 8}$$

,where H_{total} is total hydration heat of the cementitious materials(KJ/Kg), and α_u is ultimate degree of hydration.

$$H_{total} = H_{cement} \times p_{cement} + H_{FA} \times p_{FA} + H_{Slag} \times p_{FA} + H_{Slag} \times p_{Slag} \quad \text{Equation 9}$$

,where, H is total hydration heat of cement, fly ash, and slag, p is weigh of cement, fly ash and slag.

The equations below could be used to predict heat development by knowing the weight ratio of that cementitious compound to cement, or cementitious material. HI is hydraulic index to account for the different types of slag.

$$H_{total} = 500C_3S + 260C_2S + 866C_3A + 420C_4AF + 1186freeCaO + 850MgO + 624SO_3 + 461slag + FA(15.9 \cdot (pCaO \times 100) + 74.3) \quad \text{Equation 10}$$

$$\tau = 2.649 \cdot C_3S^{-0.541} \cdot C_3A^{-0.122} \cdot {SO_3}^{-1.191} \cdot Blaine^{-0.567} \cdot \exp(3.018 \cdot slag + 8.365 \cdot FA \cdot FA - CaO) \quad \text{Equation 11}$$

$$\beta = C_3S^{0.280} \cdot C_3A^{0.143} \cdot {SO_3}^{1.378} \cdot Blaine^{-0.994} \cdot \exp(-9.210 \cdot slag \cdot (1 - 0.568 \cdot HI) + 11.272) \cdot (1 - 0.519 \cdot FA) \quad \text{Equation 12}$$

$$\alpha_u = \frac{1.31 \cdot w/cm}{0.194 + w/cm} + 0.361 \cdot FA + 4.285 \cdot slag \cdot (0.730 \cdot HI - 1) \leq 1 \quad \text{Equation 13}$$

$$HI = \frac{CaO + MgO + Al_2O_3}{SiO_2} \quad \text{Equation 14}$$

,where $C_3S,\ C_2S,\ C_3A,\ C_4AF, SO_3, CaO, freeCaO, MgO,$ are weigth ratios to cement, $slag, FA,$ are weight ratio to cementitious material,$FA - CaO$ is weight ratio to fly ash.

2.4.2 Ultimate Compressive Model

Strength development with maturity for different cementitious materials can be predicted based on statistical analysis of existing database as well. Iowa strength prediction

models are summarized in Ge's dissertation and shown below. R^2 value for this prediction is 0.975:

$$S=Su*\exp\left(-\left(\frac{\tau}{t_{eq}}\right)^{\beta}\right) \quad \text{Equation 15}$$

$$Su = \exp(-1.810 * w/c + 10.143) * (1 - 0.051 * Air) * (C_2S \cdot 0.143 + 2.155 * FA - 3.544 \cdot FA^2 + 0.711 \cdot Slag - 0.367 \cdot Slag^2 \quad \text{Equation 16}$$

$$\tau = \exp[-4.462 * (FA - CaO - 0.2711) - 2.147 * (HI - 1.519)] * [EXP\left(3.401 * \frac{w}{c} - 2.709\right) * C_3S^{-1.659} * C_3A^{-0.378} * SO_3{}^{-1.154} * Blaine^{-0.229} + 120.306 * FA + 190.939 * Slag + 1221.717 * FA * Slag \quad \text{Equation 17}$$

$$\beta = [\exp(3.039) \cdot (C_3S + C_2S)^{-0.653} \cdot C_3A^{0.303} \cdot Blaine^{-0.6.25} - 0.463 \cdot FA + 1.377 \cdot FA^2 - 0.427 \cdot Slag + 1.392 \cdot Slag^2] \cdot \exp(1.993 \cdot (FA - CaO - 0.2711) + 0.924 \cdot (HI - 1.519) \quad \text{Equation 18}$$

,where τ, β are hydration parameters, C_3S, C_2S, C_3A, $C_4AF, SO_3, CaO, freeCaO, MgO,$ are weigth ratio to cement, $slag, FA,$ are weight ratio to cementitious material, $FA - CaO$ is weight ratio to Fly ash.

In developed regression analysis for MEPDG computer program, Iowa data has strength prediction model as following:

$$f'c, t = -134119 + 103000w/b + 978uw + 125CMF + 30.6\log(t) - 752w/b * uw - 0.865uw * CMF \quad \text{Equation 19}$$

,where w/b is water-cement ratio, uw is the unit weight of concrete, CMF is cementitious material factor, t is the age of concrete (Ge Z. , 2005).

However, compressive strength could vary for different dimensions of concrete, difference in curing condition, and other influences. To develop the mass concrete input of computer software, measuring compressive strength development is recommended.

2.4.3 Elastic Modulus Model

Numbers of models are established to predict the relationship between modulus of elasticity and compressive strength empirically. Most equations could be obtained by regression analysis. ACI proposed an equation for obtaining elastic modulus by assuming the normal weight of concrete is 145 pcf as shown in Equation 20.

$$E_c = 57000(f'_c)^{1/2} \quad \text{Equation 20}$$

In MEPDG Pavement report elastic modulus could be obtained based on regression analysis results from available Iowa data. (Kejin W., Jiong H., and Zhi G., 2008).

$$E_c = 80811(f'_c)^{0.4659} \quad \text{Equation 21}$$

In Ge Zhi's thesis, elastic modulus relationship can be concluded as following considering the cementitious material effects:

$$Ec = 22100 * f_E * p_{C3A}^{0.3} * p_{C4AF}^{0.25} * Blaine^{0.35} \quad \text{Equation 22}$$

$$f_E = 1 - 1.05 * p_{FA} * \left(1 - \frac{p_{FACaO}}{0.4}\right) + 0.4 * p_{Slag} \quad \text{Equation 23}$$

,where, f_E is modification factor for SCMs, bliane is specific surface area of cement(Kg/m^2) and p_{C3A},p_{C4AF},p_{FA} and p_{Slag} are weight ratio of them in terms of the total cement content. .p_{FACaO} is the weight ratio of CaO content of fly ash (Ge Z. , 2005).

In Kyle's dissertation, equivalent age Elastic Modulus has following equation to predict:

$$E = E_c \times f'^{\,E_e}_c \times w^{1.5} \quad \text{Equation 24}$$

, where w is the unit weight, f_c is the compressive strength, E_c and E_e are fit parameters, in ConcreteWorks prediction computer program, it generally used as E_c=33, E_e=0.5 (Riding, 2007).

2.4.4 Tensile Strength Model

Like elastic modulus, numbers of empirical formulas are suggested relating tensile strength. According to ACI 207, the empirical relationship between modulus of rupture and compressive strength is shown below (ACI Committee 207, 2007):

$$f_{sp} = 7.11 \times fc^{0.5} \quad \text{Equation 25}$$

Since the Linear Logarithmic Model for creep compliance contains elastic modulus, the calculation model in ConcreteWorks is used to get maturity and elastic modulus relationship by compressive strength and maturity equation.

$$f_t = 1.019 \times fc^{0.7068} \quad \text{Equation 26}$$

For equivalent age splitting tensile strength,

$$f_t = f_{tc} \times fc^{fte} \quad \text{Equation 27}$$

where f_c is the compressive strength, f_t is the tensile strength, and f_{tc} and f_{te} are fit parameters. In CocnreteWorks, it used as f_{tc}=1.7,fte=0.666 (Riding, 2007) .

2.4.5 Creep Prediction Model

Creep is a consequence of the concrete being under a constant stress at an elevated temperature so that it continuously deform with time. Creep is one of the concrete mechanics properties that is affected work hardening. This work hardening effectively prevents any further deformation from taking place if the stress remains approximately constant. Many prediction models have been developed to consider creep effects. Some examples are discussed in this section.

First, the triple power law by Bazant and Chern in Equation 28 and 29, and the extended triple power law in Equation 30 to Equation 33 are shown below (Westman, 1999).

$$J(t,t0) = \frac{1}{E_0} + \frac{\varphi 1}{E0}(t_0^{-m} + \varsigma)(t\text{-}t_0)^n \quad \text{Equation 28}$$

where, E_0 is the so called asymptotic modulus. φ, ς, n and m may be obtained by formulas modeling dependence. Times t_0, and t are expressed in days. The long term creep relationship is modeled using the triple power law.

$$J(t,t0) = \frac{1}{E_0} + \frac{\varphi 1}{E0}(t_0^{-m} + \varsigma)[(t\text{-}t_0)^n\text{-}B(t,t_0;n)] \quad \text{Equation 29}$$

$$J(t,t0) = \frac{1}{E_0} + \frac{\varphi 1}{E0}(t_0^{-m} + \varsigma)[(t\text{-}t_0)^n\text{-}B(t,t_0;n)] + \frac{\Psi 1(t_0)}{E_0} + \frac{\Psi 2(t,t_0)}{E_0} \quad \text{Equation 30}$$

$$\varsigma = \frac{1}{40(w/C)} \quad \text{Equation 31}$$

$$\Psi 1(t_0) = \gamma_1\left(\frac{t_1 - t_0}{t_1 - t_{s0}}\right)^{a_1} \quad \text{Equation 32}$$

$$\Psi 2(t,t_0) = \gamma_2\left[1 - \exp\left(-\left(\frac{t-t_0}{t_2}\right)^{a_2}\right)\right]\left(\frac{t_3 - t_0}{t_3 - t_s}\right)^{a_3} \quad \text{Equation 33}$$

where t_0 -equivalent age when the loading is applied, days

t_s - apparent setting time of the concrete days

$t_1$and t_3 - time limits for adjustments at early ages, days

t_2 and a_2 - parameters for the development of the time function, days

$t\text{-}t_0$ - actual time period after loading days.

γ_1 - initial value of function $\Psi 1(t_0)$ at $t_0=t_s$

a_1 -parameter modifying the shape of $\Psi 1(t_0)$

γ_2 - the end value of function $\Psi 2(t,t_0)$ for $t_0=t_s$

a_3 - parameter modifying the end value of $\Psi 2(t,t_0)$, $t_0>t_s$

Another creep relationship is the Linear Logarithmic Model which is used to calculate the early-age concrete stress relaxation. This model is often used in computer program simulations. This method describes the early-age concrete creep compliance function as a series or lines in log scale shown as Figure 2.

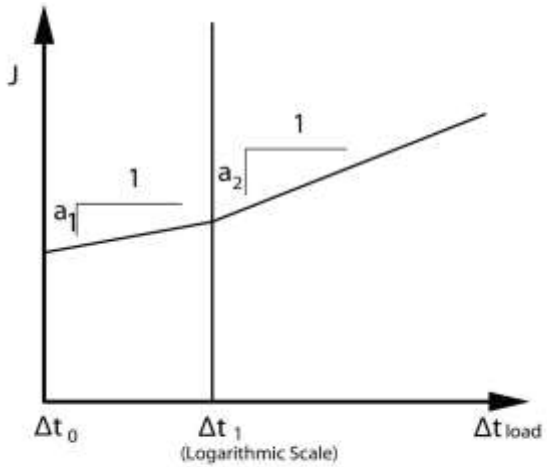

Figure 2 Creep Compliance modeled using the Linear Logarithmic Model (Larson, 2003)

The predicting equations are listed below from Equation 34 to 37. Volumes for parameters in the equation are shown in Table 4.

$$J(\Delta t_{load,} t_0) = \frac{1}{(E(t))} + \Delta J(\Delta t_{load,} t_0) \quad \text{Equation 34}$$

For $\Delta t_0 \leq \Delta t_{load} < \Delta t_1$

$$\Delta J(\Delta t_{load,} t_0) = a_1 * \log(\frac{\Delta t_{load}}{\Delta t_0}) \quad \text{Equation 35}$$

For $\Delta t_{load} \geq \Delta t_{t1}$

$$\Delta J(\Delta t_{load,} t_0) = a_1 * \log\left(\frac{\Delta t_{load}}{\Delta t_0}\right) + a_2 * \log\left(\frac{\Delta t_{load}}{\Delta t_0}\right) \quad \text{Equation 36}$$

$$a_i(t_0) = a_i^{min} + (a_i^{max}\text{-}a_i^{min}) * \exp(-(\frac{t_0 - t_s}{t_{ai}})^{n^{ai}}) \quad \text{Equation 37}$$

,where, $J(\Delta t_{load,} t_0)$=creep compliance (1/Pa)

E(t) -the concrete elastic modulus at the time of load application, which could be obtained based on laboratory testing or previous models

$\Delta J(\Delta t_{load,} t_0)$=the change of creep compliance (1/Pa)

Δt_{load} =the time since load application (days)

t_0= the time of load application (days)

Δt_1= the time of the change in creep compliance slope (days)

t_s=the concrete time offset

a_i^{min}, a_i^{max}, $t_{ai,} n_{ai}$=fit parameters

Table 4 Modified Linear Logarithmic Model Parameter

Modified Linear Logarithmic Model Parameter	Value	Units
delta t_0	0.001	days
delta t_1	0.1	days
$a_1$min*(10^-12)	0.1	1/Pa
a_1 max*(10^-12)	60	1/Pa
n_{a1}	1.19	
a_2 min*(10^-12)	5	1/Pa
a_2 max*(10^-12)	30	1/Pa

2.4.6 Thermal Cracking Potential Prediction

Several methods could be used for predicting thermal cracking risk, ranging from simple temperature difference requirements to stress and strength ratio. Thermal cracking of concrete can be predicted by the allowable stress design method. The level of cracking could be defined based on stress and strength ratio shown below:

$$\eta^{\max} = \left[\frac{\sigma_t(t)}{f^*_{ct}(t)}\right]^{\max} \qquad \text{Equation 38}$$

,where η^{max} is the maximum cracking risk in the member, σ_t is the tensile stress (MPa), and f^*_{ct} is the tensile strength at time t (MPa) (Riding, 2007).

Several researchers have explored the probability of cracking due to thermal stress using assumed mean and standard deviations of the concrete strength and stress. Generally, concrete cracking occurs at tensile stress/strength ratio of the concrete equals to 1. The stress at failure may not always be equal to the concrete tensile strength. Based on testing results in Riding's dissertation (Riding, 2007), there is 50% probability of cracking occurring at a stress to strength ratio of 0.63 with corrections. In previous study, the value of 0.75 tensile stresses to strength ratio is close to the 50% probability of cracking using Figure 3 (Raphael, 1984).

The probability of cracking may be summarized into low, medium, high and very high cracking potential based on different levels of stress/strength ratio. Generally when tensile stress/strength ratio is over 1, the cracking may have large potential to occur. In an

actual cracking potential prediction, which considers a safety factor as 1.3, the mass concrete has very high cracking potential when the stress/strength ratio is over 0.75. A low cracking potential could be defined as probability of 25%, between 25% and 50% could be considered as moderate cracking risk, and between 50% to 75% probability may be classified as a high cracking probability. A very high cracking risk will be any cases over 75% probability. A concrete cracking probability versus stress to strength ratios for various splitting tensile strength models is shown in Table 5 below (Riding, 2007). The tensile strength model used in later study could obtain similar tensile strength developments as Raphael mentioned.

Table 5 Concrete Cracking probability versus cracking stress to tensile strength ratios for different splitting tensile strength models (Riding, 2007)

Failure Probability	Test Results of this Study	Relationship Developed in This Study	Raphael 1983	ACI 318-05, Chapter 18	Carino and Lew 1982
75%	0.64	0.63	0.74	0.85	0.76
50%	0.57	0.56	0.67	0.78	0.69
25%	0.51	0.51	0.61	0.72	0.63
10%	0.46	0.46	0.56	0.66	0.57
5%	0.44	0.43	0.54	0.64	0.55
1%	0.39	0.38	0.49	0.58	0.50

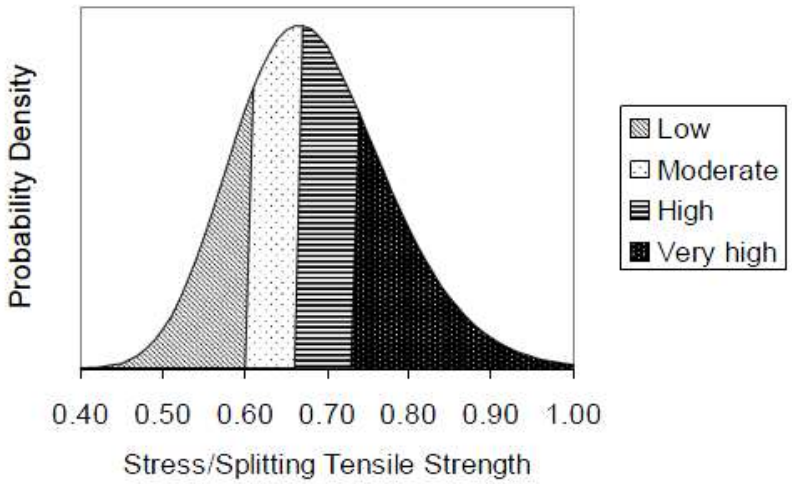

Figure 3 Cracking Probability categories for versus stress to splitting tensile strength ratios using the Raphael (1984) model (Raphael, 1984)

2.5 Simulation Computer Programs

In order to fulfill the research goal, existing simulation computer programs are investigated. Some of the computer programs are user friendly, but most of the computer software requires considerable background knowledge and lengthy processing times. ConcreteWorks is capable of performing thermal analysis for mass concrete. However, this program does not predict detailed cracking potential, or consider the effects of cooling pipes. Several other available programs were explored and compared for this project including STADIUM, ANSYS, and 4C Temp&Stress. At last, 4C Temp&Stress was selected for use for this research. Comparisons between computer programs are discussed in this section.

2.5.1 Currently Available Computer Programs

Several highlights of current available computer programs are listed and compared in Table 6. ConcreteWorks is empirical software developed at the Concrete Durability Center at the University of Texas. This software can be used to predict mass concrete temperature development, and Alkali Silica Reaction (ASR) and DEF susceptibility. The database established in ConcreteWorks can be applied in many projects involving mass concrete construction. The program is very user friendly and has less requirement for user's concrete background regarding the thermal development of concrete. Users can choose provided construction conditions as project needs. Furthermore, ConcreteWorks can also be used as an aid for mix design by varying the input aggregate and cementitious materials while noticing how thermal development is affected.

STADIUM is a program which is used to perform numerical simulations to estimate the service life of a concrete structure. The results from STADIUM are focused on the corrosion of mass concrete, instead of temperature or stress prediction. The advantage of this program is that it is capable of comparing different codes and is user friendly.

ANSYS is a finite element computer simulation program which could be used to analyze mechanical, dynamics, design life, and fatigue of structures. It is challenging to operate and requires background in computer programing. However, the results provided using ANSYS are very detailed and useful for researchers.

4C-Temp&Stress (4C) is focused on concrete thermal and stress analysis. The program could calculate the temperature and stress in concrete structures during the material

development using a two dimensional polygonal area. The required inputs of this computer program are more complex than ConcreteWorks but the program is easier to use than ANSYS. 4C shows the predicted results of temperature, maturity, strength, and stress as functions of time. In addition it also provides iso-curves of temperature, maturity, strength and stress at a given time, based on the finite element method. Iso-curves appear to be similar as contour lines and indicate the development of those properties at the cross section of the concrete.

Table 6 Comparison between different computer programs

Computer Software Package	Major Advantages	Major Disadvantages
ConcreteWorks	• Requires fewer inputs • Provides visualizations of cracking potential	• Limits analysis period up to 14 days • Cooling pipes cannot lie • Users are not allow to establish databases as other programs for concrete, insulation materials and etc.
STADIUM	• Simulates concrete service life • Compares different codes and standards	• No temperature and stress prediction s are available
ANSYS	• Comprehensive FEM program • Considers structure design impact	• Users' program experience and knowledge on structural design are required
4C Temp&Stress	• Emphasize concrete thermal behavior analysis • Allow user to establish input database • Iso-curves results are available • Tensile Stress/Strength ratio results are available • Considers cooling pipe effects	• Only SI units available • Detailed concrete properties inputs required

2.5.2 General Information and Application Suggesting for 4C Temp&Stress

4C Temp&Stress (4C) is selected for this research project to evaluate mass concrete thermal behavior. The 4C program is developed by Danish Technological Institute, which provides the abilities to outline concrete geometry, carry out full or approximated calculations, and view the results in a graphical interface. The program can perform thermal analysis and stress analysis. Thermal analysis is based on internal heat generation and thermal boundary conditions such as ambient temperature, insulation, and cooling pipes/heating wires. Stress analysis is based on external support, thermal expansion, stiffness and stress properties and creep information. Typically, 4C analyzes linear-elastic disks in a plane stress or plane strain situation for hardening and restrained concrete structures.

Since the mid-1990s 4C-Temp&Stress has been used to document curing and early-age requirements on several large civil structures around the world, including: (4C-Temp&Stress for concrete - Description)

- The Øresund Link between Copenhagen and Sweden
- Copenhagen Minimetro, bored tunnels and deep stations
- Marmaray Railway crossing, Istanbul, Bosphorus Strait. Bored tunnel, cut and cover, deep stations, Gama-Nurol JV
- Sitra bridges, Bahrain, Gamuda Berhad Contractors
- Funder highway bridge, Denmark, Züblin - Dyvidag JV
- Funder highway bridge, Denmark, Züblin - Dyvidag JV

Furthermore, HETEK- Danish R&D projects on high performance concrete also adopted this program. The main advantages of 4C Temp&Stress are that it can present iso-curves for temperature, maturity, strength and stress at a given time. It also produces isocurves for tensile stress/strength ratio. Tensile stress/strength ratio is an important criterion to predict if concrete cracking happens. The 4C program analyzes concrete members by generating finite element meshes, and finer mesh size provides more accurate results. The detailed introduction of 4C program will be discussed in Chapter 3.

2.6 Important Findings from the Literature

Available literatures discussed several factors impacting the thermal behavior of concrete, such as the dimensional size of concrete, fresh placement temperature, and insulation. Potential construction and design recommendations for thermal cracking control were also provided in literature, but were general and far-ranging. To minimize thermal damage of mass concrete, it was recommended to use low heat mix design and materials, take pre-cooling and post cooling precautions, and provide proper insulation. However, no visualized influences of the factors were presented in past study due to different thermal behavior of different concrete mix design. Prediction models of concrete properties were studied to help understand mass concrete thermal behavior, but were not convenient for contracts to use. Furthermore, current software packages of mass concrete prediction were identified to have variable limitations. The importance of this study is:

- Exploring available computer software to simulate mass concrete behavior
- Using Iowa existing mass concrete mix design to visually present how those factors affect concrete thermal behavior in construction
- Refining current recommendations on mass concrete construction.

CHAPTER 3 INTRODUCTION TO 4C TEMP&STRESS

This chapter discusses the application of 4C Temp&Stress program. Section 3.1 explained the assumptions and limitations of 4C program. Section 3.2 discussed the general inputs and outputs of 4C. The models applied in 4C program are presented in section 3.3. Advantages and disadvantages of 4C program are shown in section 3.4.

3.1 Assumptions and Limitations of 4C Program

The main calculation assumptions in the program are shown in Table 7. Thermal analysis method is generally chosen to be transient, where the calculated temperatures are as a function of place and time. For the temperature prediction after a very long period, a stationary method can be used. Stress analysis is mostly assumed to be based on thermal results including thermal expansion and material properties. If the stress analysis is not based on thermal results, only the impact of external load will be considered. Analysis dimensions can be chosen as 2 dimensional or 2½-dimensional. Two dimensional identifies geometry as a disk. 2½-dimensional identifies a plane strain situation where it is possible to specify cross-sectional load and support conditions. Time specifications, nonlinear calculations, mesh, node generation, circles and self-weight parameters can be either defined, or set as the default values. There are certain limitations in 4C-Temp&Stress about task-size that 4C can analyze. Generally, 4C program is capable to analyze river bridge foundations. Thermal and stress analysis requires a large amount of computer memory.

Other assumptions on defining the database are discussed in Chapter 5 when actual analyzing case is applied. The specific heat of cement, aggregates, GGBFS, and fly ash could be defined by measurements or recommended values. In this study, the specific heat of the materials is assumed to be the same and is equal to 0.84 KJ/Kg/°C. The thermal conductivity recommended values can be found in engineering tool box website (Engineering Tool Box). The water temperature in the cooling pipes is assumed to be 10 °C in this study. In concrete properties input section, activation energy factors are assumed to be 33500J/mol, and 1470J/mol/°C as default values in 4C program.

Assumptions of the locations for minimum temperature and maximum temperature are at the surface of the concrete member and at the mid-center of the concrete member. The surface temperature is assumed to be equal to averaged 7-day ambient temperature during whole analysis period, which is inputted as sin curve format. Wind velocity is assumed constant during analysis period instead of varying every day. The maximum temperature difference is assumed to be the difference between the maximum temperature and the temperature at top surface sensor. The top surface sensor is assumed to be placed at 3 inches below the surface.

For stress approximation analysis, if the poisson ratio is assumed to be zero, the analysis can be divided into two separate parts. The first part determining the stress distribution perpendicular to the cross section is very simple and is performed together with the temperature calculation. The reason is the computational work required by the general stress calculation is rather heavy, and the approximate stress calculation is a short cut to obtain an indication of whether or not the general stress calculation will yield an acceptable result. Further assumptions for different sensitivity study and case study were addressed where the actual study were discussed.

Table 7 Assumptions of Calculation Parameters default input in 4C program

Time specifications	
Total process time	300 hr
Time step, desired	1 hr
Time step factor	0.5
Nonlinear calculation	
Convergence criteria	As a start value of 1.0e-3
Mesh, node generation	**Percentage of the largest extend**
Min. distance to boarder	0.01%
Density, internal nodes	10%
Density, border nodes	10%
Density around Cpipe/Hwire	5%
Radius around Cpipe/Hwire	20%
Circles	
No. of faces	12
Self weight	off

3.2 General Inputs and Outputs for 4C

In order to correctly utilize 4C program, inputs of 4C are studied in this section. Several assumptions of using 4C program, which are discussed in section 3.1, should also be considered. 4C program contains three main parts: project editor, project solver and result viewer. The following section discusses these three parts in detail.

Project Editor is where the user edits and outlines the projects, including the construction, placing, cooling pipes, boundary conditions and loads. In this section, concrete member volumes, cooling pipe or heating wires are drawn using drawing tools. After defining volumes shape, the volume properties, such as material type, size, temperature, and start time, are defined. Then, define surfaces and thermal boundary conditions. Boundary conditions are significant parameters for simulation. Inputs for boundary conditions include: temperature, wind velocity, shield definition, heat transfer coefficients, and radiation. Therefore, temperature and shield definition are essential to be defined for each volume. Usually **Sine Curve** is chosen as ambient temperature input to simulate boundary conditions. Curve parameters for **Sine Curve** include: start time (h), minimum temperature (°C) and maximum temperature (°C). Shield definition could be used to define the formwork and curing method. Heat transfer coefficient will be automatically generated after above information is defined. If any cooling pipes, or heating wires are designed, input information of faces, diameter and boundary conditions for pipes are required. No load input is necessary to simulate thermal behavior of concrete in 4C. Definition of proper load support, such as point support or line support is important to get a more accurate stress analysis.

Project Solver is where the temperature, maturity, approximated stress and stress development of mass concrete are generated and calculated. Eight calculation parameters need to be selected or input. Thermal analysis method includes transient, stationary. Stress analysis methods can be chosen with thermal results or without thermal results. Dimensions can be plane stress, plane strain in 2-dimensional, or 2½-dimenstional including no strain in z-direction, no rotation around x-axis, or no rotation around y-axis. Usually, 2½-dimenstional is selected with no rotation and strain. Furthermore, time specifications, nonlinear calculations, mesh, node generations, circles, and self-weight parameters are needed to define. The detailed calculation parameters inputs will be discussed in Chapter 4. In concrete

database section, current concrete information can be chosen to be used, or to add new concrete database. Creating new data base requires input information about mixture proportions, heat, E-modulus, poisson ratio, thermal expansion coefficient, properties (slump, W/C ratio, air content and so on) initial strain, creep, compressive strength and tensile strength. Mixture proportions could be defined an using existing material database or by creating a new database. Material database in 4C program are mostly applied in European concrete industry, so new material base should be established with the new mix design information about density, specific heat, and thermal conductivity. Detailed information on how to establish a database will be discussed later.

Result Viewer is where the results are displayed. The process is generating mesh, calculating temperature and then calculating stress. Generate finite element mesh is used to activate the project solver, and then user could perform temperature calculation. Stress calculation should be performed after thermal calculation. The results that 4C is capable to presented are shown in the following Table 8.

Table 8 List of graphic results generated by 4C Computer Program

The generated finite element mesh	
x/y-diagram in specified points as a function of time showing	temperature maturity strength approximated stress stress
x/y-diagram for each cast as a function of time showing the min./max.	temperature maturity strength approximated stress stress
x/y-diagram for each cast as a function of time showing the average	temperature maturity strength approximated stress stress

Iso-curves in the cross section at any specified time after casting showing	temperature maturity strength approximated stress stress
An x/y-diagram showing either external or internal temperature difference as function of time.	

In order to analyze the desired mass concrete structure, the structure should be drawn in project editor first, and then boundary conditions are defined based on environmental conditions and construction insulating conditions. A proper concrete database for specific mass concrete mix design should be established and assigned to the analyzing volume. The next step is to define the calculation properties. Either default values or modified mesh sizes can be applied to analysis. Mesh size should be generated before conducting analysis. At last, the results could be viewed in result viewer. 4C inputs for mass concrete thermal analysis are listed in Table 9. Detailed information will be defined for different concrete structures later when actual analysis is preceded.

Table 9 Required Inputs information for 4C

Concrete volume	current size type and name			
	Placement temp.			
	Boundary condition:			
	Top:	temperature	wind velocity	shield definition
	Side:	temperature	wind velocity	shield definition
Concrete properties	**Concrete information** : slump, w/c ratio, air content, measured density, specific heat, thermal conductivity Act. Energy factor 1, Act. Energy factor 2 maturity vs. heat development data maturity vs. E-modulus maturity vs. poison ratio maturity vs. compressive strength maturity vs. tensile strength creep			

Concrete volume and boundary conditions could be obtained from data provided by the Iowa DOT. The formwork and top insulation method removal time may not be defined as the most effective interval, whereas it is based on the real construction conditions. Ambient temperature, wind velocity could be obtained from historical weather station from historical weather stations (Season Weather Averages). Most concrete properties could be found in thermal control plan provided by CTL Group. Specific heat and thermal conductivity inputs used the value from the literature survey. Maturity could be calculated based on the equations in Chapter 2, and then the relationship between maturity and other properties as inputs are plotted. Detailed procedure to get curvature parameters of these concrete properties will be explained in Chapter 5. Furthermore, calculation parameters can be varied in the program such as mesh sizes, and analysis period.

3.3 Prediction Model Used in 4C

General inputs of 4C program to perform thermal analysis have been discussed in the previous section. Fresh concrete properties of the concrete mix can be specified at the beginning of the mass concrete project. Usually, a pre-pour of the mix design is conducted, and temperature development is monitored. The relationship between maturity with heat development data, E-modulus, compressive strength, and tensile strength of concrete are important input parameters for 4C program. These parameters could either be obtained through testing or prediction models.

Maturity related equations are shown in Equation 1 and 2 in Chapter 2. Heat development data is generally measured from the heat of hydration process. Generally, a laboratory testing of heat hydration for a 2*2*2 inch cube should be conducted with the same mix design as the real project. The larger the testing size of sample is, the more accurate the heat development data collected will be. When heat development data is not available, the experienced model could be used as discussion in section 2.4.1. Compressive strength, tensile strength, elastic modulus and creep information could also be measured in the laboratory. Otherwise, many empirical models could be applied to calculate and plot above mechanical properties as discussed in section 2.4.2 to 2.4.6. Curvature parameters or developmental data of above information should be input in 4C computer program. The flow chart used to obtain

the required inputs for 4C program is shown in Figure 4. Examples of developing those inputs using the models will be illustrated in Chapter 5 when a specific case is mentioned.

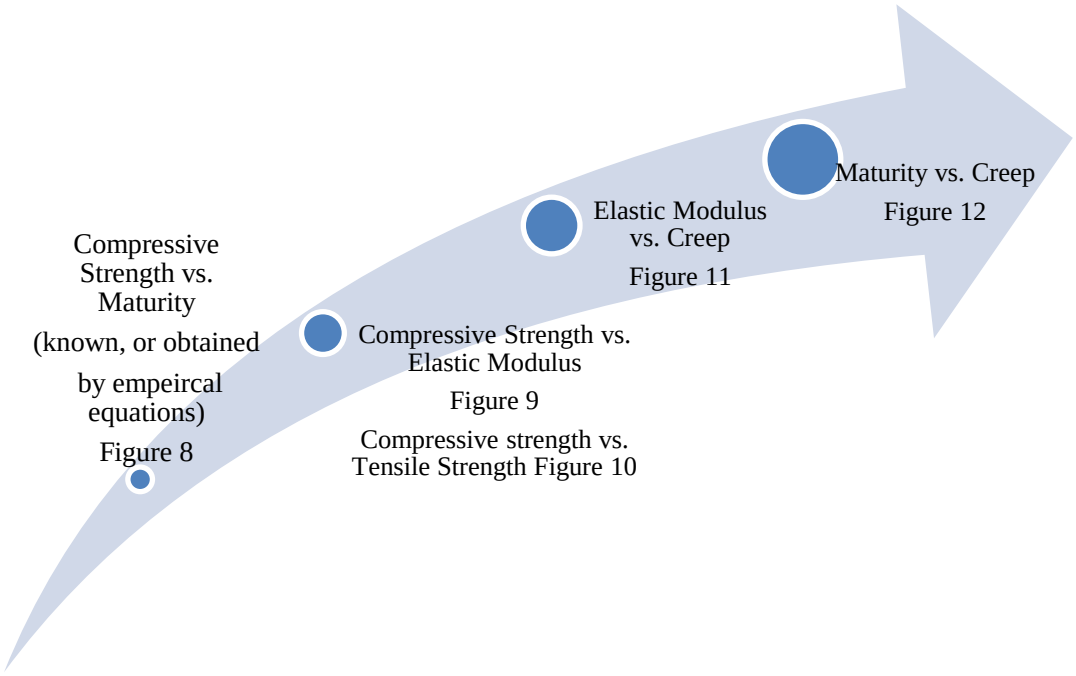

Figure 4 How to simulate several mechanical properties as inputs for 4C program

3.4 Advantages and Disadvantages of 4C Program

Compared to ConcreteWorks, another computer software package used in the first phase of DOT project, 4C-Temp&Stress has capacity to build databases for structures, concretes, formwork/insulation, and materials etc., but users can only choose established concrete database and geometry of concrete member in ConcreteWorks. 4C program has the other advantage of presenting more detailed temperature data. The comparison is shown in the Table 10.

In 4C program, the analysis at specific points could also be applied on maturity, strength and stress results demonstration. Not only multiple choices to exhibit analysis results along the time are available, showing iso-curves at a given time is also an advantage of 4C-Temp&Stress. An iso-curve is a curve along which the function has a constant value in the cross section of concrete structure. In ConcreteWorks, the temperature changes are only shown as animation, which is hard to get output results from. Most analysis results from 4C are accessible to output as "dat." format files. Furthermore, 4C also considers the effects of

cooling pipes or heating wires, which are not considered in ConcreteWorks. Users can define the cooling pipe/ heating wires used in the project and simulate thermal development more closely to the real construction.

Table 10 Temperature outputs comparison between 4C and Concreteworks computer program

Output Items	4C	ConcreteWorks
Max. temperature of the volume	x	x
Min. temperature of the volume	x	x
Max. temperature of specific point	x	
Min. temperature of specific point	x	
Max. temperature difference of the volume		x
Ambient temperature	x	x
Average temperature of the volume	x	
Average temperature of specific point	x	

In addition, 4C Temp&Stress software package is more effective in terms of calculation time than ConcreteWorks, and longer analysis period could be designed while ConcreteWorks could only consider 14days temperature prediction and 7 days cracking potential prediction.

The following points could be considered as the challenge for users of 4C-Temp&Stress.

- 4C software normally works in Windows XP environment, and might be compatible with Windows 7 with 32 bit but not 64 bit.
- Comparing both programs, ConcreteWorks is a free software and uses English units, which makes the program more applicable in the US states, while 4C is a commercial program with SI units only.
- In addition, 4C-Temp&Stress has more inputs that require users to be more knowledgeable to collect the information and make reasonable assumptions, while ConcreteWorks has many defaults and does not require so much information to input.

- The other shortage of 4C is exhibited when the volume of concrete becomes extremely large, generated meshes are finer or cement content is raised extremely high, the calculation could not be analyzed for very long period.
- Ambient temperature inputs are not flexible as well. It could only be assumed as sine-curve or constant while actual ambient temperature varies day by day, so that the prediction results might be different from actual measurements.
- Furthermore, cross-section results viewer can only be shown at the mid span along the longest edge of the concrete. No diagonal or other perpendicular cross section results can be estimated and presented.

CHAPTER 4 METHODOLOGY

I-80 Bridge project and 4C program are selected for the following study. WB I-80 Missouri River Bridge mass concrete construction data was collected by construction contractor: Jensen's Company and Cramer, at the beginning of the research. The information about mass concrete structure dimensions, construction environment, and monitored temperature development data were obtained from the Iowa DOT. More information including, mix design, insulation method; sensor location could be obtained from literatures, thermal control plan for the bridge project and interviews. This chapter will discuss the study approaches by utilizing 4C computer program. Section 4.1 briefly discusses the original data collected from the Iowa DOT and several interviews with experienced construction inspectors or contractors. Study plan on how to apply 4C program to do sensitivity study and case study are discussed in section 4.2.

4.1 Data Collection & Interviews

This section discusses collected excel data from the Iowa DOT including temperature data, estimated compressive strength for each concrete structure, and information obtained from thermal control plan and interviews, which provided more facts related to mass concrete construction. Then a proper input for 4C program was developed for the following study.

4.1.1 General Project Information

In order to analyze mass concrete thermal behavior using computer program, Data is collected from West Bound I-80 Bridge mass concrete construction by the Iowa DOT. This bridge was completed over the Missouri River at Council Bluffs, Pottawattamie County, Iowa. Bridge plans and thermal control plans are provided by the Iowa DOT. Bridge plans outline the dimension of concrete members and construction layout of each pier. Thermal control plans are majorly provided by CTL Group, which indicate the recommendation for mix design, sensor location and thermal control procedures. Two construction companies were involved in this project, Cramer &Associate, Inc. and Jensen Construction Company. Jensen hired CTL Group to provide thermal control plan for precast concrete and followed

the provided recommendations. Recommended temperature difference limit to compressive strength for the applied mix design is shown in Figure 5 below. Table 11 below describes the thermal control plan difference from two companies.

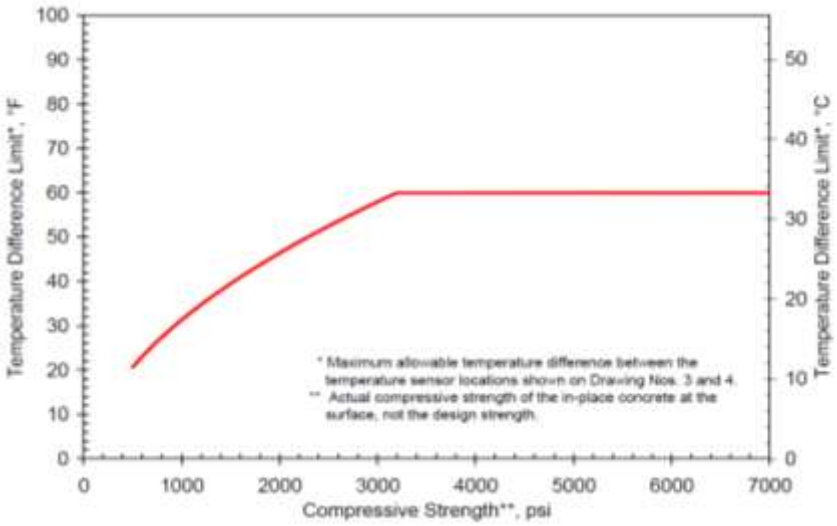

Figure 5 Temperature difference limit for the applied mix design from Jensen's thermal control Plan (for footings of Piers 3, 5, 7, 8 and 9)

Table 11 Comparison between thermal control plan from Cramer & Associate, Inc. and Jensen Construction Company

Thermal Control Plan	Cramer	Jensen
Specific concrete structures	Pier 1,2,and 4 footing	Pier 3,5,7,9 footing
Maximum temperature limits	160°F	160°F
Placement concrete temperature	45-85°F	maximum 85°F
Maximum temperature difference	less than60F	see Figure 7
Insulation method	Insulating blanket for top surface R-2.5 formwork on side	recommended to use plastic sheeting on top recommended to use extruded polystyrene board insulation covered by plywood for formwork
	two sensors in the center two sensors at mid-point of the side exterior surface with min. 2 in cover.	two sensors in the center(one primary and one backup) two sensors at mid-point of the side exterior surface at the depth of rebar

Sensor	two sensors at mid-point of the top exterior surface with min. 2 in cover two sensors to monitor the air temperature	two sensors at mid-point of the top exterior surface at the depth of rebar two sensors to monitor air temperature two sensor to monitor water temperature
Cooling pipe	3/4" PVC Placed 3 feet on center in the middle of the footing	3/4" PVC assumed 2 1/4*3ft or 2 1/2*3ft see layout drawing in Appendix B

The Ready Mixed Concrete Co.'s "IOWA MASS CONCRETE w/Slag" concrete was approved for use in this project shown in Table 12. Available concrete properties include: the pretested 7-day compressive strength of the cylinders was 5230 psi in average, tensile strength is 580 psi, and elastic modulus is 4.27 $*10^6$ psi. Measured coefficient of thermal expansion is $4.1*10^6$/°F.

Table 12 Concrete mix design for I-80 Bridge project

Description	Weight(lb/cubic yard)	Volume
Cement, IPF	420	2.28
Slab GGBFS	207	1.13
water(263#)	w/c ratio 0.42	4.21
#557 Limestone	1586	9.70
Air Content	1322	793.00
Water Reducer	6.5	1.75
High Range Water Reducer	3oz 100#	0.00
	4-8oz 100#	0.00
		27.00

The collected structures information includes general construction conditions, temperature development after concrete placed until formwork removed, and estimated in-place compressive strength at surface sensor. A total of 26 concrete structures from the project were recorded containing: footings from pier 1 to pier 6 and pier 8, columns from pier 1 to pier 7 and pier 10, stems from pier 1 to pier 5, pier 7 and pier 9. Furthermore, caps from pier 1 to 5 were provided. Collected concrete members also can be classified as mass

concrete member with cooling pipes, and mass concrete structures without cooling pipes. The recommended cooling pipe layouts for I-80 project by CTL group are shown in Appendix B. The least dimension, which is defined as depth of concrete, is less than 5 feet for Pier 1 footing as 4.5ft, thus the structure may not be considered as mass concrete. A summary of collected items are listed in Table 13.

Table 13 Concrete members from collected data

Pier No.	Type	Cooling Pipes	Size(ft)	Date Cast	Notes
1	Footings	no	43*15*5	10/20/2008 1pm	
2	Footings	no	43*27*7.25	10/30/2008/15:30pm	
3	Footings	no	43*15*5	11/19/2008/15:30pm	
4	Footings	no	43*19*6.5	11/4/2008/6:30pm	
5	Footings	no	46*18*5.75	2/3/2009 5pm	
6	Footings	no	43*25*6.75	11/4/2008 7am	• ft*ft*ft-length*width*thickness of structure
8	Footings	yes	77*39.6*10.5	12/30/2008	
1	Columns	no	4	12/4/2008	
2	Columns	no	5	2/18/2009	
3	Columns	no	6	1/23/2009	
4	Columns	no	5	3/5/2009	
5	Columns	no	5	3/31/2009	
6	Columns	no	8.33	1/6/2009	
7	Columns	yes	7	10/15/2008	
10	Columns	no	8.33	5/21/2009	
1	Stems	no	39*4*7	12/4/2008	• ft-least dimension of the structure
2	Stems	no	38*5*19	1/9/2009	
3	Stems	no	38*6*16	11/21/2008	
4	Stems	no	38*5*18	12/10/2008	
5	Stems	no	38*5*20	2/17/2009	
7	Stems	yes	38*7*35	9/3/2008	
9	Stems	yes	46*9*34	6/30/2009	
1	Caps	no	4	1/23/2009	
2	Caps	no	5	3/20/2009	
3	Caps	no	6	2/25/2009	
4	Caps	no	5	3/20/2009	
5	Caps	no	5	5/5/2009	

4.1.2 Data Collection from Interviews

Interviews of several inspectors and contractors provided more practical information of mass concrete construction that was helpful on making assumptions in the research. The persons interviewed include: Jeremy Purvis, who was a quality control supervisor, who had worked working on mass concrete construction, Jason Cole, who was the inspector of I-80 Bridge, and Dan Timmons, vice president of Jensen Road Company. The major conclusions from interviews are discussed below. In mass concrete construction, the top surface is generally covered by plastic sheeting and using wet curing blanket could reduce the temperature difference. However, wet curing shall be limited to a certain condition. Excessive application of wet curing is not economical. Wood or steel formwork is generally used only on side surfaces, and the forms are generally removed 5-7 days after the casting of massive structures. Sometimes, forms are not moved until they are not required any more. The temperature limit is generally consistent as thermal control plans. 85°F placement temperature limit, 160°F maximum temperature limit, and 35°F maximum temperature difference limit are recommended. Cooling pipes are generally installed for massive bridge foundation pours because the water source is convenient. However, cooling pipes are not always applied even if they are installed. The applications of cooling pipes are based on monitored temperature on site. Recently, CTL Group recommends cooling pipes must be run if they are installed. Running water through cooling pipes after excessive heat is observed may lead to thermal shock and crack in side of concrete.

4.2 Study Plan to Use 4C Program

One of the purposes of the study is to better understand the effects of concrete properties, construction practice, and environmental conditions based on computer software analysis results. Then, apply the findings to real mass concrete projects. In order to achieve the purpose, three main studies are conducted, including computer program verification, sensitivity study, and case study. The flow chart of how 4C program works is shown in Figure 6.

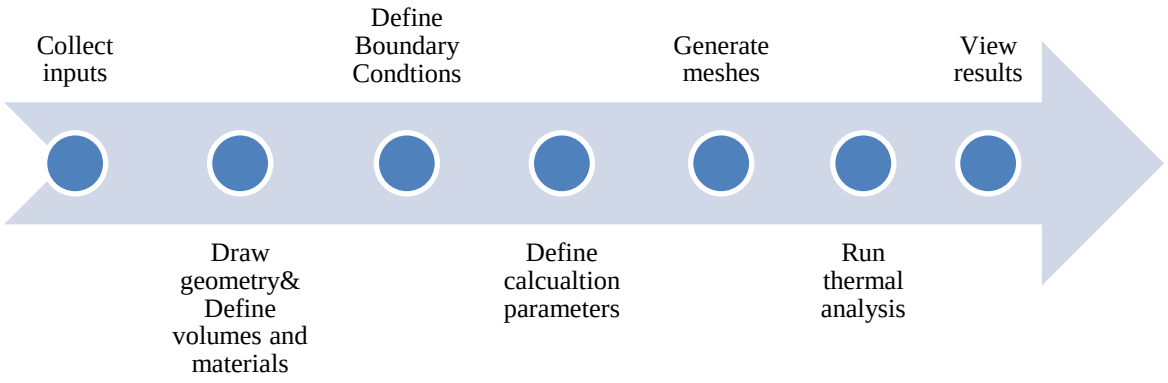

Figure 6 How 4C program perform analysis

The process of the study is discussed as following. Literature review on mass concrete, related concrete properties, and related computer programs are studied at the beginning of the study. As a result, 4C program was selected to predict mass concrete thermal behavior and cracking potential. In order to get accurate computer simulation results, inputs of the computer program should be studied before using it in practice. Data is collected and interviews are accomplished to make practical assumptions prior to computer calculation. Afterwards, available information is used to predict thermal behavior of mass concrete at the early age. The applicability of 4C program is verified using analyzed I-80 Bridge data. Sensitivity study and case study are conducted after verification of computer program. Based on the studies, better mass concrete construction conditions will be understood, and thermal control recommendations will be made for field practices.

Since several inputs for 4C program are simulated, verification of program analysis should be conducted before conducting further study. The verification will be discussed in Chapter 5. First, pier 1 to 8 footing are drawn and analyzed in 4C program based on collected data and discussed assumptions. Temperature development data and stress/strength ratio are obtained. The temperature results are plotted as the relationship between time and temperature development including maximum temperature at center, minimum temperature

at top or side surface, and calculated temperature difference. In order to predict thermal cracking potential, tensile stress/strength ratio is the major result. Then, compare 4C temperature outputs with collected data to verify the accuracy of the computer program. Statistic method is used for verification. 30 or 50 data points are chosen for each pier from computer output and collected results. Each data pair includes actual measurement and 4C predicted values at a specific time. Sensitivity study is developed after verified of 4C program.

Sensitivity studies are designed to predict the effects of concrete properties, construction procedures and environment impact. The sensitivity study is conducted considering various parameters such as cooling pipe installation, placement temperature, and thermal properties of aggregate, which will be detailed introduced in Chapter 6. A series of sensitivity studies are conducted for two baselines, pier 1 footing and pier 3 footing. For pier 1 footing, the effect of substructure material used soil and concrete. Since the least dimension of pier 1 footing is 4.5 ft, which is less than 5 ft and not classified as mass concrete structure, pier 3 footing was designed for additional set of sensitivity study. Pier 3 footing's sensitivity study uses soil as substructure for baseline. Detailed cooling pipe sensitivity study are analyzed including layout of cooling pipes, diameter of cooling pipes and water temperature. Some conclusions could be obtained from sensitivity study, which could be used as recommendations for mass concrete construction.

To apply the computer program to real mass concrete construction, further case studies are analyzed in Chapter 7. First, I-80 Bridge footings, columns, stems, and caps are computed. The relationship of maximum temperature difference and stress/strength ratio are discussed. Recommendations will be provided based on this study. Furthermore, example footings analyses of US 34 Bridge project are performed. US 34 Bridge is constructed over Missouri River on US 34, and is located at Glenwood, Iowa. The flow chart of research progress is shown in Figure 7.

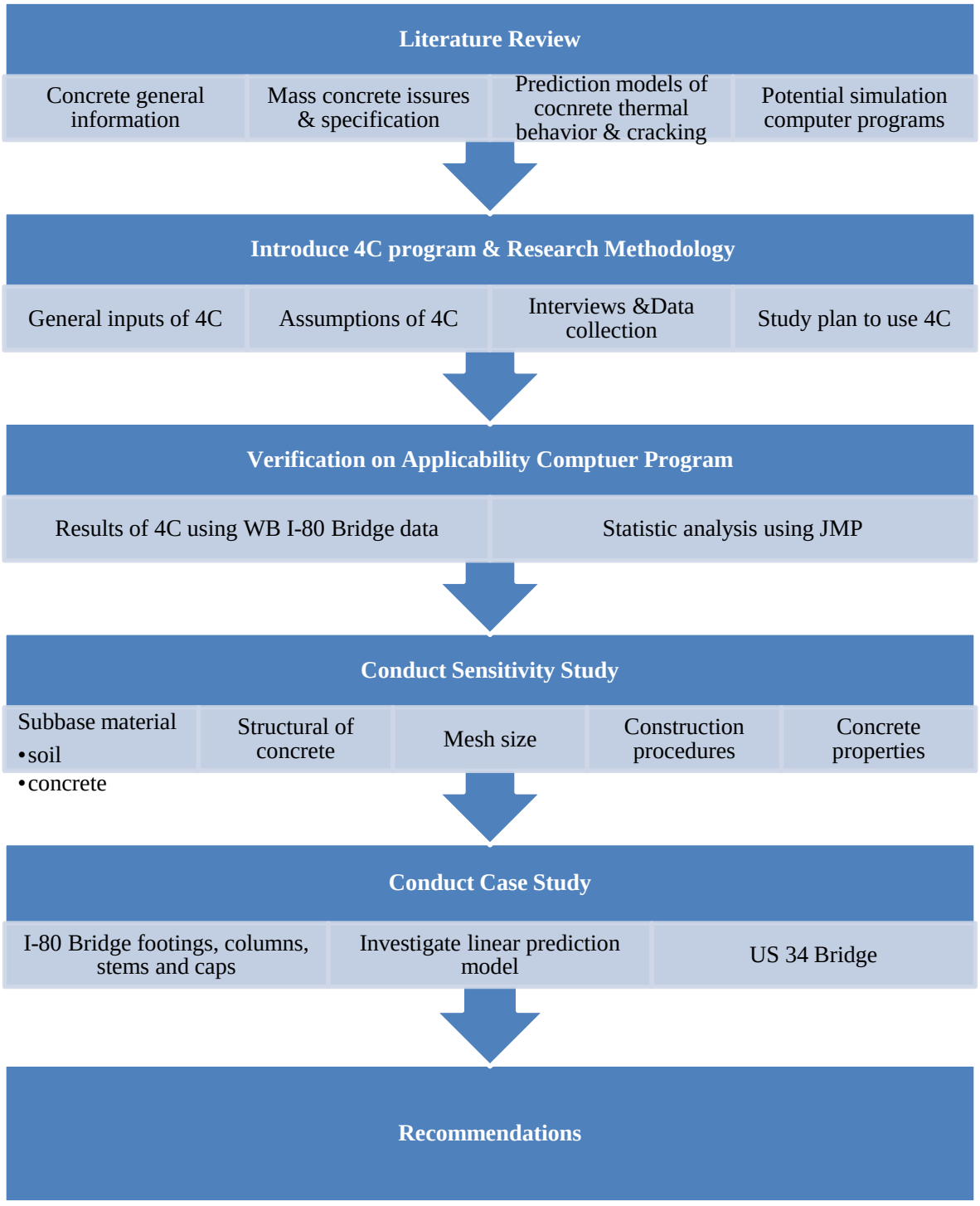

Figure 7 Study Plan for the research on mass concrete thermal behavior

CHAPTER 5 4C PROGRAM VERIFICATION

In this chapter, the model developed inputs for 4C program are illustrated in section 5.1 based on the discussion in literature review and 4C prediction models in section 3.3. Verification of the program is accomplished by comparing difference between actual measured (CTL) and 4C predicted (4C) values, including maximum temperature, and temperature difference. Detailed comparison is illustrated in section 5.2.

5.1 4C Examples of Inputs from Prediction Model

The concrete inputs of compressive strength, elastic modulus, creep, and tensile strength are required before conducting 4C analysis. During I-80 Bridge construction, temperature development, and estimated compressive strength development data were collected. The compressive strength development was estimated based on lab tests by CTL Group. The maturity was information collected by contractor. Since the research didn't perform additional lab tests to obtain other required inputs, simulation is used to get heat development data by measured temperature during the construction period. The inputs for heat development of concrete structures is developed by changing the curvature parameters until the temperature results is close to collected measured data. Temperature development is simulated based on pier 1 footing for no cooling pipe condition, and pier 8 footing for cooling pipe installed condition. The maturity and compressive strength information was estimated by CTL Group, which contained two groups of values, one was at the top, and another was at the side of the concrete member. The averaged value between top and side are finally used as 4C input. With known maturity and compressive strength, tensile strength development, elastic modulus development, and creep development can be derived using prediction models. Detailed procedures are discussed below along with figures.

Based on collected data, relationship between compressive strength and maturity could be obtained as shown in Figure 8. Elastic modulus development can be obtained based on Equation 21, which is an experienced prediction model for Iowa concrete. The relationship is developed as compressive strength to elastic modulus shown in Figure 9. Tensile Strength development could be obtained based on Equation 26 plotted as Figure 10.

Predicted results for creep based on elastic modulus are shown in Figure 11 using Equation 34 to 37.

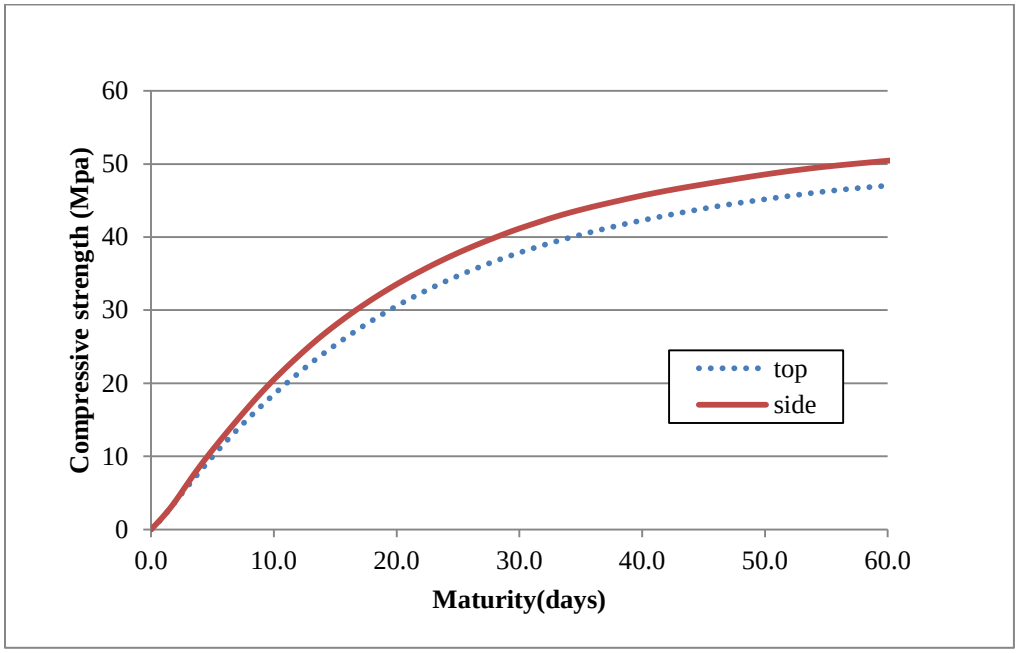

Figure 8 Pier 8 footing's maturity and compressive strength relationship

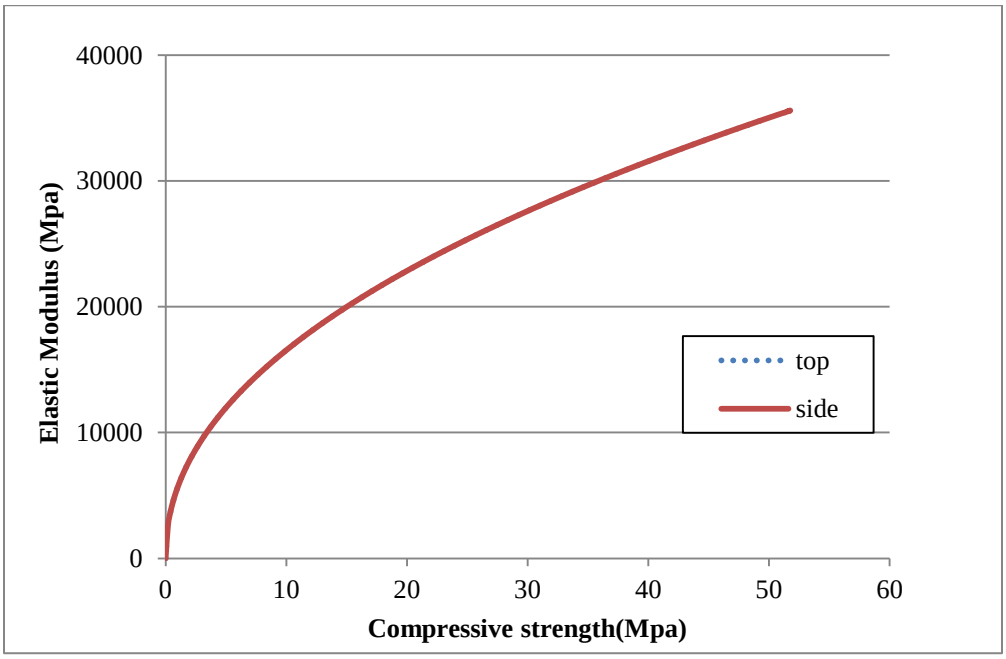

Figure 9 Pier 8 footing's compressive strength and elastic modulus relationship ("top" and "side" data is coincident)

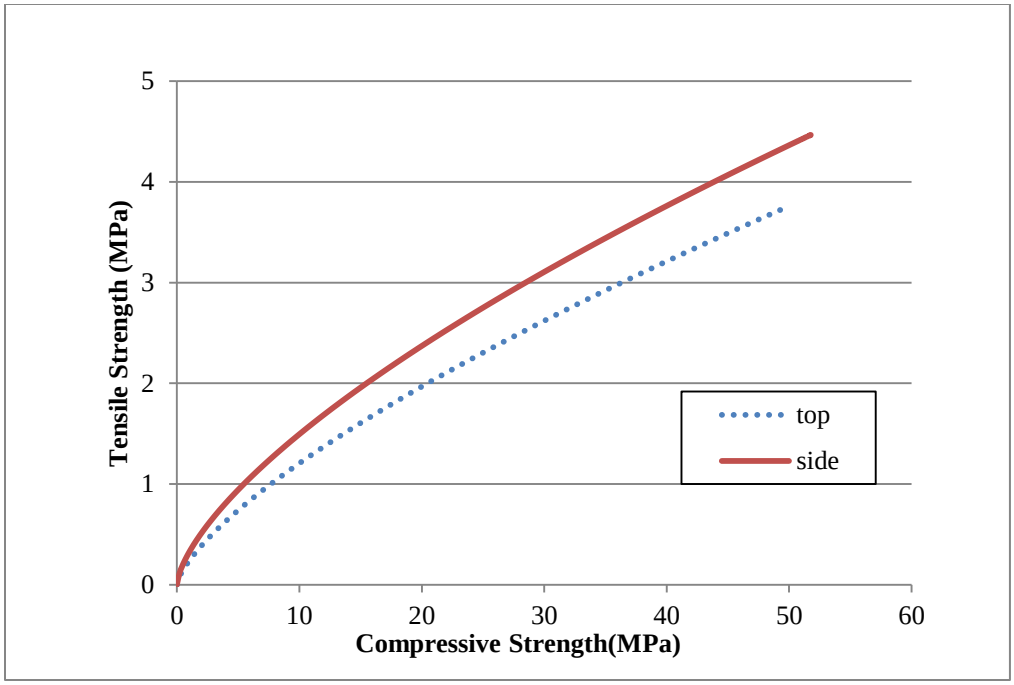

Figure 10 Pier 8 footing's compressive strength and tensile strength relationship

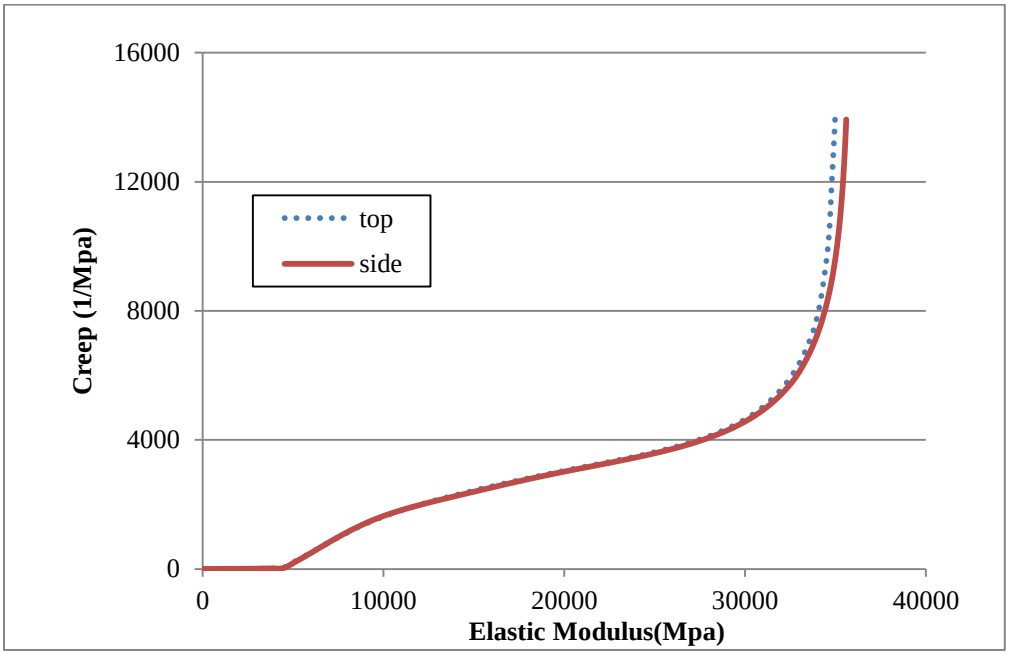

Figure 11 Pier 8 footing's elastic modulus and creep relationship

With the development data for mechanical concrete properties, the relationships among each factor to maturity are shown Figure 12 to Figure 14 to simulate the curve in 4C program, which are achieved by changing curvature parameters.

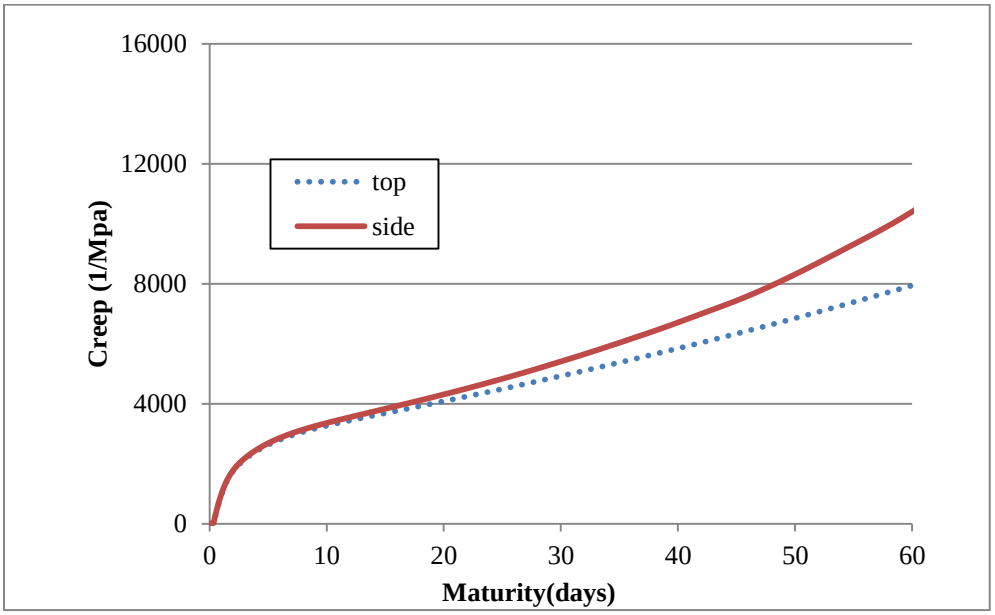

Figure 12 Pier 8 footing's maturity and creep relationship

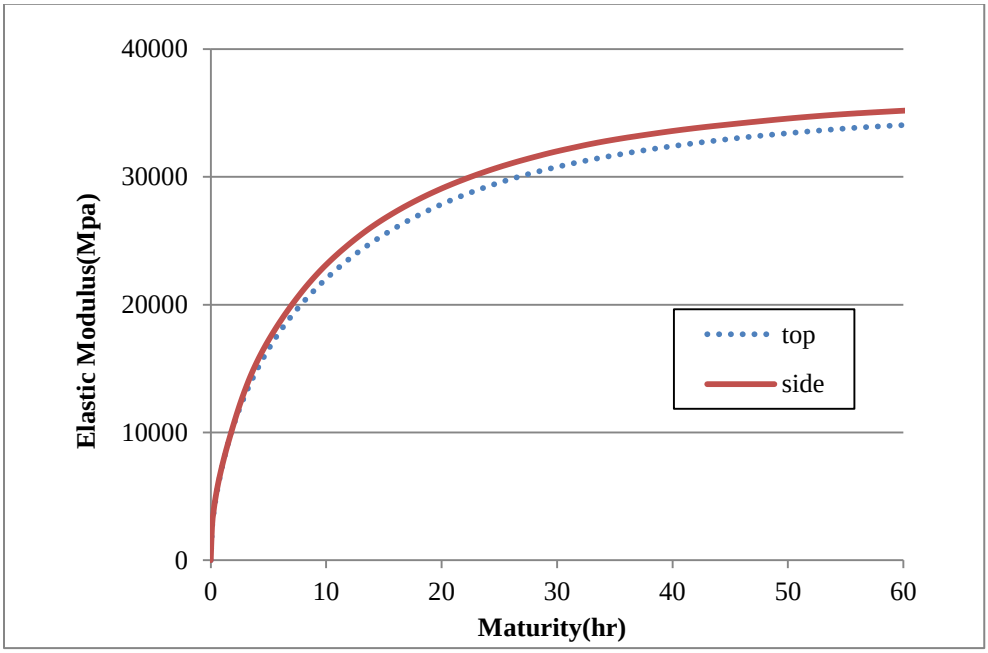

Figure 13 Pier 8 footing's maturity and elastic modulus relationship

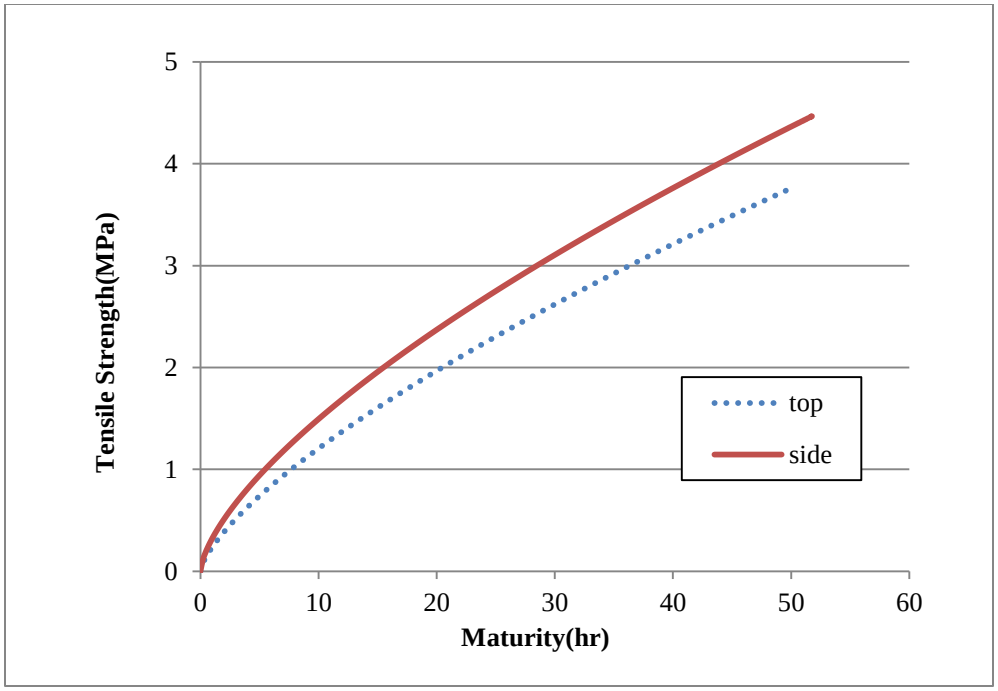

Figure 14 Pier 8 footing's maturity and tensile strength relationship

Using similar methods, concrete curvature parameters for structures with cooling pipes can be simulated as well. A summary of the 4C inputs including concrete geometry, boundary conditions, concrete properties are listed in the Table 14 below.

Table 14 4C program inputs summary for I-80 Missouri River Bridge analyses

Description	Input Value	Notes
Concrete Volume		
Current size type and name	Varies	Obtained from data collection
Placement temp.	Varies	Obtained from data collection
Boundary Condition		
Top: temperature	Average ambient temp.	Obtained from data collection
Wind velocity	Obtained from weather station	Obtained from data collection
Shield definition	Plastic foil/ 5 mm air foam, duration	Obtained from data collection
SIDE: temperature	Average ambient temp.	Obtained from data collection

Wind velocity	Obtained from weather station	Obtained from data collection
Shield definition	Plywood formwork, interval	Obtained from data collection
Concrete Properties		
Slump	101mm	Obtained from data collection
W/c ratio	0.42	Obtained from data collection
Air content	6.50%	Obtained from data collection
Measured density	2320Kg/m^3	Obtained from data collection
Specific heat	0.84Kj/kg/°c	Obtained from data collection
Thermal conductivity	13	Obtained from data collection
Act. Energy factor 1	33500 J/mol	Default in 4c program
Act. Energy factor 2	1470 J/mol/°c	Default in 4c program
Material Properties		
Maturity vs. Heat development data	W/o cpipes: total:650 KJj/Kg, time :28h, curvature: 0.7 W/ cpipes: total:490 KJ/Kg, time :28h, curvature: 0.7	Based on temp. Development data from collected data
Maturity vs. E-modulus	Total:40000 Mpa, time :15h, curvature: 0.8 cementitious material	Based on model prediction
Maturity vs. Poison ratio	Total: 0.17, time: 22.4 hr, curvature :1, fresh: 0.34	Default value in computer program
CW'S default value	0.00000736 /c	Obtained from data collection
Maturity vs. Compressive strength	Total:50Mpa, time :70h, curvature: 0.7	Based on estimated compressive strength data from collected data
Maturity vs. Tensile strength	Total:4.5Mpa, time :70h, curvature: 0.41	Based on model prediction
Creep		Based on model prediction

Concrete database for I-80 Bridge mass concrete simulation could be established based on above information. Concrete volume in 4C program is drawn afterwards as shown in bridge plans. Verification of the computer programs will be discussed in section 5.2.

5.2 Verification of 4C Computer Program

Several inputs for 4C program are based on the literature review or prediction equations. The accuracy of the analyzed results should be studied before using this program to conduct further study. Concrete members from I-80 Bridge are used for comparison between collected temperature data and predicted temperature data. In verification, 6 footings, 7 stems, 5 caps and 7 columns are selected to compare by visualized temperature plot with time as x axis and used to do statistical comparison as well. Examples of visualized comparison for pier 1 footing are shown in Figure 15 and Figure 16. More comparison figures of maximum temperature will be shown in Appendix C. Pier 8 footing uses new heat development data for concrete structure using cooling pipes, which also produce similar temperature difference results as pier 1 footing. Generally, CTL and 4C present close maximum temperature values, while 4C predictions decrease faster.

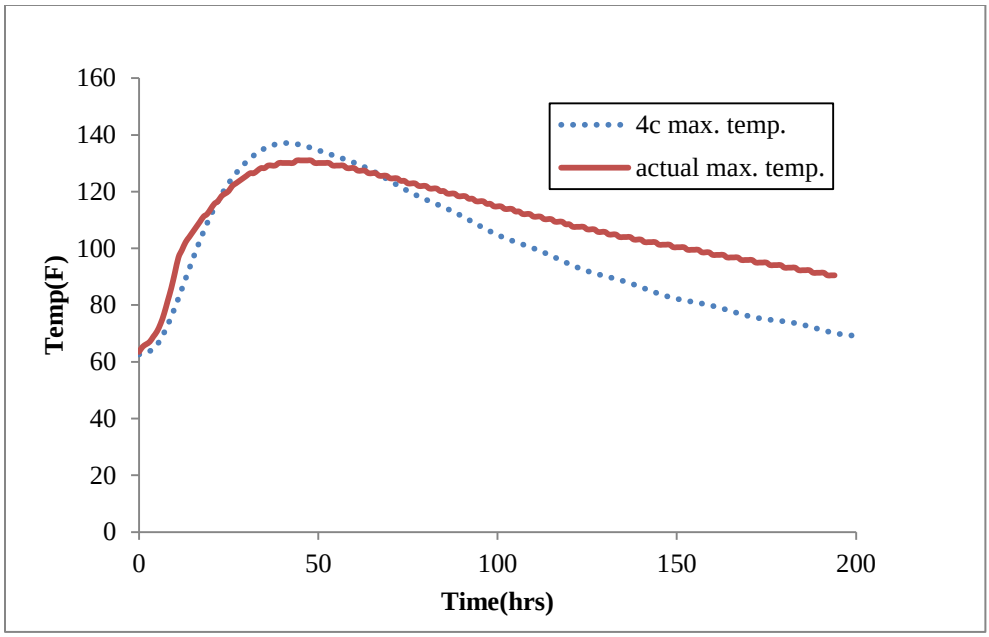

Figure 15 Maximum temperature development for pier 1 footing comparison between measured (actual) and predicted (4C)

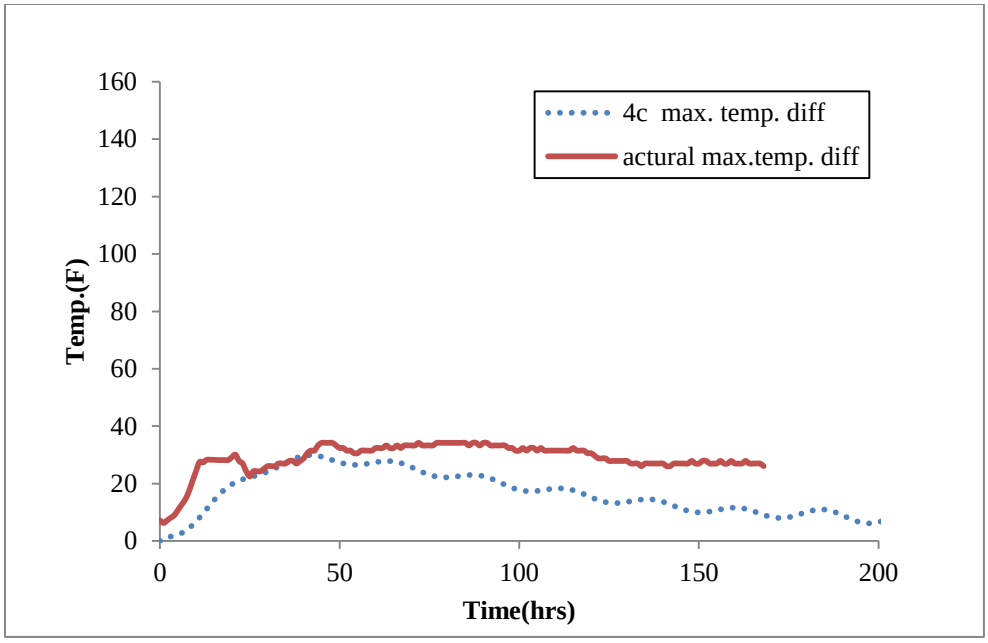

Figure 16 Maximum temperature difference development for pier 1 footing comparison between measured (actual) and predicted (4C)

Figure 17 to Figure 18 present linear equality analysis results of concrete members without cooling pipes to compare measured and predicted results at all chosen time. Concrete structures used to analyze are No.1 to 6 pier footings, No.1 to 7 and 10 pier columns, No. 1 to 5, 7, and 9 pier stems, and No. 1 to 5 pier caps, total 26 concrete members. 30 recorded maximum temperatures and maximum temperature difference are selected as 30 data sets for each concrete member from CTL measurements and 4C predictions, which reflects the temperature development for mass concrete structure. The time of data set for each structure is selected every three hours. The points on the straight line of equality represent CTL and 4C values are identical. Figure 17 describes 26 data set collected for peak temperatures of all concrete members. The predicted data is close to line equality with R^2 value of 0.89. However, the prediction has the trend to underestimate maximum temperature.

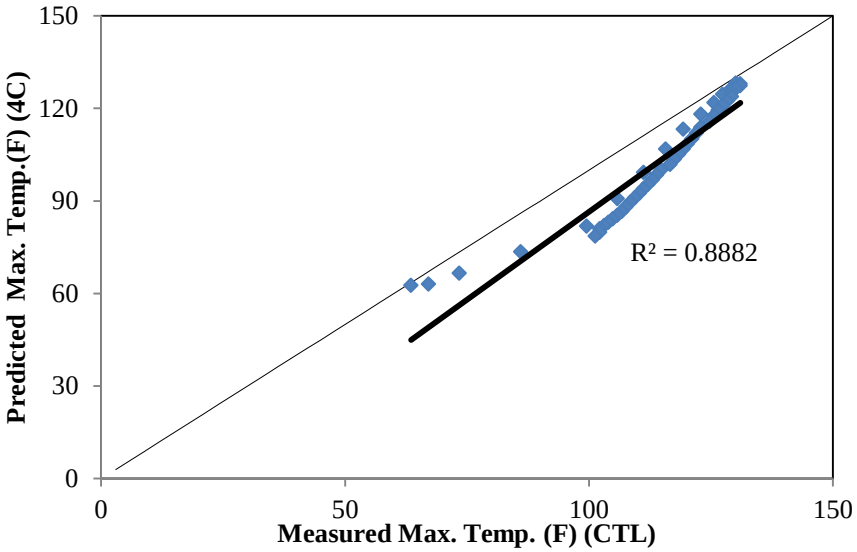

Figure 17 Line of equality analysis for CTL and 4C maximum temperature results for 26 concrete members

Figure 18 shows maximum temperature of all concrete members' results at all chosen times, in the total of 780 data points. The figure indicates the data are arranged close to line of equality with R^2 value of 0.4851, which shows the maximum temperature predicted values are acceptable. Figure 19 indicates maximum temperature difference predictions are not recommended for use with scattered plot data and low R^2 value of 0.29.

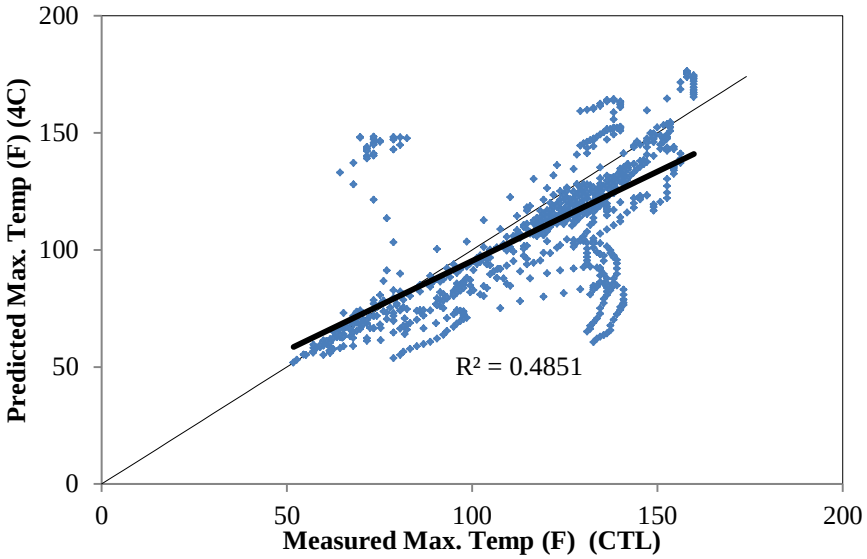

Figure 18 Line of equality analysis for CTL and 4C maximum temperature results

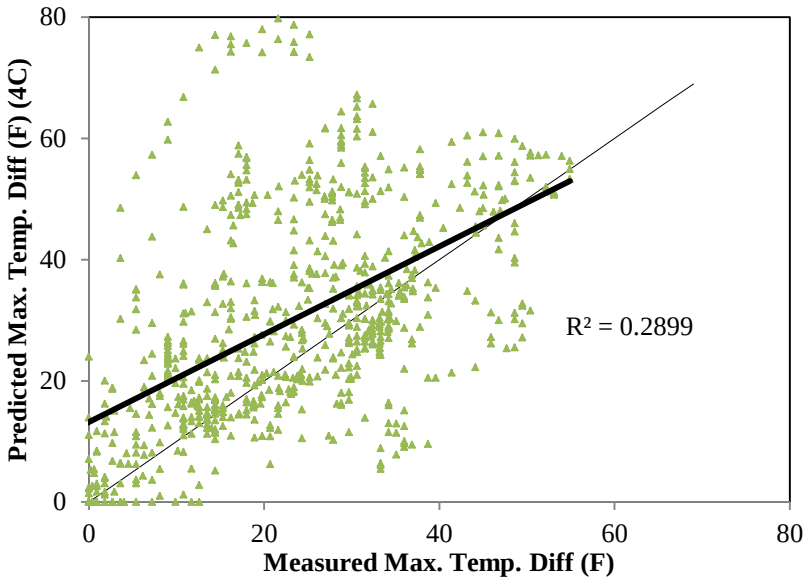

Figure 19 Line of equality analysis for discrepancy of maximum temperature difference prediction results

In order to better understand the prediction results of the 4C program, a statistical evaluation of discrepancy between actual measurements and 4C prediction is conducted. In the statistical analysis, the discrepancy in maximum temperature and maximum temperature difference are calculated and analyzed as shown in Figure 20 to Figure 24. The distributions of the discrepancy values for 26 concrete structures at different time points are displayed as side-by-side box plots in Figure 20 and 21. The values on the x-axis represent the time points as illustrated in Table 14. Positive values on the y axis mean measured values are larger than predicted values, and negative values mean measured values are smaller than predicted values. For example, time point No.1 presents temperature at 0 hours after placement and time point No. 2 presents temperature at 3 hours after placement etc.

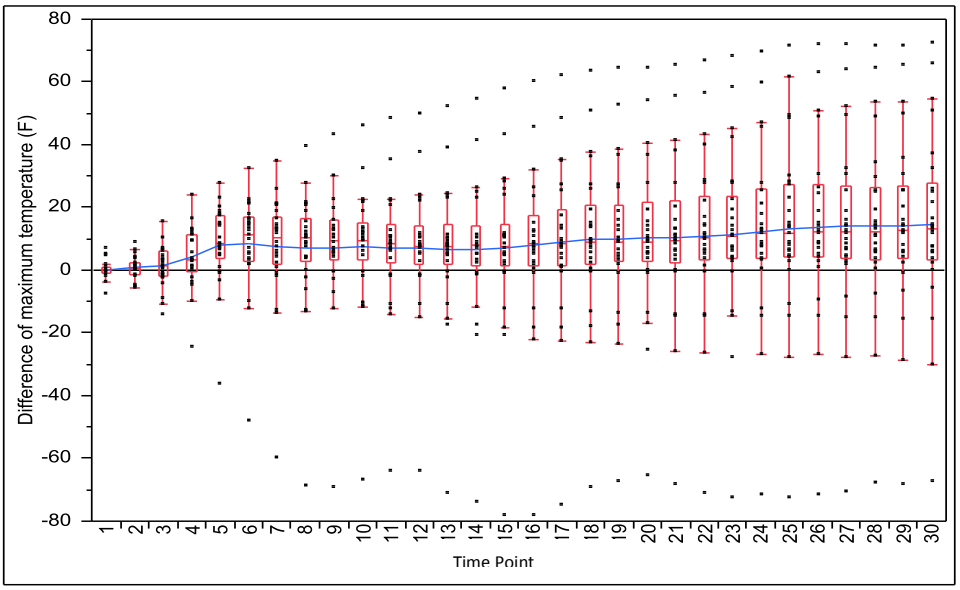

Figure 20 Box Plot and Connected mean for discrepancy between measured and predicted maximum temperature

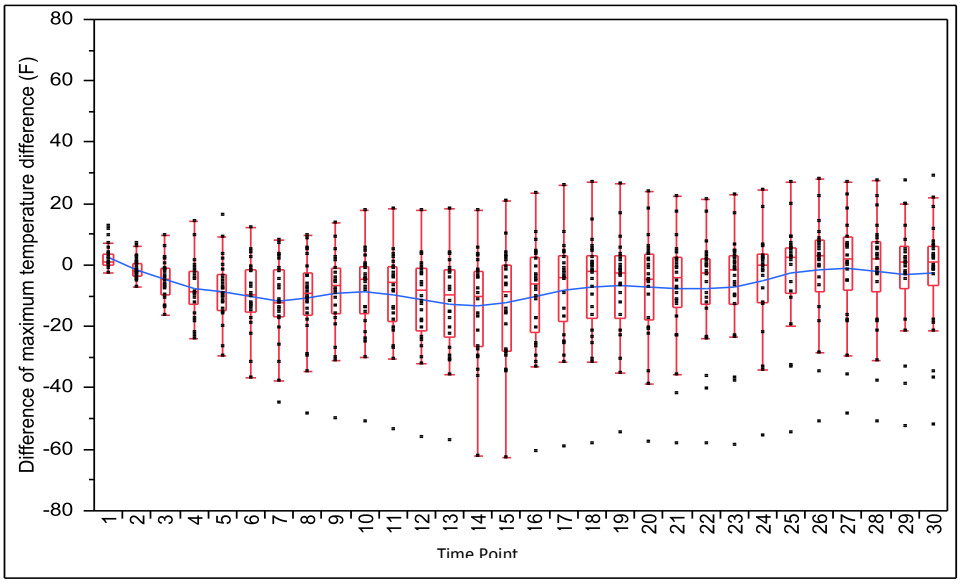

Figure 21 Box Plot and Connected mean for discrepancy between measured and predicted maximum temperature difference

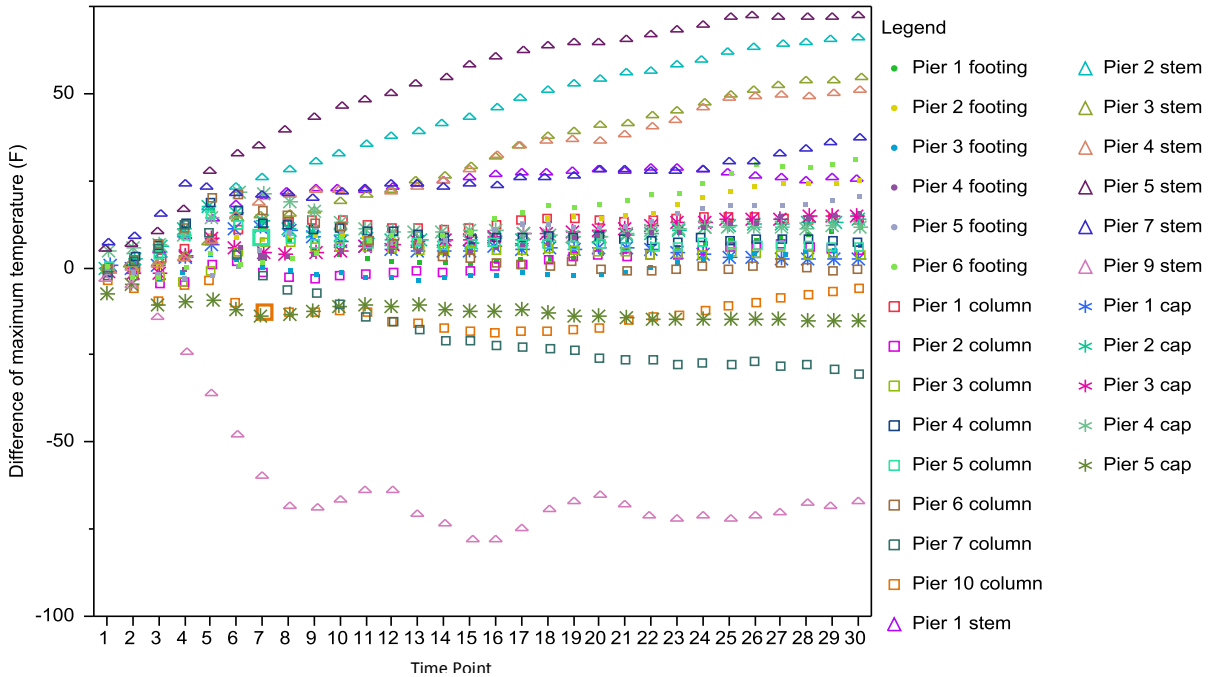

Figure 22 Discrepancy of maximum temperature between measured and predicted vs. Time interval with different types of concrete structure

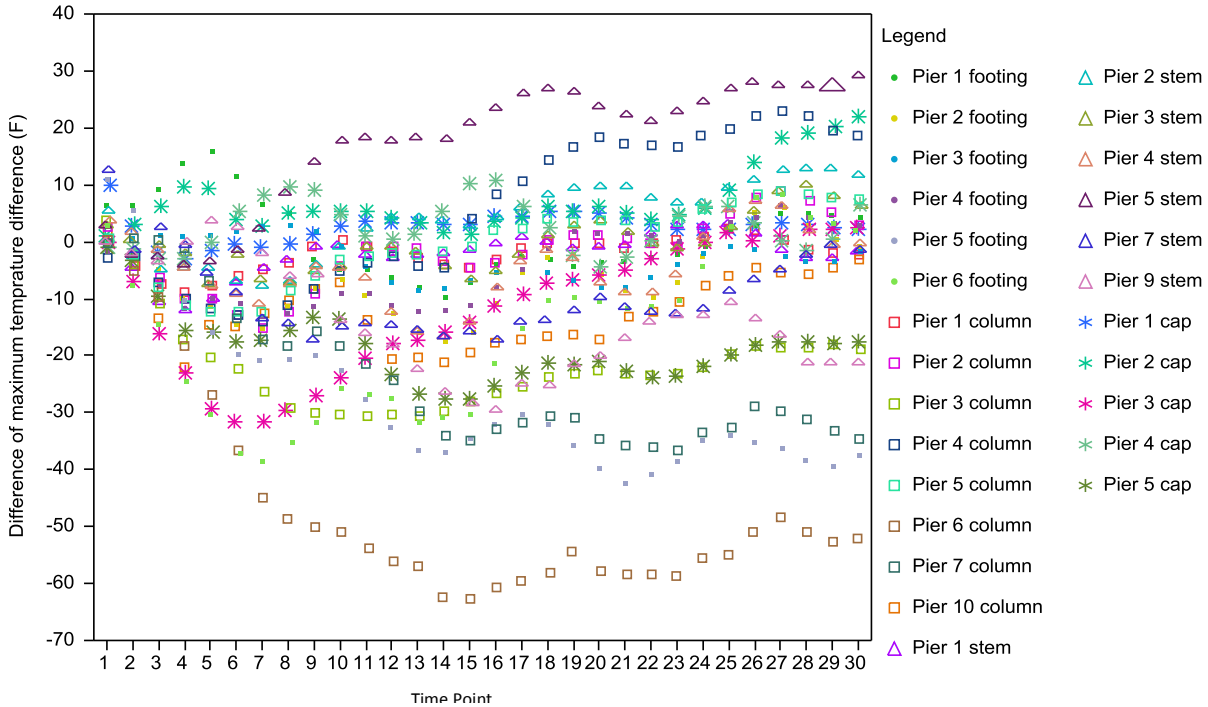

Figure 23 Discrepancy of maximum temperature difference between measured and predicted vs. Time interval with different types of concrete structure

Table 15 X- axis representation of Figure 20 to Figure 23

Time Point	Represent hours	Represent Concrete structure
1	0	footing 1
2	3	footing 2
3	6	footing 3
4	9	footing 4
5	12	footing 5
6	15	footing 6
7	18	column 1
8	21	column 2
9	24	column 3
10	27	column 4
11	30	column 5
12	33	column 6
13	36	column 7
14	39	column 10
15	42	stem 1
16	45	stem 2
17	48	stem 3
18	51	stem 4
19	54	stem 5
20	57	stem 7
21	60	stem 9
22	63	cap 1
23	66	cap 2
24	69	cap 3
25	72	cap 4
26	75	cap 5
27	78	
28	81	
29	84	
30	87	
50	187	

The box plots of prediction discrepancy for maximum temperature and maximum temperature difference are presented in Figure 20 and Figure 21. The connected means are shown as the blue line in the figures. The average means for the prediction discrepancy are about 10°F for maximum temperature and -15°F for maximum temperature difference. Comparing interquartile ranges of the box plots, the spread of the maximum temperature distributions increases. The prediction of maximum temperature differences have the largest interquartile ranges during time point 13 to 16, described as the time between 39 hours to 48 hours. This indicates relative low prediction accuracy during this period. These box plots also indicate that outliers may exist because those points appear in the tails of the distribution. These potential outliers can be identified as pier 2 stem, pier 4 stem and pier 9 stem. Left skewness is the most common attribute of these data distributions seen in the box plots in these figures, which implies that predictions more likely underestimate the observed values.

Three concrete members display a maximum discrepancy larger than 60°F for maximum temperature. The connected mean of the discrepancies is larger than zero in Figure 20 and smaller than zero in Figure 21, then 4C predictions overestimate maximum temperature development and underestimate maximum temperature difference, respectively. Additional figures of Figure 22 and Figure 23 indicate the discrepancies more directly for different structure types. In Figure 22, the stem structures display low prediction accuracy, thus 4C program may not be recommended on thermal analysis for stem structures. Figure 23 also indicates pier 6 column may be an outlier, because it has a maximum discrepancy larger than 45°F for maximum temperature difference. The mean of the prediction discrepancy for maximum temperature is 10°F with lower and upper 95% confidence intervals of -8.587°F and 23.483°F, when standard error is 4.4307. Means of discrepancy for maximum temperature difference at specific analysis time are between -15°F to 5°F.The lower and upper 95% confidence intervals are -19.31°F and 9.407°F, when large standard error is 2.9993.

Some of very large discrepancy between CTL and 4C are very large might due to neglecting effects of ambient temperature variance, concrete shape and dimensions, and some other random difference of field construction. Constant maximum and minimum ambient temperatures for several days are assumed while ambient temperature varied day by

day in measurements. Also the discrepancy may be caused by heat development model inside the program. The predicted maximum temperatures drop faster after 70 hours than measurements in most cases. In addition, the influence of precast foundation member is not considered in the case studies, which exists in actual construction field. For example, the late heat development of columns after 25 days has impact on the heat development of the newly poured stems above it. The most important factor in terms of the discrepancy of maximum temperature differences is because the actual sensor locations are not at recommended place. Construction variances may lead the analysis results have large prediction errors, such as vibration of concrete during construction and deeper rebar locations.

Different organization of data set will results in different statistic results. Compare the CTL and 4C maximum temperature based on different concrete types as footing, columns, stems and caps separately. Each member will have 30 or 50 data point as discussed above. Box plots along with statistic summary are shown in Appendix C.4-C.7. The extreme large discrepancies are more likely to occur for stems. 4C perfections on footings and columns produce relatively smaller maximum temperature discrepancy to actual measured maximum temperature. Caps have lowest error, +/- 13°F with 95% confidence interval. Columns and footings produced around +/-20°F error between CTL and 4C. The average mean of each stem analysis are all exceed 20°F, with 50°F error. No matter how the data sets are assigned R^2 values over than 0.6 are presented in all cases, which considered as high significance forecast error (Peter M. F., David H.). This analysis also indicates that when predicted models at different time are ignored, the errors might increase.

During peak maximum temperature, the thermal stress may approach the largest range, and create high thermal cracking potential. Additional verifications on several time intervals where peak maximum temperature occurs are conducted as Table 15 to Table 16 shown. During 24 hours to 72 hours, the peak temperature is reached, which is the important period for engineers to consider thermal control, in order to avoid thermal cracking. T-test and Welch test are performed on prediction error to test equal mean and equal variance. Equal mean represents the predictions and actual measurements are equal. The researcher ignored stems prediction results, use 19 concrete members to conduct the following tests. The p-values are larger than 0.05 during 36 hours to 72 hours, which indicates the non-

hypothesis of the mean is not equal to zero is rejected with 95% confidence interval. The results indicate that even large discrepancies up to 60°F exist; the accuracy of prediction is still acceptable for maximum temperature results. The maximum temperature difference presents significant difference during 54 hours to 63 hours with p-value smaller than 0.05, which means significant differences exist in temperature difference prediction. This may due to the different sensor locations of the minimum temperature in the field.

Table 16 T-test summary of max. temperature at different time after placement

Prediction @ Time (hr)	Standard Dev.	Ttest: Test mean=0 (p-value (prob>|t|)
24	7.867	0.002
27	8.448	0.018
30	8.266	0.019
33	8.157	0.048
36	8.518	0.098
39	8.675	0.146
42	9.337	0.233
45	9.74	0.221
48	10.428	0.161
51	10.81	0.138
54	11.138	0.122
57	11.167	0.12
60	11.507	0.133
63	11.537	0.117
66	11.833	0.097
69	12.33	0.081
72	21.845	0.678

Table 17 T-test summary of max. temperature at different time after placement

Prediction @ Time (hr)	Standard Dev.	Ttest: Test mean=0 (p-value (prob>|t|)
24	15.506	0.004
27	14.695	0.003
30	14.311	0.004
33	14.901	0.002
36	15.547	0.001
39	15.4359	0.004
42	16.26	0.0006
45	17.908	0.002
48	17.69	0.008
51	17.21	0.016
54	17.4	0.034
57	17.12	0.031
60	18.32	0.029
63	18.552	0.025
66	18.452	0.026
69	18.539	0.039
72	17.972	0.069

Table 17 summarized the prediction accuracy for different structure types. In Welch ANOVA tests, the probabilities larger than F are very small, which indicate the means are not equal to zero. This concludes if the whole analysis period is considered, the prediction accuracy will decrease.

Table 18 Welch test results summary of max. temperature at different time after placement

	Test of equal variance Prob >F (Levene)	Test of equal mean Prob>F
Footings	<0.001	<0.001
Columns	<0.001	<0.001
Stems	<0.001	<0.001
Caps	0.1384	<0.001

CHAPTER 6 SENSITIVITY STUDY

In order to investigate the effects of variables on mass concrete thermal behavior and verify the prediction results from 4C program, a sensitivity study is conducted based on various constructions, environmental and thermal properties parameters as follows:

1) Construction Parameters
    a. Temperature sensor location
    b. Dimensional size
    c. Insulation method
    d. Form removal time
    e. Substructure material
    f. Cooling pipes
2) Environmental Parameters
    a. Fresh placement temperature
    b. Ambient temperature
3) Mix Proportion, Thermal Properties and others
    a. Cement content, fly ash, GGFBS
    b. Thermal conductivity
    c. Coefficient of Thermal Expansion
    d. Creep
    e. Coarse degree of meshes

Section 6.1 illustrates the baseline condition of the sensitivity study. Section 6.2 discusses the sensitivity study regarding construction parameters except cooling pipe effects, section 6.3 shows effects of environmental parameters, and section 6.4 considers the effect of mix proportion, thermal properties and mesh size. Each section describes the sensitivity study for pier 1 footing and pier 3 footing. Section 6.5 discusses the sensitivity study on cooling pipe installation. Section 6.6 summarizes the major conclusions from sensitivity study, and compares the results obtained from ConcreteWorks to 4C.

6.1 Baseline Conditions of Sensitivity Study

The baselines of sensitivity studies are defined based on WB I-80 Missouri River Bridge collected data for pier 1 and pier 3 footing. The form removal time is reduced to 4 days (96 hours) for pier 1 footing to be able to compare the results with ConcreteWorks, because ConcreteWorks can only calculate 7 days cracking potential. Baseline inputs are shown in Table 19 below. The sensitivity study plan and detailed inputs are shown in Table 20 and detailed variables in sensitivity study are shown in Table 21. The ranges of different parameters are selected to better identify effects on concrete thermal behavior. Several results from wide-range parameters are unrealistic to real world practice such as extremely high maximum temperature, temperature differences and tensile stress/strength ratio. However, the trends and concepts shown should be correct. Furthermore, substructure material sensitivity study of pier 1 footing on substructure considers soil and concrete two types of material, and pier 3 footing use soil sub-material. Each subbase material will be used to conduct a series of sensitivity study on construction, environmental and other parameters.

The additional sensitivity study for pier 3 footing is to confirm the results from pier 1 footing. Furthermore, the least dimension of pier 1 footing is not large enough to consider it as a mass concrete structure based on the Iowa DOT definition of mass concrete. Concrete material properties and calculation parameters for pier 3 footing baseline are the same as pier 1 footing, except 400 hours processing time will be used due to formwork removal time is 371hours for top insulation and 312 hours for side formwork. Other inputs for pier 3 footing are adjusted based on collected data such as dimensional size, and ambient temperature and form removal time. The updated sensitivity study information for pier 3 footing is shown in Appendix D. Pier 3 footing will not discuss sensor location and substructure material sensitivity.

Table 19 Actual and Baseline inputs comparison for pier 1 footing

Group	Input	Actual	Baseline
General	Material Type	Concrete	Concrete
	Material **Name**	Pier 1 ftg	Pier 1 ftg
	Thickness	3.7m	3.7m
	Start Time	0	0
	Fresh Temperature	17°C	17°C
Dimensional Size	Width	1.4m	1.4m
	Length	13.1m	13.1m
	ambient temp.	min. :7.5° C, max. :14°C, start time :5 hr	min. :7.5 °C, max. :14°C, start time :5 hr
	wind speed	5m/s	5m/s
Surface Boundary Condition	top concrete insulation material	Plastic foil	Plastic foil
	top concrete insulation removal time	192 hr	168 hr
	side concrete insulation material	Plywood formwork	Plywood formwork
	side concrete insulation removal	192hr	96hr
	bottom concrete insulation material	none	none
	bottom concrete insulation removal	none	none
	substructure insulation material	none	none
	Substructure insulation removal	none	none
Material Properties		see Table 14	see Table 14
Concrete Properties		see Table 14	see Table 14
Calculation parameters		see Table 7	see Table 7
Subbase material		Concrete	Soil/Concrete

Table 20 Pier 1 footing sensitivity study summary

Group	Input	Dim. Size	Fresh Plcmt. Temp.	Top Insul.	Side Insul.	Form Rem. Time	Plmt. Date	Cement Content
General	Material type	Concrete	Con.	Con.	Con.	Con.	Con.	Con.
	Material name	Pier 1 ftg	Pier 1 ftg	Pier 1 ftg	Pier 1 ftg	Pier 1 ftg	Pier 1 ftg	Pier 1 ftg
	Thickness	Varies	3.7m	3.7m	3.7m	3.7m	3.7m	3.7m
	Start time	0	0	0	0	0	0	0
	Fresh temperature	17 C	Varies	17 C	17 C	17 C	17 C	17 C
Dim. Size	Width	Varies	1.4m	1.4m	1.4m	1.4m	1.4m	1.4m
	Length	Varies	13.1m	13.1m	13.1m	13.1m	13.1m	13.1m
Surface Boundary Condition	Ambient temp.	Min. :7.5 °C, Max. :14°C, Start Time :5 hr					Varies	Min. 7.5 °C, Max. 14°C, Start Time :5 hr
	Wind speed	5m/s	5m/s	5m/s	5m/s	5m/s	5m/s	5m/s
	Top con. insul. mat.	Plastic foil	Plastic foil	Varies	Plastic foil	Plastic foil	Plastic foil	Plastic foil
	Top con. insul. rem. time	168 hr	168 hr	168 hr	168 hr	168 hr	168 hr	168 hr
	Side con. insul. mat.	Plywood formwork	Plywood formwork	Plywood formwork	Varies	Plywood formwork	Plywood formwork	Plywood formwork
	Side con. insul. rem. time	96hr	96hr	96hr	96hr	Varies	96hr	96hr
	Bottom con.insul. material	none	none	none	none	none	none	none
	Bottom con. insul. rem.time	none	none	none	none	none	none	none
	Substructure insul. mat.	none	none	none	none	none	none	none
	Substructure insul. rem. time	none	none	none	none	none	none	none
Material Properties		See Table 14	See Table 14	See Table 14	See Table 14	See Table 14	See Table 14	Varies
Concrete Properties		See Table 14	See Table 14	See Table 14	See Table 14	See Table 14	See Table 14	See Table 14
Calculation parameters		See Table 7						
Sub-structure material		Soil/Concrete						

Table 21 Variables summary for pier 1 footing sensitivity study

	Dimension	Placement Temp.	Top. Insulation	Side Insulation	Removal time	Placement Date	Cement Content
Parameter(Width* Length*_Depth_)	12'*43'*4.5'	40-90° F	See Table 25	See Table 25	48-194 hr	10/20/2008	560-760 pcy
	12'*43'*5'	10°F Increment			24 hour increments	7/20/2008	100pcy Increments
	12'*43'*6'					Placement Temp.	**CTE value**
	12'*43'*7'					40-90° F	7.36,9,11,13
	15'*43'*4.5'					10°F	*10^{-6}/°C
	25'*43'*4.5'					increments	
	30'*43'*4.5'						**Thermal Cond.**
Parameter(_Width_* Length*Depth)	35'*43'*4.5'						
	40'*43'*4.5'						5.39,8.4,10,13,18
	12'*30'*4.5'						(KJ/kg/°C)
	12'*50'*4.5'						
Parameter(Width* Length*Depth)	12'*60'*4.5'						
	12'*70'*4.5'						
	12'*77'*4.5'						

Table 22 Substructure material properties

Substructure Properties	Soil	Concrete
Density(kg/m^3)	1700	2350
Specific heat(KJ/kg/C)	1.1	0.84
Thermal conductivity(KJ/m/h/C)	6	8
Thermal expansion (1/C)	0	7.36*e-6
E-Modulus(Mpa)	10	400000
Poisson ratio	0	0.17
Compressive strength(Mpa)	120	50
Tensile strength(Mpa)	120	4.5

Table 23 Baseline of pier 3 footing sensitivity study

Group	Input	Actual	Baseline
General	Material type	Concrete	Concrete
	Material name	Pier 3 ftg	Pier 3 ftg
	Thickness	8.23m	8.23m
	Start time	0	0
	Fresh temperature	20.5°C	20.5°C
Dimensional Size	Width	2.2m	2.2m
	Length	13.1m	13.1m
Surface Boundary Condition	Ambient temp.	min. :8° C, max. :20.5°C, start time :11 hr	min. :8 °C, max. :20.5°C, start time :11 hr
	Wind speed	5m/s	5m/s
	Top concrete insulation material	Plastic foil	Plastic foil
	Top concrete insulation removal time	371 hr	371 hr
	Side concrete insulation material	Plywood formwork	Plywood formwork
	Side concrete insulation removal	312 hr	312 hr
	Bottom concrete insulation material	none	none
	Bottom concrete insulation removal	none	none
	Soil insulation material	none	none
	Soil insulation removal	none	none
Material Properties		see Table 14	see Table 14
Concrete Properties		see Table 14	see Table 14
Calculation parameters		see Table 7	see Table 7
Subbase material		Soil	Soil

Substructure material properties are shown in Table 22. Default soil property values from 4C program are used as one type of substructure information, while assuming no elastic properties for soil. Concrete properties were developed based on the mix design used in the I-80 Bridge project. The calculation in 4C program is required to change the units from English to SI, and converted back from SI to English after calculation to better understanding

the effects. The results as English unit of sensitivity study are discussed in three main parameters: maximum temperature, maximum temperature difference, and tensile stress/ strength ratio. The outputs are presented in the following sections.

6.2 Sensitivity Study on Structure and Construction Parameters

Construction parameters including sensor location, dimensional size, insulation method and form removal time will be discussed in this section. The discussion on influence of different substructure materials is combined.

6.2.1 Sensor Location

In order to obtain practical maximum temperature difference as real practice, the minimum temperature of the concrete member is used at the sensor location instead of the surface of the concrete structure predicted by ConcreteWorks. In the WB I-80 Bridge thermal control plan, CTL Group recommended sensors should be placed at “surface and “center”, which were discussed in Table 11. The locations of the sensor are studied to verify the temperature development in the concrete member, temperature development of several locations. Figure 24 is the 3D layout of analyzed structure, where recommended top sensor location and analyzed cross section are presented. Figure 25 shows the geometry output of cross-section for pier 1 footing at the middle of concrete structure, and the potential sensor locations. The maximum temperatures at different locations are listed in Table 24. The triangles in the figures present meshes generated to calculate the results.

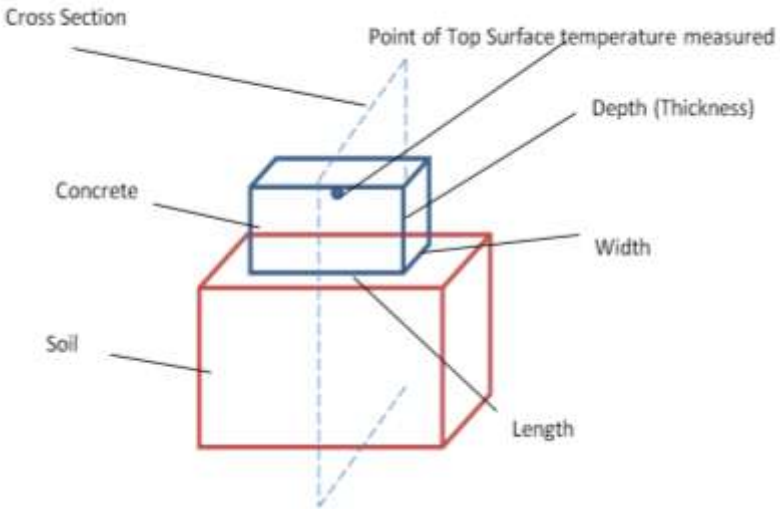

Figure 24 3-Dimensional structure geometry of mass concrete and substructure

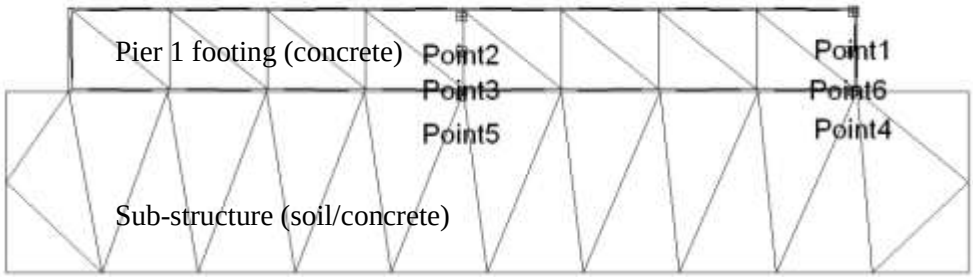

Figure 25 Pier 1 footing Geometry of Potential Sensor Location

Table 24 Sensor location study temperature results for pier 1 footing

Point	Location	Maximum Temperature (F)
1	Top edge surface	71
2	3in below top surface	101
3	Center	136
4	Bottom surface	61
5	Bottom edge surface	76
6	3in below mid-side surface	109

The maximum temperature occurs inside of the center of the structure. The middle of the bottom long edge produces the lowest temperature. The temperature close to surface has little variation during heat hydration process compared to center of the concrete. The temperature closed to surface has little variation during heat hydration process compared to center of the concrete. The temperature development at the corner of the concrete cannot be studied using 4C because the analyzed cross section cannot be changed. In addition, sensors embedded directly at the corner of the concrete member could easily be broken without protection from concrete cover. From this study, the maximum temperature difference should be obtained from the difference between center (point 3) and top surface (point 2) or side surface (point 6), whichever is cooler. For pier 1 footing, temperature is lower at 3 inches from the top surface than 3 inches from the side surface before plywood form work removed. Sometimes, the minimum temperature may occur at side surface due to ambient temperature and insulation method varies.

The location of minimum temperature sensor is evaluated using 4C computer program in terms of how deep the sensor should be installed. The effect of two directions of sensor location and longitudinal and lateral are investigated. The cross-section is cut through the middle of concrete volume along the longest direction is shown in Appendix D. Ten points are selected from the mid-top or mid-side surface to inside of the concrete. The interval between each point is 3 inches in depth. The shown units of data points in 4C program are metrics. The temperature results of sensor study on top (longitudinal) and side (lateral) surface are summarized after converting units in Figure 26 and Figure 27. When the sensors are installed deeper from the surface, the temperature rises higher. The maximum temperature varies less when the sensors are closer to internal concrete and less effects of ambient temperature to concrete as well. The recommended surface sensor is recommended to install at 3 inch below concrete cover, where the sensor could be easily attached on the steel rebar.

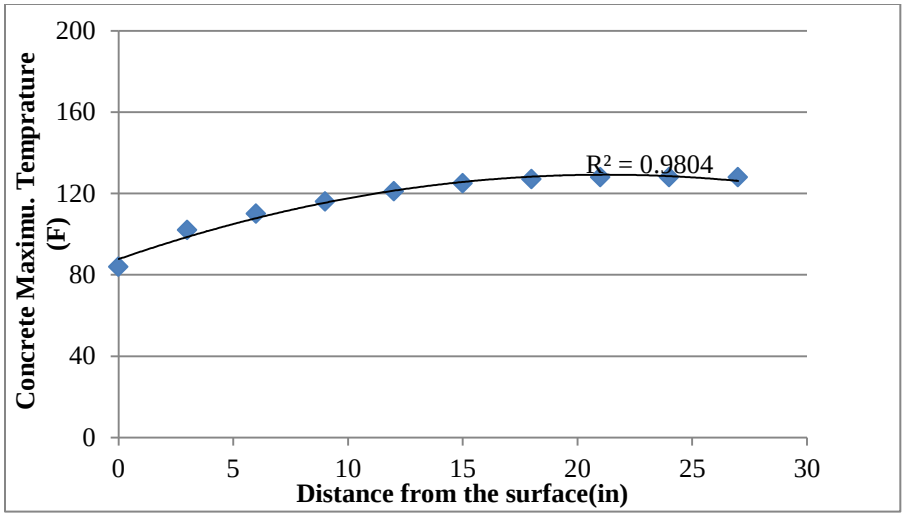

Figure 26 Relationship of longitudinal distance and maximum temperature

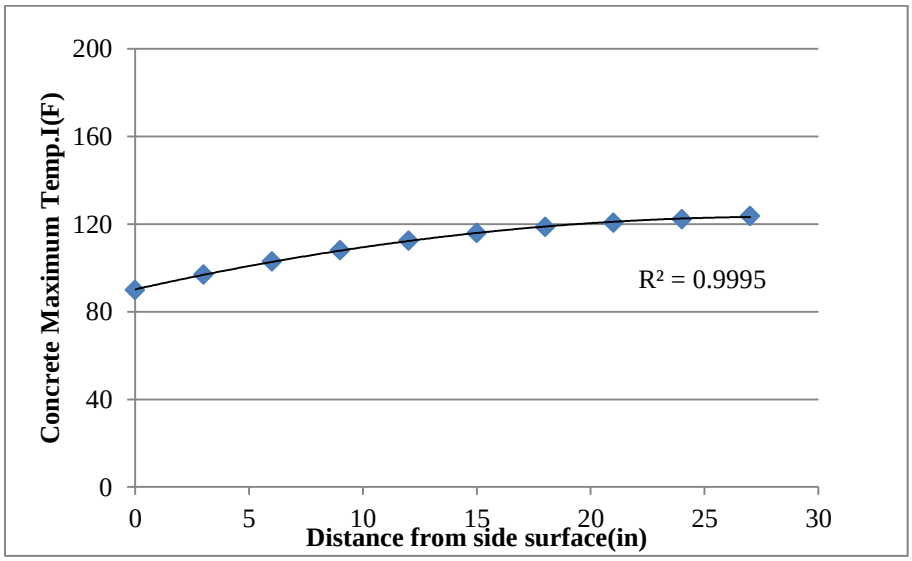

Figure 27 Relationship of lateral distance and maximum temperature

6.2.2 Dimensional Size

Generally, larger size concrete structure generates more heat and results in higher maximum temperature, larger temperature differences, and higher possibility to thermal cracking and delayed ettringite formation. A sensitivity study is conducted to determine the effect of dimensional size on thermal development of concrete structure. Dimensions are selected by varying depth, width and length of concrete structure shown in Appendix D. Depth represents the least dimension (thickness) of the structure, length is the longest

dimension of the structure, and width is the shorter dimension of a surface from top view. Stress/strength ratio is the ratio between tensile stress and tensile strength created by concrete thermal development, which is categorized as the maximum ratio before form removal and the maximum ratio after form removal. The results are presented in Figure 28 to Figure 34 below. For different substructure materials, temperature results are the same in 4C analysis. The difference occurs only at stress/strength ratio.

According to the dimensional size sensitivity study, the most significant factor is the depth of the concrete. When material under the concrete is soil, the maximum temperature, temperature difference and the stress strength ratio are increased as the least dimensions increase. If length and depth are fixed, increasing concrete width not too much influence exhibits on maximum temperature. However, the maximum temperature difference increases as the stress/strength ratio increase. Changes of concrete length do not have big effects on temperature and stress/strength ratio. When the substructure material is concrete, the temperature results are similar to soil substructure analyzed results, but the trend of stress/strength ratios is changed. The increasing of the least dimension results in slightly decreasing stress/strength ratio before form removed and significant increasing stress/strength ratio after form removed. Results of maximum temperature and tensile stress/strength ratio development for depth along with time are shown in Appendix D. The length units in Appendix are in metrics. The maximum stress/strength ratio was not be affected by only changing the length and width of the concrete structure.

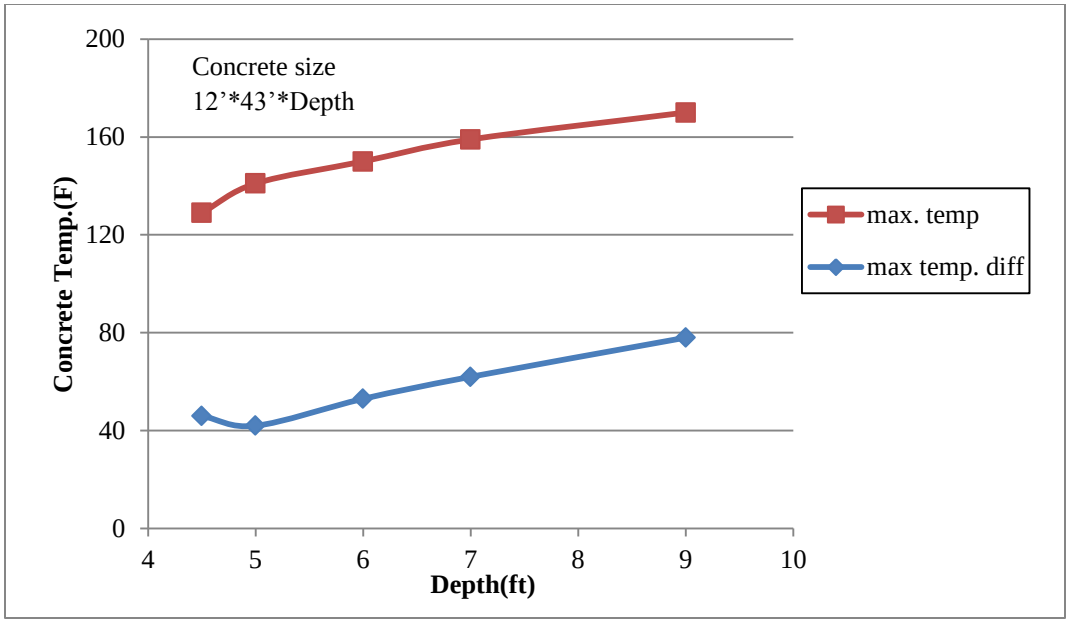

Figure 28 Relationship between least dimension (depth) and temperature for pier 1 footing

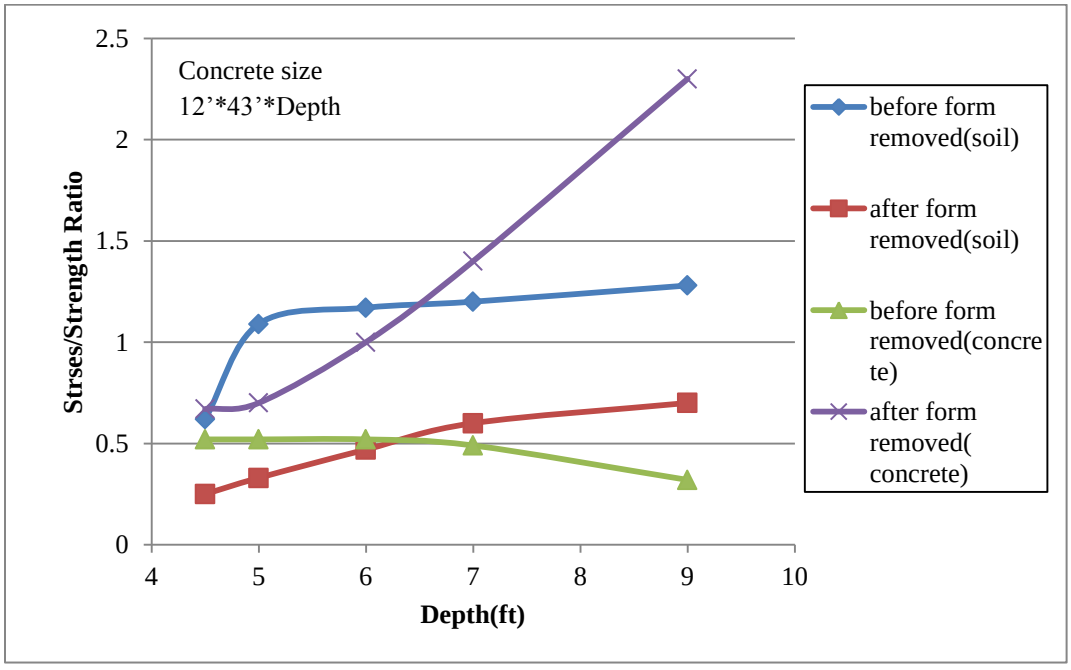

Figure 29 Relationship between least dimension (depth) and stress/strength ratio for pier 1 footing

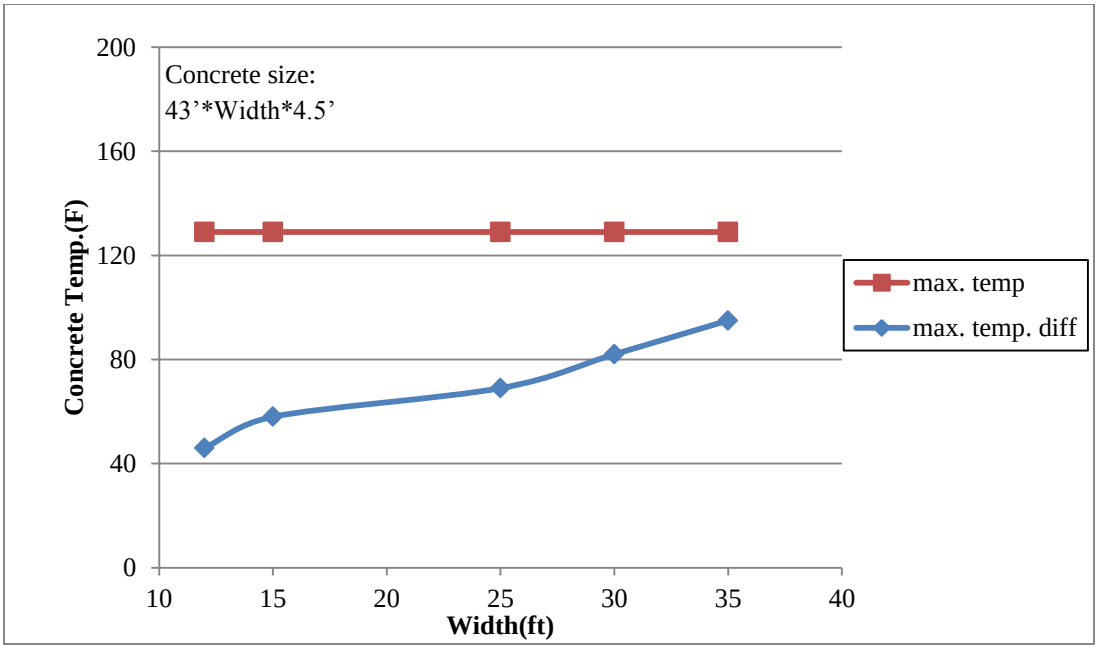

Figure 30 Relationship between width and temperature for pier 1 footing

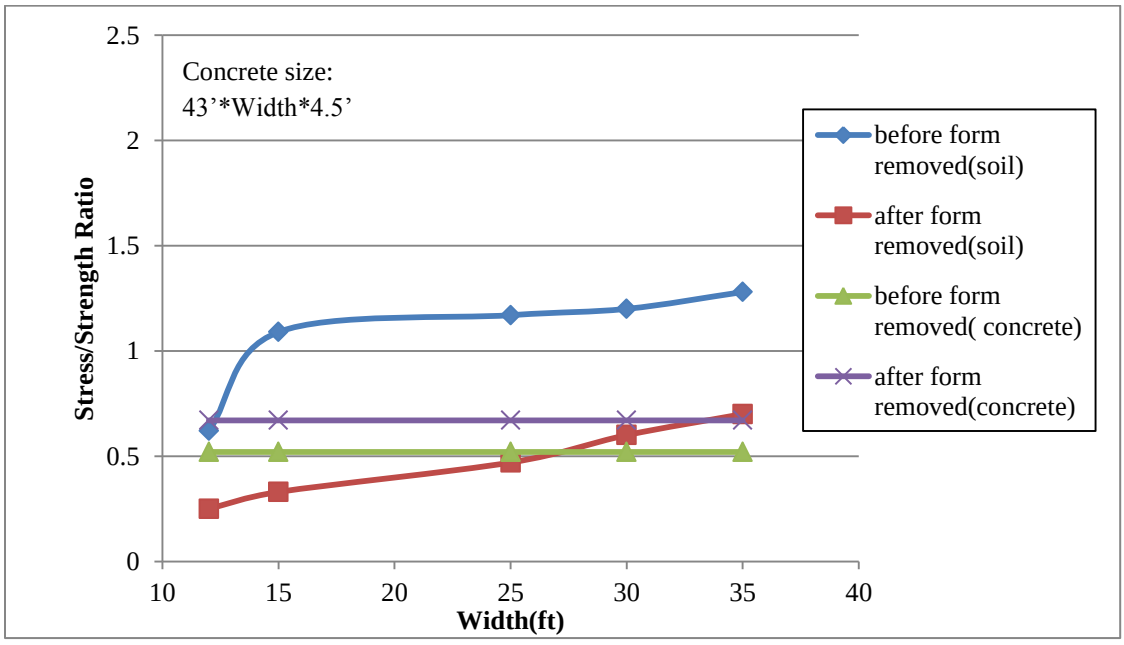

Figure 31 Relationship between width and stress/strength ratio for pier 1 footing

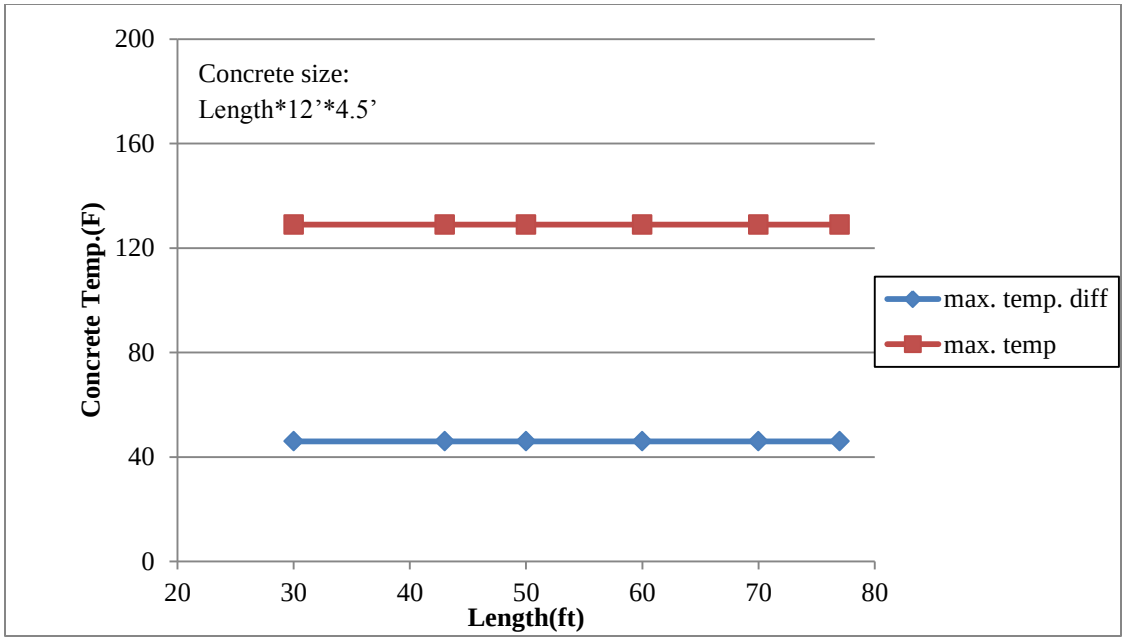

Figure 32 Relationship between length and temperature for pier 1 footing

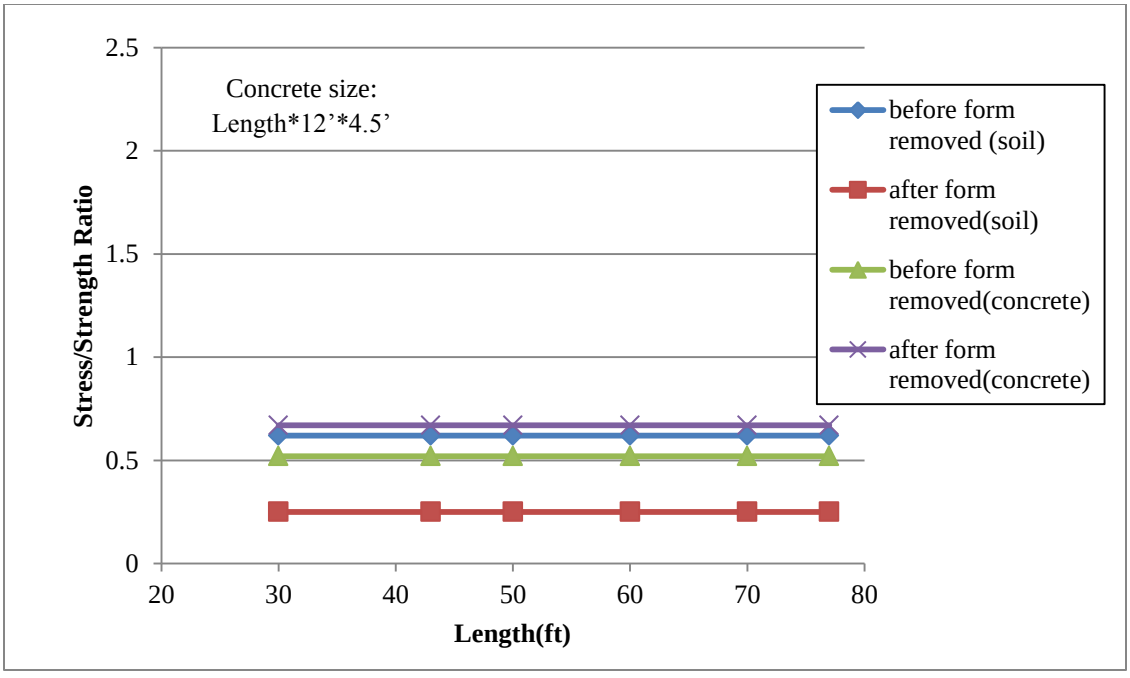

Figure 33 Relationship between length and stress/strength ratio for pier 1 footing

Based on pier 1 footing sensitivity study, the least dimension is the critical dimensional parameter. Therefore, only least dimension sensitivity study is conducted for

pier 3 footing as shown in Figure 34. The same conclusion could be drawn as pier 1 footing sensitivity study.

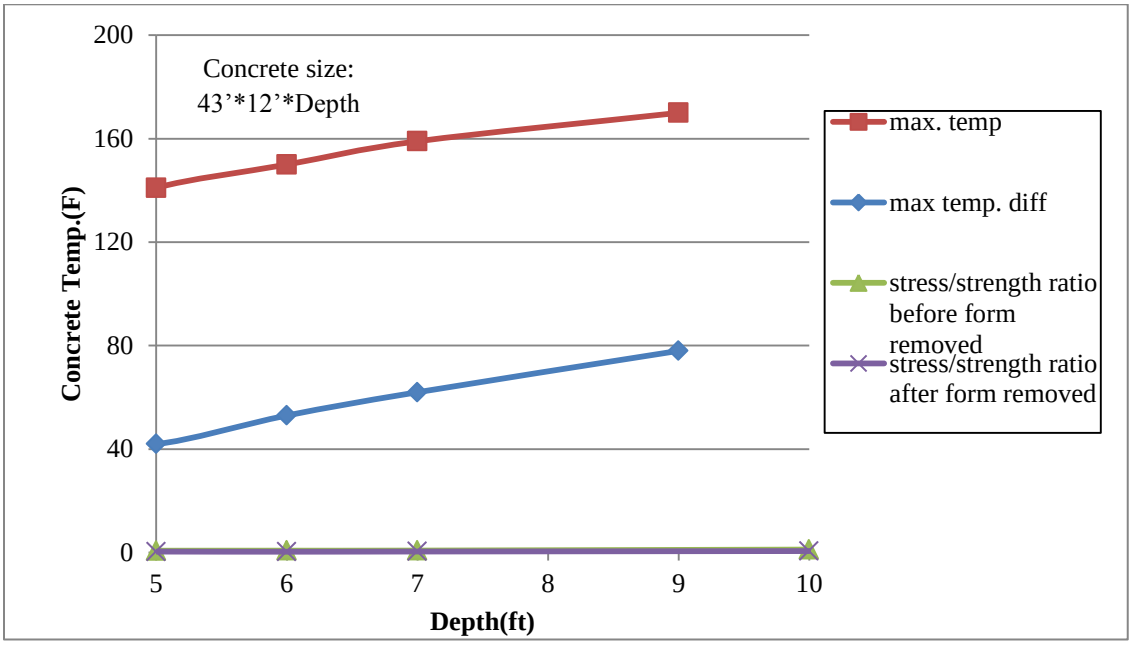

Figure 34 Relationship between least dimension (depth) to stress/strength ratio and temperature for pier 3 footing

6.2.3 Insulation Method

Formwork and curing practices are essential to reducing heat diffusion rate and preventing moisture loss on the surface of the concrete. The insulation promotes complete cement hydration, improves the abilities to gain strength, and minimizes early drying shrinkage. Insulation methods are defined as boundary conditions in 4C Program. The program database provides fifteen materials having individual thermal conductivity and thickness information as shown in Table 25. In the sensitivity study, all materials are used for side or top boundary condition. The ratio of thickness to thermal conductivity is recorded as R-value, which is also known as the resistance to thermal conductivity. R-value evaluates how well the insulating material functioned. The material with higher R-value indicates less heat dispute during insulation process. The recommended R-value of formwork for I-80 bridge project is 2.5, and plastic sheet are the recommend top curing method. The default insulation materials are selected based on the recommendations with plywood formwork around side and plastic foil on top of the concrete structure. Figure 35 to Figure 36

graphically shows the results when soil and concrete are both used as material underneath the concrete structure. Temperature development results are still the same for different substructure materials. The results in Figure 37 and Figure 38 indicate maximum temperature is not affected by using different side insulation material, while temperature difference varies. However, top insulating material has influence on maximum temperature, and maximum temperature difference development. Similar conclusions could be drawn from Figure 39and Figure 40.

Table 25 Insulation Material for sensitivity study

No.	Material Type	Thermal conductivity (KJ/m/h/C)	Thermal conductivity (btu/hr/ft/f)	Thickness (m)	Thickness (in)	R-Value
1	Construction joints	0	0	0	0	0
2	Etha Foam 6 mm	0.144	1.041	0.006	0.236	2.72
3	Foam Plast 10mm	0.144	1.041	0.01	0.394	4.54
4	Foam Plast 20mm	0.144	1.041	0.02	0.787	9.07
5	Foam Plast 30mm	0.144	1.041	0.03	1.181	13.61
6	Foil with 5mm air space	0.21	1.519	0.006	0.236	1.86
7	Form bord 19mm	0.36	2.603	0.019	0.748	3.45
8	Form bord 25mm	0.36	2.603	0.025	0.984	4.54
9	Plast foil	0.14	1.012	0.001	0.039	0.46
10	Plywood	0.5	3.616	0.018	0.709	*2.35*
11	Plywood form work	0.36	2.603	0.0135	0.531	*2.45*
12	Steel form 8 mm	300	2169.349	0.008	0.315	0
13	Timber formwork 32mm	0.43	3.109	0.032	1.26	4.86
14	Winter mat 100mm	0.16	1.157	0.1	3.937	40.83
15	Winter mat 55mm	0.16	1.157	0.055	2.165	22.45
16	Free	0	0	0	0	0

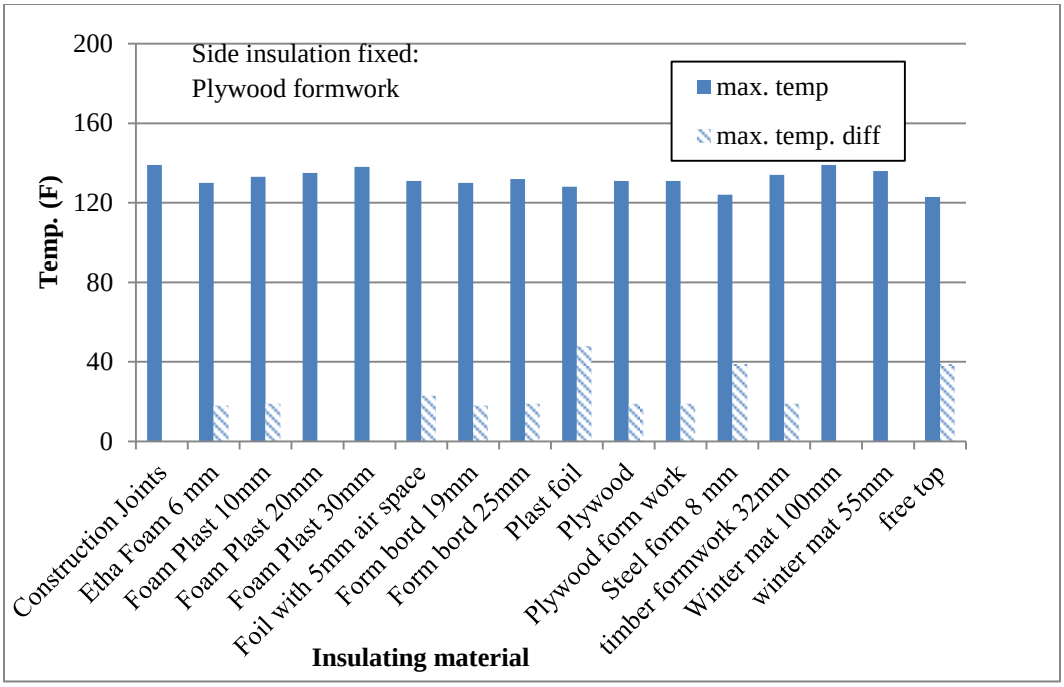

Figure 35 Temperature results with top insulation varies for pier 1 footing

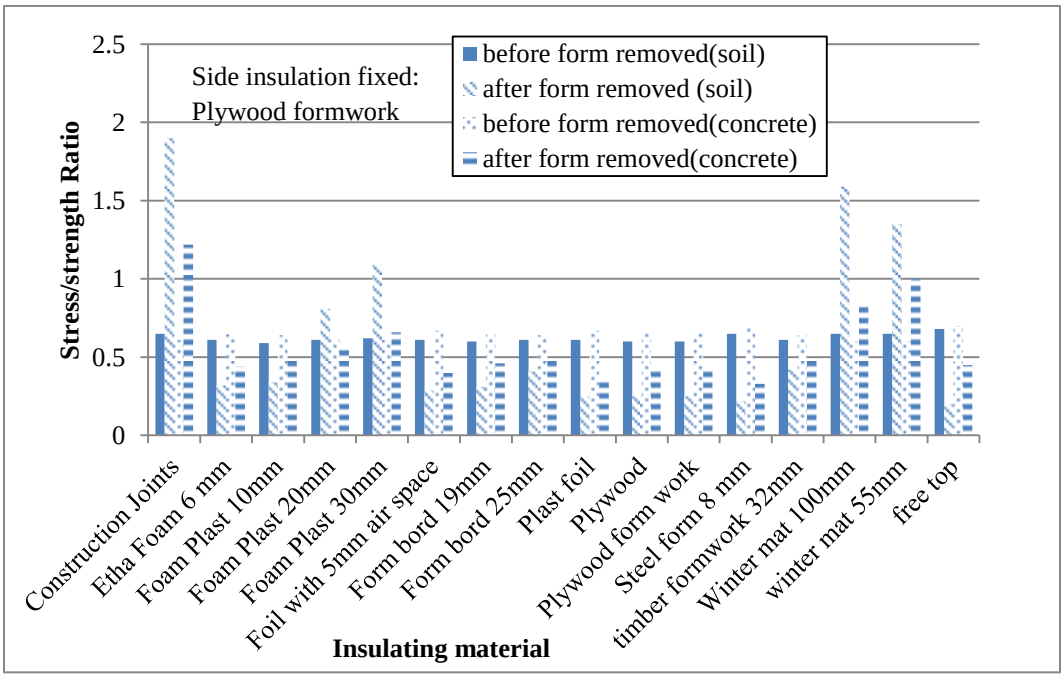

Figure 36 Stress/strength ratio with top insulation varies for pier 1 footing

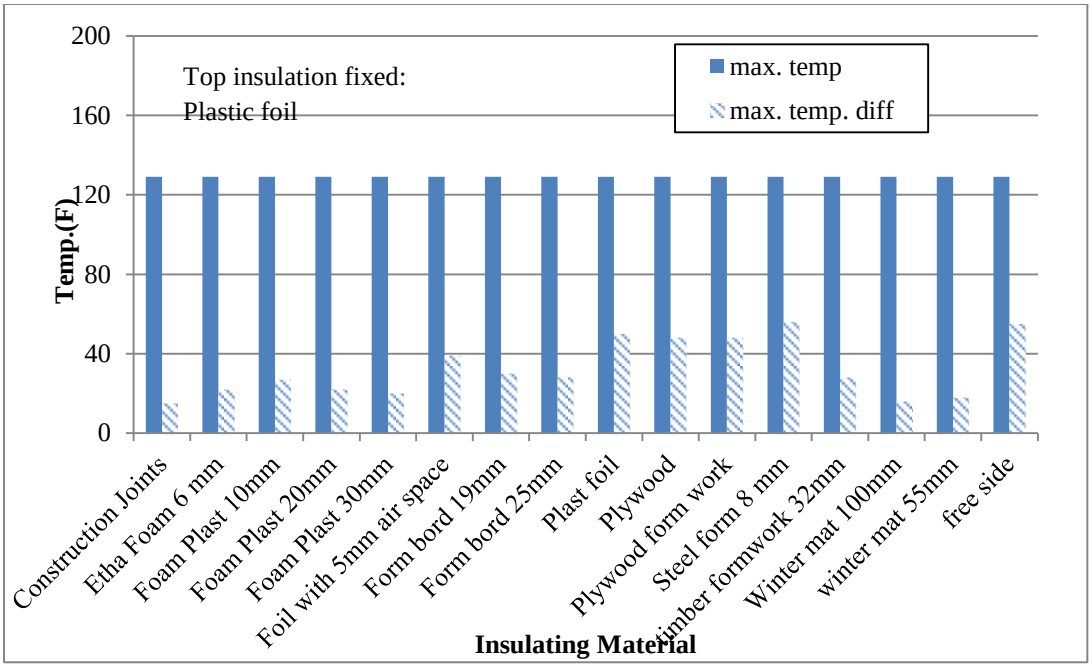

Figure 37 Temperature results with side insulation varies for pier 1 footing

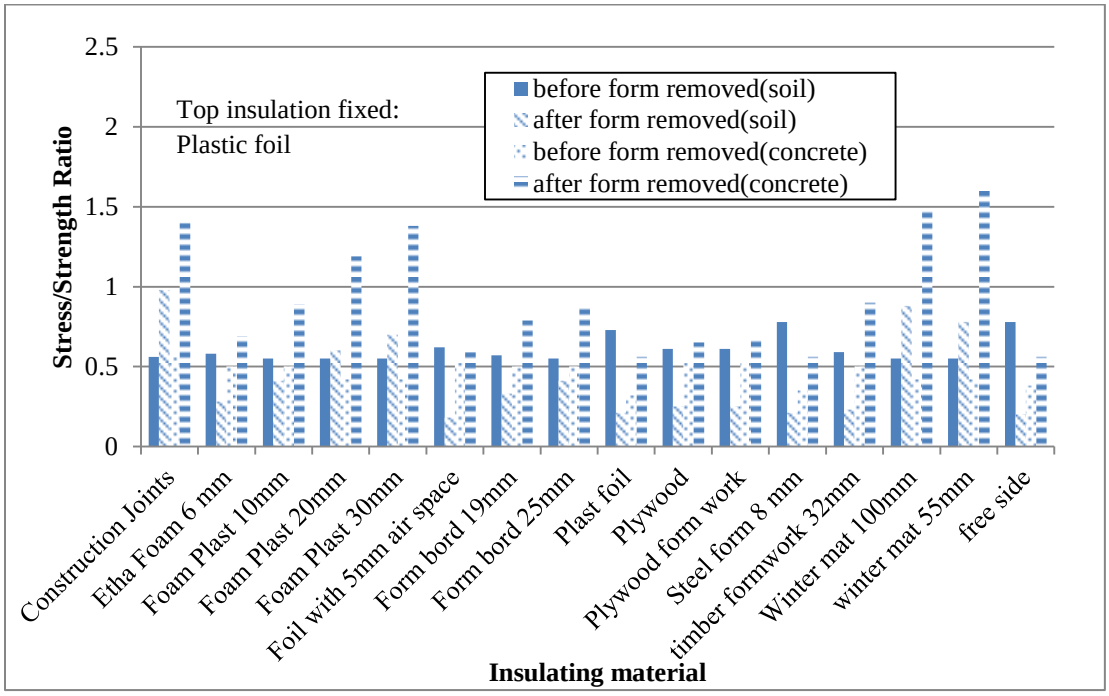

Figure 38 Stress/Strength ratio results with side insulation varies for pier 1 footing

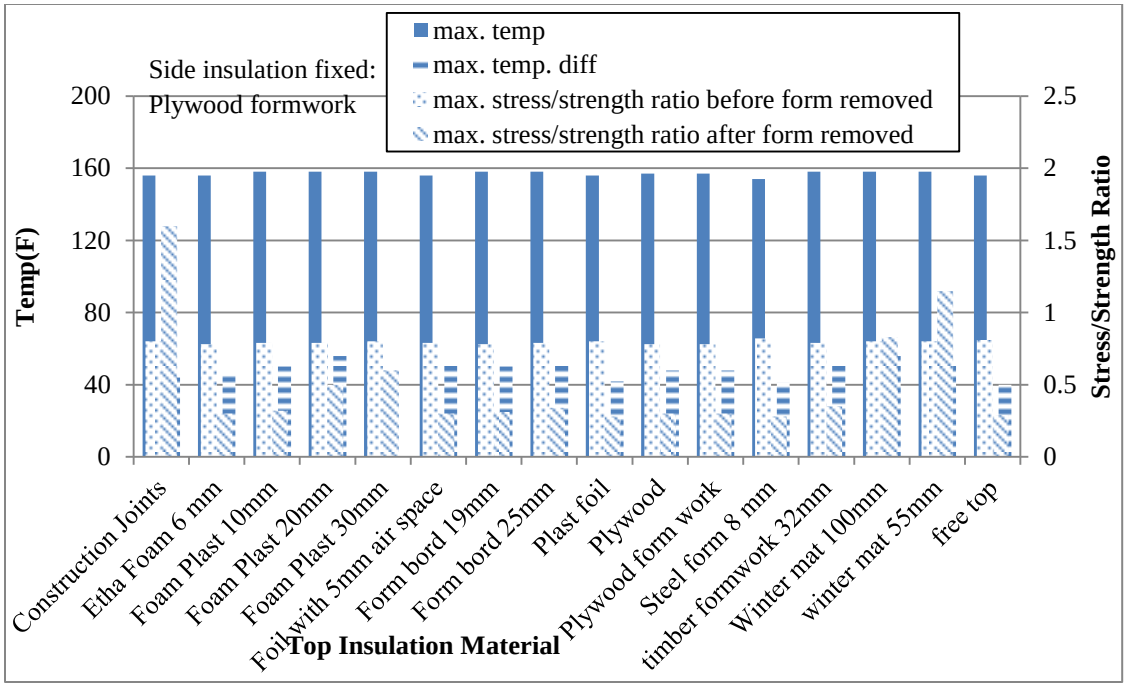

Figure 39 Temperature and stress strength ratio results with top insulation varies for pier 3 footing

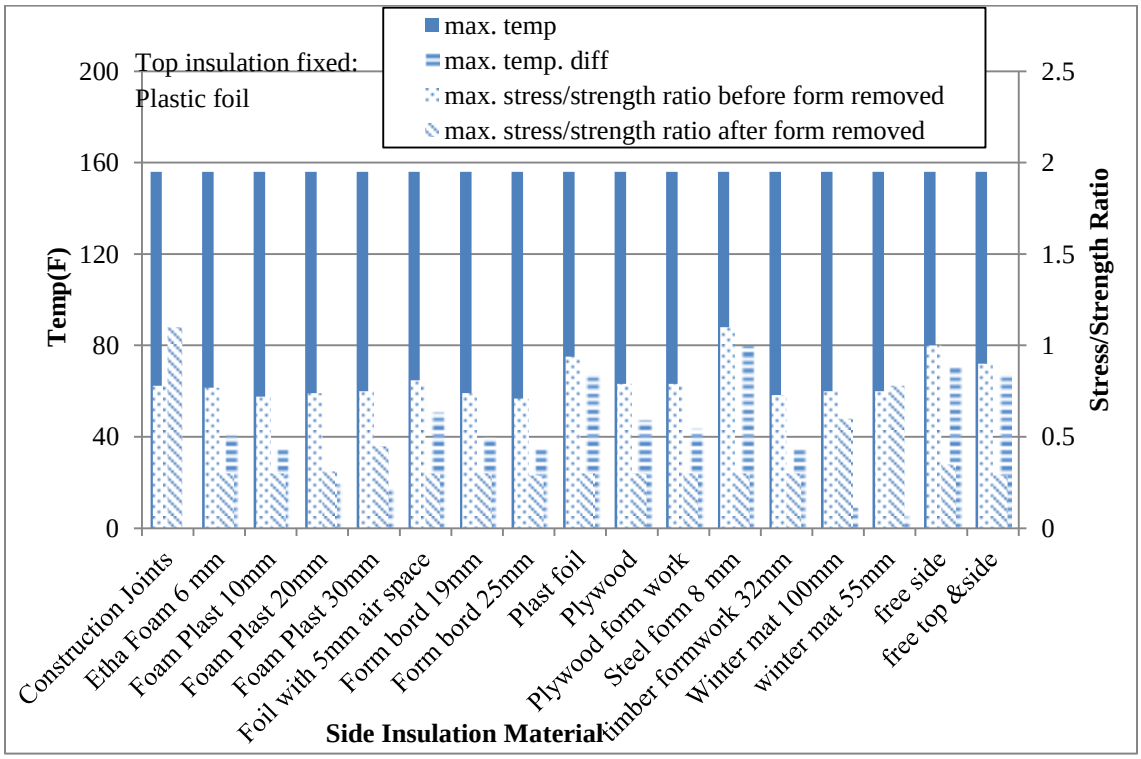

Figure 40 Temperature and stress/strength ratio results with side insulation varies for pier 3 footing

By comparing temperature and stress/strength, it could be found that some insulation materials are beneficial to control cracking before formwork removal. Some of them were good to control thermal cracking after form removal. Top insulating material results from pier 1 footing indicate using steel could be very efficient to control the maximum temperature of concrete. However, the temperature difference is increased due to less insulating effect of steel and the minimum temperature at sensor decreased dramatically. Pier 3 footing results also indicate larger temperature differences using steel and winter mat.

In top insulation sensitivity study, construction joints, thick plastic form and winter mat have very large R-values, which can control the rate of heat dissipation, and generated heat from the concrete might be kept by the insulation caused negative temperature difference. The maximum temperature difference results in Figure 35 are marked as zero for those materials. To evaluate the potential of thermal cracking, stress/strength ratios are examined. The tensile stress/strength ratios are very high compared to other low R-value materials. The conclusion could be made, for those different insulating materials obtained unreasonable temperature, thermal cracking potential might be very high.

Changing side insulating formwork materials does not have a significant effect on maximum temperature. The reason is that farther distance exists from side insulation to center of the concrete. However, the maximum temperature differences of the concrete members change. Construction joints and winter mat provide low temperature difference but high tensile stress/strength ratio. So the material selection should not only be based on temperature results but stress/strength ratio. Other findings from insulation material study will be summarized in Chapter 8.

6.2.3 Form Removal Time

Form removal time is the length of time after the concrete is placed till the formwork is removed. Form removal time is related to side insulation for boundary condition definition in 4C analysis. Formwork or another insulating material should be kept in place for a period of time which allows the concrete to gain strength and dissipates enough heat to prevent thermal cracking. When the formwork is removed, the high temperature difference between concrete and ambient may lead thermal cracking. Therefore, it is preferable to keep the formwork on as long as possible. However, from the construction point of view, contractors

may want to remove it earlier to reuse the formwork. It becomes important to know the optimum form removal time. Form removal time sensitivity studies are evaluated for 2 to 8 days for pier 1 footing and 2 to 13 days for pier 3 footing. 2 days is selected to be the minimum form removal time because mass concrete might finish heat development after 2 days and form can be removed without significant impact on mass concrete development. The end day of the sensitivity study is selected based on real formwork removal time, 194hour, and 371 hours.

The results indicate formwork removal time has no effect on the maximum temperature in the placement. With increasing of form removal time, maximum temperature differences decreases until some level where the temperature difference does not change. Stress/strength ratios after the form is removed decrease as shown in Table 26. In a word, longer form removal time gives longer time for concrete to gain strength before experiencing large temperature gradient by removing formwork. Applying longer form removal time can decrease the stress/strength ratio and present lower cracking potential of mass concrete. Different form removal time does not have effect on cracking potential before formwork or side insulation is removed. Comparing stress/strength ratio after formwork removed, the results indicate later formwork removal decreases the cracking potential. For pier 3 footing, the maximum temperature difference is changed when the removal time varies as shown Table 27. This difference between pier 1 footing and pier 3 footing may due to the increased depth of pier 3 footing as it has a more significant influence on form removal time.

Table 26 Sensitivity study summary on side insulation removal time for pier 1 footing

Form Removal Time	Max. Temp	Max. Temp. Diff (Surface)	Cracking Potential			
			Soil		concrete	
			Before removed	After removed	Before removed	After removed
48hr	129	46	0.61	0.64	1.01	0.62
72hr	129	46	0.61	0.4	0.81	0.65
96hr	129	46	0.61	0.25	0.55	0.64
120hr	129	46	0.61	0.16	0.51	0.58
144hr	129	46	0.61	0.12	0.51	0.58
168hr	129	46	0.61	0.09	0.51	0.57
196hr	129	46	0.61	0.11	0.51	0.57

Table 27 Sensitivity study summary on side insulation removal time for pier 3 footing

Form Removal Time (hr)	Max. Temp(F)	Max. Temp. Diff (Surface) (F)	Cracking Potential	
			Before removed	After removed
48	156	72	0.78	1.5
72	156	66	0.78	1.17
96	156	60	0.78	0.86
120	156	59	0.78	0.65
144	156	50	0.78	0.47
168	156	42	0.78	0.42
192	156	42	0.78	0.42
216	156	42	0.78	0.41
240	156	42	0.78	0.4
264	156	42	0.78	0.38
288	156	42	0.78	0.34
312	156	42	0.78	0.3
336	156	42	0.78	0.3

6.3 Sensitivity Study on Environmental Parameters

Environmental temperature has obvious influence on mass concrete thermal behavior. In this section, fresh placement temperature and placement date are discussed. Fresh placement temperature is defined as the temperature of the concrete when it is placed. Fresh placement temperature is directly related to the thermal development of the placement. Literature indicates that lowering the placement temperature can lower the maximum temperature of the placement and reduce the thermal gradient.

Ambient air temperature can change dramatically in different seasons. Sensitivity studies are conducted to examine the effects of fresh placement temperature and ambient temperature. The Iowa DOT developmental specification limited the fresh placement temperature should be in the range of 40°F - 70°F (ACI 207 2006). Recently, the Iowa DOT allowed the maximum fresh placement temperature up to 80°F. Fresh placement temperature is analyzed in the range of 40-90°F for this study while the ambient temperatures are chosen at two different days in a year, with a dramatic temperature difference, October, 2008, and July 20th, 2008. The winter date is chosen as October instead of December is to avoid

complications with freezing conditions. The results were shown in Figure 41 to Figure 42 below. Pier 3 footing fresh placement temperature results are shown in Figure 43 and Figure 44. Placement dates are selected at July 30th, 2008 for summer condition and November 19th, 2008 for winter condition.

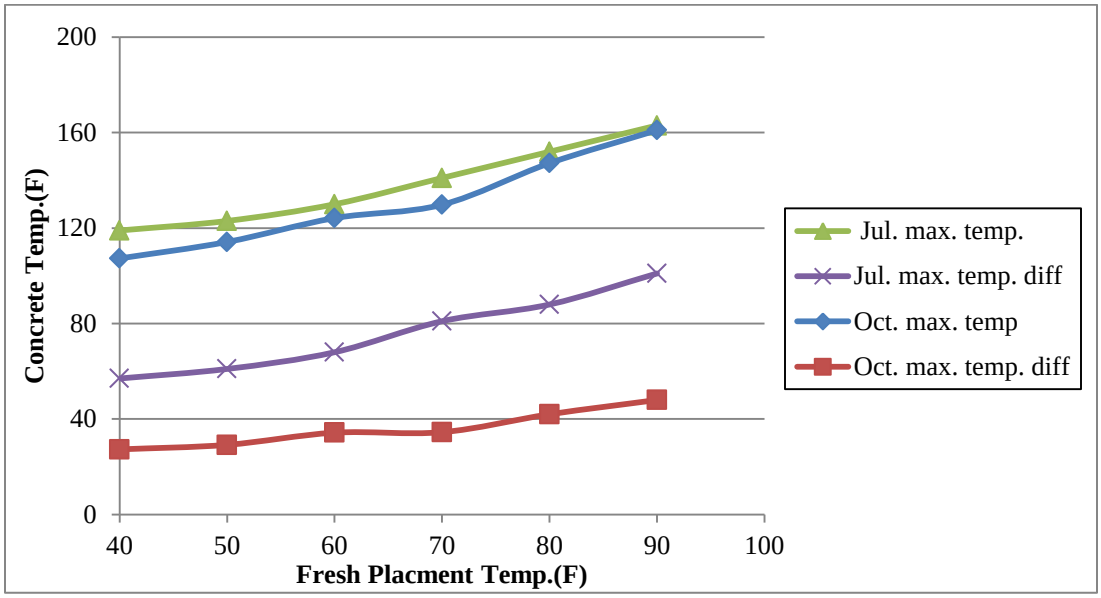

Figure 41 Relationship of temperature to fresh placement temperature for pier 1 footing

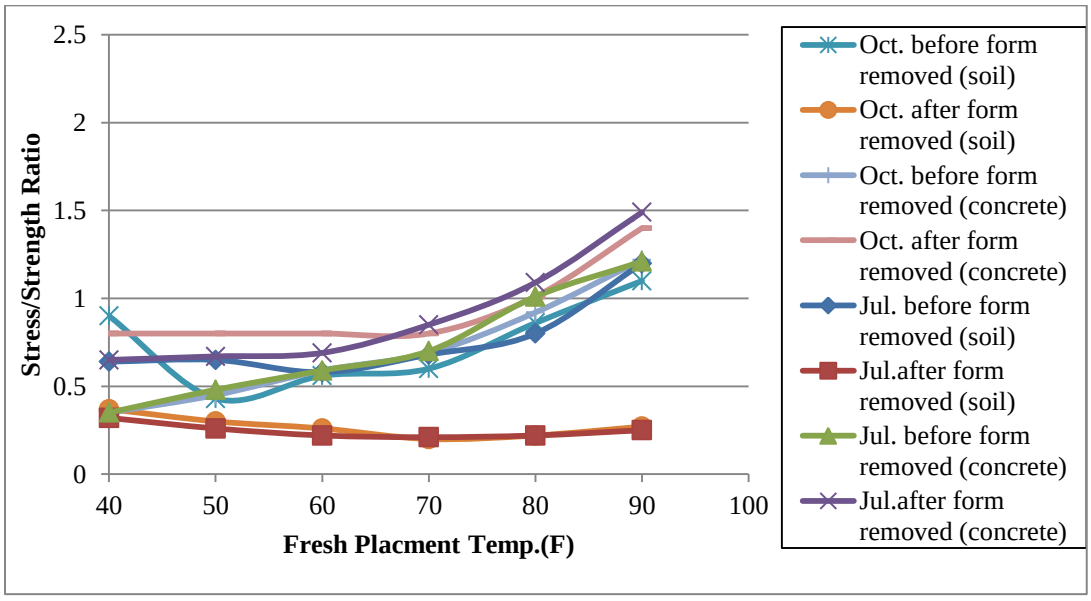

Figure 42 Relationship of stress/strength ratio to fresh placement temperature for pier 1 footing

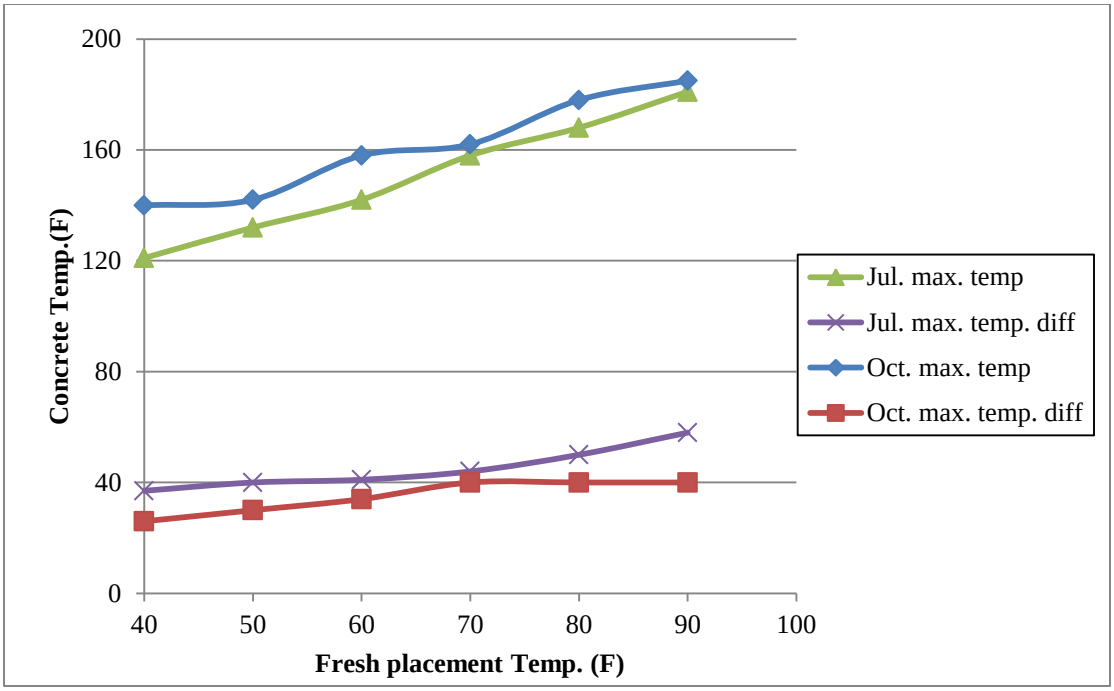

Figure 43 Relationship of temperature to fresh placement temperature for pier 3 footing

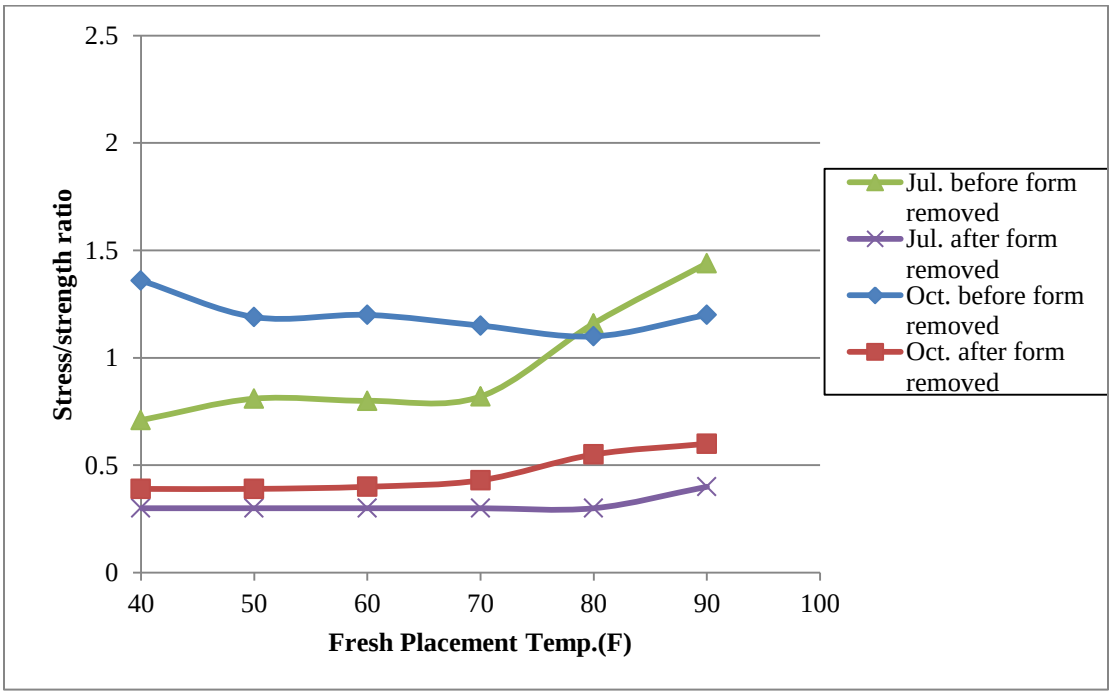

Figure 44 Relationship of stress/strength ratio to fresh placement temperature for pier 3 footing

The sensitivity study results indicate that lower fresh placement temperatures generally result in lower maximum temperatures and maximum temperature differences. Figure 41 and Figure 43 present lower ambient temperatures can reduce maximum developed concrete temperature and decrease the maximum temperature difference. Especially for pier 1 footing which is smaller than pier 3 footing, lower ambient temperature dramatically decreases the maximum temperature difference.

In terms of cracking potential before form removal, lower fresh placement temperature leads to lower stress/strength ratio with concrete sub structure material. For soil substructure of pier 1 footing, the lower fresh placement is better only showed in temperature range of 50°F to 90°F for winter condition, and 60°F to 90°F for summer condition. When fresh placement temperature is 40°F or 50°F, the cracking potential increases compared to fresh placement temperature is 50°F or 60 °F. Construction may not be able to economically reach fresh placement temperature as low as 40°F. To pier 3 footing, lower fresh placement temperature is better for summer condition as pier 1 footing results. In winter condition, higher fresh placement temperature is better, but not over 80°F.

After formwork is removed, the cracking potential is very low for soil substructure, no matter what the ambient temperature is. The maximum stress/strength ratio decreases from 40°F to 70°F, and slightly increases from70°F to 90°F. However, these changes do not affect cracking possibility. Concrete substructure material produces higher stress/strength ratio compared to soil after form removal. The stress/Strength ratio is increased from 60°F to 90°F, and winter construction results in higher cracking potential than summer. To pier 3 footing, no obvious differences of stress/ strength ratio are shown after formwork is removed. The discussion on high stress/strength ratio before formwork removal will be discussed in case study. In a word, higher fresh placement temperature generally results in higher stress/strength ratio after form removal, but the ratios are smaller than 0.7, which are considered as not high cracking potential.

6.4. Sensitivity Study on Mix Proportion, Thermal Properties and Others

In this section, sensitivity studies of mix proportion, thermal properties and mesh sizes are discussed. Due to the inputs limitation of 4C program, only cement content could be varied without doing laboratory tests to obtain new heat development data. For mix

proportion discussion, only cement content is discussed for both pier 1 and 3 footing. SCMs of fly ash or GGBFS should have new heat and strength development data through testing. Pier 3 footing is chosen to study the effects of SCMs using the heat development data and compressive strength data simulated in ConcreteWorks. Thermal property discussion includes thermal conductivity and coefficient of thermal expansion. At last, mesh size effect will be investigated.

6.4.1 Mix Proportion

Concrete mix proportion plays a very important role on mass concrete temperature and strength development. In 4C program, heat of development data should be constructed for each mix design. Conducting sensitivity study of the mix proportion using 4C program without measuring new heat development data and strength data may lead to inaccurate prediction. 4C program assumes the influence of different cement content without requiring new heat development. However, when fly ash or slag content of a certain mix design is changed, a new concrete database should be established. In the pier 1 footing study only studied the influence of cement content varies. For pier 3 footing, influences of fly ash and slag are considered by simulating new heat and strength development data from ConcreteWorks outputs.

In literature, cement has a large contribution to concrete heat development and strength. The more cement contained in a concrete mix, the more heat of hydration generated, and the more strength gained. The Iowa DOT currently had a developmental specification limiting the minimum total cementitious material content to 560 lb/cy for mass concrete, and recommendations for adding SCMs.

A sensitivity study on pier 1 footing baseline examines the effects of cement content 560, 660, and 760 lb/cy. Even the maximum temperature and stress/strength ratio is very high. The trend of results should still be applicable. With the increasing of Portland cement content, maximum temperature and maximum temperature difference in the placement increases as shown in Figure 45 to Figure 46. The cracking potential also increases as the cement content increases due to increased temperature gradient and stress. For pier 3 footings,

427pcy to 727 pcy cement with 100 pcy increments are analyzed as shown in Figure 47. Substitutions of SCMs are analyzed shown in Figure 48 to Figure 50.

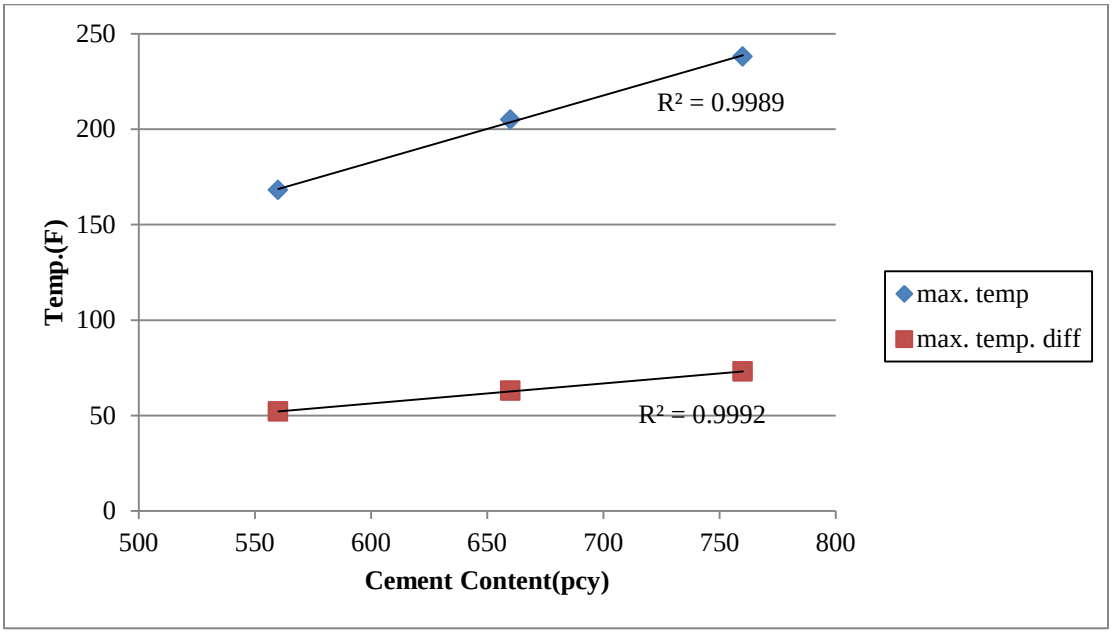

Figure 45 Relationship of temperature to cement content for pier 1 footing

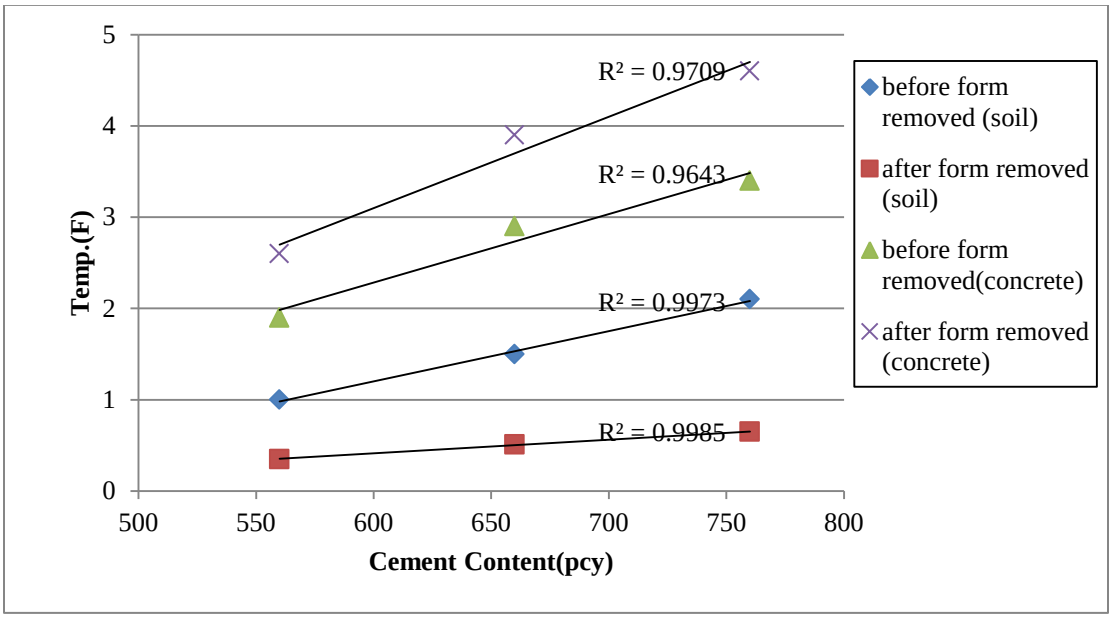

Figure 46 Relationship of stress/strength to cement content for pier 1 footing

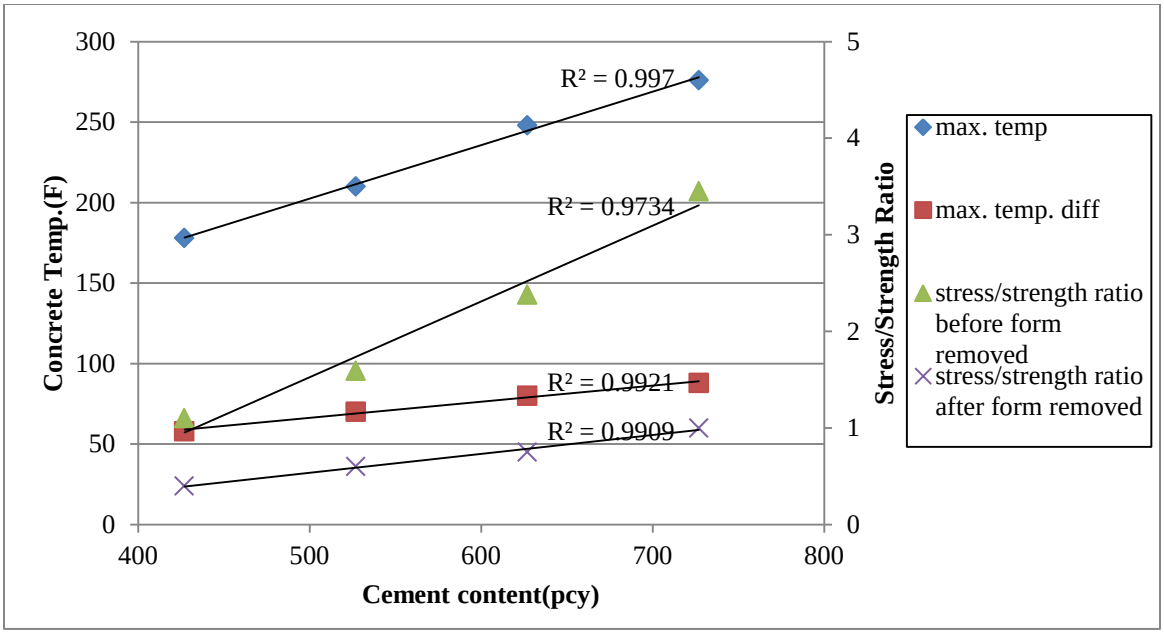

Figure 47 Relationship of stress/strength to cement content for pier 3 footing

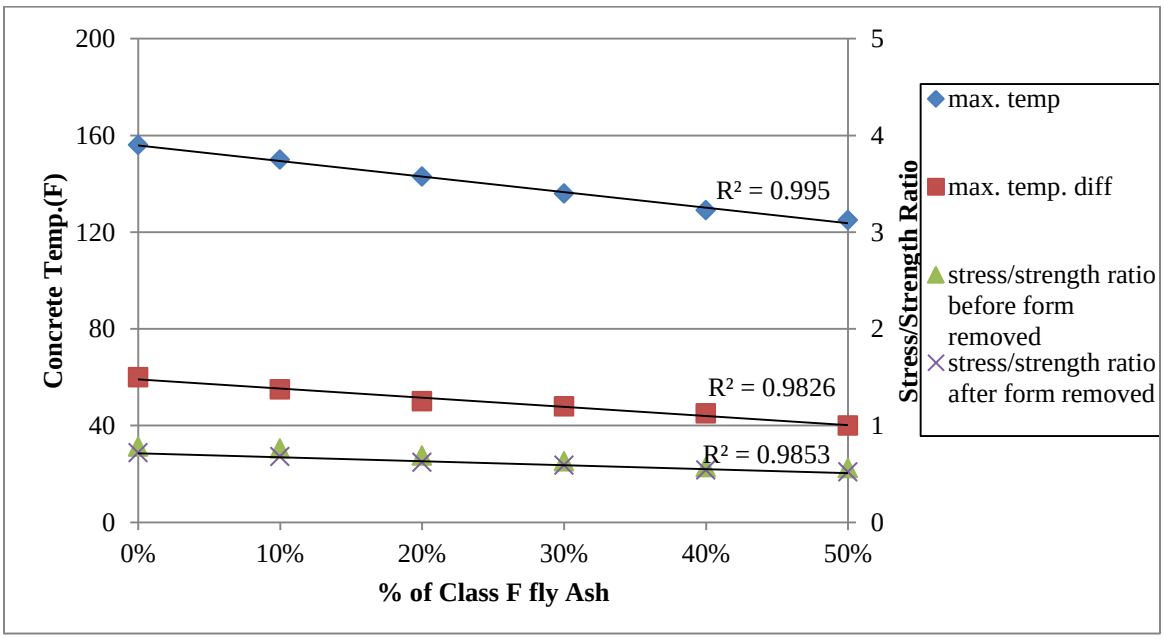

Figure 48 Relationship of temperature and stress/strength to class F fly ash for pier 3 footing

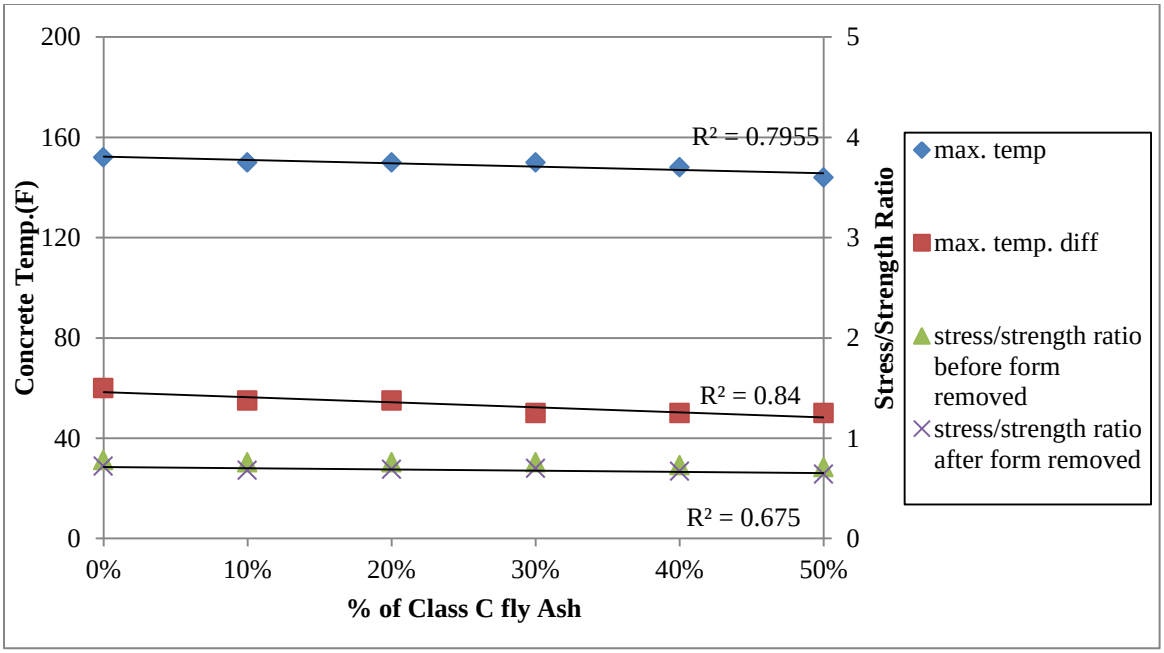

Figure 49 Relationship of temperature and stress/strength to class C fly ash for pier 3 footing

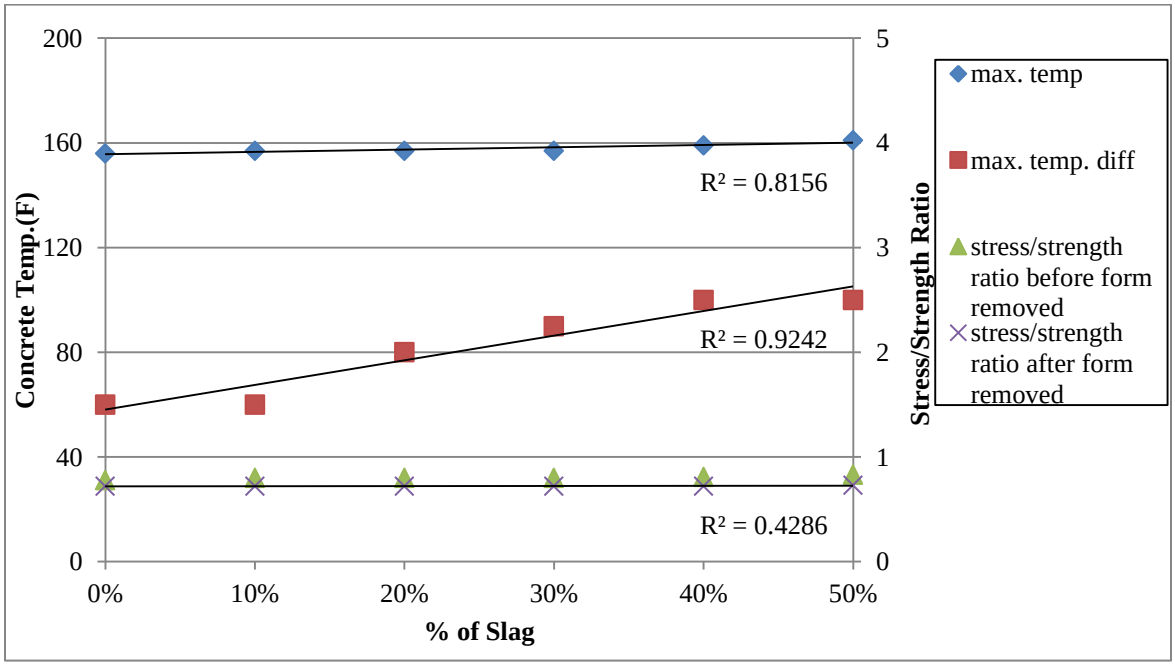

Figure 50 Relationship of temperature and stress/strength to Slag for pier 3 footing

Table 28 below indicates that SCMs may decrease peak temperature of concrete. Substitution of cement with Class F fly ash decreases the maximum temperature, which leads

to lower stress/strength ratio and temperature difference. However, no obvious influence is found of using Class C fly ash. Slag does not have obvious effects on maximum temperature development, but increases maximum temperature difference significantly especially higher 20% slag is added. Then, cracking potential is increased slightly.

Table 28 Sensitivity study summary on SCMs for pier 3 footing

Description		ConcreteWorks			4C
		Max. Temp. (F/C)		max. temp. diff(F)	Stress/Strength Ratio(before-after)
Class F Fly Ash	0%	156	68.89	60	0.78-0.72
	10%	150	65.56	55	0.76-0.68
	20%	143	61.67	50	0.69-0.62
	30%	136	57.78	48	0.63-0.59
	40%	129	53.89	45	0.57-0.54
	50%	125	51.67	40	0.56-0.52
Class C Fly Ash	0%	152	66.67	60	0.78-0.72
	10%	150	65.56	55	0.76-0.68
	20%	150	65.56	55	0.76-0.69
	30%	150	65.56	50	0.76-0.70
	40%	148	64.44	50	0.73-0.67
	50%	144	62.22	50	0.71-0.64
Slag	0%	156	68.89	60	0.78-0.72
	10%	157	69.44	60	0.80-0.72
	20%	157	69.44	80	0.80-0.72
	30%	157	69.44	90	0.80-0.72
	40%	159	70.56	100	0.81-0.72
	50%	161	71.67	100	0.83-0.73

6.4.2 Thermal Conductivity

Thermal conductivity is described as the rate of thermal conduction for materials. The range of thermal conductivity is selected based on Iowa concrete thermal properties from literature. Figure 51 to Figure 52 present the results for pier 1 footing and Figure 53 shows pier 3 footing findings. The range of this study is selected based on general thermal conductivity of concrete listed in Table 1.

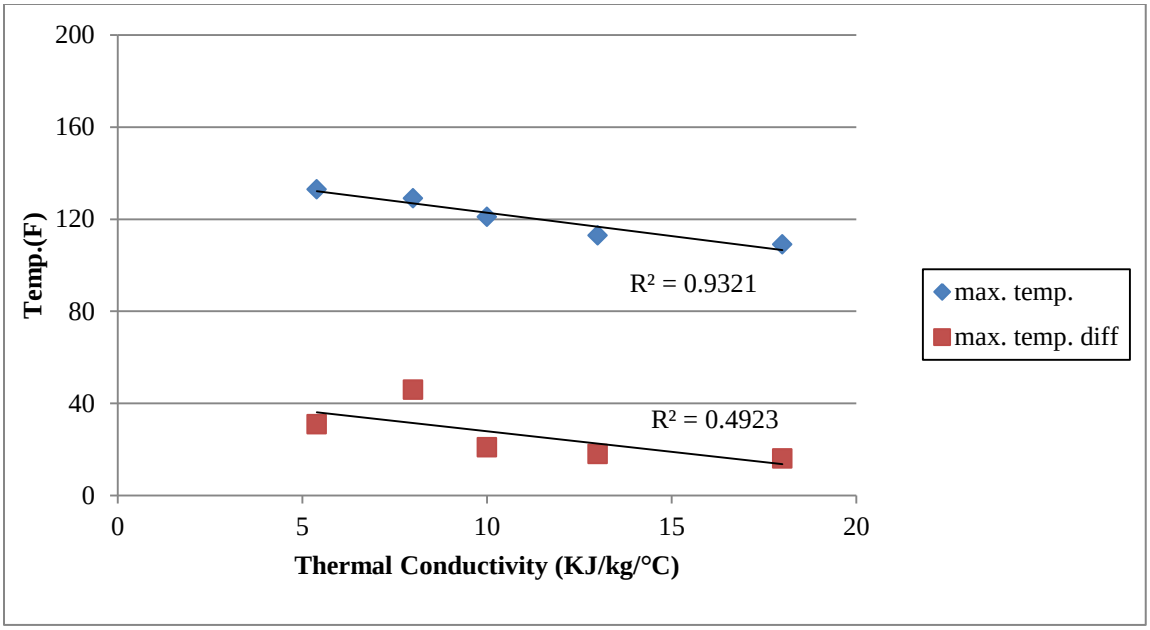

Figure 51 Relationship of temperature to thermal conductivity of concrete for pier 1 footing

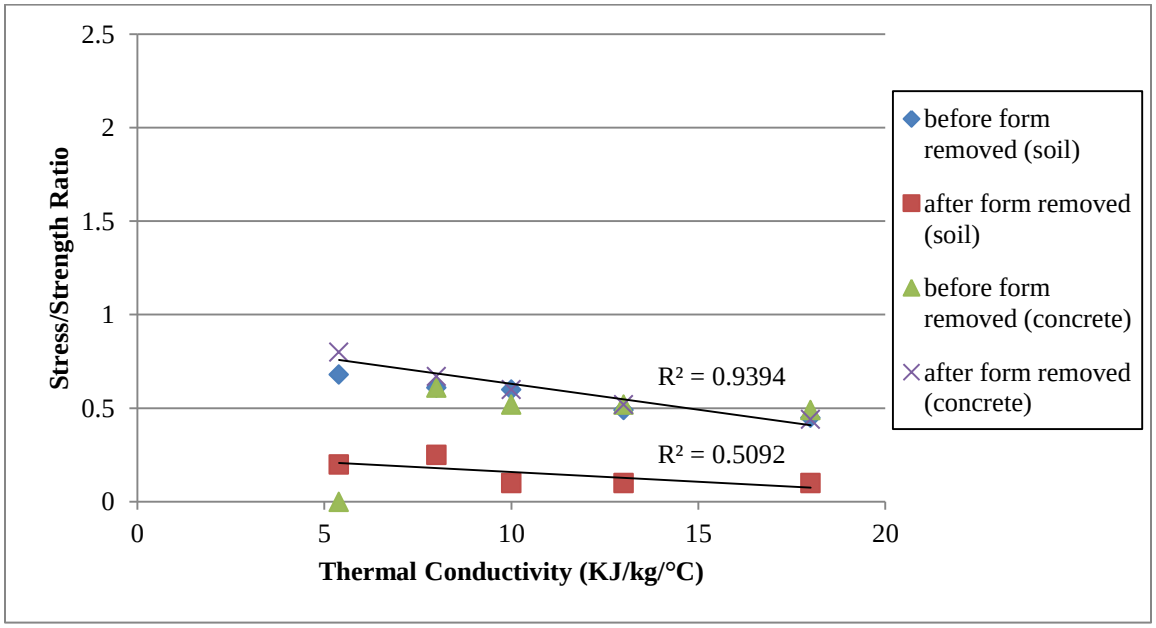

Figure 52 Relationship stress/strength ratio to thermal conductivity of concrete for pier 1 footing

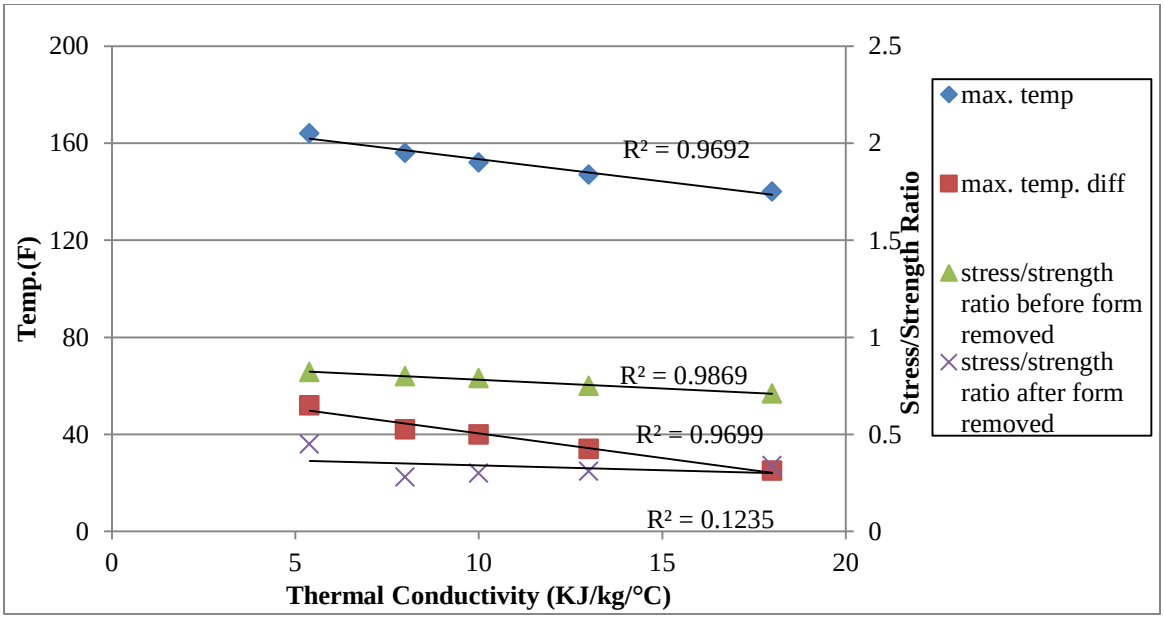

Figure 53 Relationship temperature and stress/strength ratio to thermal conductivity for pier 3 footing

Based on above results, higher thermal conductivity materials better control on maximum temperature and temperature difference. The maximum temperature can vary up to 30°F for pier 1 footing and 25 °F for pier 3 footing during the general concrete thermal conductivity range. The stress strength ratio results indicate the higher the thermal conductivity of concrete, the lower possibility of cracking. Furthermore, larger size concrete members have less effect on variable thermal conductivity. In concrete structures, aggregate thermal conductivity plays a very important role. Therefore, the selection of different aggregates can be important to control thermal cracking.

6.4.3 Coefficient of Thermal Expansion

Coefficient of Thermal Expansion (CTE) measures a material's expansion or contraction with temperature. Large variation in CTE exists for different types of aggregate. Due to the significant influence of the aggregates, it is important to measure the coefficient of the thermal expansion for the particular concrete under investigation. The range of CTE is $4.1*10^{-6}$ to $7.2*10^{-6}$ (1/°F) ($7.4*10^{-6}$ to $13*10^{-6}$ (1/°C)), which was selected based on Iowa concrete thermal properties from literature.

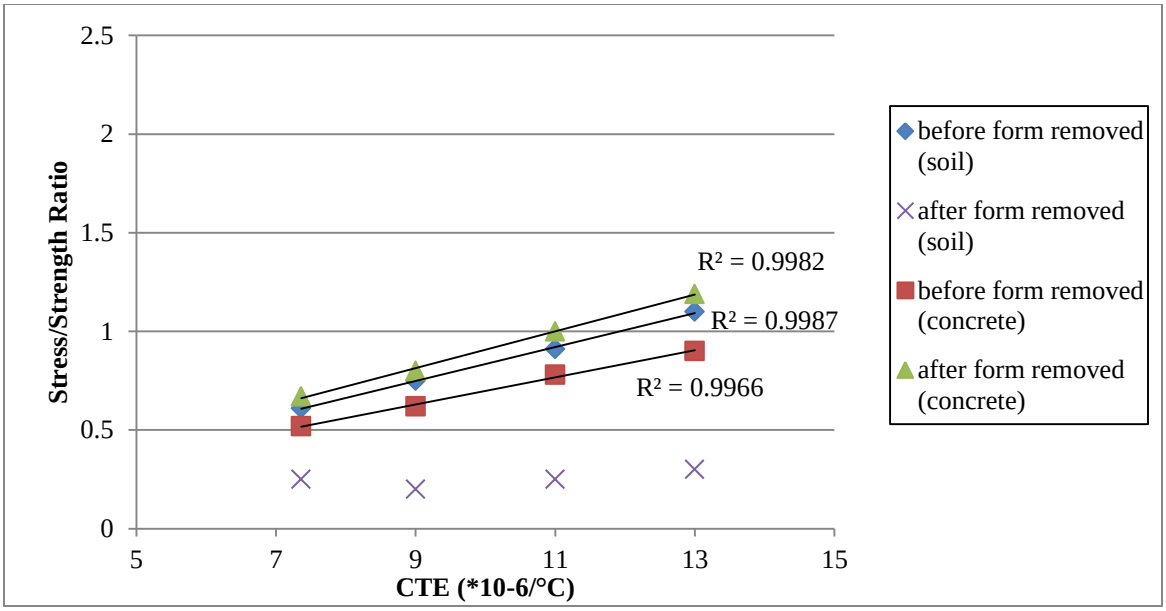

Figure 54 Relationship stress/strength ratio to CTE for pier 1 footing

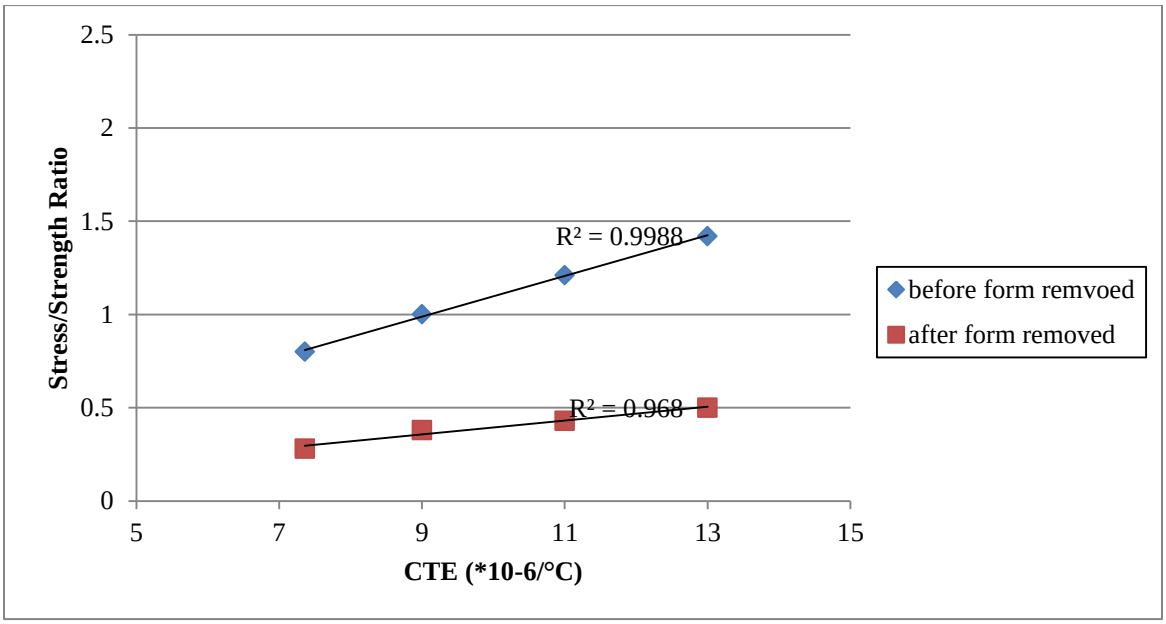

Figure 55 Relationship stress/strength ratio to CTE for pier 3 footing

Sensitivity results in Figure 54 to Figure 55 indicate lower CTE decreases the stress/strength ratio especially during first 48 hours, while maximum temperature and maximum temperature difference of concrete member are not affected. Therefore, selection of aggregate type can effectively control thermal cracking. For instance, limestone aggregate

has a lower CTE than concrete containing siliceous aggregate, which will reduce the potential of thermal cracking.

6.4.4 Creep

Creep is a vital component to evaluating mass concrete cracking. Sensitivity study for structures with and without creep information are discussed in this section. As literature discussed, concrete creep effects can reduce the cracking potential by creating small deformation to release stresses. As models presented in literature section 2.5, the creep information for 4C inputs can be obtained as Figure 56 and Figure 57 shown. The tensile stress/strength ratios of the sensitivity study are presented in Figure 58. The cracking potential is significantly decreased by considering creep effect.

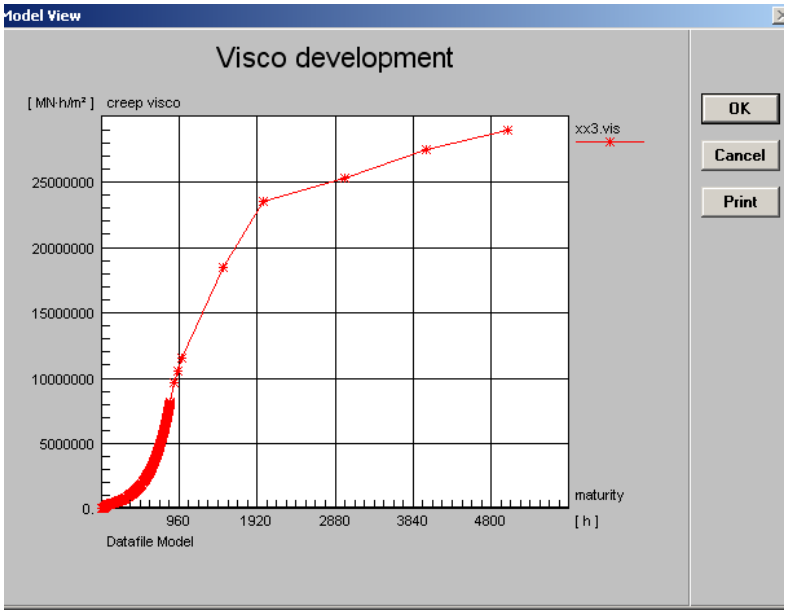

Figure 56 Visco 1 input view as creep information

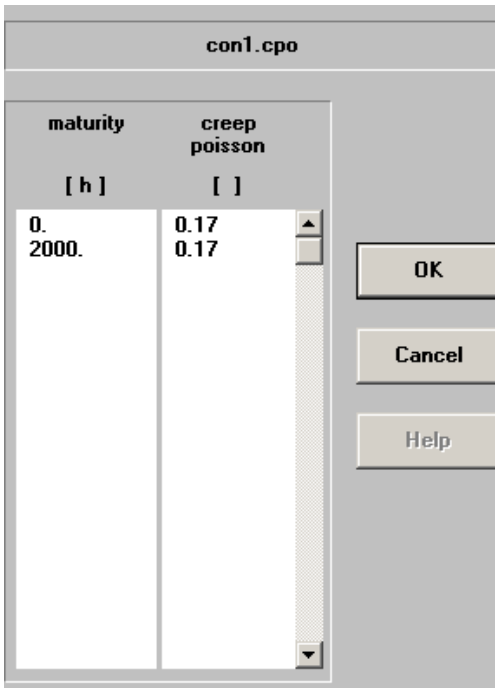

Figure 57 Creep possion input

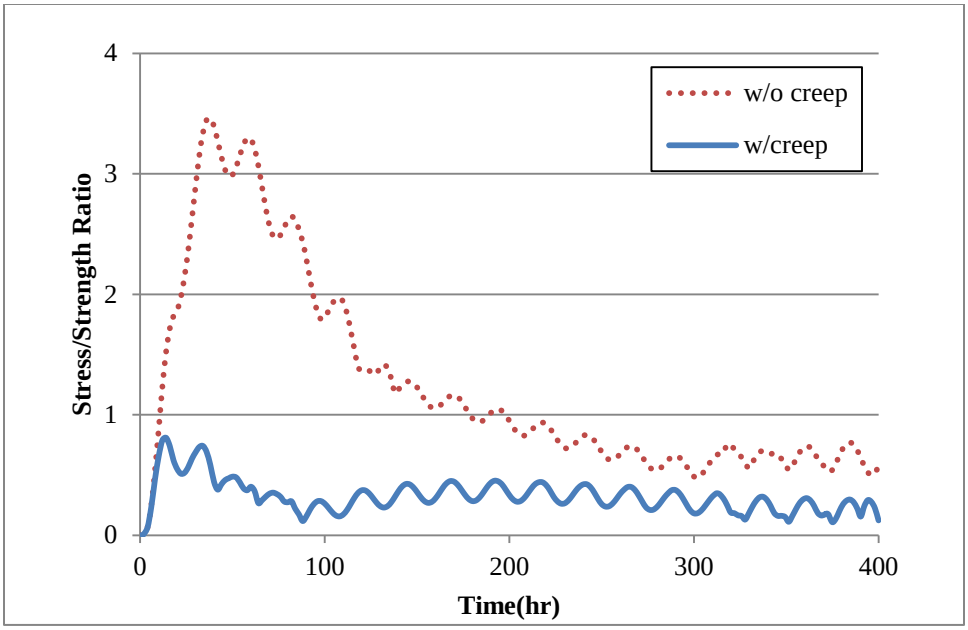

Figure 58 Sensitivity study of stress/strength ratio to creep information for pier 3 footing

6.4.5 Meshes

In finite element program, generating mesh is an important process before calculating. Mesh stands for the number of dimensions generated to calculate. The size of mesh is related to calculation accuracy. Generally, finer meshes result in more accurate calculation, and simulate closer result to actual measurements. Mesh sensitivity study for cases with and without cooling pipes are analyzed. Inputs are discussed in Table 29. When the percentage of density for nodes is smaller, meshes is finer to do calculation, which means the same size of analysis member is divided into more small sections to analyze. Pier 1 footing and pier 3 footing baselines are used for meshes study under no cooling pipe condition, and the results are shown in Figure 59 to Figure 60.

Table 29 Calculation parameters and results summary for mesh size sensitivity study

% of the largest extend	Baseline(Coarse Mesh)	Fine Mesh
min. distance to border(%)	0.01	0.1
density, internal node(%)	10	2
density, border nodes(%)	10	2
density around cpipe/hwire (%)	5	5
radius around cpipe/hwrie (%)	20	10
Pier 1 footing Max. Temp(F)	128	128
Pier 1 footing Stress/strength Ratio	0.6-0.19	0.6-0.21
Pier 3 footing Max. Temp(F)	159	160
Pier 3 footing Stress/strength Ratio	0.81-0.44	0.83-0.49

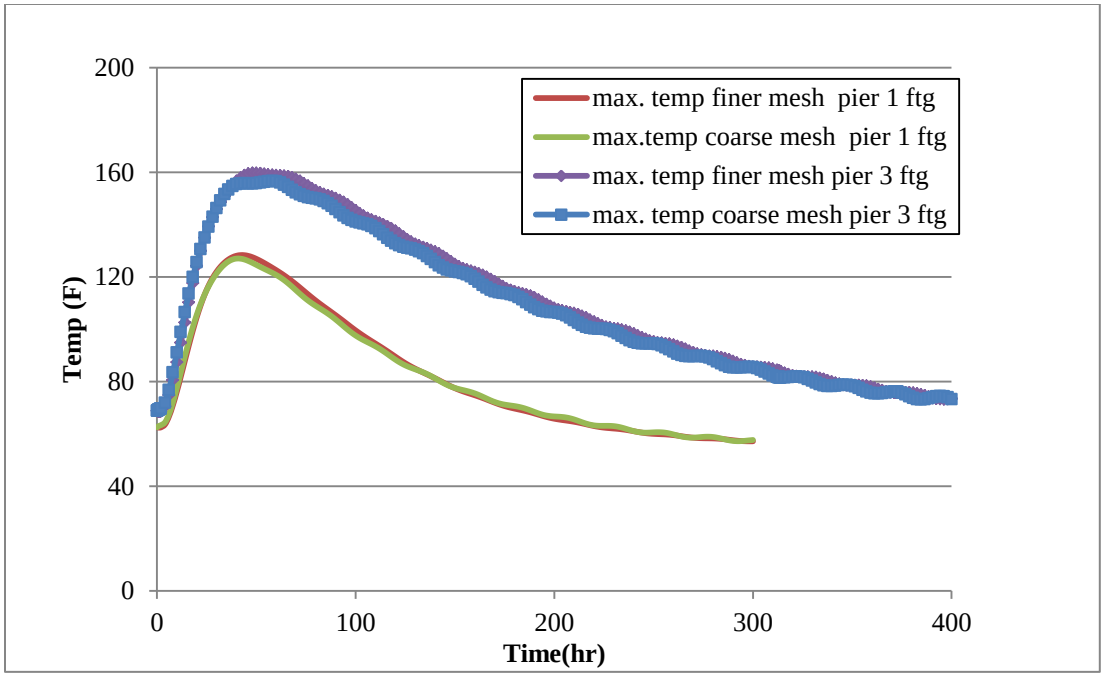

Figure 59 Temperature results for mesh size without cooling pipes sensitivity study

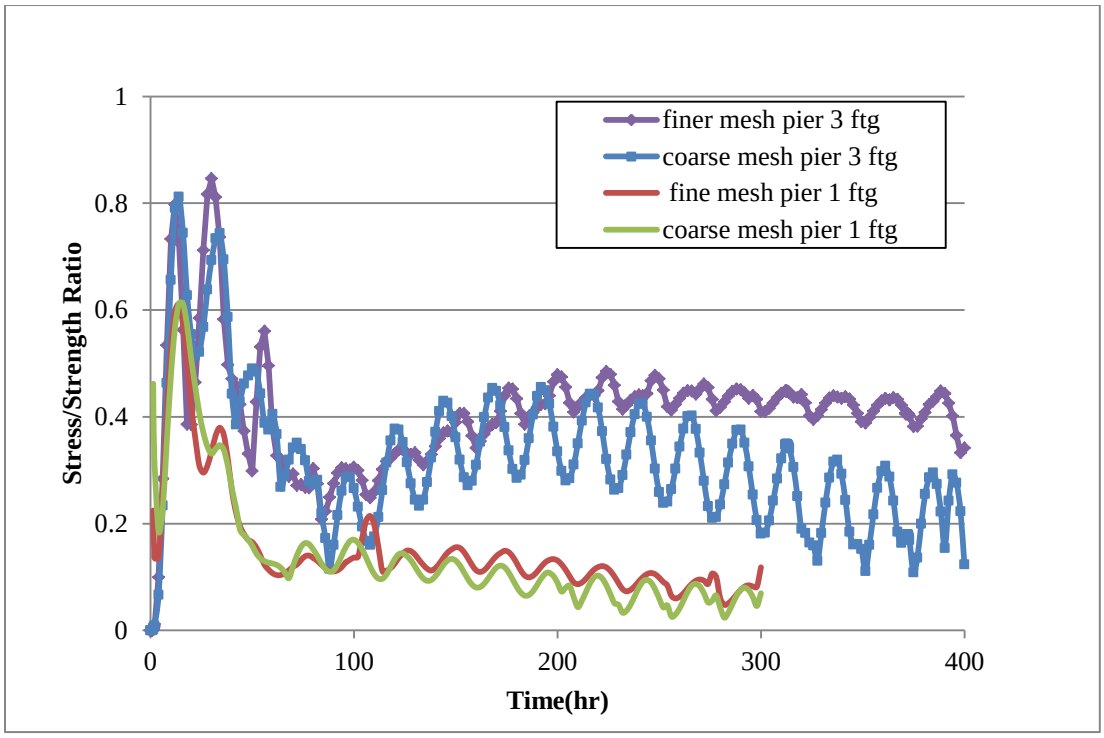

Figure 60 Stress/strength ratio results for mesh size without cooling pipes sensitivity study

Pier 3 footing is used to conduct mesh size sensitivity study with cooling pipes. All the cooling pipe results will be discussed in section 6.6. Finer meshes could obtain slightly higher temperature within 1°F and get little stress/strength ratios difference. Generally higher stress/strength ratio is obtained by reducing the meshes size. The obvious difference happens right after form removal.

6.5 Sensitivity Study to Cooling Pipe

Application of cooling pipes is recommended as an effective construction practice in literature to reduce temperature rise of concrete. In this section comparison between using and not using cooling pipes are discussed in section 6.6.1. Then, a series of sensitivity studies to evaluate the effect of cooling pipes are presented in section 6.6.2

6.5.1 Influence of Using Cooling Pipes

In order to control stress from volume change primarily by temperature change in mass concrete, cooling and insulating systems are often required. Embedded cooling pipes (cpipes) with cool water running through help to transfer heat from the core, and reduce the differential temperature. The temperature of the concrete can be decreased to about 30 °F below the initial peak value by embedded cpipes. The material of embedded pipes can be aluminum or thin-wall steel tubing, plastic, and polyvinyl chloride (PVC). Most common material is PVC. 4C allows the user to draw in cooling pipes and simulates post cooling effects. The baseline of the sensitivity study is pier 3 footing. The cooling pipe layout is drawn as what's recommended in CTL thermal control plan for I-80 bridge project shown in Figure 61. The inputs are similar to pier 3 footing without cooling pipes, except concrete heat development data is changed. The distance from top surface to first row of cooling pipes and bottom surface to last row of cooling pipes is 1.25 feet. The distance from side surface to first column of cooling pipes is 2.5feet. The spacing between cooling pipes is 2 feet vertically and 3 feet horizontally. For different concrete structures, these values may vary but should have similar interval to ensure the efficiency of the cooling pipes.

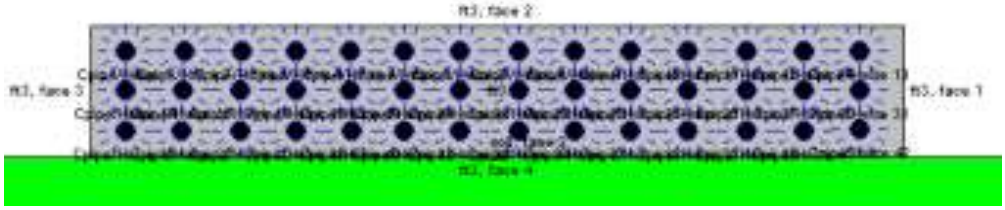

Figure 61 4C drawn layout of cooling pipes for pier 3 footing recommended by CTL Group

Figure 62 indicates cpipes significantly reduce maximum temperature developed in the concrete about 30°F and slightly reduces stress/strength ratio after 12 hours as presented in Figure 63.

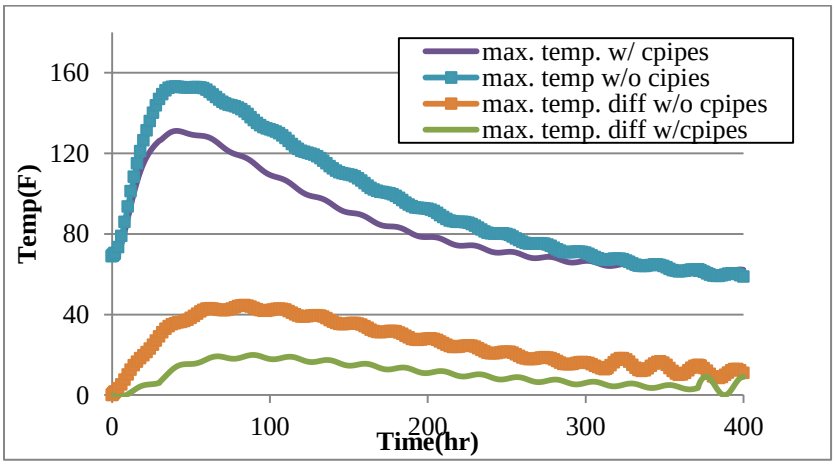

Figure 62 Temperature results for cooling pipes sensitivity study

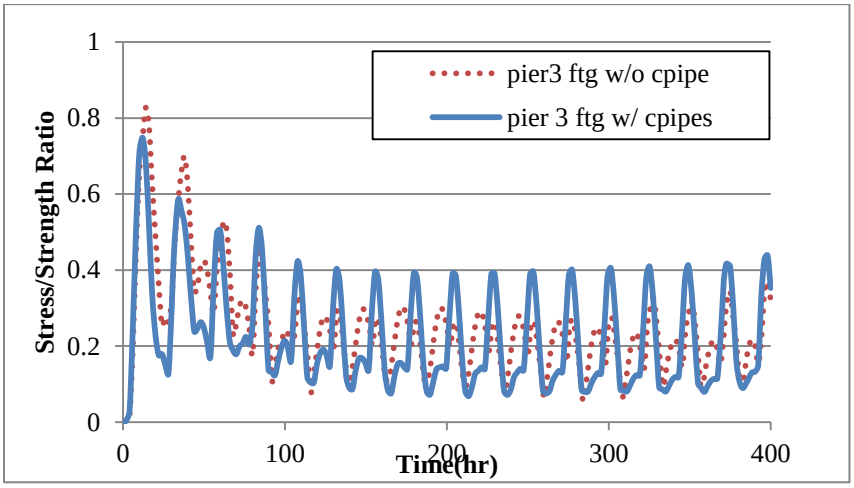

Figure 63 Stress/strength ratio results for cooling pipes sensitivity study

6.5.2 Cooling Pipes Sensitivity Study

In this section, comparison between I-80 Bridge known (CTL/actual) and predicted (4C) temperatures, and cpipe sensitivity studies regarding to area ratio between cpipes and concrete member in a cross section are shown. First, study comparing temperature data for pier 3 footing with or without cpipes in I-80 Bridge thermal control plan is discussed. CTL Group provided temperature data, which is considered as known temperature information and has already been proven to contribute reliable mass concrete thermal results. Calculations using pier 3 footing are conducted to compare with known maximum temperature and maximum temperature difference while fresh placement temperature are different at ambient temperature is 20°F, 50°F and 80°F as Table 30 and Table 31 shown.

Table 30 Comparison between CTL Group and 4C prediction for pier 3 footing without cooling pipe used

W/O Cpipes Ave. Air Temp(F)	Fresh Temp.(F)	Max. Concrete Temp(F)			Max. Temp. Diff(F)			Max. Stress/Strength Ratio
		4C	CTL	Diff. between 4C and CTL	4C	CTL	Diff. between 4C and CTL	
20	45	115	117	-2	56	33	23	0.65
	55	126	129	-3	63	36	27	0.81
	65	141	140	1	73	39	34	1.05
50	45	131	122	9	42	24	18	0.52
	55	137	133	4	50	27	23	0.61
	65	149	144	5	59	30	29	0.78
80	55	145	138	7	39	19	20	0.75
	65	156	148	8	41	22	19	0.8
	75	167	158	9	46	25	21	0.9
	85	179	169	10	55	28	27	0.97

Table 31 Comparison between CTL Group and 4C prediction for pier 3 footing with cooling pipe used

W/ Cpipes		Max. Concrete Temp(F)			Max. Temp. Diff(F)			Max. Stress/Strength Ratio
Ave. Air Temp (F)	Fresh Temp.(F)	4C	CTL	Diff. between 4C and CTL	4C	CTL	Diff. between 4C and CTL	
20	45	95	92	3	48	20	28	0.57
	55	105	102	3	51	23	28	0.70
	65	114	114	0	58	26	32	0.82
50	45	100	102	-2	30	15	15	0.3
	55	108	111	-3	32	17	15	0.38
	65	117	121	-4	39	19	20	0.9
80	55	120	126	-6	21	13	8	0.43
	65	126	134	-8	22	15	7	0.4
	75	134	143	-9	30	17	13	0.39
	85	143	153	-10	37	19	18	0.47

The above table indicates that 4C program tends to underestimate maximum temperature when ambient and fresh placement temperature are high, and overestimate peak temperature when ambient and fresh temperatures are low. Furthermore, as previous sensitivity study indicated that higher ambient temperature, higher fresh placement temperature and deeper sensor installation contribute to higher maximum temperature and maximum temperature difference of concrete. Cooling pipes reduce the maximum temperature around 20°F in this comparison. However, the temperature difference is increased. When the minimum temperature is taken at the side surface of concrete, 4C calculated maximum temperature difference is close to CTL prediction. When the minimum temperature is taken at top surface, higher temperature difference is presented.

When prediction is higher actual temperature, the values are recorded as positive; otherwise, the values are presented as negative values. Comparing the difference between actual measurements and 4C predicted temperature; the results indicate the predictions are close to professional company information in terms of maximum temperature. When averaged air temperature became higher around 80°F, 4C program predicts higher maximum

temperature for cases without cpipes, and lower maximum temperature for cases with cpipes. Average difference for maximum temperature comparison is +/- 4.5°F. Comparing maximum temperature difference between actual measurements and prediction, 4C always predicts approximate 20°F higher temperature difference in average.

The tensile stress/strength ratio from 4C is plotted in Figure 64 below. , The application of cpipes decreases the stress/strength ratio. In addition, cracking potential increases with increasing of fresh placement temperature when ambient temperature is 20°F and 50°F.

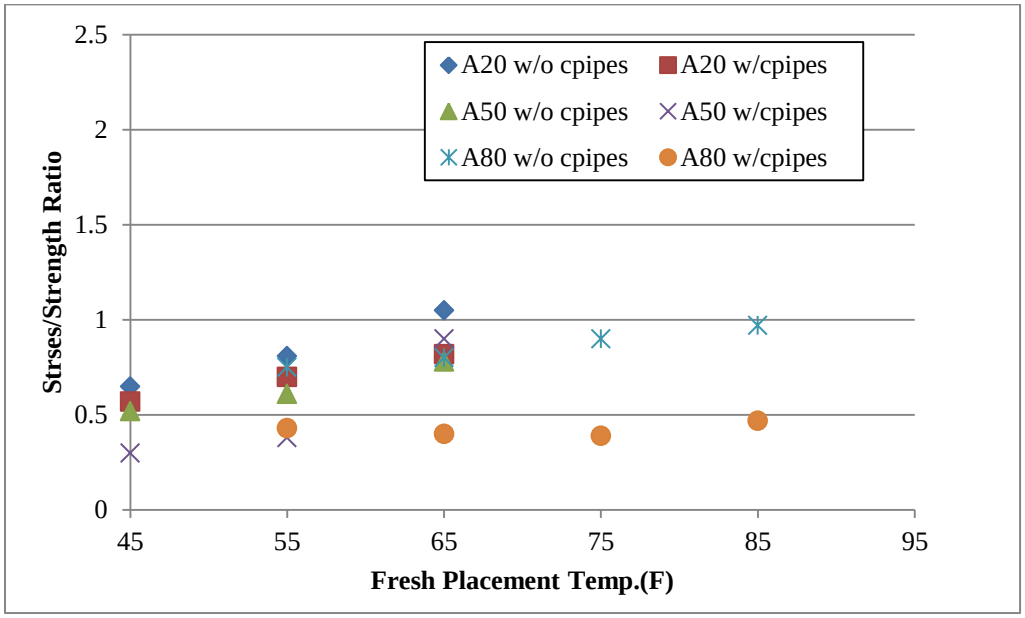

Figure 64 Effect of fresh placement temperature and air temperature from 4C prediction for pier 3 footing without and without cooling pipe used

A series of cooling pipe studies are conducted for baseline of pier 3 footing with c pipes based on the area ratio. The area ratio is defined as the ratio between total surface area of cooling pipes and the concrete area through cross section, which is represented by α. The study incorporates two situations: when α is constant, and when α is not constant.

The area ratio of baseline condition with cooling pipes is calculated as 0.09. When α is constant, the sensitivity study is conducted based on constant pipes layout and varied pipes layout. Under the same layout of cooling pipes condition, analyses regarding different

temperature of water running through pipes and vertical spacing between pipes are calculated. Furthermore, different layout and diameter of pipes are adjusted to keep the constant α.The results are shown in Figure 65 to Figure 66 below. Layouts of pipes are also shown in figures but not in scale.

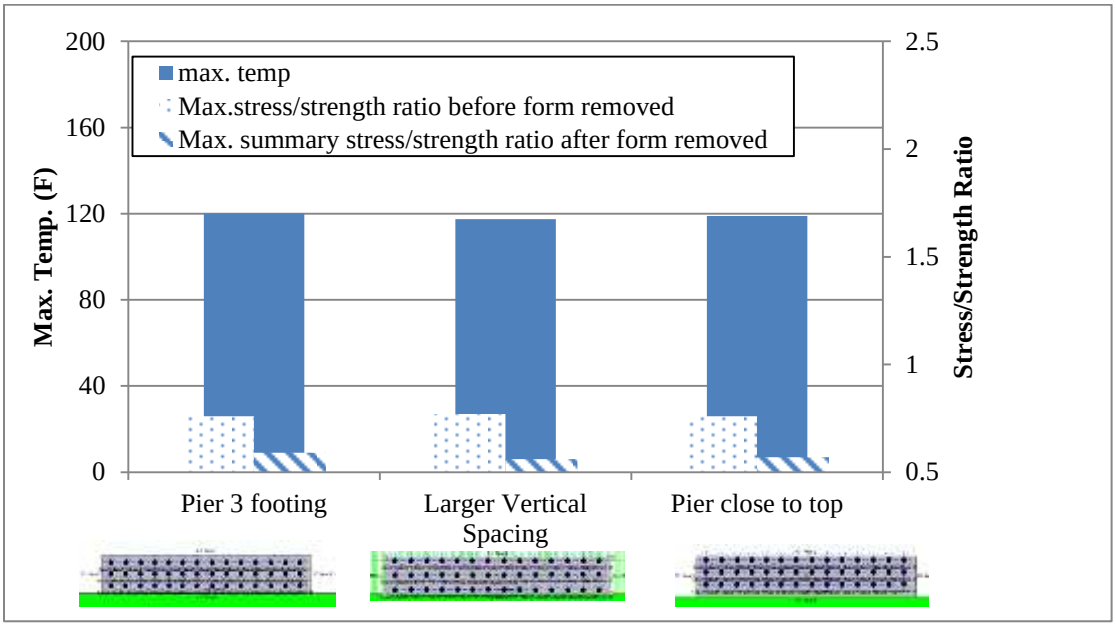

Figure 65 Max temperature and stress/strength ratio results when location of cooling pipes is different while α isconstant

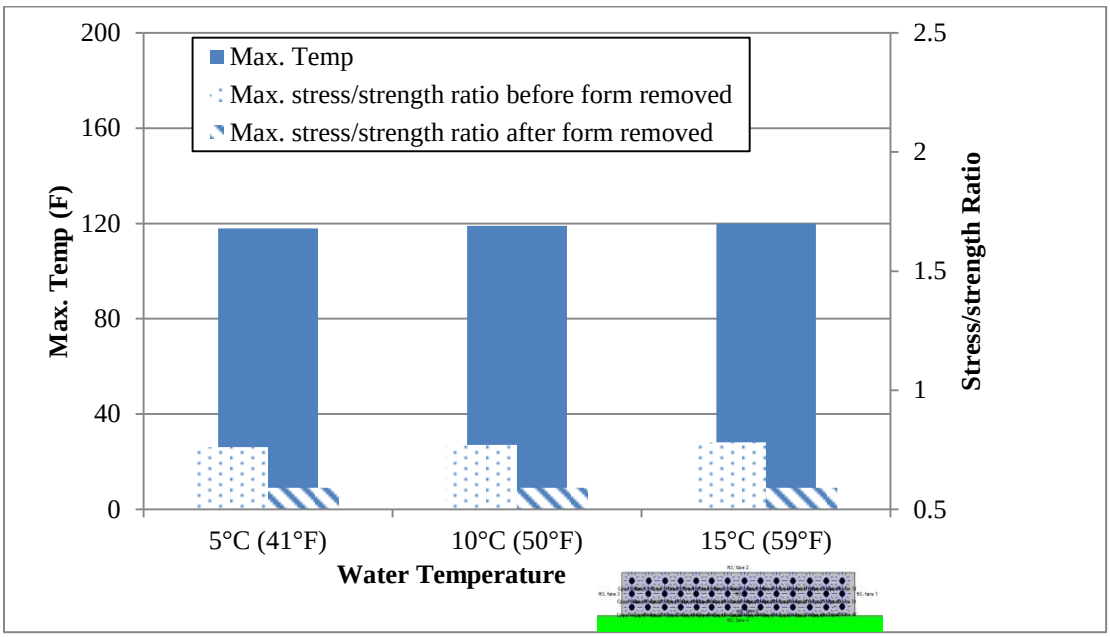

Figure 66 Max temperature and stress/strength ratio results when water temperature is different while location of cooling pipes and α are constant

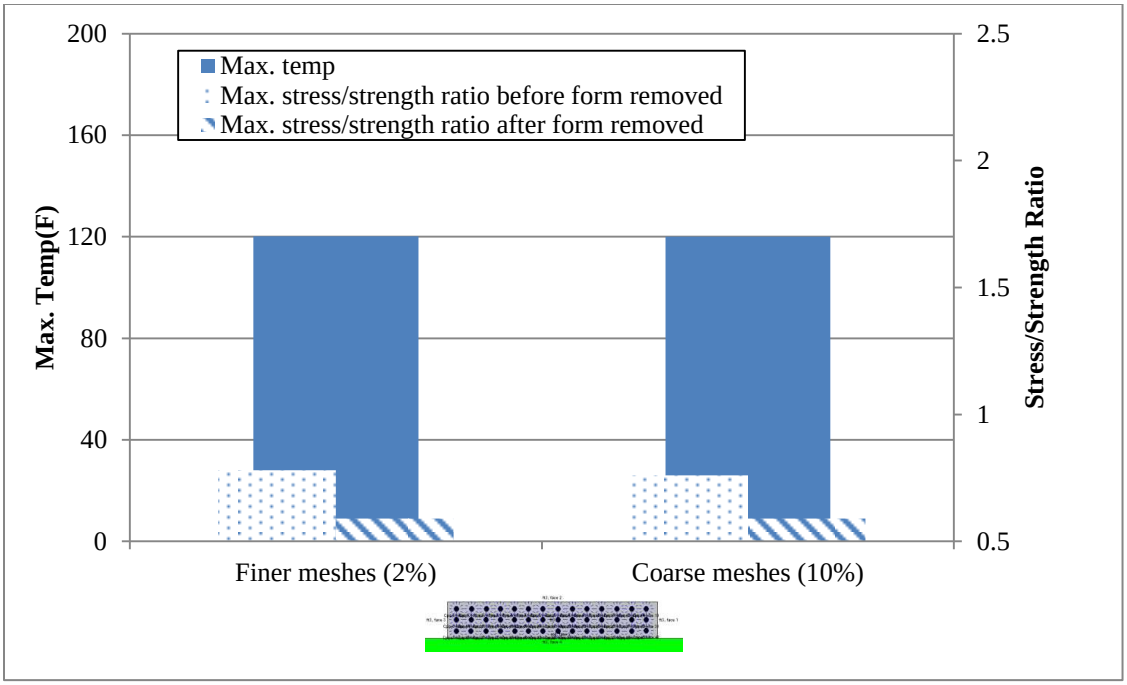

Figure 67 Max temperature and stress/strength ratio results when meshes are different

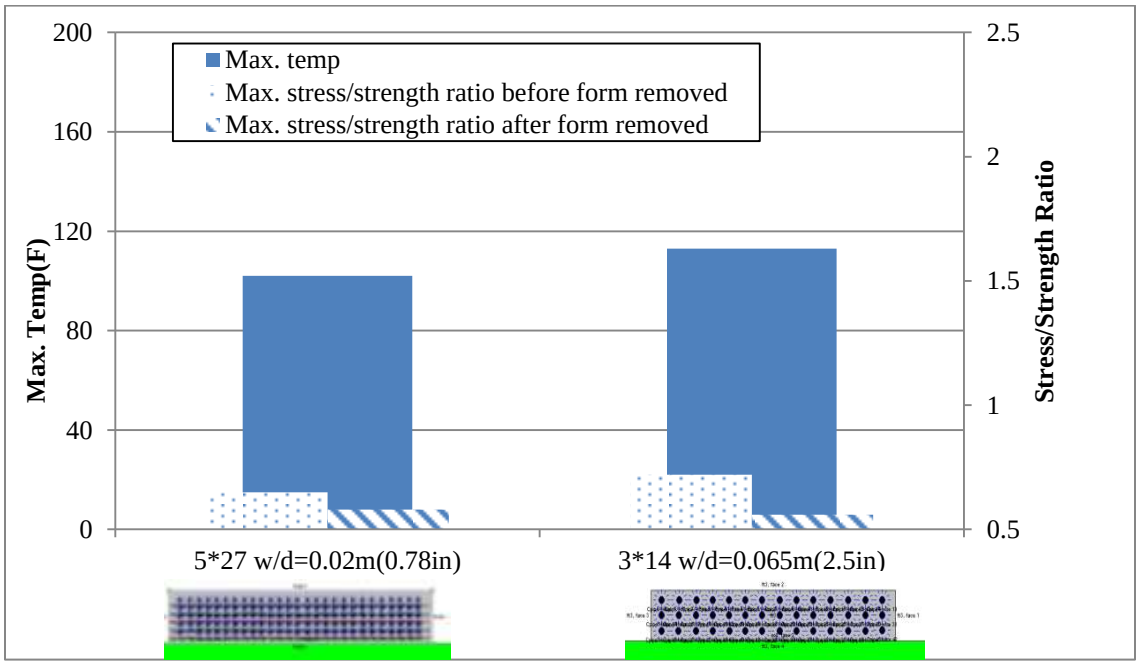

Figure 68 Max temperature and stress/strength ratio results when layout of cooling pipes are different and α are constant

Figure 65 shows the effect of different distance from pipes to surface. Pier 3 footing uses the recommended layout, which was discussed in section 6.6.1. When the distance between pipes are kept constant, moving pier footing closer to top surface or closer to bottom surface have little effect on maximum temperature and stress/strength ratio. Vertical spacing between pipes is increased by 2.6 feet through decreasing distance from pipes to surface. The maximum temperature drops and stress/strength ratio drops 0.3 after form removal. Changing of water temperature in pipes can also slightly affect maximum temperature and stress/strength ratio. Higher water temperature results in about 1°F higher maximum temperature and 0.1 higher stress/strength ratio with increment of 5°C (or 9°F) as shown in Figure 66. Furthermore, finer meshes result in higher stress/strength ratio before form removal in Figure 67. Figure 68 illustrates the effect of numbers of pipes, while α is approximately constant to 0.29. In order to obtain constant α, diameter of cooling pipes are varied. For example, "w/d=0.02m" represents pipes with the diameter of 0.02m. The result indicates that more pipes have better effect on decreasing maximum temperature of concrete and lower the cracking potential.

Results while α is different are shown in Figure 69 and 70. Increasing of horizontal spacing between pipes for pier 3 footing reduces the number of pipes and changes the layout to 3 rows of cpipes with 7 pipes in each row (3*7). The maximum temperature increases approximately 2°F and stress strength ratio increases by 0.2 due to the decrease of α. When the same layout and similar α are used for concrete member, the maximum temperature and stress/strength ratio does not change for longer or shorter pier footings. The result with less cpipes is compared with smaller size concrete (length decrease to 34.75ft), while area ratio α is decreased. The layouts are shown in Figure 69 for less pipes (2*14) and smaller piers (3*14). Less pipes result in higher maximum temperature and higher stress/strength ratio.

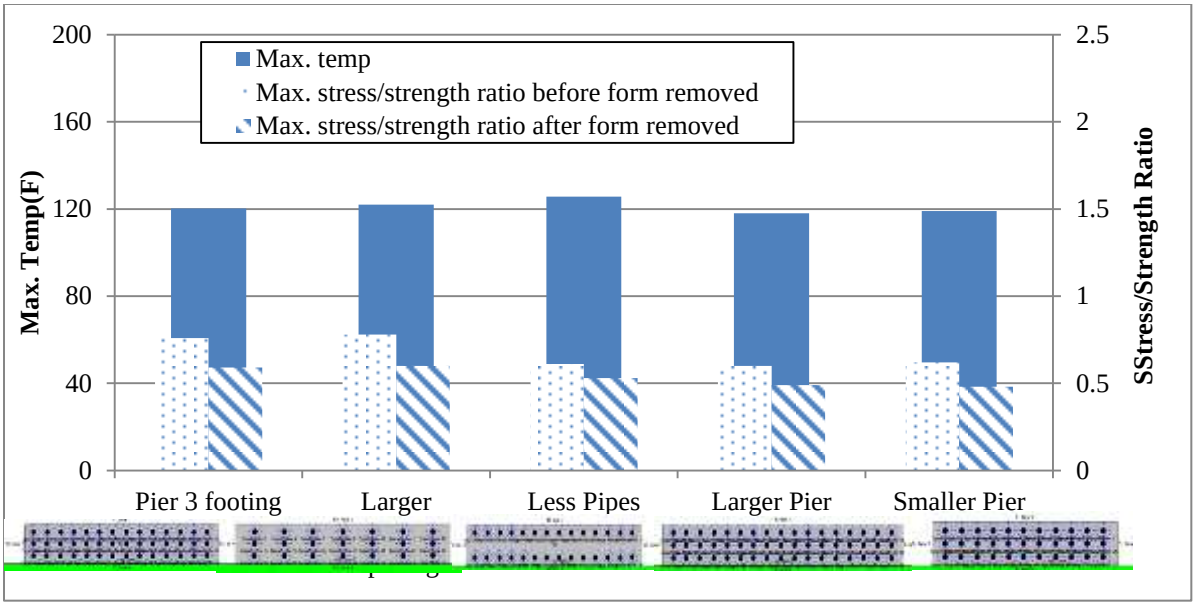

Figure 69 Max temperature and stress/strength ratio results when layout of cooling pipes and α is different

While the layouts of cpipes for pier 3 footing are kept the same, the area ratios are varied by changing the diameter of the pipes shown in Figure 70. The studied diameter may be unrealistic to practice, but the trend should be correct. The maximum temperatures are decreased by increasing the diameter of cooling pipes, and stress/strength ratios before form removal are significantly decreased, especially when diameter is 4 inches. After form is removed, the stress/strength ratio is decreasing but not apparent when the diameter under 15 inches. When the diameter is as large as 15 inches, the cracking potential is increased. The reason probably is larger diameter of cpipes affect the homogeneity of the material, so that the cracking potential is increased. In addition, the flow rate of water is constant, excessively large cpipes can only result in low efficiency and uneconomic practices.

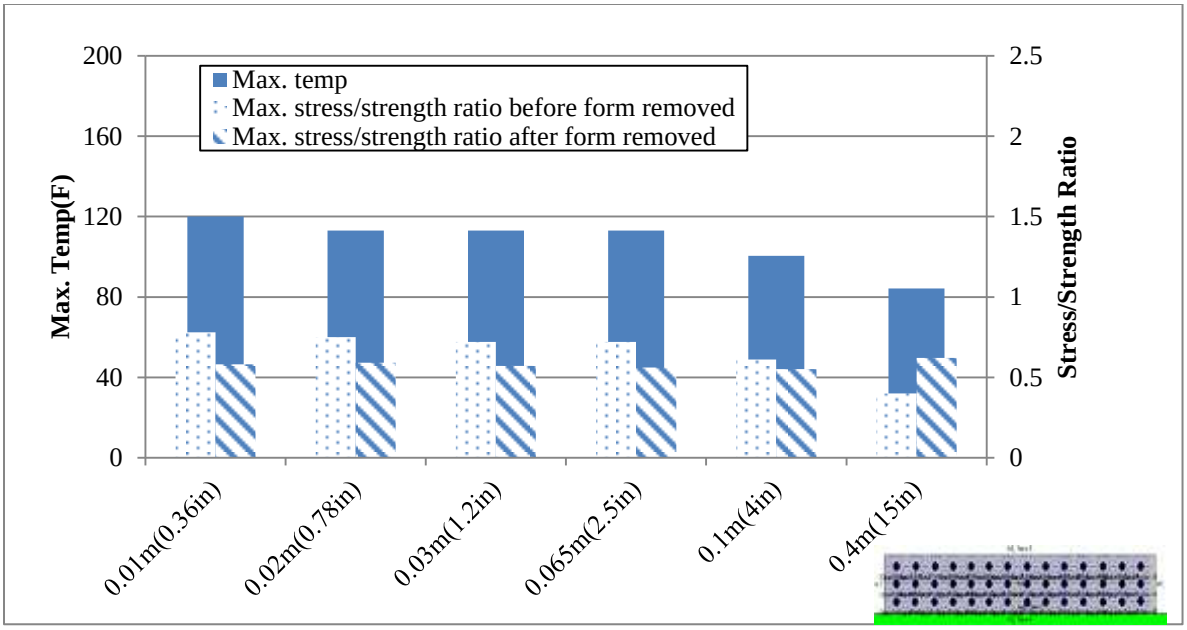

Figure 70 Max temperature and stress/strength ratio results α is different (diameter is different)

Based on above study, area ratio α plays an important role in controlling maximum temperature and stress/strength ratio. Generally larger α gives smaller maximum temperature and less stress/strength ratio. In real construction project, the cooling pipes layout is similar to the study baseline. General relationship between stress/strength ratio and α can be obtained through sensitivity study by changing cooling pipe diameter under the same layout shown as Figure 70.

As mentioned in literature, when the stress/strength ratio is above 0.75, the cracking potential will be considered very high. From Figure 71, the smallest area ratio α is recommended as 0.09 as CTL thermal control plan recommended. This recommended ratio presents the minimum pipes requirement for mass concrete construction. The equation below can also be used to determine the numbers and diameter of cooling pipe when concrete dimensional size is known.

$$\text{Stress/strength Ratio}=0.1509\,\alpha^2-0.4905\,\alpha+0.7928 \qquad \text{Equation 39}$$

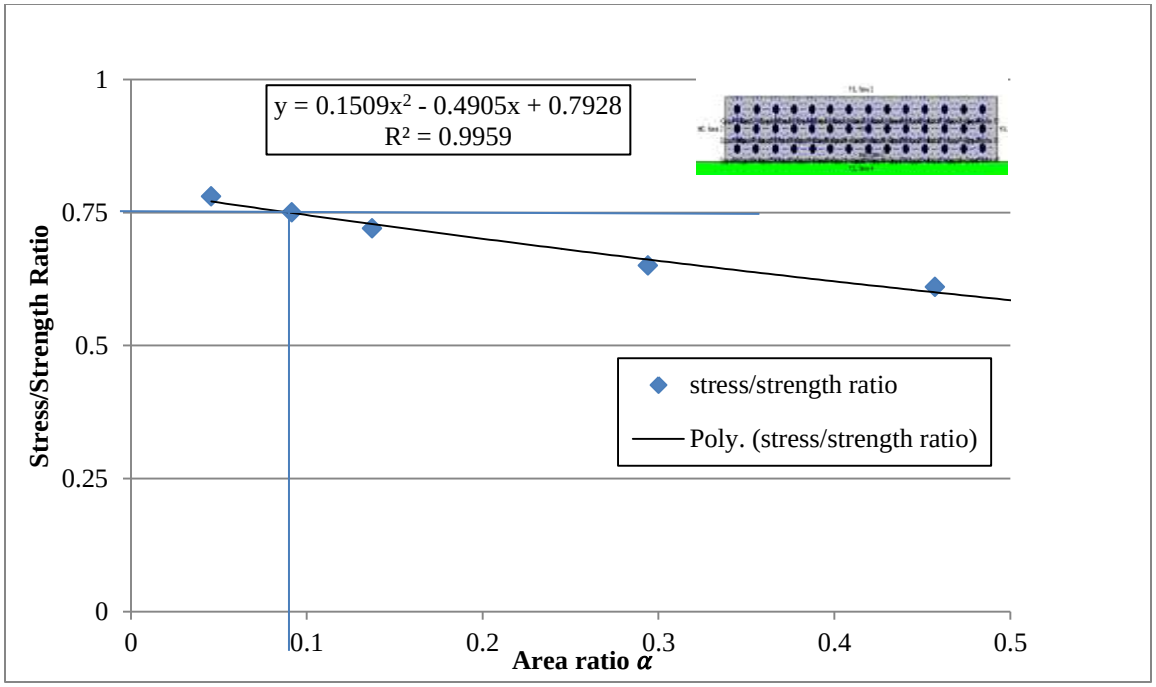

Figure 71 Relationship between area ratio α and stress/strength ratio

6.6 Major Findings of Comparison between Concreteworks and 4C Temp&Stress Results

The sensitivity study using 4C is compared to ConcreteWorks outputs concluded by Jacob Shaw. (Shaw, 2011) Following findings could be summarized:

- With same concrete and construction condition used for computer calculation, similar trends were found that maximum temperature and maximum temperature difference increased with:
    - The increase of the least dimensional size
    - The increase of fresh Placement Temperature in winter (October).
    - The decrease of form removal time
    - The increase of cement content
- The results of maximum temperature and maximum temperature difference between two computer programs were different. ConcreteWorks concludes higher temperature difference, which calculates the temperature difference between maximum predicted temperature at the center and minimum predicted temperature at the surface. The

temperature at the surface was not often used in construction. The surface temperature was significantly influenced by ambient temperature. 4C program outputs could adjust the minimum temperature location at sensor, which is about 3 inches deep from the surface. The temperature values were higher than surface temperature, and resulted in less maximum temperature difference.

- The mix design sensitivity study was not reliable from 4C program. In order to get accurate prediction using 4C, measured concrete properties should be provided. ConcreteWorks was developed considering the influences of different mix design. The results should be reasonable. Even the trend from 4C was confirmed by ConcreteWorks program, the maximum concrete temperatures were significantly different. It is recommended to use measured heat development and compressive strength in4C program when mix design of concrete is changed.
- Several forming method and insulation method were provided in ConcreteWorks. The analysis using 4C confirmed the recommendations from ConcreteWorks. 4C provided more options on forming and insulation materials.
- The effect of placement date = was also confirmed by ConcreteWorks. Generally, winter construction developed smaller maximum temperature difference and less cracking potential. In summer, mass concrete construction had lower cracking potential, when fresh placement temperature under 70°F.
- ConcreteWorks can not calculate the tensile stress/strength ratio, while 4C program can provide iso-curve development during analysis period. Iso-curve results for the case, pier 3 footing with cooling pipes, were presented at time 12 hours, 48 hours, 96 hours, 168 hours and 312 hours in Appendix E. High temperature always occurred in the center of concrete structure. Figure 72 shows the iso-curve of temperature development for half-right cross section of concrete member at 48 hours when concrete reached peak temperature during analysis period. Highest stress/strength ratio occurs during first 24 hours at edges and corners of concrete member. With time passing, the higher stress/strength ratio is likely to appear at the center of the structure. Examples of iso-curve on stress/strength ratio are shown in Figure 73 and Figure 74.

The iso-curve graphic results are generated by 4C program. User could zoom in and out the cross section to get readable iso-curve results.

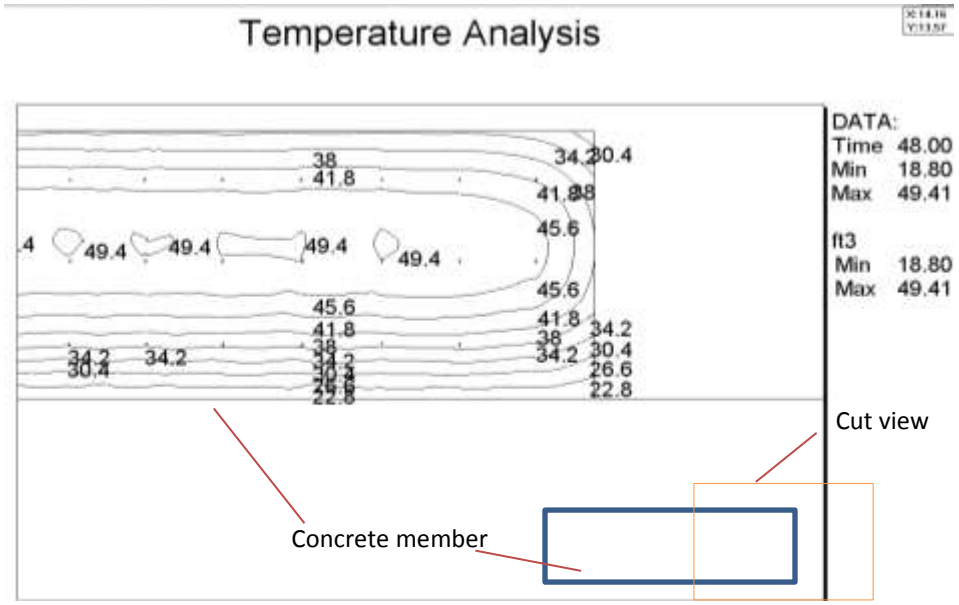

Figure 72 Example temperature development iso-curve results for right-half cross section of pier 3 footing with cooling pipe applied at 48 hours (not in scale)

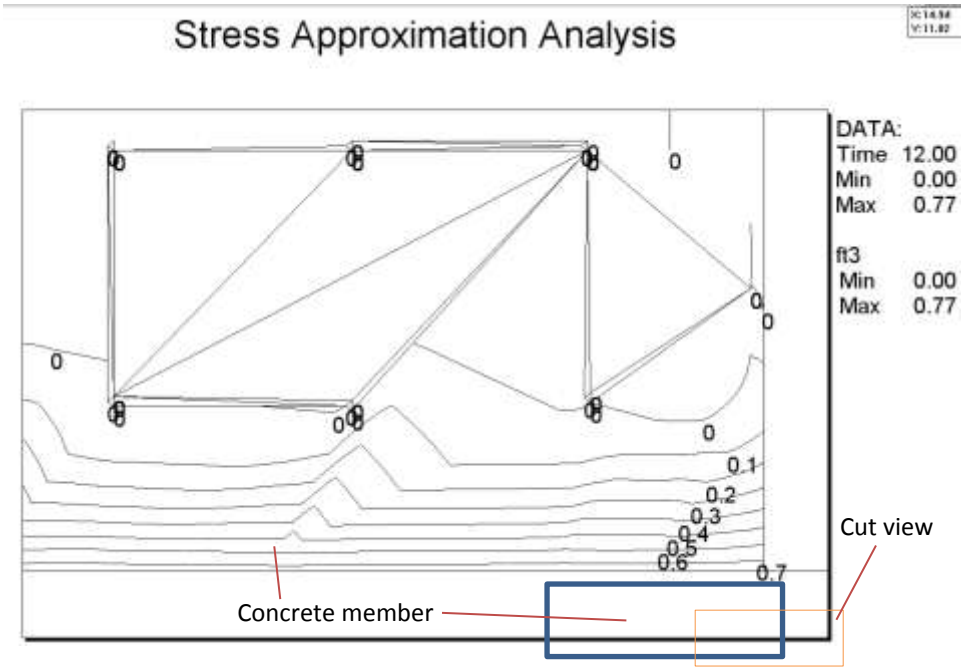

Figure 73 Example tensile stress/strength iso-curve results for lower right corner of cross section of pier 3 footing with cooling pipe applied at 12 hours(not in scale)

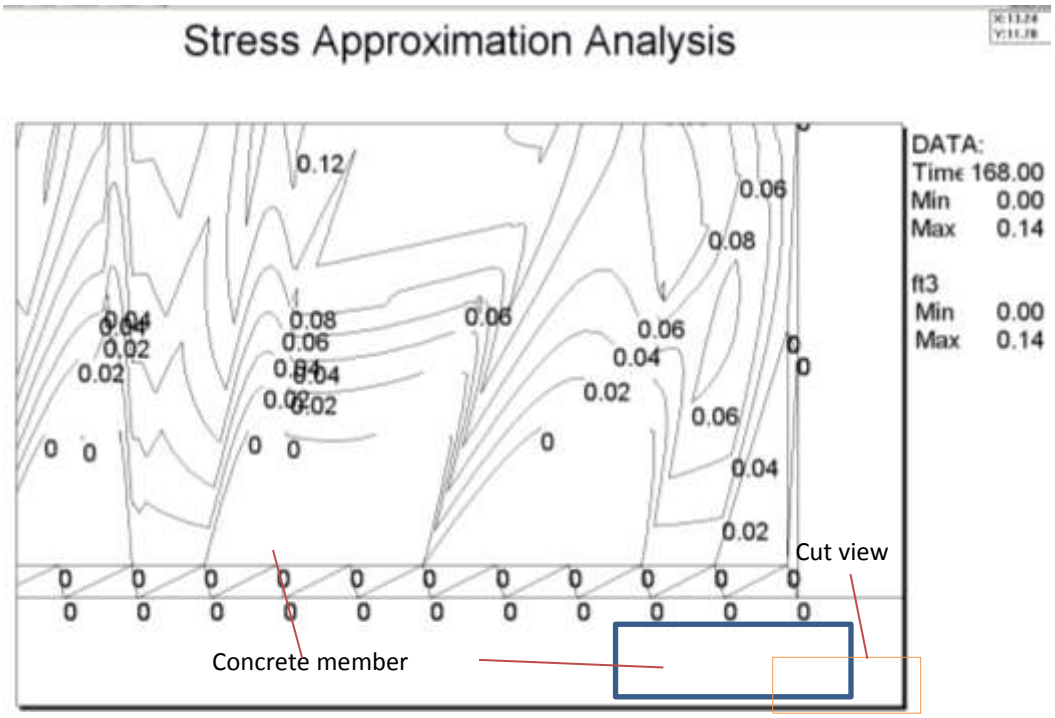

Figure 74 Example tensile stress/strength iso-curve results for lower right corner of cross section of pier 3 footing with cooling pipe applied at 168 hours(not in scale)

CHAPTER 7 CASE STUDY

In this chapter, results are developed and calculated based on I-80 Bridge project. The predicted temperature difference and stress/strength ratio are discussed for footings and columns in the project. The recommendations of maximum temperature difference to avoid high cracking potential can be obtained from case studies. After analyzing I-80 footings and columns, the effect of fresh placement temperature and concrete least dimension is investigated. A relationship between these two inputs to maximum temperature, stress/strength ratio can be obtained. At last, a case study for US-34 Glenwood Bridge construction is conducted as additional thermal-control recommendation.

7.1 I-80 Bridge Case Study

Sensitivity studies help to understand how 4C Temp&Stress works, how factors affect the thermal behavior of mass concrete, and how reliable 4C results is. Case studies continue to explore the relationships between some factors and mass concrete thermal cracking. The first case study is conducted on footings and columns of the I-80 Bridge, on which no cooling pipes were used. The material underneath all mass concrete members is assumed to be soil, which assumes no restrains exist during concrete hardening period. Ambient temperatures are different for each concrete member based on historical weather data (Weather Underground, 2012). The analysis results are concluded with maximum concrete temperature, maximum temperature difference, and stress/strength ratio shown in Appendix F. The stress/strength ratios are discussed in four time intervals based on temperature difference limits provided by the Iowa DOT developmental specifications.

Maximum temperature difference is set as limitation to avoid thermal cracking in construction. In CTL Group thermal control plan, the maximum temperature difference limit is higher than the Iowa DOT developmental specifications as shown in Figure 75.

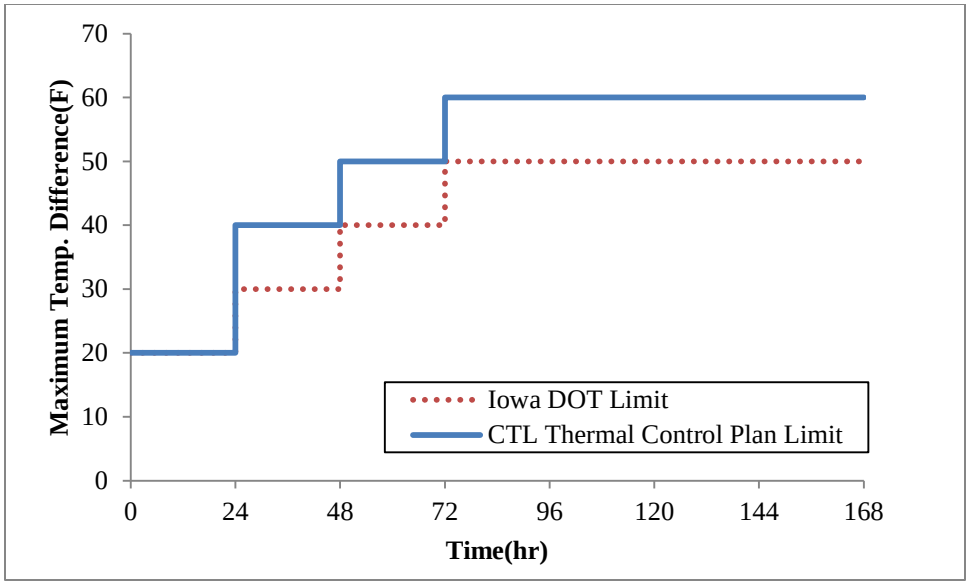

Figure 75 Comparison of maximum temperature difference limit from CTL and Iowa DOT

7.1.1 Study on Maximum Temperature Difference and Stress/Strength Ratio

Footings and columns are used to investigate the relationship between maximum temperature difference and stress/strength ratio. In order to evaluate maximum temperature difference, the definition of concrete minimum temperature is important. 4C program predictions allow the minimum temperature to be taken at surface or at 3 inches below surface, thus the maximum temperature difference can be obtained both at the surface and the sensor. Comparison between maximum temperature difference for actual measurements and 4C prediction are provided in Table 32. Positive values under prediction-actual comparison mean predictions are underestimated. Several actual temperature differences for I-80 bridge project are over DOT temperature difference limit but not over CTL limit. However, these members do not present thermal cracking. The 4C program predicted temperature difference at sensor location, pier 3, 6, and column challenge both limits shown in Table 32. However, no thermal cracking is observed in I-80 Bridge project. The Iowa DOT limitation is conservative.

Table 32 Summary of maxium temperature difference & difference between computer calculated (4C) and actual (CTL)

	Maximum Temp Diff. of Concrete (F)			Temp. Diff between Actual measured (CTL) and 4C prediction (F)	
Concrete Member	**Measured**	**4C(surface)**	**4C(sensor)**	**Temp. Diff between measured to 4C sensor**	**Temp. Diff between surface and 3 in below surface (sensor)**
Pier 1 Footing	34.2	46	27	7.2	19
Pier 2 Footing	34.2	58	44	-9.8	14
Pier 3 Footing	56.5	67	50	6.5	17
Pier 4 Footing	51	54	42	9	12
Pier 5 Footing	50.4	69	58	-7.6	11
Pier 6 Footing	50.4	72	60	-9.6	12
Pier 1 Column	15.3	36	27	-11.7	9
Pier 2 Column	38.7	67	53	-14.3	14
Pier 3 Column	28.7	78	64	-35.3	14
Pier 4 Column	34	58	43	-9	15
Pier 5 Column	39.5	55	42	-2.5	13
Pier 7 Column	50.4	101	88	-37.6	13
Pier 10 Column	52.2	77	66	-24.8	11

The relationship between maximum temperature differences and maximum stress/strength ratios during a certain time interval are shown in Figure 76 to Figure 77. The graphs combine the relationship for different concrete structure, footing and columns while subbase is soil, when minimum temperature is obtained from sensor or surface. Four time intervals are selected based on the Iowa DOT provided information as 0 to 24 hours, 24 to 48 hours, 48 to 72 hours, and after 72 hours. The cracking potential is generally increasing with the increase of temperature difference, no matter where the minimum temperature is measured.

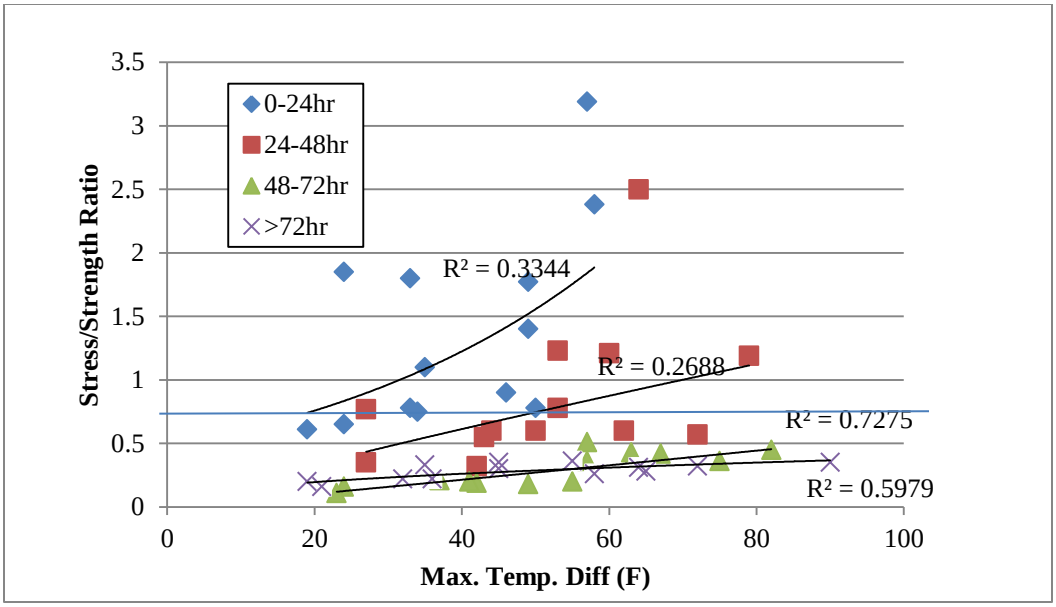

Figure 76 Relationship between temp. diff &cracking potential soil substructure (min. temp. at sensor)

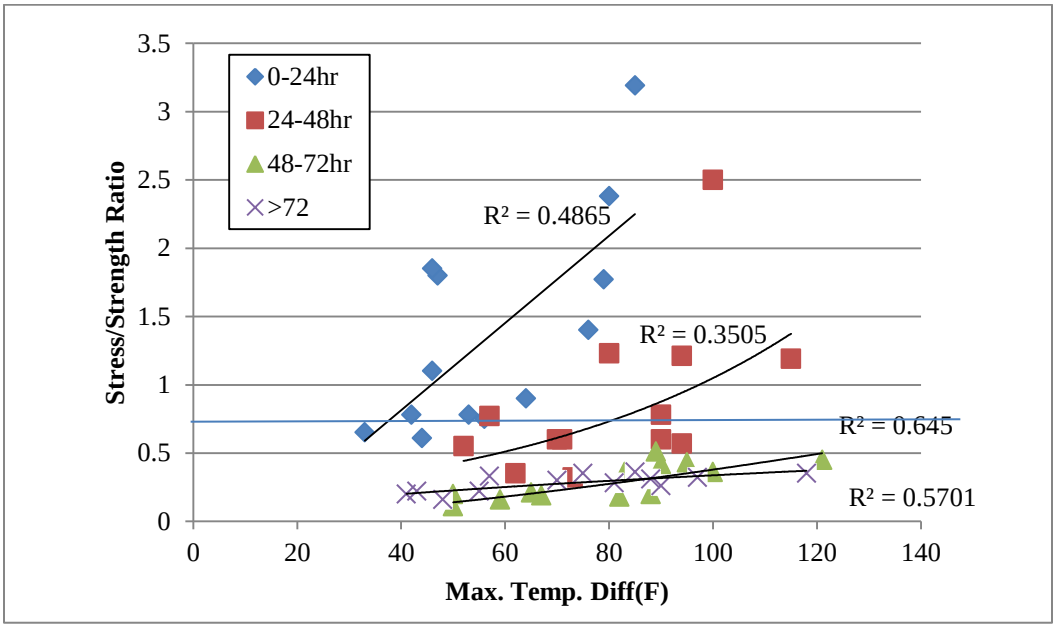

Figure 77 Relationship between temp. diff &cracking potential soil substructure (min. temp. at surface)

The stress/strength ratios during first 24 hours are mostly over 1, which indicates very high potential of cracking to occur. Generally, the peak stress/strength ratio is achieved around 20 hours. However, the high stress/strength ratio during this period is considered as not reliable enough for soil subbase material due to concrete setting and elastic properties.

Generally the final set of fresh concrete with fly ash occurs at 10 to 13 hours after placing. During first 12 hours, the concrete is still hardening, not enough strength could be gained during this period and the concrete is still restrained by substructure and formwork. Even the tensile stress/strength ratio is large; the concrete might be too elastic to propagate cracks (Ge, Dec. 2003). Other factors delaying setting time includes decreasing concrete temperature, using slag, excessive plasticizer, and water to cement ratio. The peak stress/strength ratio around 20 hours after casting may due to concrete final set. Furthermore, a concrete member may be divided into several sections to cast instead of one piece of concrete simulated in this study. The stress/strength ratio will decrease if the dimensions of concrete reduce. For example, a concrete column is simulated in 4C program as a one-pour structure, but the column is actually casted in 3 times in practice. Each time casting will wait until the bottom section is set.

When peak maximum temperature of concrete occurs, large temperature gradient will occur, and result in higher stress/strength ratio. After final set, concrete temperature keeps rising and the concrete will experience peak temperature around 48 hours. Large temperature difference may occur at this time which results in large stress/strength ratio. Thus, the stress/strength ratio during 24 to 48 hours should be considered as important criteria on evaluation of mass concrete thermal cracking when a structure is placed on soil substructure.

The trends in the above figures indicate that the stress/ strength ratio is significantly increases as the temperature difference increases, especially during 24- 48 hours for concrete substructures of soil. The temperature difference relationship with ratio has similar trends no matter the temperature difference was obtained from surface or sensor. After 48 hours, the stress/strength ratios are under 0.5 no matter how large the temperature differences are in these trials. Combined relationship of maximum temperature and maximum stress/strength ratio during different two time intervals are shown in Appendix E. Lower R^2 is exhibited due to combining two different structure elements.

When substructure is concrete, the relationships between maximum temperature difference and stress/strength ratio are shown in Figure 78 and Figure 79 for footings and columns. The results indicate the stress/strength ratios are low during the first 24 hours and increasing with time. The highest stress/strength ratio generally occurs after 72 hours for

concrete substructure instead of 24-48 hours for soil substructures. In first 48 hours after concrete is placed on concrete substructure, most data shows the stress/strength ratio is lower than 0.5. With the time increasing, the stress/strength ratio is increased, and indicates high cracking potential.

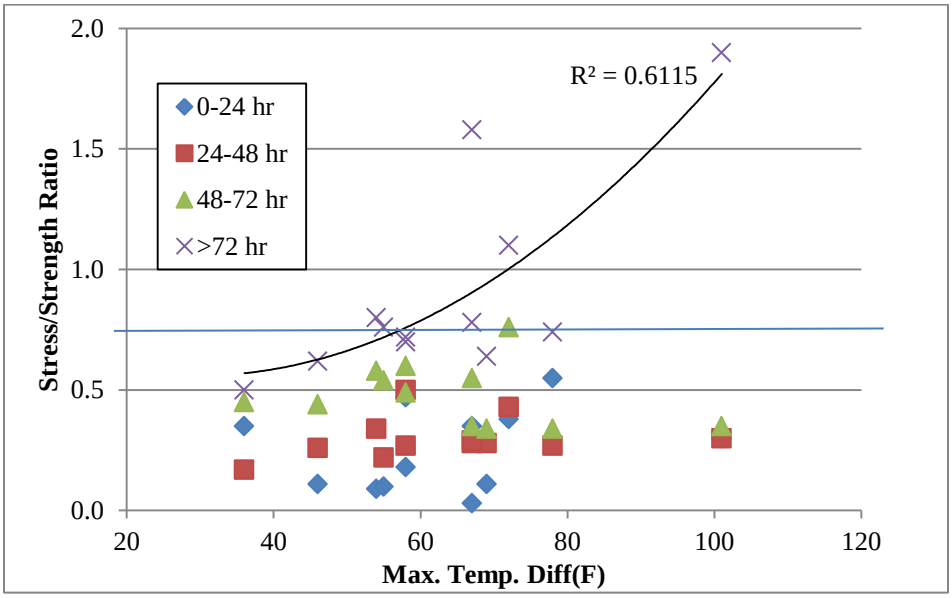

Figure 78 Relationship between temp. diff &cracking potential concrete substructure (min. temp. at surface)

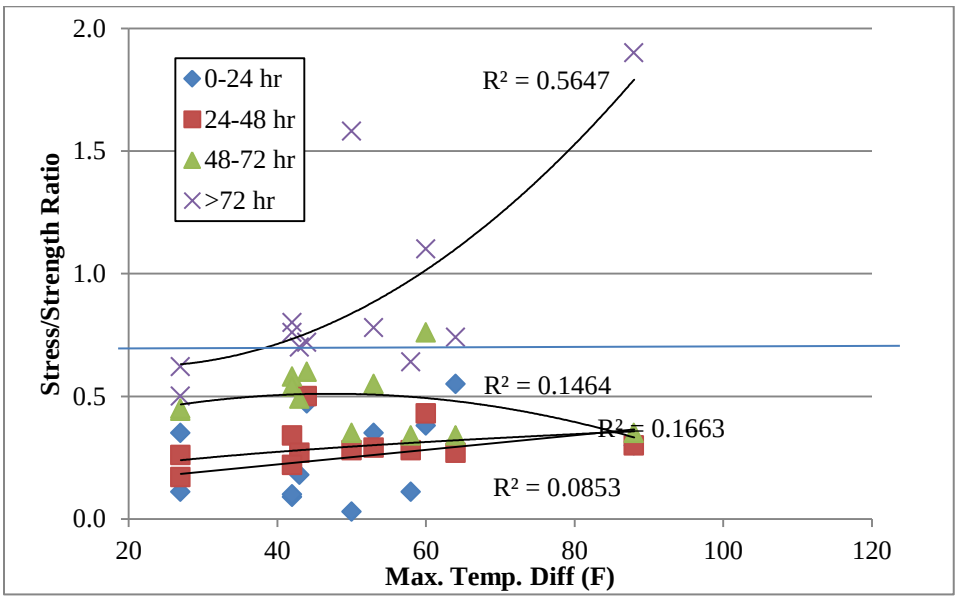

Figure 79 Relationship between temp. diff &cracking potential concrete substructure (min. temp. at sensor)

From Figure 76 to Figure 79, the maximum temperature difference can be estimated and summarized in Table 33 below. Iowa developmental specifications indicate the maximum temperature difference of 50°F was conservative for footing structures constructed on soil and all concrete structures on concrete. Columns constructed on soil may be impractical using 4C program.

Table 33 4C predicted temperature difference limit based on case study

		Temp. Diff Limit(F)	
Substructure	**Structure**	**Surface**	**Sensor**
	footings	64	50
Soil	columns	57	38
Concrete	footings &columns	62	40

7.1.2 Relationship between Maximum Temperature Difference and Stress/Strength Ratio

Maximum temperature difference is found to be an important factor to evaluate mass concrete cracking potential. The relationship between maximum temperature difference and stress/strength ratio are investigated using a statistical computer software system JMP in this section. The study is based on the results of 4C prediction for pier 1 to 6 footings, pier 1 to 5 columns and pier 10 columns in the total of 13 concrete structures. Each structure is modeled in 4 different time intervals as discussed in section 7.1.1. The time intervals are labeled as 1 through 4. Time interval 1 represents the analysis period during 0 to 24 hours, time interval 2 the time between 24 and 48 hours, and time interval 3 is 48 to 72 hours. The fourth time interval is all analysis periods after 72 hours. Two substructure conditions, soil and concrete, are considered when the temperature differences are evaluated at sensor location.

In order to establish a relationship between the maximum temperature difference and stress/strength ratio, the total observations of 52 ratios are assumed to be a random sample generated from some population. The normal quartile plots of the ratios by time interval are shown in the top two graphs of Figure 80. The ratios are highly skewed for time interval 1 and 2 when substructure is soil and time interval 4 when substructure is concrete. The

skewness is due to the fact that the variances of the ratios for 4 time intervals are not homogeneous. Thus, transformations may be attempted to stabilize the variances of the stress/strength ratio distributions. The natural log transformation is commonly used to normalize the distribution and establish equal variance in these situations. The normal quartile plots of the transformed data, displayed in the bottom two graphs in Figure 80 show fairly similar slopes. The variance of transformed stress/strength ratios decreases and the slopes of the plots are approximately parallel.

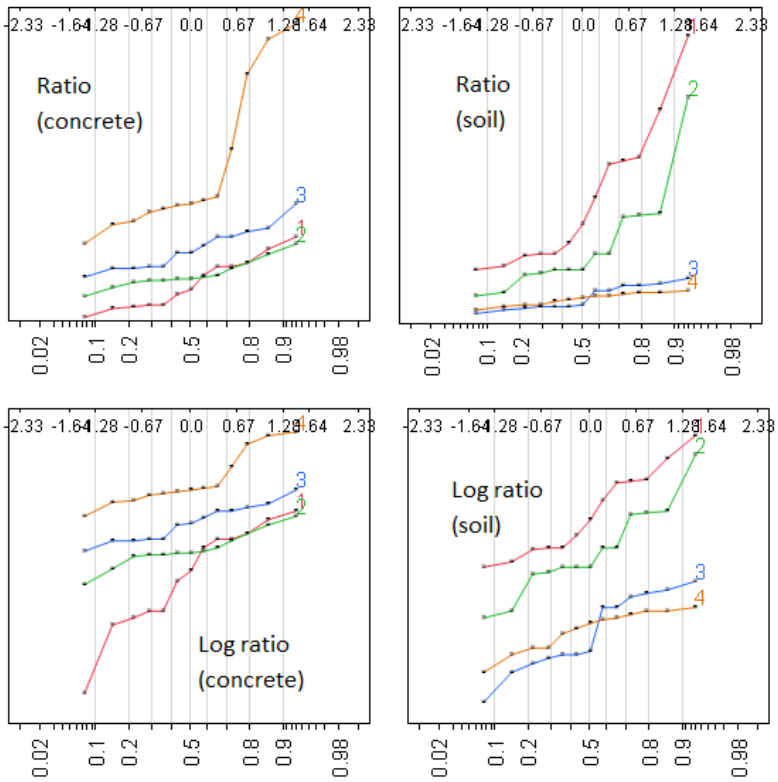

Figure 80 Normal Quintile Plot of stress/strength ratio for different subbase material

Covariance model is a general linear model with a continuous outcome variable and two or more predictor variables. The analysis of covariance (ANCOVA) is a merger of ANOVA and regression for continuous variables, which is based on linear regression. The assumption for ANCOVA is homogeneity of regression which requires the relationship between covariate and the dependent variable should be similar across all groups of the independent variables.

The covariance models are considered to study the relationship of the maximum temperature difference and the log transformed stress/strength ratio by time interval where the time interval is considered as the category variable. This method assumes the transformed ratios are normally distributed and homoscedastic. Straight-line models with equal slopes and unequal intercepts are first fitted for the data. Using these models, the null hypothesis of unequal variances can be tested. This is rejected with a F Ratio equals to 3.3113 and p-value equals to 0.028 for soil base for soil subbase, and with F Ratio equals to 8.0266 and p-value equals to 0.0002. The tests of the variance are equal are conducted as Figure 81 shown. Concrete subbase demonstrated unequal slopes corresponding to the results from tests of variance summarized in Table 34 below.

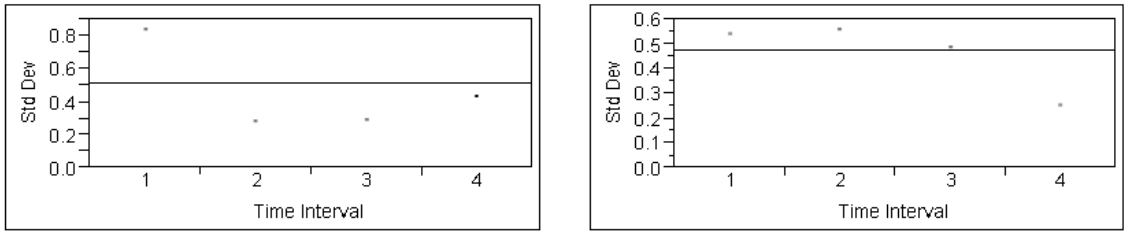

Log ratio (concrete) Log ratio (soil)

Figure 81 The variance results of stress/strength ratio

Table 34 Summary for the tests of equal slope

	Source	DF	Sum of Squares	Mean Square	F Ratio
Log(ratio)	Model	7	27.151456	3.87878	28.9856
for soil	Error	44	5.887973	0.13382	**Prob > F**
	C. Total	51	33.039429		<.0001*
Log(ratio)	Model	7	21.797642	3.11395	18.6396
for	Error	44	7.350663	0.16706	Prob > F
concrete	C. Total	51	29.148305		<.0001*

Approximately equal slopes are observed for log ratio with soil subbase in Figure 80. Line 3 and line 4 represent the ratios during time intervals of "48-72 hours" and ">72 hours". The ratios have similar trend even the lines are interacted. The interactions between other

lines are not significant. Thus, the straight lines with different intercepts and common slope could be fit for this case. Considering the influence of first 24 hours ratios, the interaction is significant and the unequal slopes will be found from log ratio with concrete subbase. Thus the models will be developed with equal slope for soil subbase, and unequal slope for concrete subbase.

The covariance models are expressed in Equation 40 to Equation44 for concrete substructures. R^2 value of the models is 0.748. The t-test results indicate time interval, the cross effect of time interval and temperature difference is significant where the p-values are larger than 0.05. The p-value is p= 0.9993 for the F-test of lack of fit. Hence, we do not reject the null hypothesis that the model is correct. R is the maximum stress/strength ratio during that period, and T is the maximum temperature difference during that time interval.

$\ln(R) = -3.3493+0.0465 \times T$	(0-24 hours)	Equation 40
$\ln(R) =-1.5406+0.0063 \times T$	(24-48 hours)	Equation 41
$\ln(R) =-0.4037-0.0084 \times T$	(48-72 hours)	Equation 42
$\ln(R) =-1.3038+0.0192 \times T$	(>72 hours)	Equation 43

The models of soil base condition are fitted with equal slope assumption as shown in Equation 45 to Equation 48. The R^2 value is 0.80. The null hypothesis of equal slope is rejected for both time interval and temperature difference with F ratio of 56.29 and 30.95, and p-value smaller than 0.0001. The p-value is p= 0.8352 for the F-test of lack of fit. Hence, we do not reject the null hypothesis that the model is correct.

$\ln(R) = -0.5019+0.0186 \times T$	(0-24 hours)	Equation 44
$\ln(R) =-1.2619+0.0186 \times T$	(24-48 hours)	Equation 45
$\ln(R) =-2.2287+0.0186 \times T$	(48-72 hours)	Equation 46
$\ln(R) =-1.9915+0.0186 \times T$	(>72 hours)	Equation 47

The cracking potential increases as ln(R) increasing. The critical ln(R) is -0.25, where very high cracking potential occurs. Figure 82 indicates the relationship between model prediction of the stress/strength ratio and temperature difference during different time interval. The lines represent the predicted ratios from models. The points are ratios from 4C prediction, which are used to establish the prediction models. Additional comparisons between predicted stress/strength ratio from established models and calculated stress/strength ratio from 4C program are shown in Appendix F.

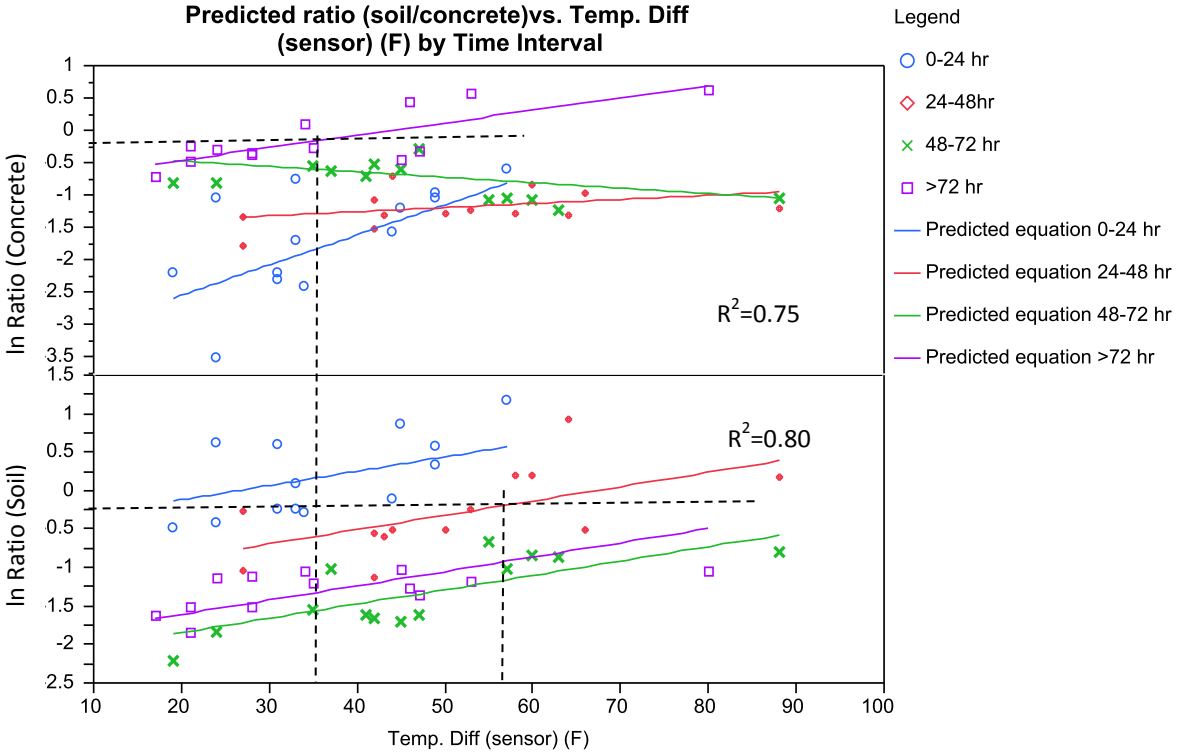

Figure 82 Relationship between maximum temperature difference and stress/strength ratio by time interval

The results show that the temperature limit is 53 °F during 24 to 48 hours when substructure is soil. The cracking potential is always high before 24 hours and low after 48 hours. When substructure is concrete, low cracking potential is exhibited during first 72 hours. After 72 hours, the cracking potential increases as maximum temperature difference increases. The maximum temperature difference limit is 32°F as shown in Table 34.

Table 35 Comparison of maximum temperature difference limits

Condition	Substructure	Temp. Diff Limit(F)
Prediction Model	Soil	57
	Concrete	35
Iowa Limitation		50
Literature		35

7.1.3 Influenced Factors of Maximum Temperature Difference

Due to the importance of maximum temperature difference to mass concrete cracking potential, the prediction accuracy and factors influencing maximum temperature difference are investigated in this section. First, the comparison between actual measured maximum temperature difference by CTL Group and predicted maximum at sensor location are presented in Table 35. Average difference between predicted and actual maximum temperature difference is -9.6°F, which means predicted maximum temperature is higher in most cases. Some predictions are much larger (above 30° F), such as pier 3 column and pier 6 column. The depth of those concrete members is large, the maximum temperature is higher. In actual construction projects, better cooling may be taken to control the temperature difference which is not specified in projects report. The predicted difference of maximum temperature difference between sensor and surface is 13.6°F in average, which verified by sensor location study in Chapter 6.

Table 36 Difference between maximum temperature difference measured in field and predicted by 4C

Concrete Member	Maximum Temp Diff. of Concrete			Temp. Diff between Actual measured (CTL) and 4C prediction (F)	
	Measured	4C (surface)	4C (sensor)	Temp. Diff between Measured to 4C sensor	Temp. Diff between surface and 3 inches below surface (sensor)
Pier 1 Footing	34.2	46.0	27.0	7.2	19.0
Pier 2 Footing	34.2	58.0	44.0	-9.8	14.0
Pier 3 Footing	56.5	67.0	50.0	6.5	17.0
Pier 4 Footing	51.0	54.0	42.0	9.0	12.0
Pier 5 Footing	50.4	69.0	58.0	-7.6	11.0
Pier 6 Footing	50.4	72.0	60.0	-9.6	12.0
Pier 1 Column	15.3	36.0	27.0	-11.7	9.0
Pier 2 Column	38.7	67.0	53.0	-14.3	14.0
Pier 3 Column	28.7	78.0	64.0	-35.3	14.0
Pier 4 Column	34.0	58.0	43.0	-9.0	15.0
Pier 5 Column	39.5	55.0	42.0	-2.5	13.0
Pier 7 Column	50.4	101.0	88.0	-37.6	13.0

Based on above case study results, effects of thickness of concrete and environmental temperature to maximum temperature differences are discussed after analyzing the data by statistic computer program, JMP 9. The environmental temperature is defined as average ambient temperature during a day in the following discussion. Figure 83 indicates that generally with the increasing of depth of concrete, the maximum temperature difference increases. Increase of ambient temperature may not have a linear relationship due to the data points being randomly scattered. However, it cannot conclude ambient temperature does not have influence on temperature development. If compared the environmental effects at the same depth of concrete as shown in Figure 84, the lower average ambient temperature has higher maximum temperature, when the depth is greater than 5 feet. When the depth is less than 5 feet, the maximum temperature does not have obvious effects on concrete temperature. Optimum average ambient temperature is in the range of 50°F to 60°F. Under this condition,

mass concrete could be constructed as deep as 7.5 ft with practical length and width. With increasing of ambient temperature, shallower mass concrete is recommended to construct.

Fresh placement temperature has a more clear relationship with depth of concrete and maximum temperature compared to average ambient temperature. The result is shown in Figure 83. Depth of concrete is one of the critical criteria to produce different maximum temperature difference. In this case study, fresh placement temperature is not presented clearly due to small range of different fresh placement temperature exhibited. Another case study to evaluate the effects of fresh placement temperature and depth to concrete maximum temperature difference will be discussed in section 7.2. Figure 85 indicates no linear relationship exists between fresh placement temperature, average ambient temperature and maximum temperature difference.

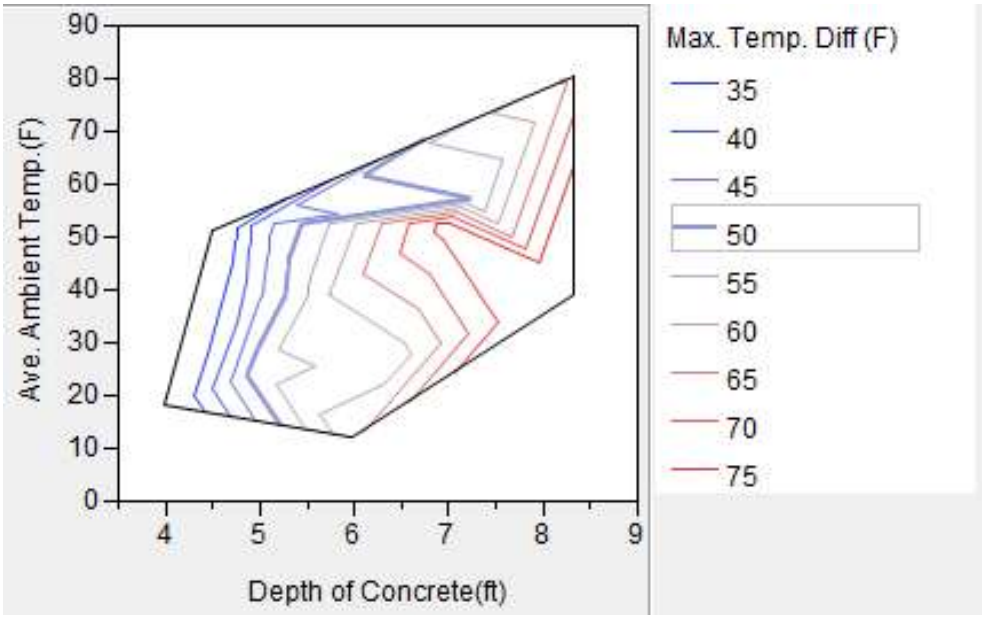

Figure 83 Contour plot of relationship of depth (least dimension) of concrete and ambient temperature to maximum temperature difference (from JMP 9)

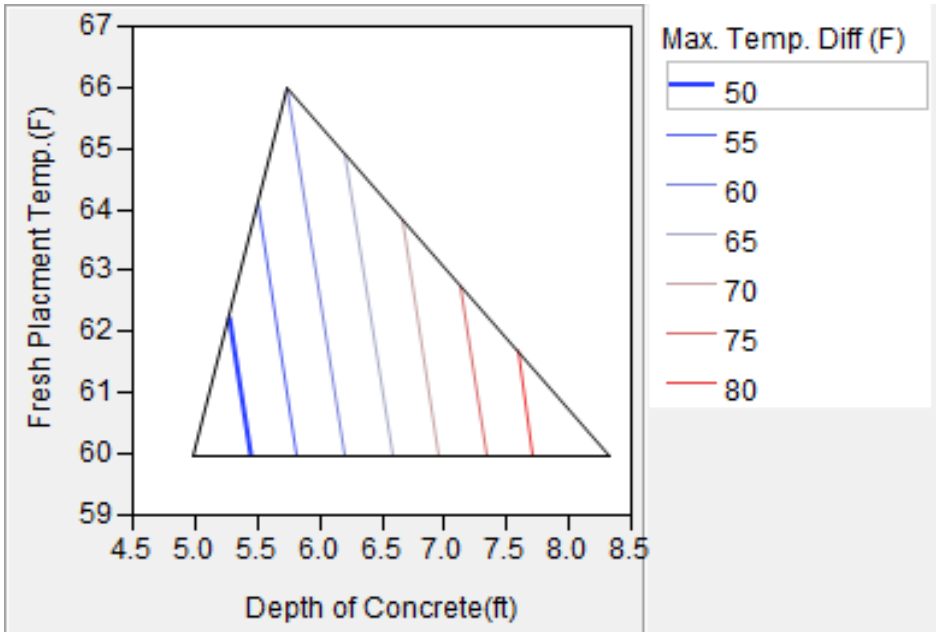

Figure 84 Contour plot of relationship of depth (least dimension) of concrete and fresh placement temperature to maximum temperature difference (from JMP 9)

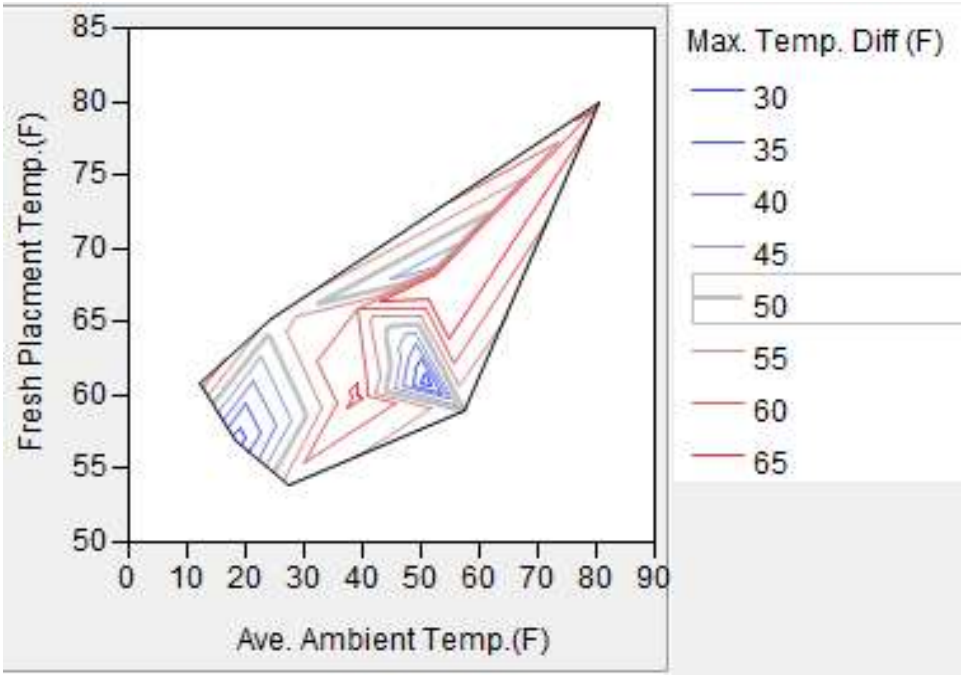

Figure 85 Contour plot of relationship of fresh placement temperature and average ambient temperature to maximum temperature difference (from JMP 9)

7.2 Case Study on Effects of Fresh Placement Temperature and Least Dimensions to Mass Concrete

Section 7.1 case studies indicate thermal cracking potential is related to maximum temperature and maximum temperature difference. Figure 83 to Figure 85 indicate fresh placement temperature and depth of concrete have significant effect on maximum temperature difference. Ambient temperature has a relatively obscure relationship to maximum temperature difference. Since relatively low ambient temperature is beneficial for mass concrete construction as found in section 7.1 and two Iowa mass concrete projects (I-80 Bridge and US-34 Bridge) were more likely to build in cold weather, the ambient temperature influence is neglected for further study. A further case study on effect of fresh temperature and depth of concrete to maximum temperature and maximum temperature difference is studied in this section. Statistical analysis is performed shown in Figure 86 and Figure 87 and Appendix F. Residual plots in Figure 86 and Figure 87 show linear regression models are appropriate for the data of maximum temperature and maximum temperature difference, while depth and fresh placement temperature are considered variables. Depths of concrete are chosen as 5 feet, 6 feet, 7 feet and 10 feet. Fresh placement temperatures are chosen from 40°F to 90°F with 10 degree increments. The statistical results in Appendix F indicate data are normal distribution. A linear regression models can be built for maximum temperature and maximum temperature difference. Surface plot in Figure 88 and Figure 89 are graphical representation of the relationship among three variables.

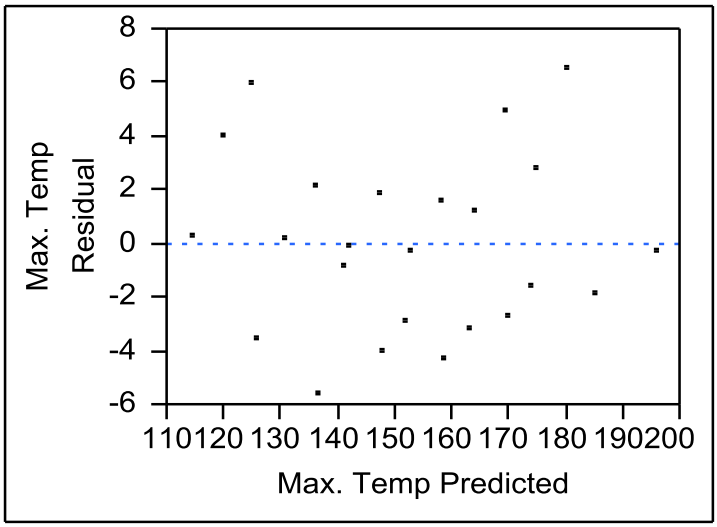

Figure 86 Max. temp. residual plot by predicted (from statistical software)

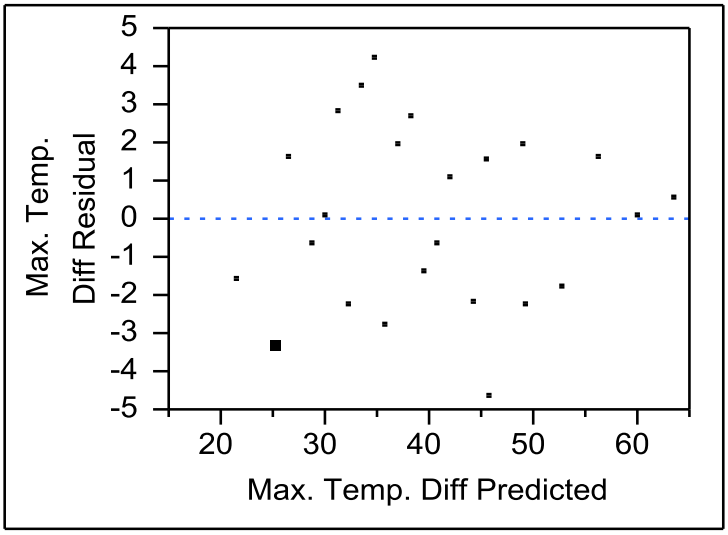

Figure 87 Max. temp. diff. residual plot by predicted (from statistical software)

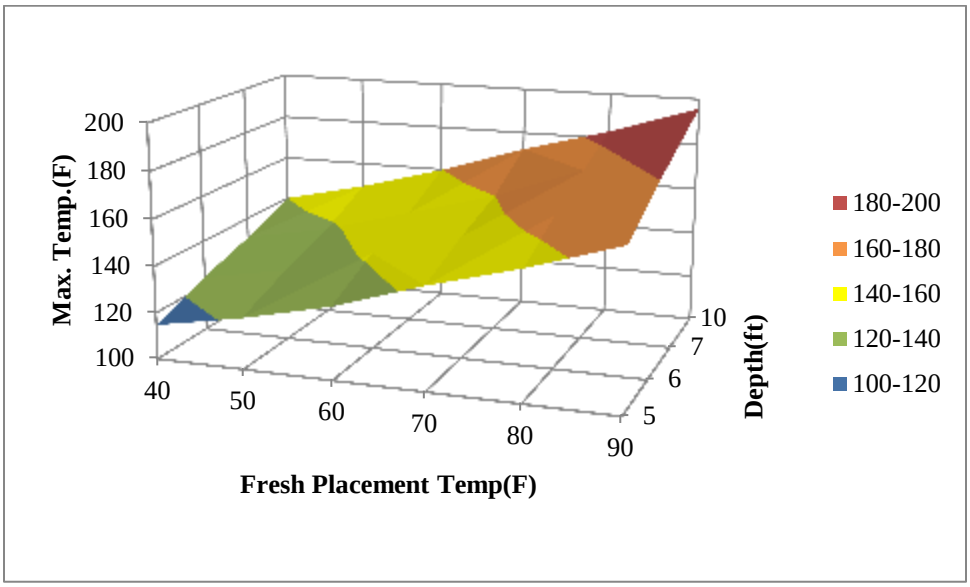

Figure 88 Surface plot for max. temp., depth and fresh placement temperature

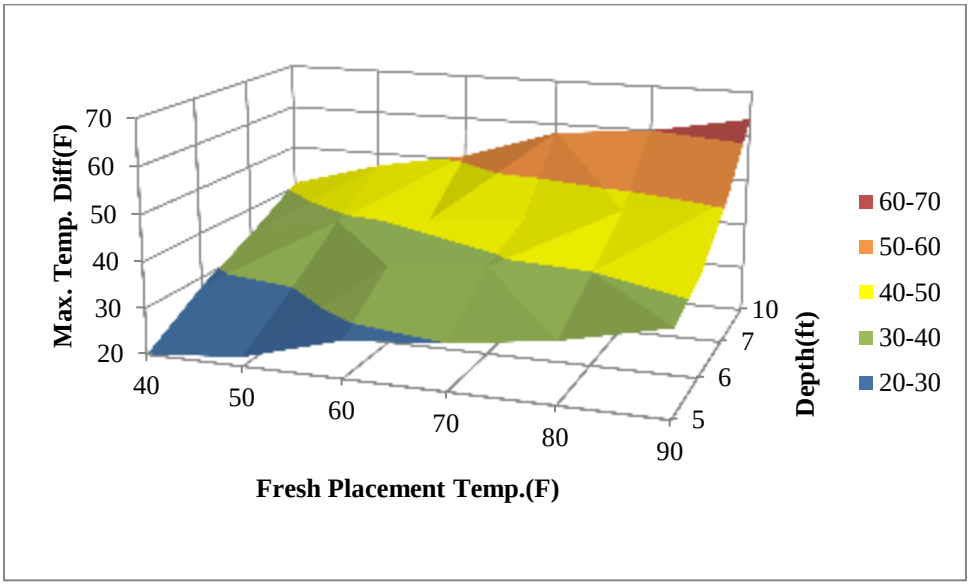

Figure 89 Surface plot for max. temp. diff., depth and fresh placement temperature

The linear model expressions can be established as Equation 7.3 and 7.4 below:

$$T_{max} = 43.9871+5.2714 \times D+1.1044 \times T_f \quad \text{Equation 49}$$

$$T_{max\ diff.} =16.7829+4.8214 \times D+0.3564 \times T_f \quad \text{Equation 50}$$

, where

Tmax- maximum temperature of the concrete (°F)

Tmax diff.- maximum temperature difference of concrete structure (°F)

D - the least dimension, depth of concrete (ft)

Tf - fresh placement temperature (°F)

R^2 values for two equations are 0.978 and 0.958, which indicate the established linear models reflect the correct relationship between these parameters. Stress/strength ratios are not proper to fit linear model from residuals plot as observed in appendix F. Non-random patterns are obtained for residual plots, and a better fit for a non-linear model are suggested. Contour plots for maximum temperature, maximum temperature difference, and stress/strength ratios relationship to fresh placement temperature and depth of concrete are also shown in Appendix F.

7.3 US 34 Case Study

4C Temp&Stress program has been validated be many projects listed in Chapter 2 and verification analysis in Chapter 5. Applying 4C program to future mass concrete construction projects is expected. This section describes two examples of US 34 Bridge project, which are pier 1 footing and pier 4 footing. The bridge approached on relocated US 34 over Missouri river at Glenwood, and was planned to be constructed from late February, 2012. The concrete mix design in this project uses the same as I-80 Bridge project. Footing dimensions are obtained in construction plans. The remaining input assumptions as made are presenting in Table 36. Ambient temperatures are based on average February temperature from historical weather station. Fresh placement temperature and form removal time are assumed based on I-80 Bridge concrete members, which were constructed around February.

Table 37 Changed 4C inputs for US 34 Case study

	Pier 1 footing	**Pier 4 footing**
Dimensional Size(ft*ft*ft)	13*12*5.5	51*20*6
Ambient Temp(F)	min:-8°C(17.6°F)	max:2°C(-37.8°F)
Fresh Place. Temp.	15.6°C(60°F)	
Insulation material	Same as I-80 Bridge	
Form removal time	200 hours	
Insulation removal	168 hours	

Analysis results are shown in Figure 90 to Figure 93. All cases do not experience high cracking potential. Since the stress/strength ratio of pier 1 footing is still increasing after 300 hours, the results of longer analysis time up to 500 hours for stress/strength ratio is presented in Appendix G, which indicates after 480 hours (20days), the cracking potential starts to decreasing. The highest stress/strength ratio after 300 hours was 0.53, still does not exceed high cracking possibility.

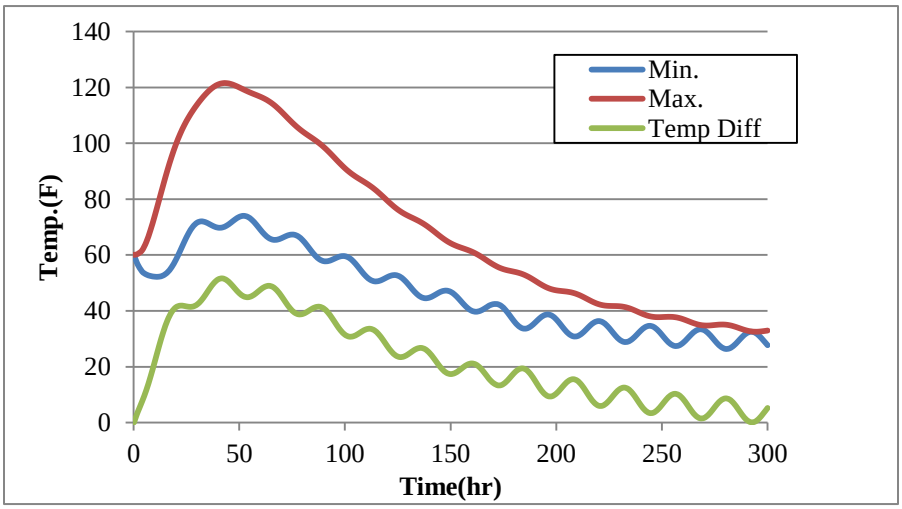

Figure 90 US34 pier 1 footing temperature results using 4C

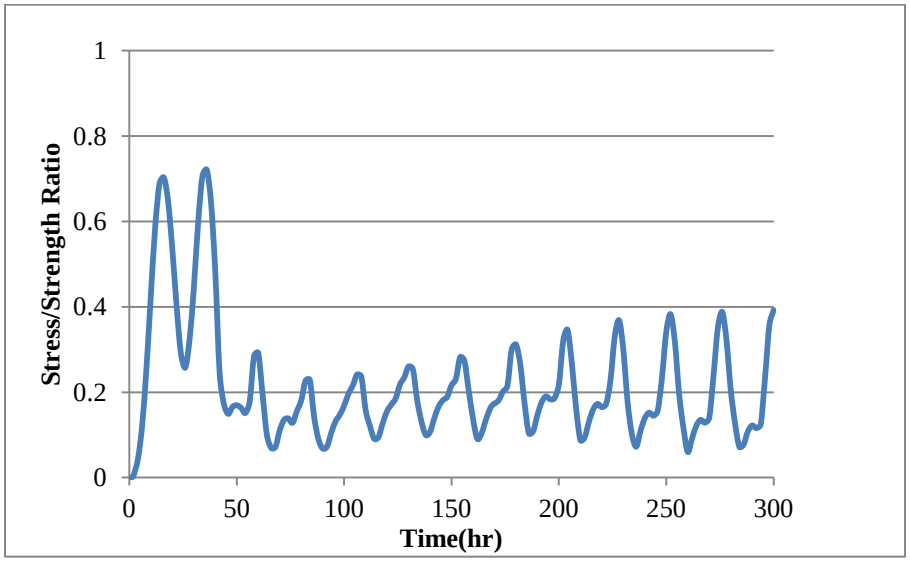

Figure 91 US34 pier 1 footing stress/strength ratio result using 4C

CTL Group indicates pier 4 footing is recommended to use cooling pipes. Case study on whether cooling pipes used are compared in Figure 92 and Figure 93. Maximum temperature drops around 20°F under cooling pipes condition. Maximum stress/strength ratio drops by 0.2 as well, which indicates application of cooling pipes have effectively controlled thermal cracking potential.

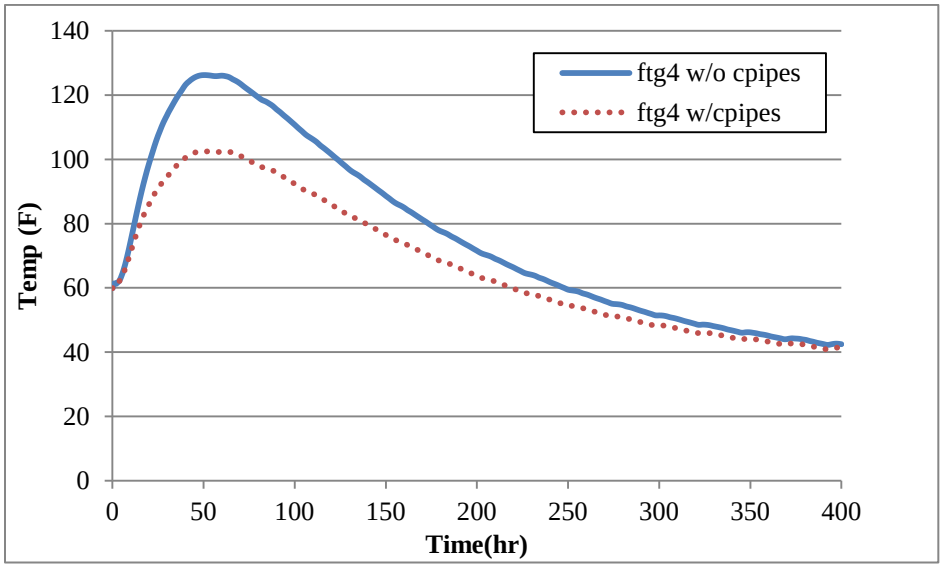

Figure 92 Maximum temperature results for pier 4 footing with or without cooling pipes

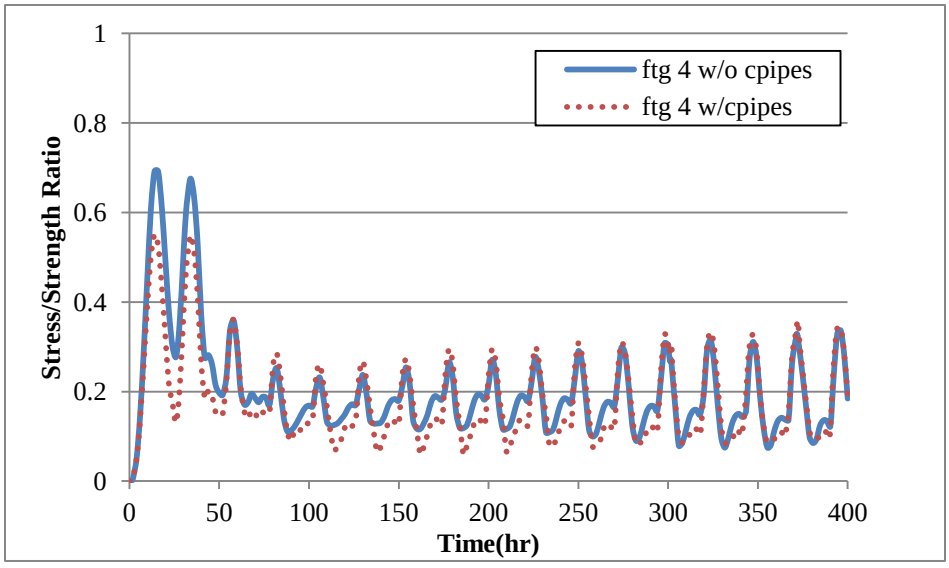

Figure 93 Stress/strength ratio results for pier 4 footing with or without cooling pipes

US 34 case study shows that pier 1 footing creates approximately the same peak stress/strength ratio with smaller dimensions (especially smaller depth). The reason may be the length and widths were smaller with relative thick depth, which limits generated heat to gradually dissipate through the concrete member. Under the same construction condition, with the same depth, longer and wider mass concrete structure will produce less stress/strength ratio.

CHAPTER 8 CONCLUSIONS, RECOMMENDATIONS AND FURTURE RESEARCH

8.1 Conclusions and Recommendations

Excessive heat of hydration in mass concrete placements may cause concrete damage due to induced thermal gradient in concrete. Mass concrete brings many challenges in regard to thermal control. However, the current specifications and guidance of mass concrete construction were varied for different states or even not developed for some states. This study investigated the parameters that might affect the thermal behavior of mass concrete using 4C Temp&Stress computer software. The objectives are to illustrate the effects of the concrete ingredient, construction, and environmental factors by conducting sensitivity studies and case studies, to provide recommendations for mass concrete based on the Iowa DOT specification. In literature, it was found using low-heat mix design, precooling, or post cooling construction practices could reduce the thermal cracking potential of mass concrete structures. The following studies verified the literature findings and provide additional recommendations for future construction. The findings from verification study on 4C program are summarized in section 8.1.1. The findings from sensitivity study and case study are summarized in section 8.1.2 and 8.1.3.

8.1.1 Conclusion and Recommendations from Verification Study

The software program has been verified through case studies to assure reliability recommendations. The following conclusions are drawn through the study:

- By comparing temperature development curves between 4C prediction and actual measurements from I-80 Bridge project, it can be concluded that the 4C program underestimated the maximum temperature development of the concrete, and overestimated the maximum temperature difference of the concrete. Using our inputs, the 4C predictions were statistically significantly different for maximum temperature difference in comparison to actual measurements, especially for stems.
- Additional statistical analysis indicated 4C program performed especially well from 0 to 72 hours in terms of prediction accuracy. The accuracy during this period is

important because the temperature of concrete approaches the peak, which may produce high thermal stress due to large temperature gradient.

- The assumptions of ambient temperature and sensor location might lead to inaccurate 4C prediction. The average predicted difference was 8.74°F for maximum temperature and 15.29°F for maximum temperature difference.
- The 4C program produced large maximum temperature differences.
- Current temperature difference limit in the Iowa DOT specification was conservative. The case study indicated that even the temperature difference over the Iowa DOT limitation, the concrete still performed as not very high cracking potential.

8.1.2 Conclusion and Recommendations from Sensitivity Study

Based on the results of sensitivity study and the comparison to ConcreteWorks, the major findings were determined as follows:

- Maximum temperature and maximum temperature difference increased with:
  - Increased depth of concrete
  - Increased fresh placement temperature (hot weather concreting)
  - Decreased fresh placement temperature (cold weather concreting)
  - Decreased form removal time
  - Increased cement content
- Generally, hot weather mass concrete construction had lower cracking potential when the fresh placement temperature was limited to 70°F. Combining current specifications and our findings, in order to effectively reduce cracking potential, it is recommended that the fresh placement temperature be limited to the range of 50°F to 70°F.
- Maximum temperature development didn't change very much for larger concrete, no matter if insulation was applied or not.
- Etha foam, plast foam (10mm), foil with 5 mm air space, and plastic foil were recommended to use as top insulation, which were resulted in lowest cracking possibilities in analysis.

- Form bord (25 mm), plywood, plywood formwork, and timber formwork were recommended to use as side formwork, which were resulted in lowest cracking possibilities in analysis.
- The R-value of the materials should be considered when designing the placement insulation. Generally, higher R-value resulted in lower maximum temperature difference and higher maximum temperature. However, cracking potential may not be low.
- Compared to concrete substructure, soil subbase caused a decrease in cracking potential after formwork removed due to the less restraint.
- The use of supplementary cementitious materials, high thermal conductivity aggregate and low coefficient of expansion aggregate could efficiently reduce the cracking potential.
- Cooling pipes efficiently controlled the maximum temperature development and reduced the thermal cracking potential. The layout and numbers of cooling pipes was significantly important in terms of reducing cracking potential and construction cost. Recommended surface area ratio was 0.09 with spacing information as described in Appendix B.
- Thermal cracking was more likely to occur at middle-bottom of concrete long edge during first 24 hours, because the highest stress/strength ratio occurs as shown in iso-curve results shown in Figure 73. With time passing, the cracking is likely to appear at the center of the concrete structure.

8.1.3 Conclusion and Recommendations from Case Study

Two sets of case study on I-80 Bridge and US 34 Bridge confirmed the previous findings in literature and sensitivity study. I-80 Bridge case study indicated the current maximum temperature difference limits in the Iowa specification was conservative for mass concrete with soil substructure. It was observed that an acceptable cracking potential was predicted when the temperature difference limits were exceeded, however, more results should be collected and calculated from different projects to validate current limits. However, the limit of temperature difference may still lead to thermal cracking, when the substructure was

concrete. The relationships between maximum temperature difference and stress/strength ratio were provided in Figure 82, which could be used to identify the maximum temperature difference limit to avoid thermal cracking.

Linear prediction models on temperature development considering depth and fresh placement temperature for a specific mix design were investigated as Equation 49 and 50 shown. The mix design used to create the models was approved by the Iowa DOT and was on the I-80 Bridge and US 34 Bridge projects. These models could be used as a quick estimation on concrete temperature development without performing program analysis and laboratory testing only on this concrete mix and similar projects.

8.2 Future Research

Based on above conclusions, the following recommendations are proposed for future research:

- Verify model-predicted inputs by laboratory testing such as heat development, elastic modulus, and creep.
- Study on the prediction model of temperature development considering ambient temperature for Iowa approved mix designs.
- Study on different mix designs and create additional temperature prediction models.
- Economical study on different mix design and construction procedures, that have been shown to reduce the cracking potential.
- Develop a new computer program on early age thermal behavior of mass concrete prediction.
    - The new program contains database for different mix design, aggregate effects, and mechanical properties of concrete instead of predicting the properties.
    - The new program should allow users to examine iso-curves of temperature development and stress/strength ratio development at different cross section in concrete.

REFERENCE

4C User Mannual. (1998). *User Mannual 4C-Temp&Stress ver. 2.0 for Windows.* DTI building Technology.

4C-Temp&Stress for concrete - Description. (n.d.). Retrieved from Danish Technological Institute : http://www.dti.dk/1265

4C-Temp&Stress for concrete - Description. (n.d.). Retrieved from Danish Technological Institute : http://www.dti.dk/1265

Abdol R.C., Muszynski L.A., Sophia T. (2003). *Determination of the Maximum Placment and Cruing Temperatures in Mass Concrete to Avoid Druiability Problems and DEF*. Florida Department of Transportation.

ACI Committe 207 1R-05. (2005). *ACI 207. 1R-05 Guide to Mass Concrete.* American Concrete Institute.

ACI Committee 207 2R-07. (2007). *ACI 207.2R-07 Report on Thermal and Volume Change Effects on Crakcing of Mass Concrete.* American Cocnrete Institute.

ACI Committee 207 4R-05. (2005). *ACI 207.4R-05 Cooling and Insulating Systems for Mass Concrete.* American Concrete Institute.

ACICommittee207. (2007). *Report on Thermal and Volume Change Effects on Cracking of Mass Concrete.* Farmington Hills, MI: American Concrete Insitutite.

ACICommittee2074R. (2005). *ACI 207.4R-05 Cooling and Insulating Systems for Mass Concrete.* American Concrete Institute.

Altoubat, S. (2000). *Early Age Stresses and Creep-Shinkage Interaction of Restrained Concrete.* Doctoral Thesis, the University of Illinois at UrbanaChanmpaign.

Andrewswift. (n.d.). *Inequality in India*. Retrieved 11 10, 2010, from The World Affairs Blog Network: http://transitionalstates.foreignpolicyblogs.com/2009/11/19/inequality-in-india/

Anoglu N.Girgin Z.C. and Anoglu E. (2006). Evaluation of Ratio between Splitting Tensile Strength and Compressive Strength for Concrete up to 120Mpa and its Application in Strength Criterion. *ACI Material Journal Vol. 103 No. 1*, 18-24.

ASTM C 150. (2005). Standard Specification for Portland Cement. In *Annual Book of ASTM Standards, Vol. 4.02*. West Conshohocken, PA: ASTM International.

ASTM C1074. (2002). Standard Practice for Estimating Cocnrete Strength by Maturity Method. In *Annual Book of ASTM Standards, Vol. 4.02.*

Carino, N. J. (n.d.). *Handbook on Nondestructive Testing of Concrete.* National Institute of Standards and Technology.

DIT-Technology. (March, 2008). *4C Temp & Stress User Manual.*

Dong Z.,Yun C., Liping J., Jun G., Jianrong Zh., and Jun-Jie Z. (2011, 83 (23)). Manganese-Doped ZnSe Quantum Dots as a Probe for Time-Resolved Fluorescence Detection of 5-Fluorouracil. *Analytical Chemstry*, 9076-9081.

Drake, A. F. (1994). Optical Spectroscopy-Principles and Instrumentation. *Methods in Molecular Biology*, p154.

Elemental Analysis of Glass. (2004, July). Retrieved 02 28, 2012, from http://www.swgmat.org/Elemental%20Analysis%20of%20Glass.pdf

Engineering Tool Box. (n.d.). Retrieved from http://www.engineeringtoolbox.com/thermal-conductivity-d_429.html

Erik J.P., Erik S.P, Helle S. (1997). *No.115 HETEK-Control of Early Age-Crackign in concrete- Phase 9: Stress Calculations and Crack Observations.*

Erik S.P, H. S. (1996). *No. 52 HETEK-Control of Early Age Cracking in Concrete-State of The Art.*

Erik S.P, Helle S. (1996). *No.59 HETEK-Control of Early Age Cracking in concree-Phase 1: Early Age Properties of Selected Concrete.*

Erik S.P, Helle S., Erik J.P.,Henrilk E.J., Mette E.A., Per F.J., Jan G.K. (1997). *No.120 HETEK- Control of Early Age Cracking in Concrete-Guidelines.*

Gajda J. Van. G. M. (n.d.). Controlling Temperatures in Mass Concrete. *Concrete Internationa l Vol. 24, No. 1*, 58-62.

Ge, K. W. (Dec. 2003). *Evaluating Properties of Blended Cements for Concrete Pavements.* The center for Portland Cment Concrete Pavement Technology.

Ge, Z. (2005). *Predicting temperature and strength development of the fieild cocnrete.* Ames, Iowa.

Gjorv, M.-H. Z. (1991). Characteristics of Lightweight Aggregates for High-Strength Concrete. *Materials Journal*, 150-158.

Hedlund H. (2000). *Hardening Concrete: Measurements and evaluation of non-elastic deformation and associated restraint stresses.* Lulea University of Technology, Division of Structral Engineering.

Inc., N. S. (n.d.). Near-field vs Far-field Theory. *Nearfield Systems Inc.*

India Economic Growth. (n.d.). Retrieved 11 10, 2010, from Economy Watch: http://www.economywatch.com/economic-growth/india.html

IowaDOT. (2010). *Developmental Specifiations for Mass Concrete- Control of Heat of Hydration DS-09047.* Iowa Department of Transportation.

Kada H., Lachemi M., Petro N., Bonneau O. and Aitcin P.c. (2002). Determination of the coefficient of thermal expansion of high performance concrete from initial setting. *Materials and Structures, Vol. 30 No. 245*, 35-41.

Kejin W., Jiong H., and Zhi G. (2008). *Task 4 Testing Iowa Portalnd Cmenet Concrete Mixtures for AASHTO Mechanistic-Empirical Pavemetn Design Procedure.* National Cocnrete Pavemetn Technology Center.

Kejin Wang, J. H. (February 2008). *Task 6: Material Thermal Input for Iowa Materials.*

Kejin Wang, J. H. (May 2008). *Task 4: Testing Iowa Portland Cement Cocnrete Mixtures for the AASHTO Mechanistic-Empirical Pavemetn Design Procedure.*

Khan, A. A. (1995). *Concrete properties and thermal stress analysis of members at early ages.* Montreal, Canada: McGill University.

Khan, A. A. (1995, July). Concrete Properties and Thermal Stress Analysis of Members at Early Ages. Canada.

Khan A.A. (1998). "Thermal Properties and Transient Thermal Analysis of Structural Members During Hydration,". *ACI Materials Journal Vol. 95 No. 3*, 293-303.

Kim, s. G. (2010). *Effect of heat generation from cemetn hydration on mass cocnrete placement.*

Kouichi Tsuji, Takashi Ohmori, and Makoto Yamaguchi. (2011). Wavelength Dispersive X-ray Fluorescence Imaging. *Analytical Chemisitry*, 83 (16),pp 6389-6394.

Larson M. (2003). *Thermal Crack Estimation in early Age Concrete – Models and Methods for Practical Application.* Luleå University of Technology.

Maria J. Moon W., David F. Chul. S. and Andre E. (2008). *Effects of Supplementary Cementing Materials on the Setting Time and Early Strength of Concrete.* Texas Departmetn of Transportaion Research and Technology Implementation Office.

Marzouk, D. W. (2007). Bond Characterisitics of High-Strength Lightweight Cocnrete. *Structural Journal ACI*, 22-29.

Mitchell L.J. (1953). Thermal Expansion Tests on Aggregates, Neat Cement, and Concretes. (pp. 963-997). ASTM V. 53.

Munich. (1994). *Thermal Cracking in Concrete at Early Ages-Proceeding of the Internatlional RILEM Symposium.* London .

N.J.Carine, H.S.Lew. (2011). *The Maturity Method: From Theory to Application.* Gaithersburg, MD: Building and Fire Research Laboratory, National Institute of Standards and Technology.

Nielsen, L. F. (1997). *No.1123 HETEK-Control of Early Age Cracking in Concrete-Phase 4B: Material Modelling -Composite Approach.*

Oluokun F.A., Burdette E.G., and Deatherage J.H.,. (n.d.). Splitting Tensile Strength and Compressive Strength Relationship at Early Ages,". *ACI Materials Journal,Vol. 88, No. 2,*, 115-121.

Oral Bu¨yu¨ko¨ztu¨rk , Tzu-Yang Yu . (2007). Far-field radar NDT technique for detecting GFRP debonding from concrete. *Construction and Building Materials*.

Peter M. F., David H. (n.d.). *Using Ensemble Prediction Systems to Estimate Medium Range Temperature Forecast Error.* University of Miami.

Poole J.L. (2007). *Modeling Temperature Sensitivity and Heat Evolution of Concrete.* The University of Texas at Austin.

Raphael, J. (1984). Tensile Strength of Concrete. *ACI Journal, Vol. (2)*, 214-219.

Riding K.A., Poole J.L., Schindler A.K., Juenger M.G., and Folliard K.J. (2006). Evaluation of Temperature Prediction Methods for Mass Concrete Members. *ACI Materials Journal*, 103(5),357-365.

Riding K.A., Poole J.L., Schindler A.K., Juenger M.G., and Folliard K.J. (2007). Calorimetry Performed On-Site: Methods and Uses. *ACI Special Publication 241CD Concrete Heat Development: Monitoring, Prediction & Management*, SP-241-3.

Riding , Kyle; et al. (n.d.). *ConcreteWorks User Mannual Verision 2.0.* Texas Department of Transportation.

Riding K.A., P. J. (2007). Temperature Boundary Condition Models for Concrete Bridge Members. *ACI Materials Journal Vol. 104*, 379-387.

Riding, K. (2007). *Early Age Cocnrete Thermal Sterss Measurement and Modeling.*

Riding, K. A. (2005). *Concrete Works Version 2.0 Users Manual.* Concrete Durability Center.

Robert, M. (n.d.). *Mass Concrete.* Retrieved 11 22, 2011, from [http://people.ce.gatech.edu/~kk92/massconcrete.pdf]

Salah A. A and David A.L.,. (2001). Creep, Shrinkage and Cracking of Restrained Concrete at Early Age.

Season Weather Averages. (n.d.). Retrieved 2011, from Weather Underground: http://www.wunderground.com/NORMS/DisplayNORMS.asp?AirportCode=KOMA

Shaw, J. J. (2011). *A Sensitvity Study of Concrete Temperature Development in Bridge Foudnations.*

Sidney M., J. Francis Y., David D. (2003). *Concrete.* Upper Saddle River, NJ: Pearson Education, Inc.

Steven H. K., Beatrix K., and William C.P. (2002). *Design and Control of Cocnrete Mixtures.* Skokie: Portland Cment Association.

Steven H. K., Beatrix K., and William P. (2008). *Design and Control of Concrete Mixtures.* Skokie, Illinois: Portland Cement Association.

Syoji Ito,* Takashi Sugiyama, Naoki Toitani, Genki Katayama, and Hiroshi Miyasaka. (2007). Application of Fluorescence Correlation Spectroscopy to the Measurement of Local. *The Journal of Physical Chemistry Bol. 111, No. 9* , American Chemical Society.

Townsend, C. (1981). *Control of Crackign in Mass Concrete Structures.* United States Department of the Interior Bureau of Reclamation.

Ulai Noomnarm and Robert M. Clegg. (2009). Fluorescence lifetimes: fundamentals and interpretations. *Photosynthesis Ressearch*, 181-194.

Viviani. (2005). *Monitoring and Modeling of Construction Materials During Hardening.* Lausanne, Switzerland: Swiss Federal Institute of Technology.

Wang, K., Hu, j., & Ge, Z. (2008). *Material Thermal Input for Iowa Materials.*

Waters, J. C. (June 29, 2009). Accruancy and Precision in Quantitative Fluorescence Microscopy. *The Journal of Cell Biology*.

Weather Underground, I. (2012). *wunderground.com*. Retrieved from http://www.wunderground.com/history/

Westman, G. (1999). *Concrete Creep and Thermal Stresses.* Sweden: Division of Structural Engineering, Lulea University of Technology.

Yahya Rahmat-Samii, Mark S. Gatti. (1985). Far-field Patterns of Spaceborne Antennas from Plane-Polar Near-Field Measurements. *IEEE Transacation on Antennas and Propagation*, Vol. Ap-33 No. 6.

Zhang, J.; Cusson, D.; Mitchell, L.; Hoogeveen, T. (2005, June 20). The Maturity Approach for Predicting Different Properties of High-performance Concrete. *7th International Symposium on the Utilization of High-Strength/High-Performance*, pp. 135-154.

APPENDIX

APPENDIX A MIX DESIGN AND CONSTRUCTION PRACTICE METHODS TO CONTROL TEMPERATURE

A.1 Lower heat-generating cement system including:

- The use of pozzolans
- The careful production control of aggregate gradings and the use of larger-size aggregates in efficient mixtures with low cement contents
- The precooling of aggregates and mixing water (or the batching of ice in placement of mixing water) to make possible a low concrete temperature as placed
- The use of air-entraining and other chemical admixtures to improve both the fresh and hardened properties of the concrete
- The use of appropriate block dimensions for placement
- The coordination of construction schedules with seasonal changes to establish lift heights and placing frequencies
- The use of special mixing and placing equipment to quickly place cooled concrete with minimum absorption of ambient heat
- The evaporative cooling of surfaces through water curing
- The dissipation of heat from the hardened concrete by circulating cold water through embedded piping
- The insulation of surface to minimize thermal differentials between interior and the exterior of the concrete

A.2 Construction practices for temperature control (ACICommittee2074R, 2005)

- Cooling batch water
- Producing aggregate during cold seasons or cool nights
- Replacing a portion of batch water with ice
- Shading aggregates in storage
- Shading aggregate conveyors
- Spraying aggregate stockpiles for evaporative cooling
- Immersion in cool water or saturation of coarse aggregates, inducing wet belt cooling
- Vacuum evaporation of moisture in coarse aggregate
- Nitrogen injection into the mixture and at transfer points during delivery
- Using light-colored mixing and hauling equipment, and spraying the mixing, conveying and delivery equipment with a water mist
- Scheduling placements when ambient temperatures are lower, such s at night or during cooler times of the year
- Cooling cure water and the evaporative cooling of cure water
- Postcooling with embedded cooling pipes
- Controlling surface cooling of the concrete with insulation
- Avoiding thermal shock during form and insulation removal
- Protecting exposed edges and corners from excessive heat loss
- Cooling aggregates with natural or manufactured chilled air and
- Better monitoring of ambient and material temperatures

APPENDIX B COOLING PIPE LAYOUT FROM CTL THERMAL CONTROL PLAN

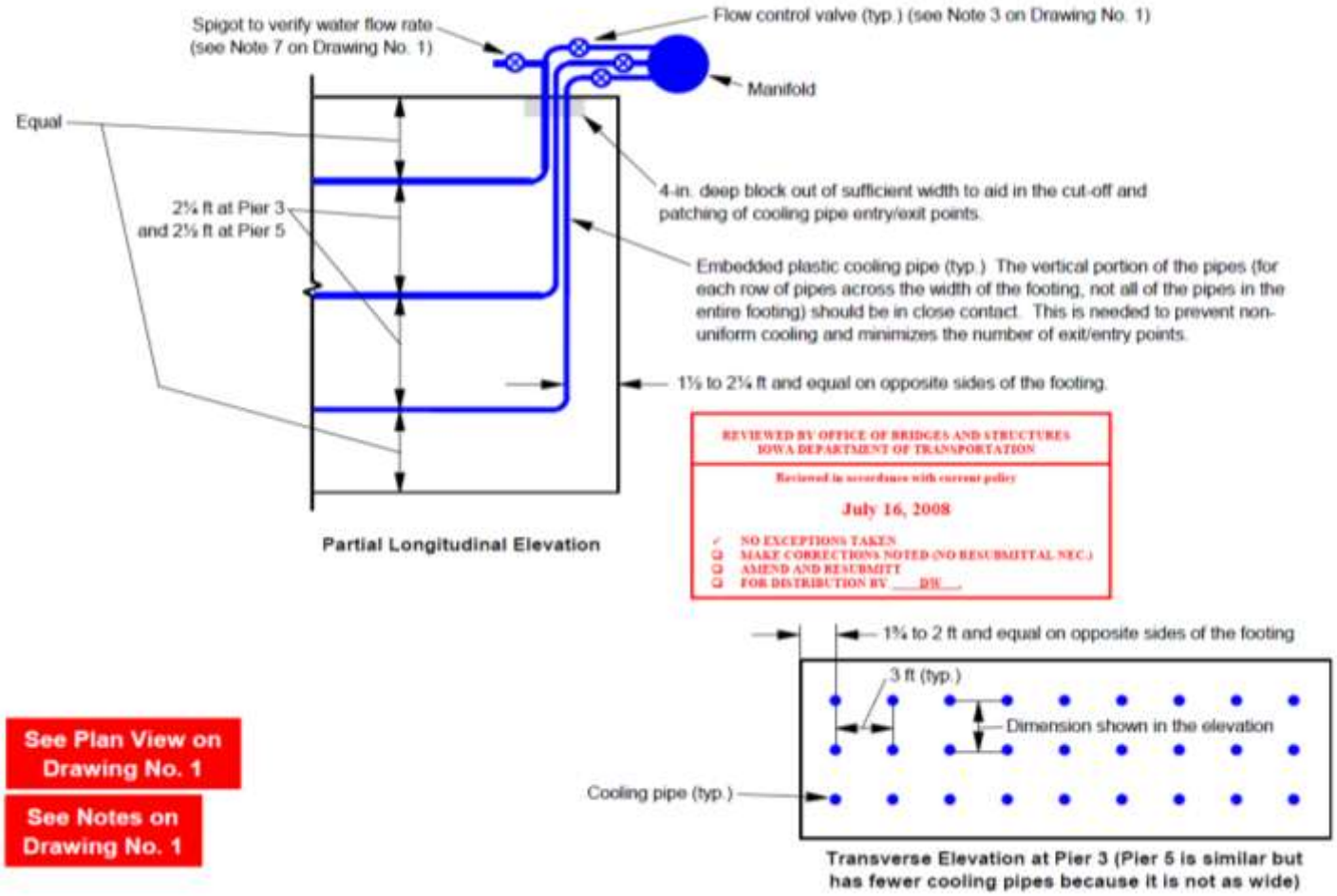

FigureB.1 Embedded cooling pipes details in the footings of pier 3 and 5 (not in scale)

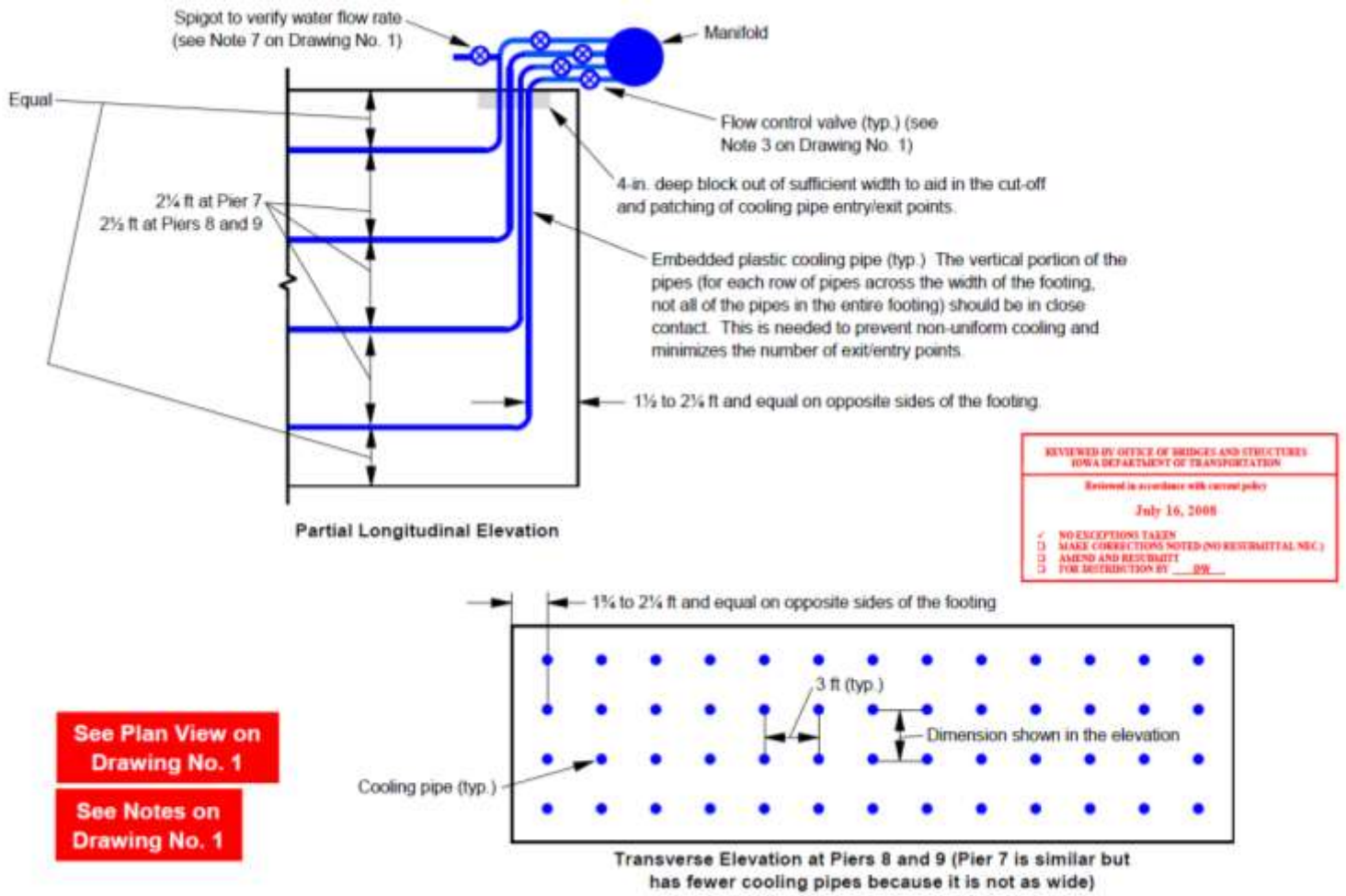

FigureB.2 Embedded cooling pipes details in the footings of pier 7, 8 and 9 (not in scale)

APPENDIX C COMPARISON BETWEEN 4C(PREDICTION) AND CTL (ACTUAL)

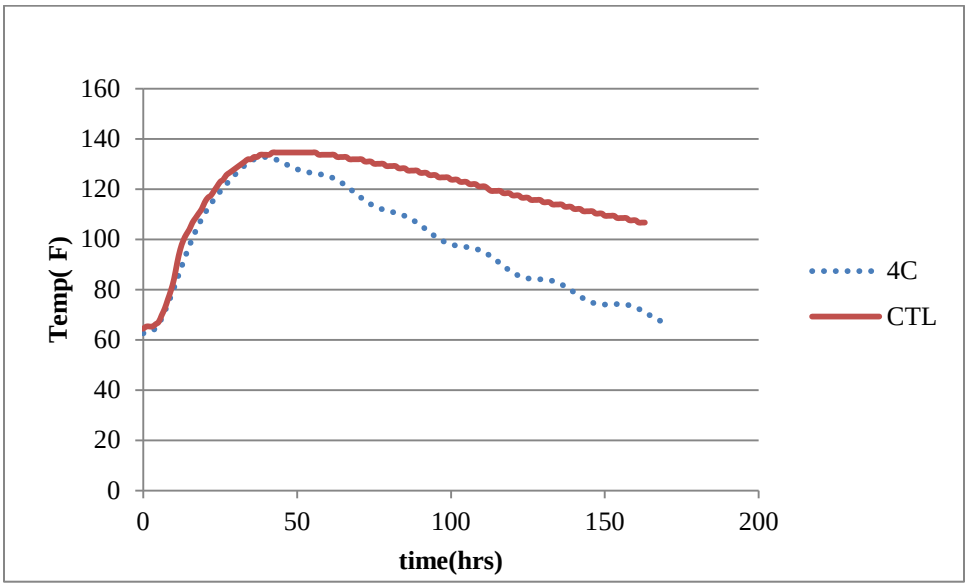

Figure C.1 Maximum temperature development for pier 2 footing comparison between measured (CTL) and predicted (4C)

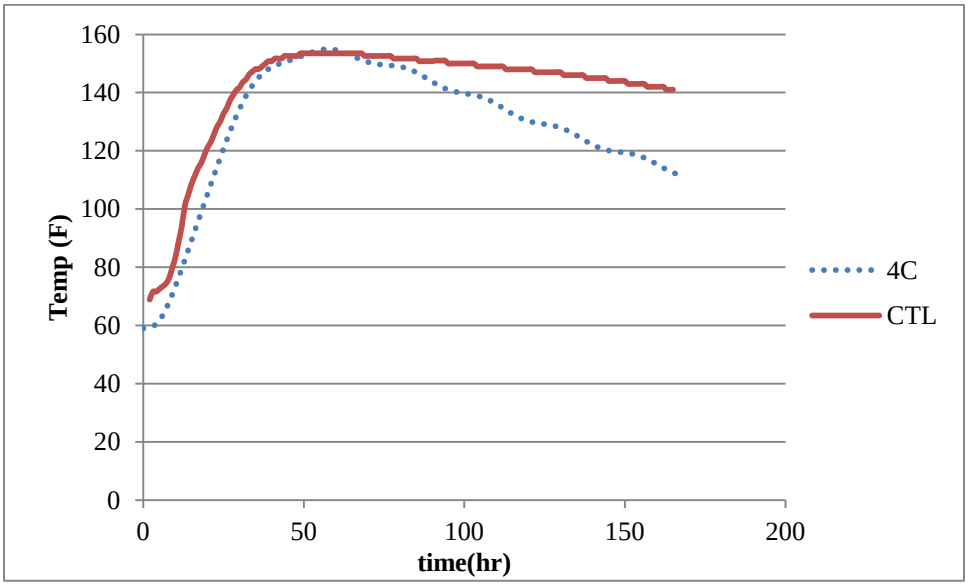

Figure C.942 Maximum temperature development for pier 3 footing comparison between measured (CTL) and predicted (4C)

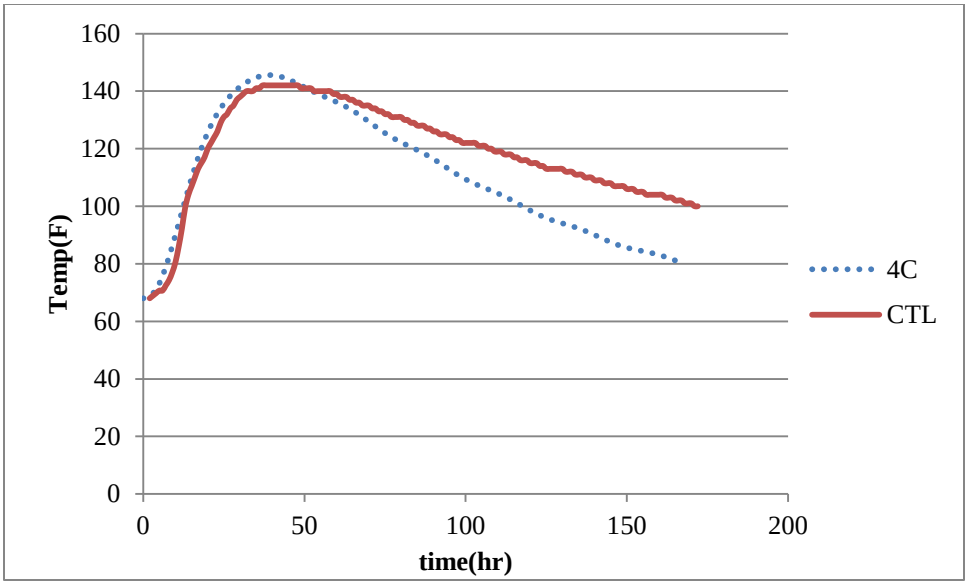

Figure C.3 Maximum temperature development for pier 4 footing comparison between measured (CTL) and predicted (4C)

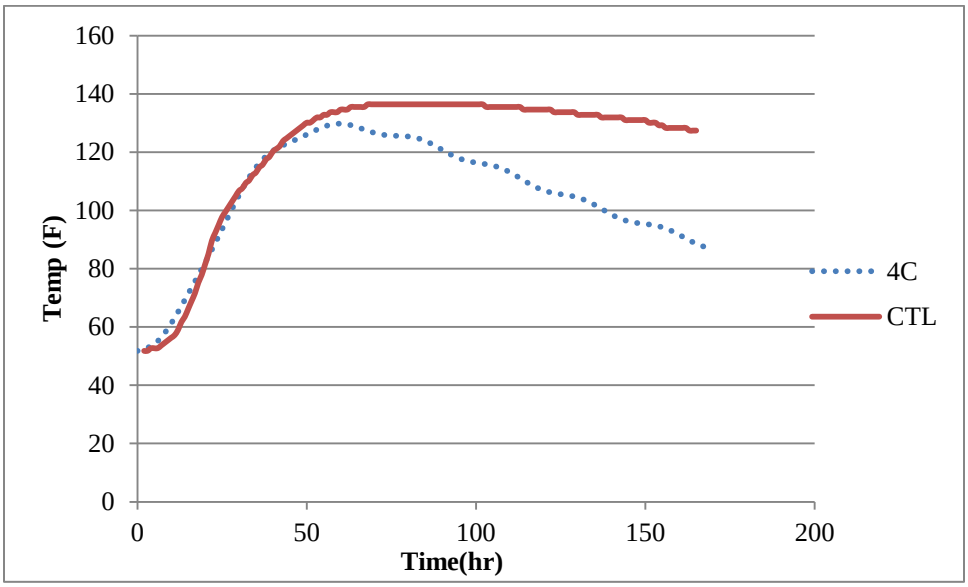

Figure C.4 Maximum temperature development for pier 5 footing comparison between measured (CTL) and predicted (4C)

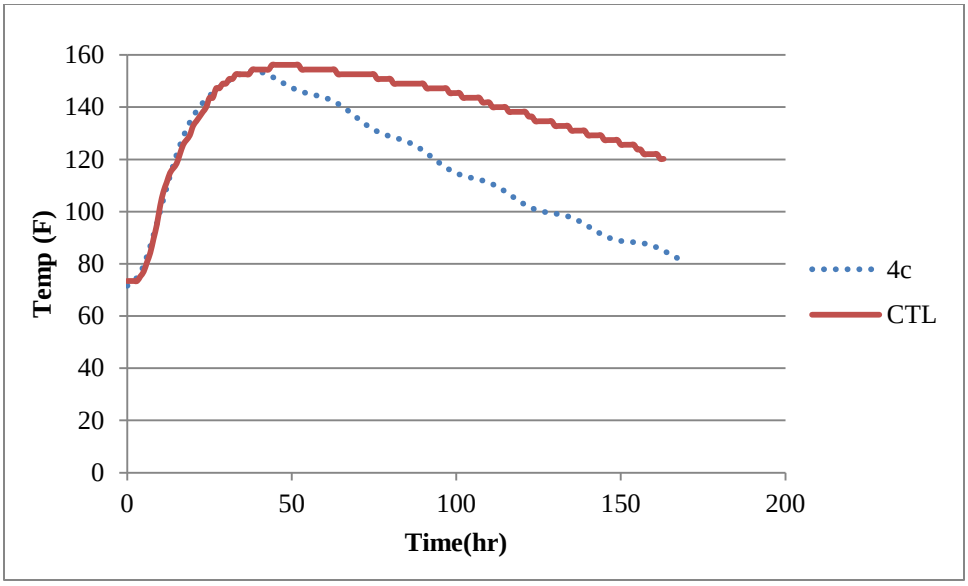

Figure C.5 Maximum temperature development for pier 6 footing comparison between measured (CTL) and predicted (4C)

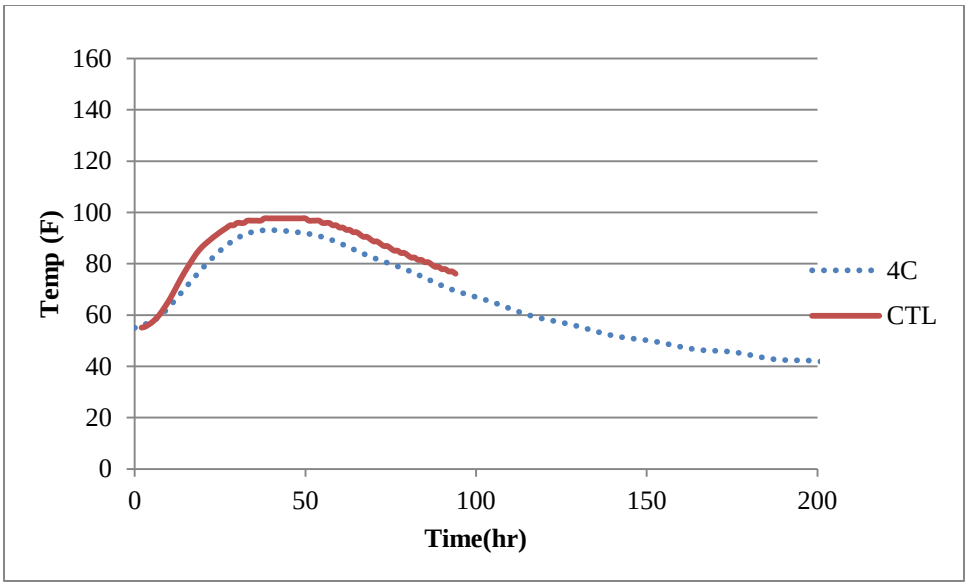

Figure C.6 Maximum temperature development for pier 1 stem comparison between measured (CTL) and predicted (4C)

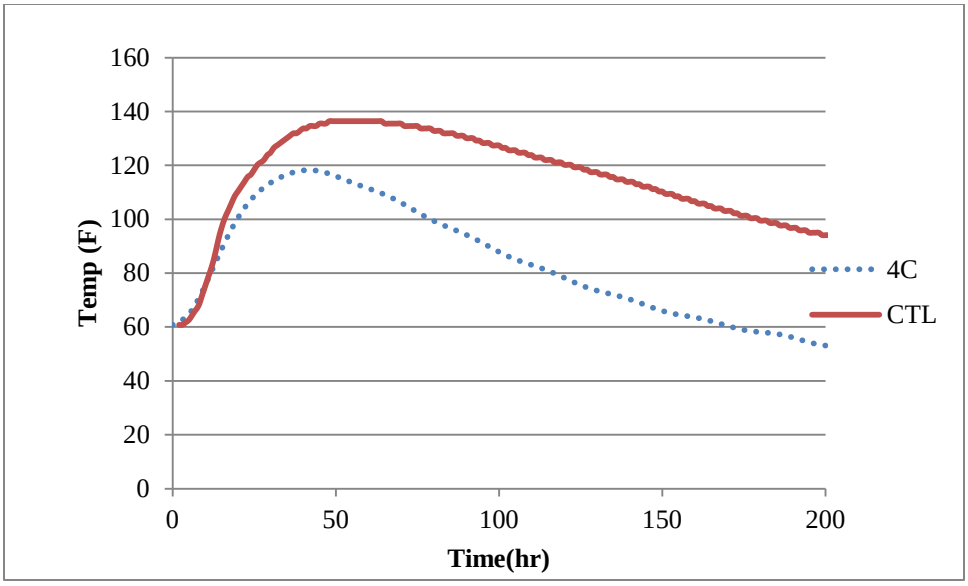

Figure C.7 Maximum temperature development for pier 2 stem comparison between measured (CTL) and predicted (4C)

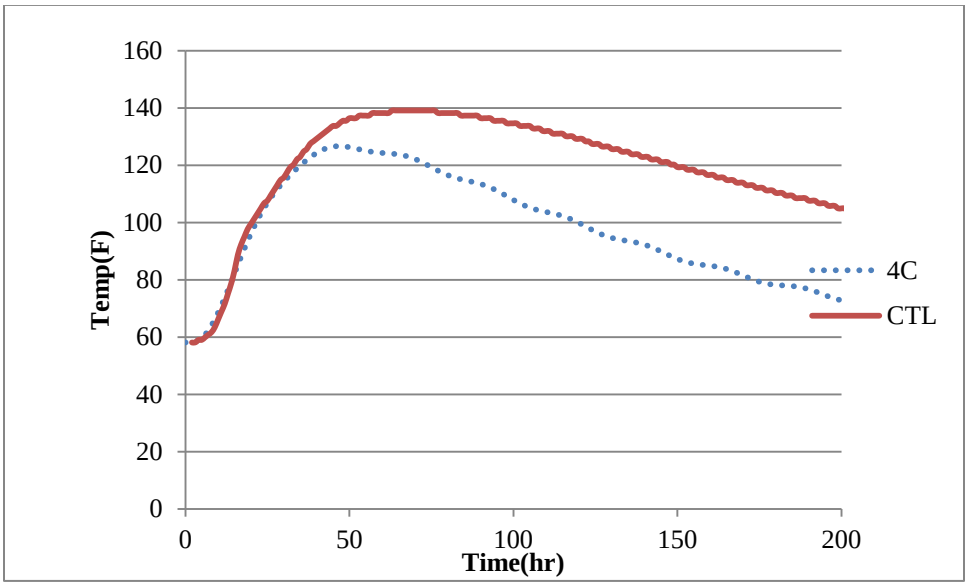

Figure C.8 Maximum temperature development for pier 3 stem comparison between measured (CTL) and predicted (4C)

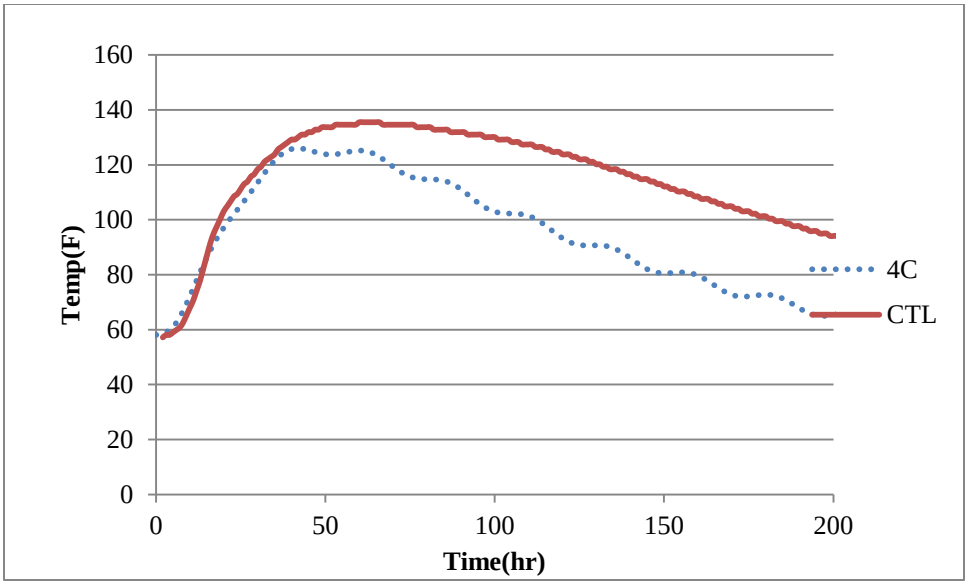

Figure C.9 Maximum temperature development for pier 4 stem comparison between measured (CTL) and predicted (4C)

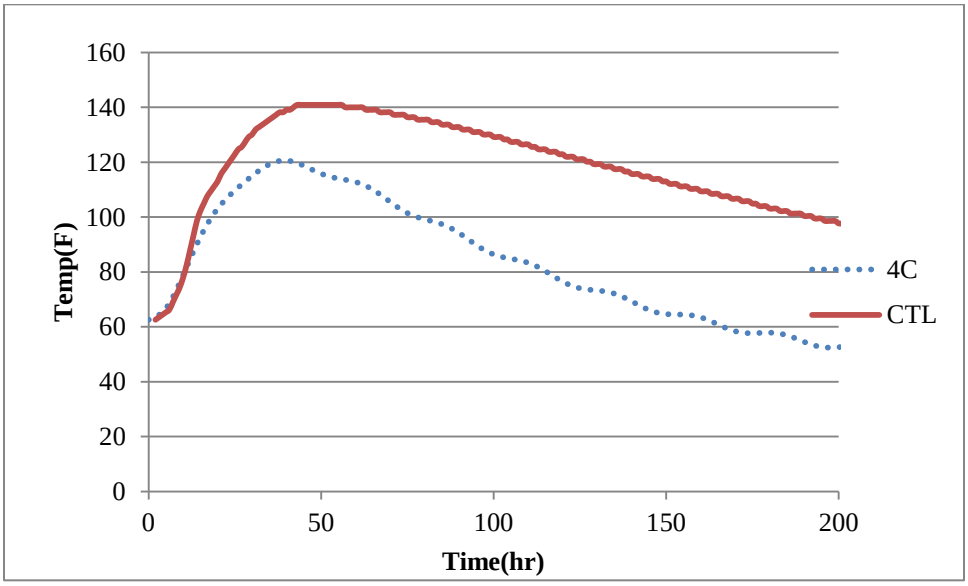

Figure C.95 Maximum temperature development for pier 5 stem comparison between measured (CTL) and predicted (4C)

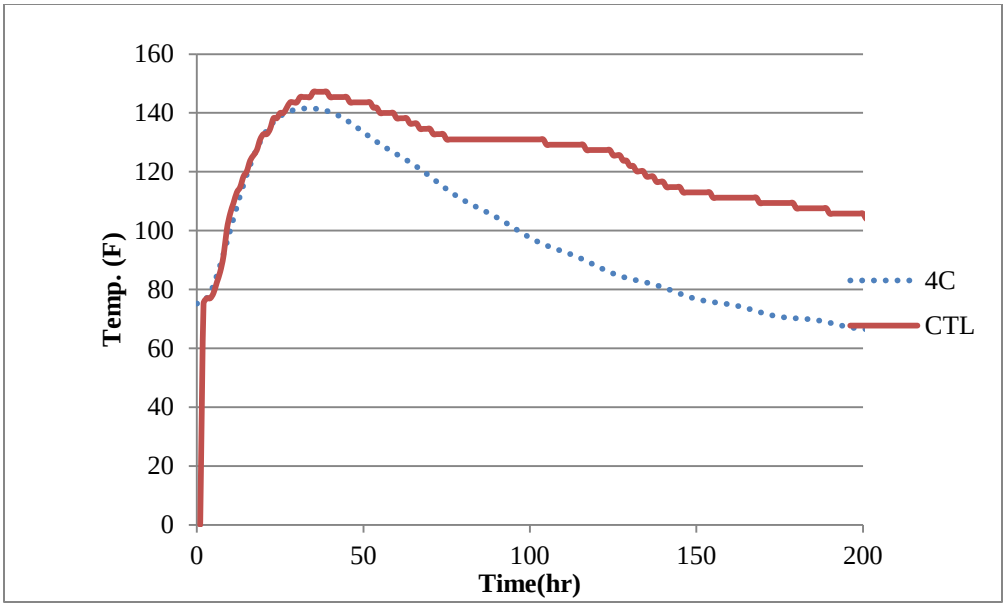

Figure C.11 Maximum temperature development for pier 7 stem comparison between measured (CTL) and predicted (4C)

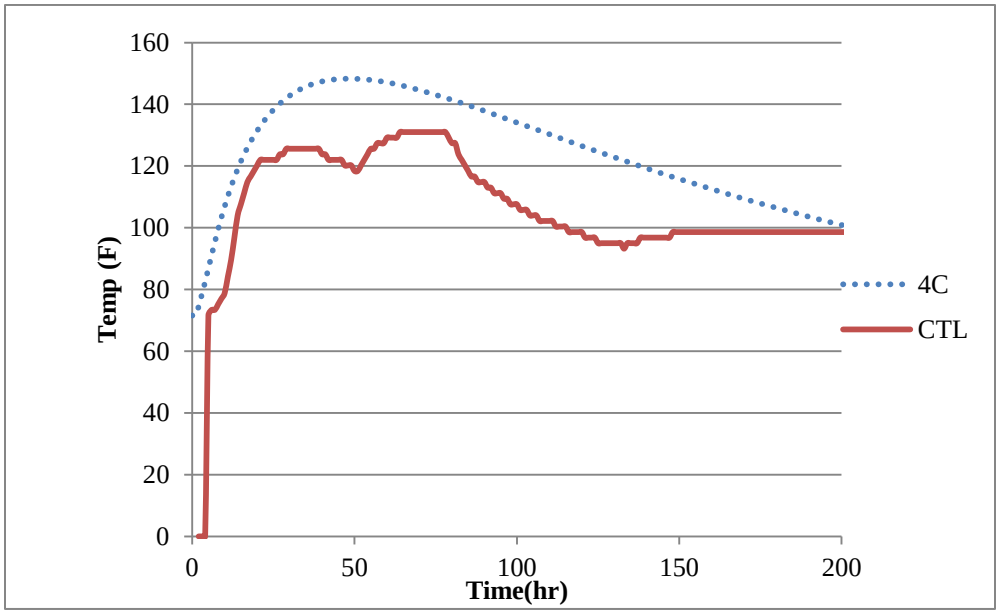

Figure C.12 Maximum temperature development for pier 9 stem comparison between measured (CTL) and predicted (4C)

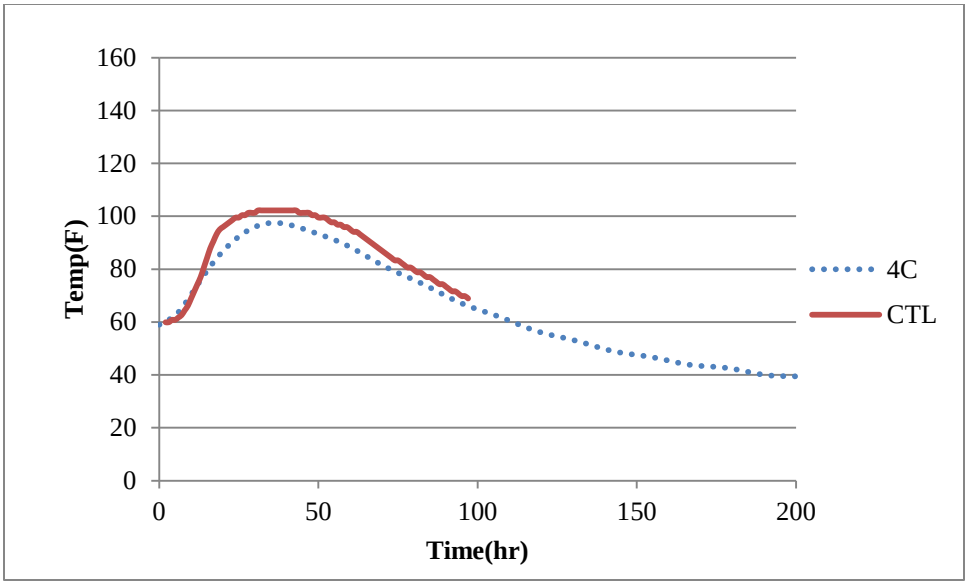

Figure C.13 Maximum temperature development for pier 1 cap comparison between measured (CTL) and predicted (4C)

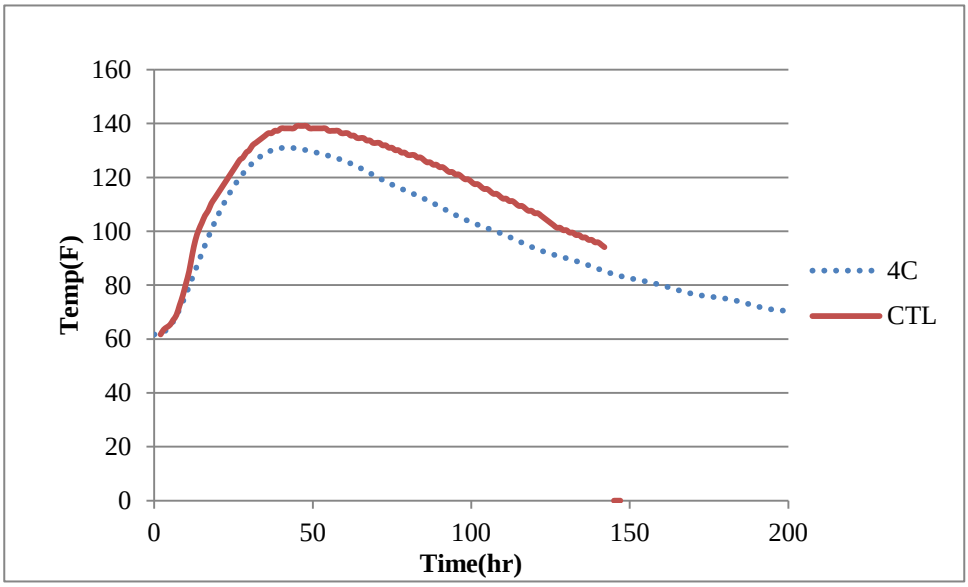

Figure C.96 Maximum temperature development for pier 2 cap comparison between measured (CTL) and predicted (4C)

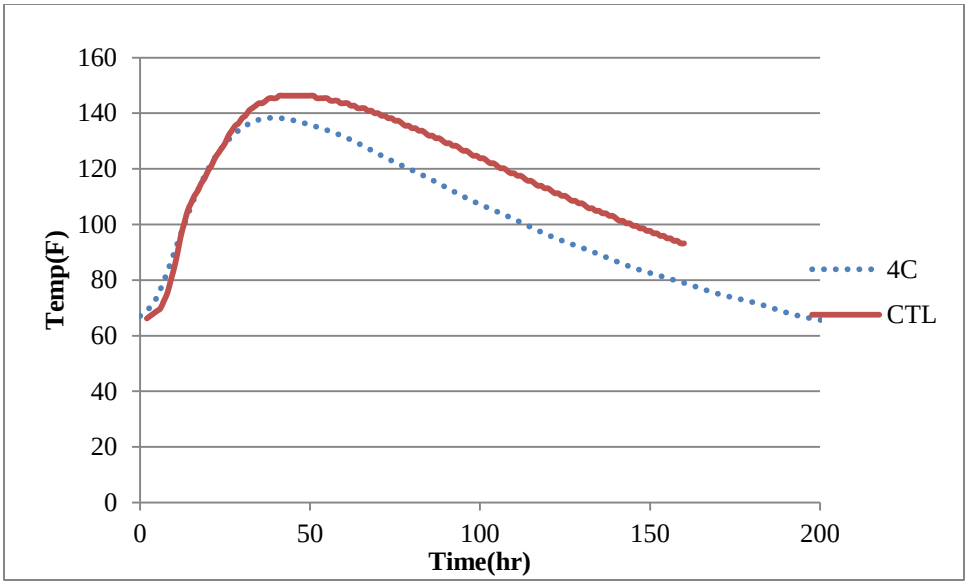

Figure C.97 Maximum temperature development for pier 3 cap comparison between measured (CTL) and predicted (4C)

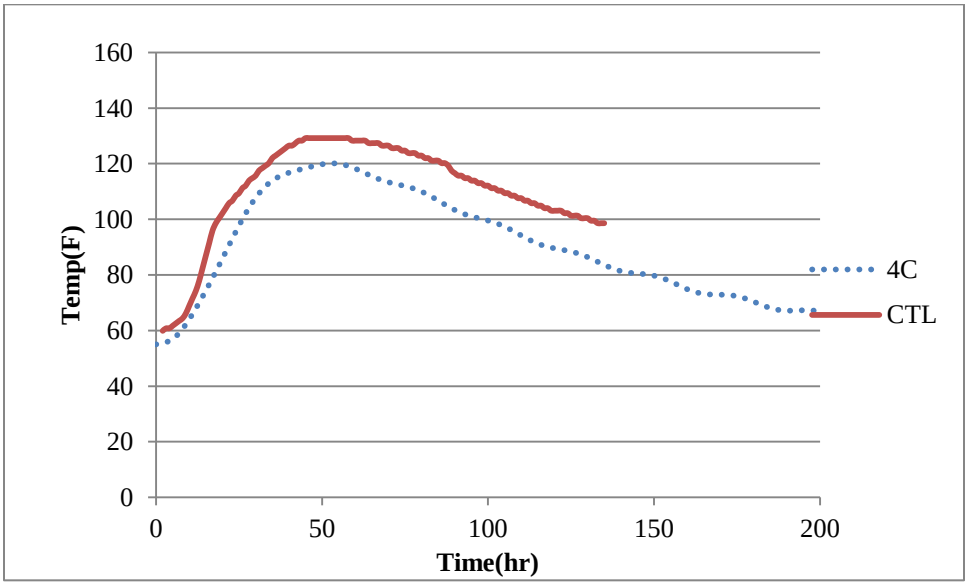

Figure C.98 Maximum temperature development for pier 4 cap comparison between measured (CTL) and predicted (4C)

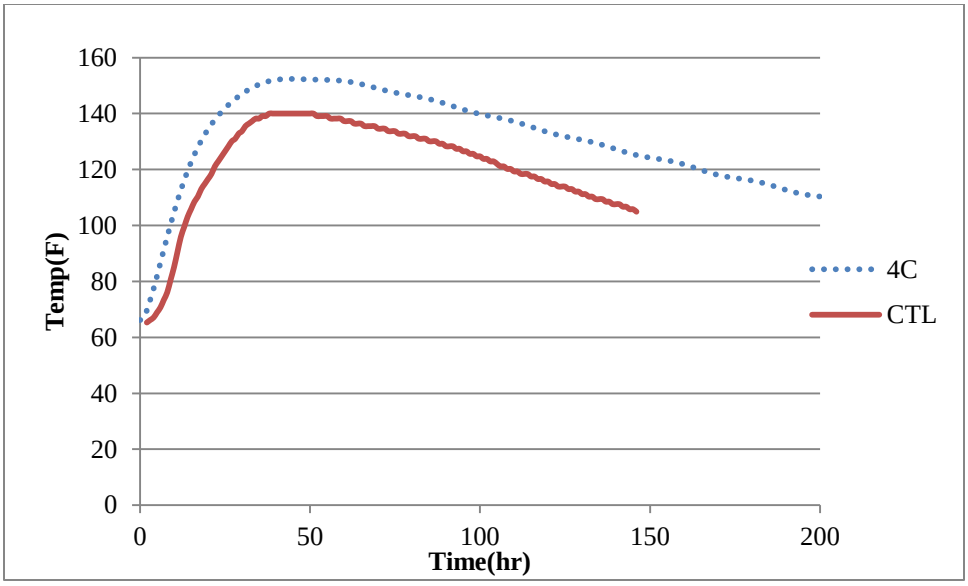

Figure C.99 Maximum temperature development for pier 5 cap comparison between measured (CTL) and predicted (4C)

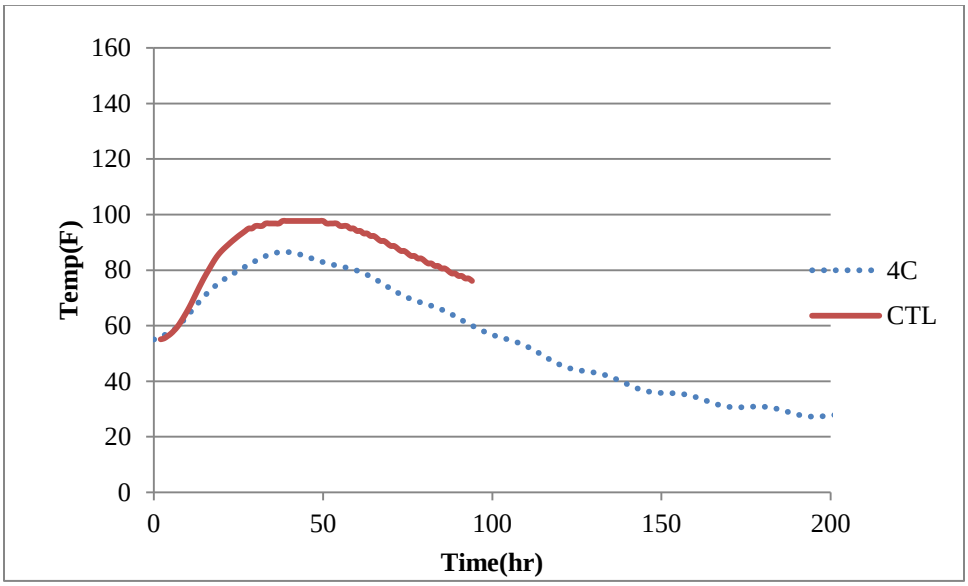

Figure C.100 Maximum temperature development for pier 1 column comparison between measured (CTL) and predicted (4C)

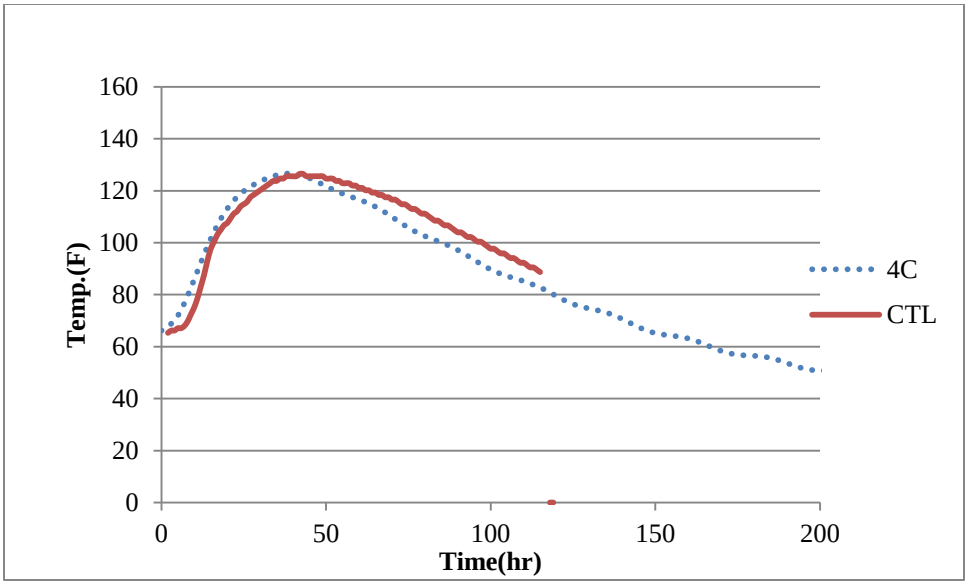

Figure C.101 Maximum temperature development for pier 2 column comparison between measured (CTL) and predicted (4C)

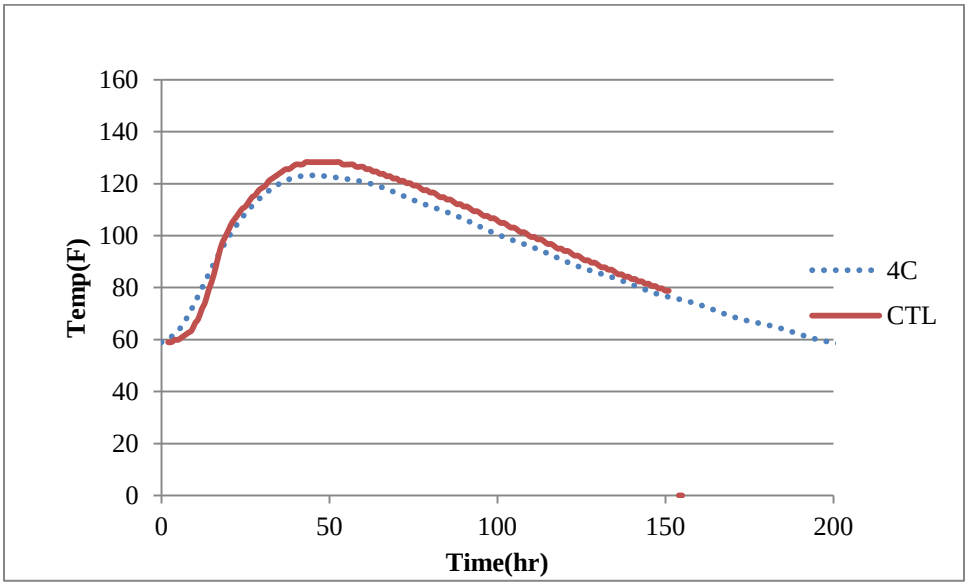

Figure C.20 Maximum temperature development for pier 3 column comparison between measured (CTL) and predicted (4C)

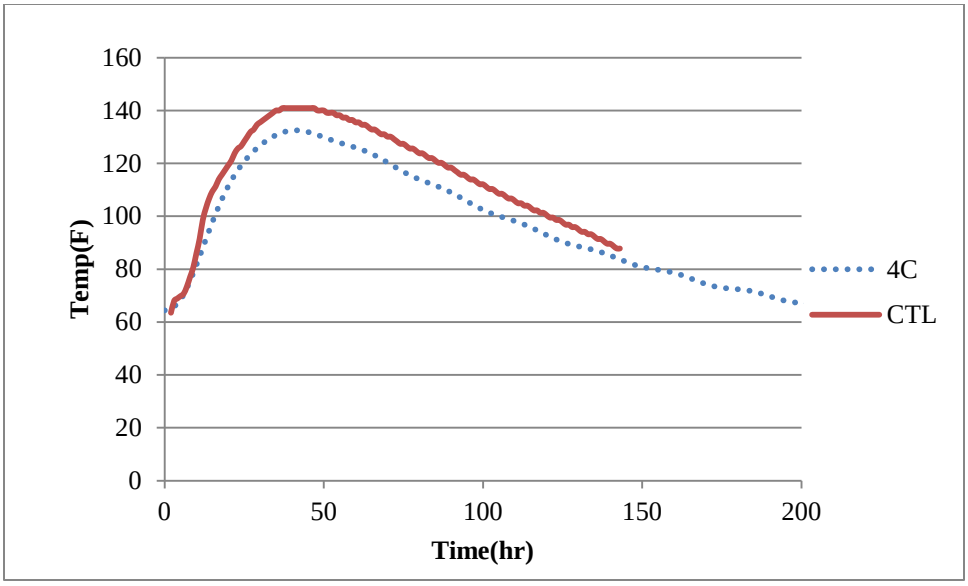

Figure C.21 Maximum temperature development for pier 4 column comparison between measured (CTL) and predicted (4C)

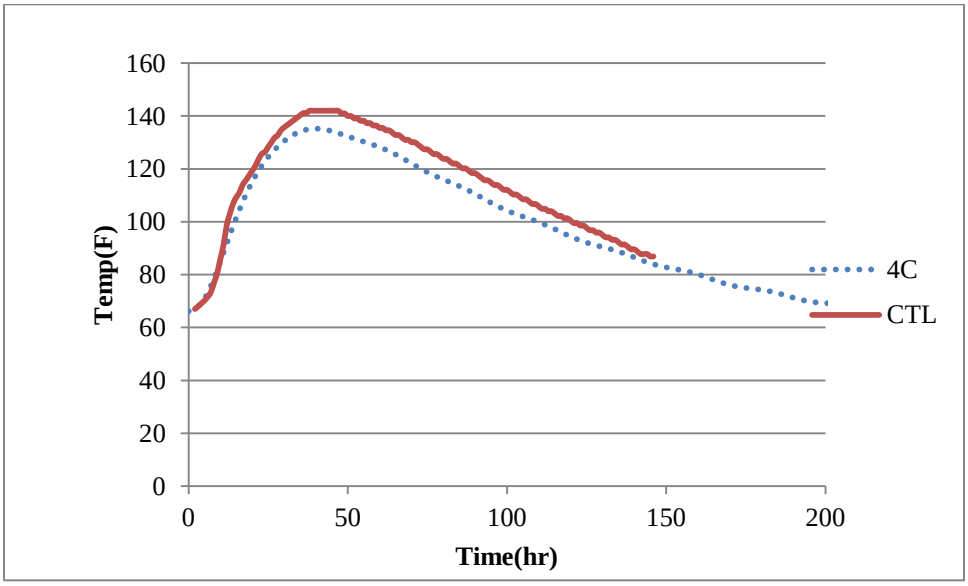

Figure C.102 Maximum temperature development for pier 2 column comparison between measured (CTL) and predicted (4C)

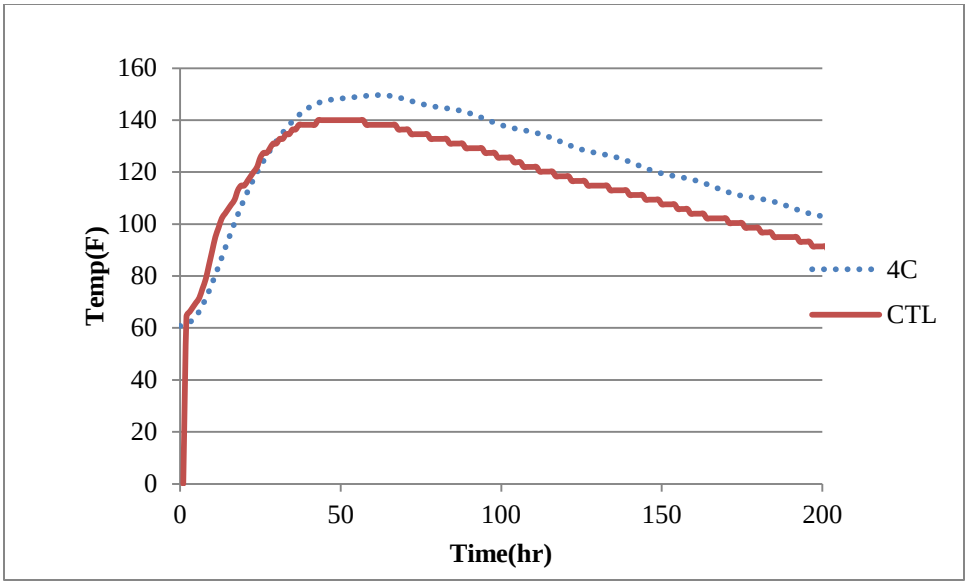

Figure C.103 Maximum temperature development for pier 7 column comparison between measured (CTL) and predicted (4C)

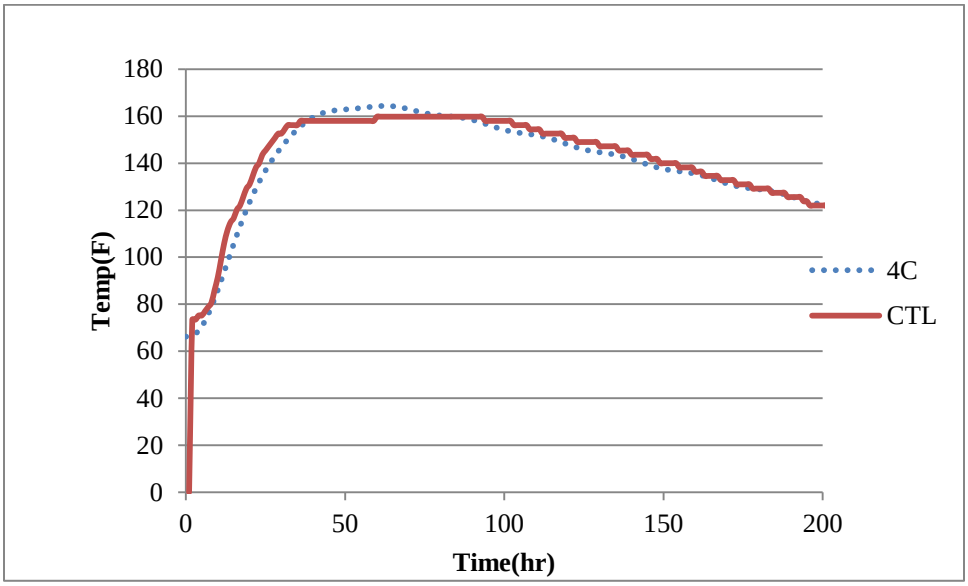

Figure C.104 Maximum temperature development for pier 10 column comparison between measured (CTL) and predicted (4C)

C.1 Bivariate Fit of 4C by CTL on maximum temperature

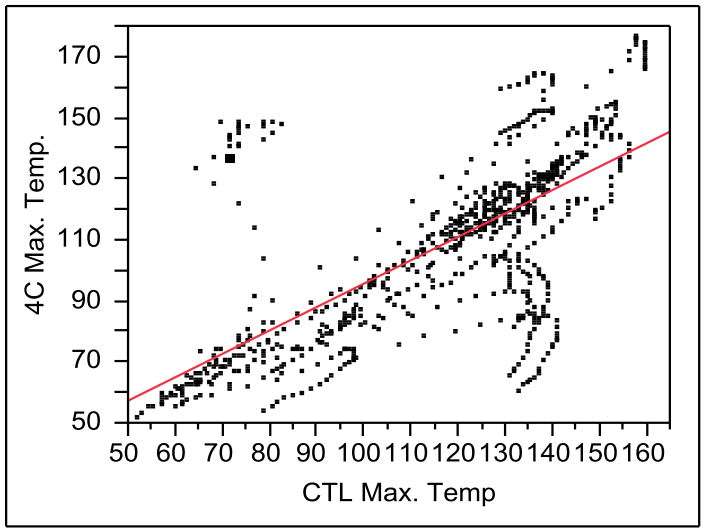

Figure C.25 Bivariate fit of CTL measured and 4C predicted results on maximum temperature

Linear Fit

Linear Fit
4C Max. Temp. = 18.939351 + 0.763973*CTL Max. Temp

Summary of Fit

RSquare	0.485122
RSquare Adj	0.48446
Root Mean Square Error	21.56174
Mean of Response	108.5216
Observations (or Sum Wgts)	780

Analysis of Variance

Source	DF	Sum of Squares	Mean Square	F Ratio
Model	1	340794.94	340795	733.0367
Error	778	361698.76	465	**Prob > F**
C. Total	779	702493.70		<.0001*

Parameter Estimates

Term	Estimate	Std Error	t Ratio	Prob>|t|
Intercept	18.939351	3.397592	5.57	<.0001*
CTL Max. Temp	0.763973	0.028217	27.07	<.0001*

C.2 Statistic oneway Analysis of difference between measured and predicted maximum temperature based on analysis time

Summary of Fit

Rsquare	0.028974
Adj Rsquare	-0.00857
Root Mean Square Error	22.59217
Mean of Response	8.736813
Observations (or Sum Wgts)	780

Analysis of Variance

Source	DF	Sum of Squares	Mean Square	F Ratio	Prob > F
Data Point	29	11422.52	393.880	0.7717	0.8012
Error	750	382804.48	510.406		
C. Total	779	394227.00			

Level	Number	Mean	Std Error	Lower 95%	Upper 95%
1	26	0.1108	4.4307	-8.587	8.809
2	26	0.8193	4.4307	-7.879	9.517
3	26	1.3802	4.4307	-7.318	10.078
4	26	4.3605	4.4307	-4.338	13.058
5	26	8.2227	4.4307	-0.475	16.921
6	26	8.4034	4.4307	-0.295	17.101
7	26	7.3932	4.4307	-1.305	16.091
8	26	7.0691	4.4307	-1.629	15.767
9	26	6.9444	4.4307	-1.754	15.642
10	26	7.3069	4.4307	-1.391	16.005
11	26	7.0368	4.4307	-1.661	15.735
12	26	6.8841	4.4307	-1.814	15.582
13	26	6.6972	4.4307	-2.001	15.395
14	26	6.5892	4.4307	-2.109	15.287
15	26	7.0668	4.4307	-1.631	15.765
16	26	8.0059	4.4307	-0.692	16.704
17	26	8.9215	4.4307	0.223	17.619
18	26	9.6474	4.4307	0.949	18.345
19	26	9.9233	4.4307	1.225	18.621
20	26	10.2084	4.4307	1.510	18.906
21	26	10.4283	4.4307	1.730	19.126
22	26	10.8570	4.4307	2.159	19.555
23	26	11.4235	4.4307	2.725	20.122
24	26	12.3868	4.4307	3.689	21.085
25	26	13.1433	4.4307	4.445	21.841
26	26	13.6476	4.4307	4.950	22.346
27	26	13.9875	4.4307	5.290	22.686
28	26	14.1269	4.4307	5.429	22.825
29	26	14.3276	4.4307	5.630	23.026
30	26	14.7847	4.4307	6.087	23.483

C.3 Statistic oneway Analysis of difference between measured and predicted maximum temperature difference based on analysis time

Summary of Fit

Rsquare	0.06513
Adj Rsquare	0.028981
Root Mean Square Error	15.29339
Mean of Response	-6.99742
Observations (or Sum Wgts)	780

Analysis of Variance

Source	DF	Sum of Squares	Mean Square	F Ratio	Prob > F
Data Point	29	12220.71	421.404	1.8017	0.0063*
Error	750	175415.86	233.888		
C. Total	779	187636.58			

Level	Number	Mean	Std Error	Lower 95%	Upper 95%
1	26	2.519	2.9993	-3.37	8.407
2	26	-1.333	2.9993	-7.22	4.555
3	26	-4.690	2.9993	-10.58	1.198
4	26	-7.647	2.9993	-13.54	-1.759
5	26	-8.804	2.9993	-14.69	-2.916
6	26	-10.347	2.9993	-16.23	-4.459
7	26	-11.652	2.9993	-17.54	-5.764
8	26	-10.613	2.9993	-16.50	-4.725
9	26	-9.424	2.9993	-15.31	-3.536
10	26	-8.813	2.9993	-14.70	-2.925
11	26	-9.736	2.9993	-15.62	-3.848
12	26	-11.205	2.9993	-17.09	-5.317
13	26	-12.601	2.9993	-18.49	-6.713
14	26	-13.425	2.9993	-19.31	-7.537
15	26	-12.366	2.9993	-18.25	-6.478
16	26	-10.053	2.9993	-15.94	-4.165
17	26	-8.129	2.9993	-14.02	-2.241
18	26	-6.896	2.9993	-12.78	-1.009
19	26	-6.744	2.9993	-12.63	-0.856
20	26	-7.355	2.9993	-13.24	-1.467
21	26	-7.809	2.9993	-13.70	-1.921
22	26	-7.735	2.9993	-13.62	-1.847
23	26	-6.932	2.9993	-12.82	-1.044
24	26	-4.886	2.9993	-10.77	1.002
25	26	-2.728	2.9993	-8.62	3.160
26	26	-1.483	2.9993	-7.37	4.405
27	26	-1.232	2.9993	-7.12	4.656
28	26	-2.282	2.9993	-8.17	3.606
29	26	-2.819	2.9993	-8.71	3.069
30	26	-2.703	2.9993	-8.59	3.185

C.4 Oneway analysis on difference of max. temp. between predicted and measured for footings

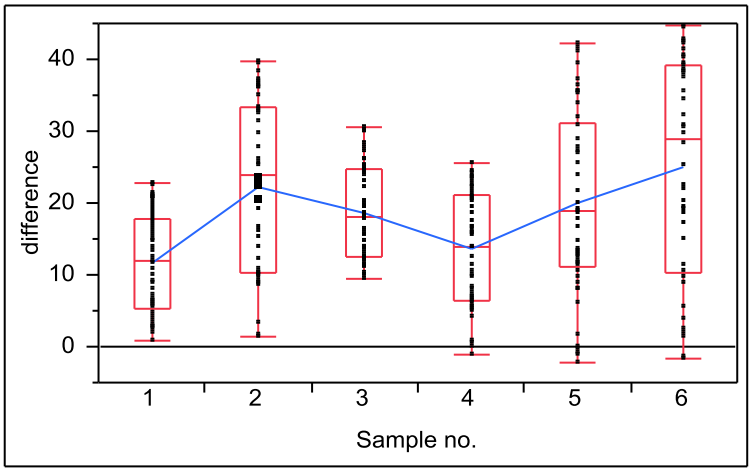

Figure C.26 Difference between measured and predicted maximum temperature based on footings from statistical analysis

Oneway Anova
Summary of Fit

Rsquare	0.15874
Adj Rsquare	0.144433
Root Mean Square Error	10.74008
Mean of Response	18.46046
Observations (or Sum Wgts)	300

Analysis of Variance

Source	DF	Sum of Squares	Mean Square	F Ratio	Prob > F
Sample no.	5	6399.100	1279.82	11.0952	<.0001*
Error	294	33912.723	115.35		
C. Total	299	40311.823			

Means and Std Deviations

Level	Number	Mean	Std Dev	Std Err Mean	Lower 95%	Upper 95%
1	50	11.6002	6.6812	0.9449	9.701	13.499
2	50	22.1246	12.0385	1.7025	18.703	25.546
3	50	18.6128	6.6310	0.9378	16.728	20.497
4	50	13.6170	7.8951	1.1165	11.373	15.861
5	50	19.8640	12.7629	1.8049	16.237	23.491
6	50	24.9443	15.2754	2.1603	20.603	29.286

Tests that the Variances are Equal

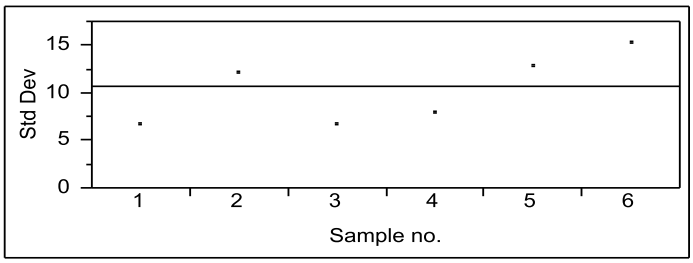

Level	Count	Std Dev	MeanAbsDif to Mean	MeanAbsDif to Median
1	50	6.68117	5.85870	5.85294
2	50	12.03852	10.77806	10.73275
3	50	6.63102	5.76852	5.73391
4	50	7.89509	6.96450	6.95888
5	50	12.76289	10.78512	10.69178
6	50	15.27541	13.60408	13.45896

Test	F Ratio	DFNum	DFDen	Prob > F
O'Brien[.5]	22.1752	5	294	<.0001*
Brown-Forsythe	17.1793	5	294	<.0001*
Levene	21.1419	5	294	<.0001*
Bartlett	12.1673	5	.	<.0001*

Welch's Test

Welch Anova testing Means Equal, allowing Std Devs Not Equal

F Ratio	DFNum	DFDen	Prob > F
13.3778	5	135.34	<.0001*

C.5 Oneway analysis on difference of max. temp. between predicted and measured for columns

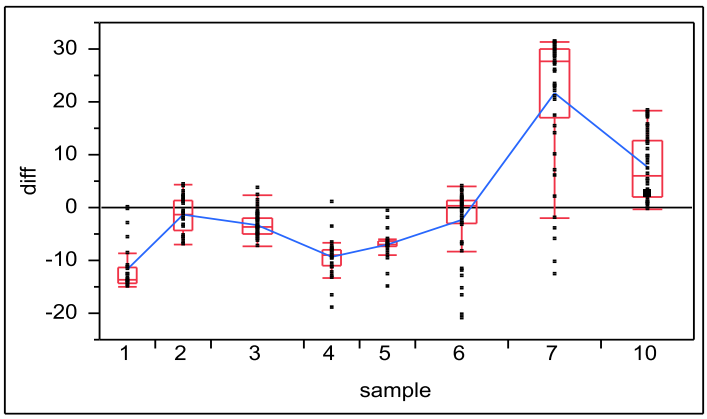

Figure C.27 Difference between measured and predicted maximum temperature based on columns from statistical analysis

Oneway Anova
Summary of Fit

Rsquare	0.731789
Adj Rsquare	0.725771
Root Mean Square Error	6.434179
Mean of Response	0.890623
Observations (or Sum Wgts)	320

Analysis of Variance

Source	DF	Sum of Squares	Mean Square	F Ratio	Prob > F
sample	7	35241.080	5034.44	121.6088	<.0001*
Error	312	12916.380	41.40		
C. Total	319	48157.460			

Means for Oneway Anova

Level	Number	Mean	Std Error	Lower 95%	Upper 95%
1	30	-11.809	1.1747	-14.12	-9.50
2	30	-1.462	1.1747	-3.77	0.85
3	50	-3.330	0.9099	-5.12	-1.54
4	30	-9.391	1.1747	-11.70	-7.08
5	30	-7.065	1.1747	-9.38	-4.75
6	50	-2.459	0.9099	-4.25	-0.67
7	50	21.553	0.9099	19.76	23.34
10	50	7.773	0.9099	5.98	9.56

Std Error uses a pooled estimate of error variance

Tests that the Variances are Equal

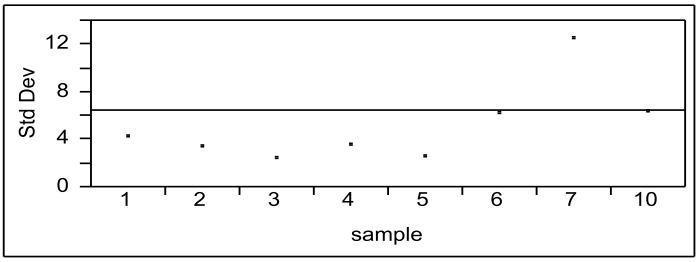

Level	Count	Std Dev	MeanAbsDif to Mean	MeanAbsDif to Median
1	30	4.14143	2.877747	2.485349
2	30	3.41292	2.974741	2.969691
3	50	2.37315	1.838566	1.803034
4	30	3.48973	2.277225	2.189503
5	30	2.54629	1.438133	1.414584
6	50	6.11605	4.529868	3.816173
7	50	12.39105	9.710453	8.342118
10	50	6.23973	5.586654	5.520114

Test	F Ratio	DFNum	DFDen	Prob > F
O'Brien[.5]	9.6483	7	312	<.0001*
Brown-Forsythe	8.6352	7	312	<.0001*
Levene	22.0626	7	312	<.0001*
Bartlett	27.3011	7	.	<.0001*

Welch's Test

Welch Anova testing Means Equal, allowing Std Devs Not Equal

F Ratio	DFNum	DFDen	Prob > F
87.9554	7	123.23	<.0001*

C.6 Oneway analysis on difference of max. temp. between predicted and measured for caps

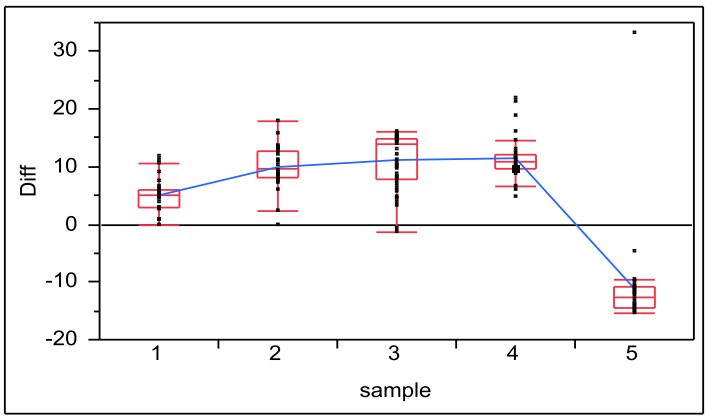

Figure C.28 Difference between measured and predicted maximum temperature based on caps from statistical analysis

Oneway Anova
Summary of Fit

Rsquare	0.721482
Adj Rsquare	0.71473
Root Mean Square Error	5.193495
Mean of Response	5.973731
Observations (or Sum Wgts)	170

Analysis of Variance

Source	DF	Sum of Squares	Mean Square	F Ratio	Prob > F
sample	4	11528.552	2882.14	106.8551	<.0001*
Error	165	4450.444	26.97		
C. Total	169	15978.996			

Means for Oneway Anova

Level	Number	Mean	Std Error	Lower 95%	Upper 95%
1	30	5.024	0.94820	3.15	6.90
2	30	9.978	0.94820	8.11	11.85
3	50	11.049	0.73447	9.60	12.50
4	30	11.578	0.94820	9.71	13.45
5	30	-11.144	0.94820	-13.02	-9.27

Std Error uses a pooled estimate of error variance

Tests that the Variances are Equal

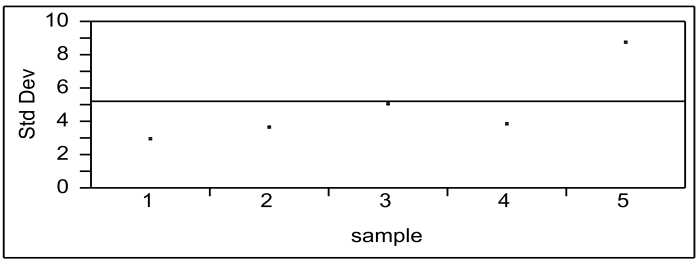

Level	Count	Std Dev	MeanAbsDif to Mean	MeanAbsDif to Median
1	30	2.908625	2.121536	2.121536
2	30	3.580015	2.646671	2.646671
3	50	4.980331	4.177220	3.866278
4	30	3.818977	2.518021	2.449074
5	30	8.700156	3.687319	3.246995

Test	F Ratio	DFNum	DFDen	Prob > F
O'Brien[.5]	0.8940	4	165	0.4689
Brown-Forsythe	0.9177	4	165	0.4551
Levene	1.7644	4	165	0.1384
Bartlett	11.6561	4	.	<.0001*

Welch's Test

Welch Anova testing Means Equal, allowing Std Devs Not Equal

F Ratio	DFNum	DFDen	Prob > F
56.2766	4	77.789	<.0001*

C.7 Oneway analysis on difference of max. temp. between predicted and measured for stems

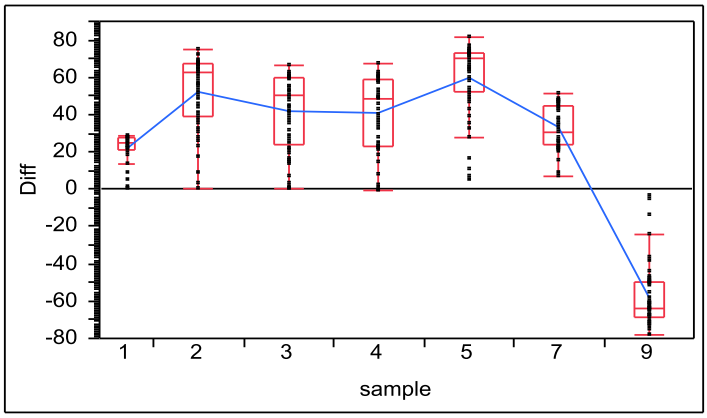

Figure C.29 Difference between measured and predicted maximum temperature based on stems from statistic analysis

Oneway Anova
Summary of Fit

Rsquare	0.822385
Adj Rsquare	0.819086
Root Mean Square Error	17.77058
Mean of Response	27.71564
Observations (or Sum Wgts)	330

Analysis of Variance

Source	DF	Sum of Squares	Mean Square	F Ratio	Prob > F
sample	6	472281.85	78713.6	249.2568	<.0001*
Error	323	102001.27	315.8		
C. Total	329	574283.12			

Means for Oneway Anova

Level	Number	Mean	Std Error	Lower 95%	Upper 95%
1	30	21.939	3.2444	15.56	28.32
2	50	51.853	2.5131	46.91	56.80
3	50	41.928	2.5131	36.98	46.87
4	50	41.106	2.5131	36.16	46.05
5	50	60.108	2.5131	55.16	65.05
7	50	32.984	2.5131	28.04	37.93
9	50	-58.219	2.5131	-63.16	-53.27

Std Error uses a pooled estimate of error variance

Tests that the Variances are Equal

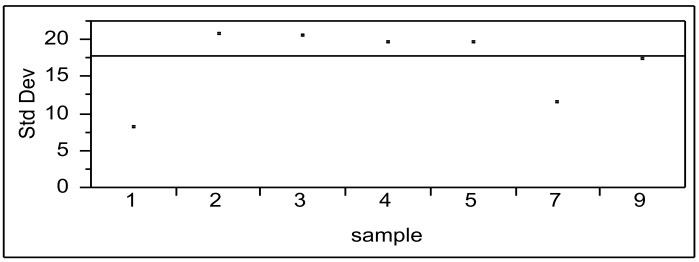

Level	Count	Std Dev	MeanAbsDif to Mean	MeanAbsDif to Median
1	30	8.07214	5.77931	5.07282
2	50	20.64782	16.88347	15.44900
3	50	20.47485	17.63632	16.94920
4	50	19.67700	16.84226	16.31940
5	50	19.49192	15.03576	12.88840
7	50	11.58031	10.25694	10.13580
9	50	17.21394	12.75883	11.54760

Test	F Ratio	DFNum	DFDen	Prob > F
O'Brien[.5]	3.1899	6	323	0.0047*
Brown-Forsythe	3.5974	6	323	0.0018*
Levene	7.2275	6	323	<.0001*
Bartlett	7.1422	6	.	<.0001*

Welch's Test

Welch Anova testing Means Equal, allowing Std Devs Not Equal

F Ratio	DFNum	DFDen	Prob > F
246.0260	6	141.84	<.0001*

C.8 Distributions @24hr

Difference of maximum temperature

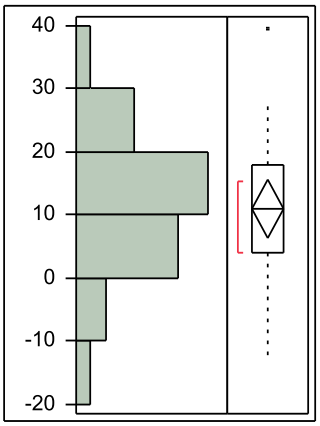

Quantiles

100.0%	maximum	39.39
99.5%		39.39
97.5%		39.39
90.0%		24.8
75.0%	quartile	17.91
50.0%	median	10.9268
25.0%	quartile	4.07978
10.0%		-4.2301
2.5%		-12.529
0.5%		-12.529
0.0%	minimum	-12.529

Moments

Mean	11.062541
Std Dev	11.087739
Std Err Mean	2.2632753
Upper 95% Mean	15.744483
Lower 95% Mean	6.3805994
N	24

Test Mean=value

Hypothesized Value	0
Actual Estimate	11.0625
DF	23
Std Dev	11.0877

Difference of maximum temperature difference

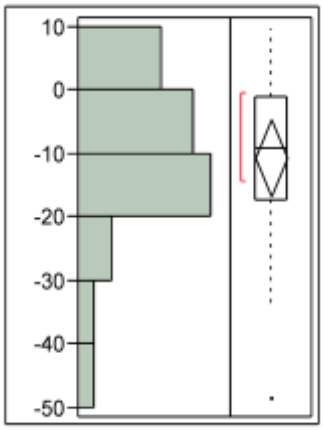

Quantiles

100.0%	maximum	9.73914
99.5%		9.73914
97.5%		9.73914
90.0%		7.12498
75.0%	quartile	-1.0841
50.0%	median	-9.2332
25.0%	quartile	-17.145
10.0%		-32.097
2.5%		-48.489
0.5%		-48.489
0.0%	minimum	-48.489

Moments

Mean	-10.59647
Std Dev	14.159988
Std Err Mean	2.8903955
Upper 95% Mean	-4.617236
Lower 95% Mean	-16.57571
N	24

Test Mean=value

Hypothesized Value	0
Actual Estimate	-10.596
DF	23
Std Dev	14.16

	t Test
Test Statistic	4.8878
Prob > |t|	<.0001*
Prob > t	<.0001*
Prob < t	1.0000

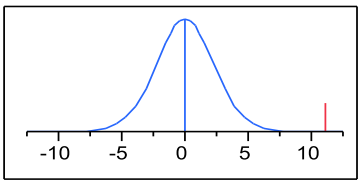

	t Test
Test Statistic	-3.6661
Prob > |t|	0.0013*
Prob > t	0.9994
Prob < t	0.0006*

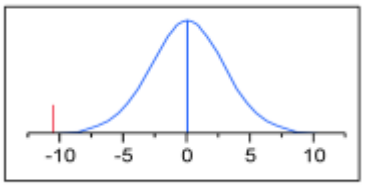

C.9 Distributions @27 hours

Difference of maximum temperature

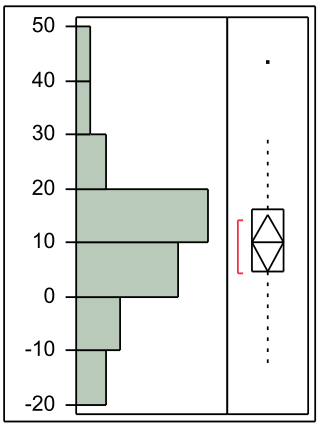

Quantiles

100.0%	maximum	43.2
99.5%		43.2
97.5%		43.2
90.0%		25.582
75.0%	quartile	16.1592
50.0%	median	10.1212
25.0%	quartile	4.69022
10.0%		-9.1901
2.5%		-12.356
0.5%		-12.356
0.0%	minimum	-12.356

Moments

Mean	9.982975
Std Dev	12.424553
Std Err Mean	2.4849106
Upper 95% Mean	15.111578
Lower 95% Mean	4.8543716
N	25

Test Mean=value

Hypothesized Value	0
Actual Estimate	9.98297
DF	24
Std Dev	12.4246

Difference of maximum temperature difference

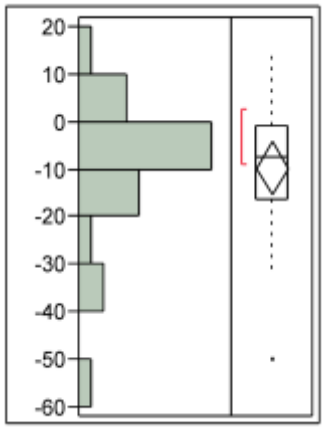

Quantiles

100.0%	maximum	13.8
99.5%		13.8
97.5%		13.8
90.0%		6.82427
75.0%	quartile	-0.9103
50.0%	median	-7.4108
25.0%	quartile	-16.436
10.0%		-30.479
2.5%		-50.088
0.5%		-50.088
0.0%	minimum	-50.088

Moments

Mean	-9.569193
Std Dev	14.026916
Std Err Mean	2.8053832
Upper 95% Mean	-3.779166
Lower 95% Mean	-15.35922
N	25

Test Mean=value

Hypothesized Value	0
Actual Estimate	-9.5692
DF	24
Std Dev	14.0269

	t Test
Test Statistic	4.0174
Prob > |t|	0.0005*
Prob > t	0.0003*
Prob < t	0.9997

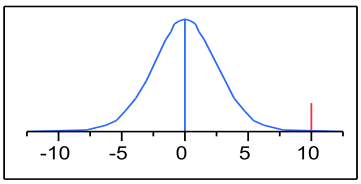

	t Test
Test Statistic	-3.4110
Prob > |t|	0.0023*
Prob > t	0.9989
Prob < t	0.0011*

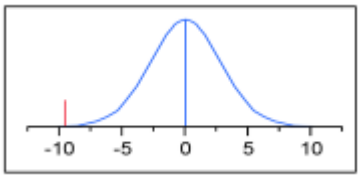

C.10 Distribution @30hours

Difference of maximum temperature

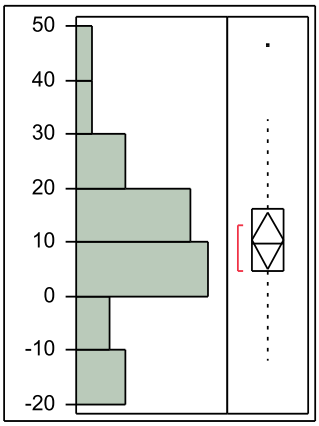

Quantiles

100.0%	maximum	46.14
99.5%		46.14
97.5%		46.14
90.0%		26.584
75.0%	quartile	16.2325
50.0%	median	9.73073
25.0%	quartile	4.81335
10.0%		-10.617
2.5%		-11.988
0.5%		-11.988
0.0%	minimum	-11.988

Moments

Mean	10.27117
Std Dev	12.996801
Std Err Mean	2.5993601
Upper 95% Mean	15.635986
Lower 95% Mean	4.9063548
N	25

Test Mean=value

Hypothesized Value	0
Actual Estimate	10.2712
DF	24
Std Dev	12.9968

Difference of maximum temperature difference

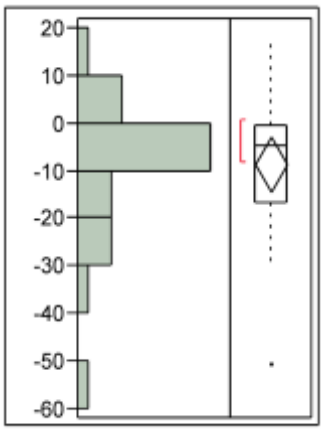

Quantiles

100.0%	maximum	17.67
99.5%		17.67
97.5%		17.67
90.0%		4.95964
75.0%	quartile	-0.4444
50.0%	median	-4.6068
25.0%	quartile	-16.576
10.0%		-27.072
2.5%		-50.765
0.5%		-50.765
0.0%	minimum	-50.765

Moments

Mean	-8.613938
Std Dev	13.956893
Std Err Mean	2.7913786
Upper 95% Mean	-2.852816
Lower 95% Mean	-14.37506
N	25

Test Mean=value

Hypothesized Value	0
Actual Estimate	-8.6139
DF	24
Std Dev	13.9569

	t Test
Test Statistic	3.9514
Prob > |t|	0.0006*
Prob > t	0.0003*
Prob < t	0.9997

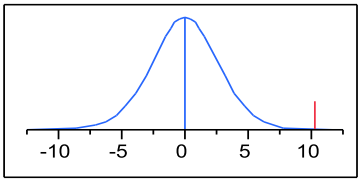

	t Test
Test Statistic	-3.0859
Prob > |t|	0.0051*
Prob > t	0.9975
Prob < t	0.0025*

C.11Distribution @ 33hours

Difference of maximum temperature

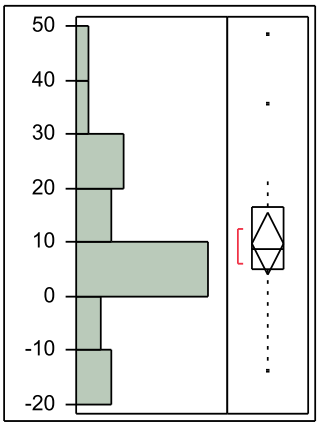

Quantiles

100.0%	maximum	48.24
99.5%		48.24
97.5%		48.24
90.0%		27.708
75.0%	quartile	16.6453
50.0%	median	8.66029
25.0%	quartile	4.92888
10.0%		-11.314
2.5%		-14.026
0.5%		-14.026
0.0%	minimum	-14.026

Moments

Mean	9.8766866
Std Dev	13.805147
Std Err Mean	2.7610295
Upper 95% Mean	15.575171
Lower 95% Mean	4.1782019
N	25

Test Mean=value

Hypothesized Value	0
Actual Estimate	9.87669
DF	24
Std Dev	13.8051

Difference of maximum temperature difference

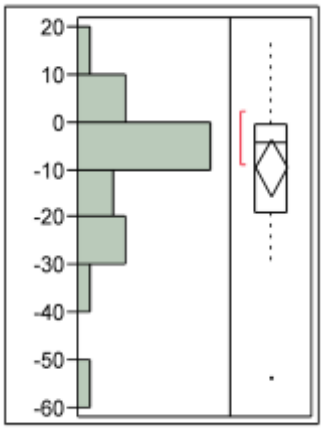

Quantiles

100.0%	maximum	18.2
99.5%		18.2
97.5%		18.2
90.0%		4.24583
75.0%	quartile	-0.6324
50.0%	median	-4.173
25.0%	quartile	-19.157
10.0%		-28.412
2.5%		-53.722
0.5%		-53.722
0.0%	minimum	-53.722

Moments

Mean	-9.483819
Std Dev	14.727939
Std Err Mean	2.9455878
Upper 95% Mean	-3.404425
Lower 95% Mean	-15.56321
N	25

Test Mean=value

Hypothesized Value	0
Actual Estimate	-9.4838
DF	24
Std Dev	14.7279

	t Test
Test Statistic	3.5772
Prob > |t|	0.0015*
Prob > t	0.0008*
Prob < t	0.9992

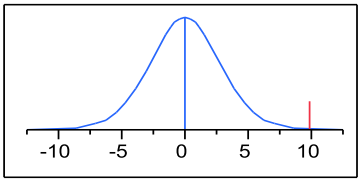

	t Test
Test Statistic	-3.2197
Prob > |t|	0.0037*
Prob > t	0.9982
Prob < t	0.0018*

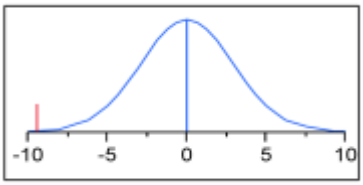

C.12Distribution @ 36hours

Difference of maximum temperature

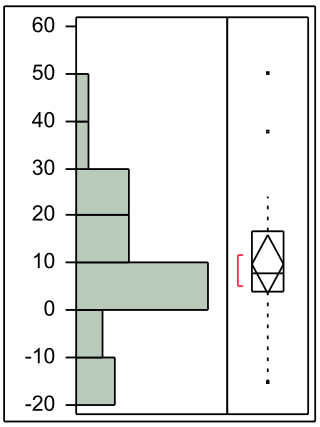

Quantiles

100.0%	maximum	49.95
99.5%		49.95
97.5%		49.95
90.0%		29.368
75.0%	quartile	16.8079
50.0%	median	7.91728
25.0%	quartile	4.00199
10.0%		-12.696
2.5%		-15.275
0.5%		-15.275
0.0%	minimum	-15.275

Moments

Mean	9.7222964
Std Dev	14.617941
Std Err Mean	2.9235882
Upper 95% Mean	15.756286
Lower 95% Mean	3.688307
N	25

Test Mean=value

Hypothesized Value	0
Actual Estimate	9.7223
DF	24
Std Dev	14.6179

Difference of maximum temperature difference

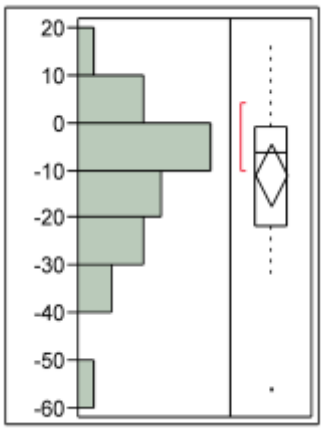

Quantiles

100.0%	maximum	17.62
99.5%		17.62
97.5%		17.62
90.0%		4.12205
75.0%	quartile	-0.7982
50.0%	median	-6.448
25.0%	quartile	-21.835
10.0%		-30.926
2.5%		-56.005
0.5%		-56.005
0.0%	minimum	-56.005

Moments

Mean	-10.92354
Std Dev	15.471846
Std Err Mean	3.0943691
Upper 95% Mean	-4.537075
Lower 95% Mean	-17.31
N	25

Test Mean=value

Hypothesized Value	0
Actual Estimate	-10.924
DF	24
Std Dev	15.4718

	t Test
Test Statistic	3.3255
Prob > |t|	0.0028*
Prob > t	0.0014*
Prob < t	0.9986

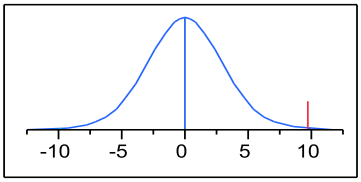

	t Test
Test Statistic	-3.5301
Prob > |t|	0.0017*
Prob > t	0.9991
Prob < t	0.0009*

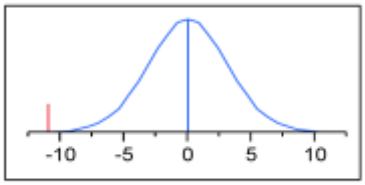

C.13 Distribution @39 hours

Difference of maximum temperature

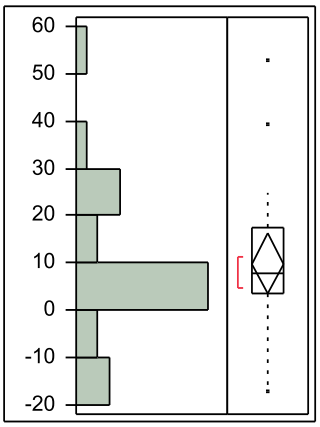

Quantiles

100.0%	maximum	52.47
99.5%		52.47
97.5%		52.47
90.0%		30.474
75.0%	quartile	17.3549
50.0%	median	7.78896
25.0%	quartile	3.70917
10.0%		-12.82
2.5%		-17.461
0.5%		-17.461
0.0%	minimum	-17.461

Moments

Mean	9.8026848
Std Dev	15.435876
Std Err Mean	3.0871752
Upper 95% Mean	16.174301
Lower 95% Mean	3.4310683
N	25

Test Mean=value

Hypothesized Value	0
Actual Estimate	9.80268
DF	24
Std Dev	15.4359

Difference of maximum temperature difference

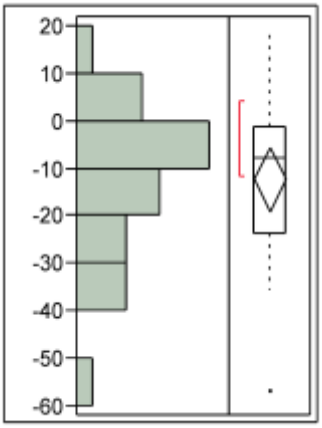

Quantiles

100.0%	maximum	18.24
99.5%		18.24
97.5%		18.24
90.0%		3.64419
75.0%	quartile	-1.4064
50.0%	median	-7.9647
25.0%	quartile	-23.517
10.0%		-33.039
2.5%		-56.904
0.5%		-56.904
0.0%	minimum	-56.904

Moments

Mean	-12.21218
Std Dev	16.289758
Std Err Mean	3.2579516
Upper 95% Mean	-5.488095
Lower 95% Mean	-18.93626
N	25

Test Mean=value

Hypothesized Value	0
Actual Estimate	-12.212
DF	24
Std Dev	16.2898

	t Test
Test Statistic	3.1753
Prob > |t|	0.0041*
Prob > t	0.0020*
Prob < t	0.9980

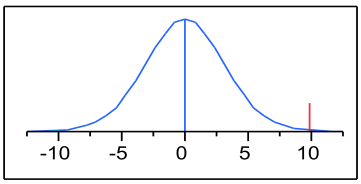

	t Test
Test Statistic	-3.7484
Prob > |t|	0.0010*
Prob > t	0.9995
Prob < t	0.0005*

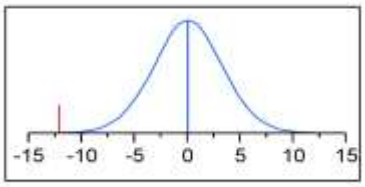

C.14 Distribution @ 42hours

Difference of maximum temperature

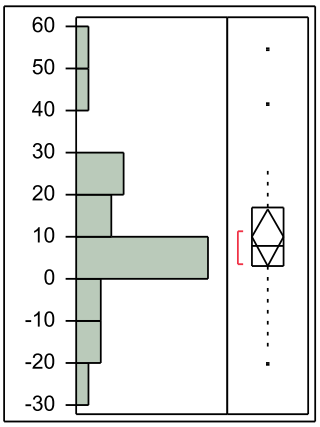

Quantiles

100.0%	maximum	54.4
99.5%		54.4
97.5%		54.4
90.0%		32.39
75.0%	quartile	17.0129
50.0%	median	7.98287
25.0%	quartile	2.96535
10.0%		-13.991
2.5%		-20.494
0.5%		-20.494
0.0%	minimum	-20.494

Moments

Mean	9.8020063
Std Dev	16.364462
Std Err Mean	3.2728924
Upper 95% Mean	16.556924
Lower 95% Mean	3.0470883
N	25

Test Mean=value

Hypothesized Value	0
Actual Estimate	9.80201
DF	24
Std Dev	16.3645

Difference of maximum temperature difference

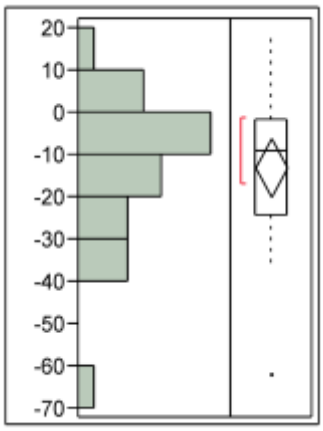

Quantiles

100.0%	maximum	17.84
99.5%		17.84
97.5%		17.84
90.0%		4.29978
75.0%	quartile	-1.8043
50.0%	median	-9.1252
25.0%	quartile	-24.347
10.0%		-34.794
2.5%		-62.364
0.5%		-62.364
0.0%	minimum	-62.364

Moments

Mean	-12.907
Std Dev	17.038536
Std Err Mean	3.4077071
Upper 95% Mean	-5.873837
Lower 95% Mean	-19.94016
N	25

Test Mean=value

Hypothesized Value	0
Actual Estimate	-12.907
DF	24
Std Dev	17.0385

	t Test
Test Statistic	2.9949
Prob > |t|	0.0063*
Prob > t	0.0031*
Prob < t	0.9969

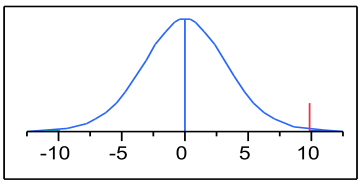

	t Test
Test Statistic	-3.7876
Prob > |t|	0.0009*
Prob > t	0.9996
Prob < t	0.0004*

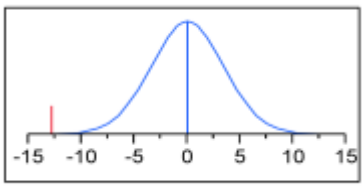

C.15 Distributions @45 hours

Difference of maximum temperature

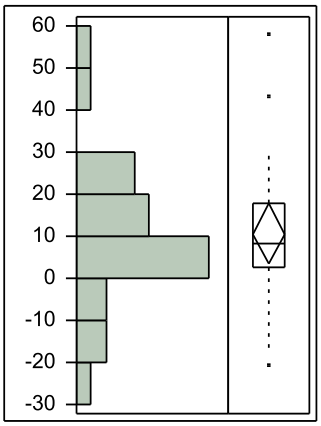

Quantiles

100.0%	maximum	58.01
99.5%		58.01
97.5%		58.01
90.0%		34.722
75.0%	quartile	17.7829
50.0%	median	8.18145
25.0%	quartile	2.47726
10.0%		-14.629
2.5%		-20.848
0.5%		-20.848
0.0%	minimum	-20.848

Moments

Mean	10.469875
Std Dev	67.164665
Std Err Mean	3.4683684
Upper 95% Mean	17.628236
Lower 95% Mean	3.3115149
N	25

Difference of maximum temperature difference

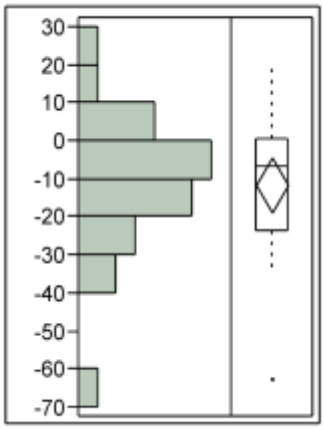

Quantiles

100.0%	maximum	20.92
99.5%		20.92
97.5%		20.92
90.0%		6.60175
75.0%	quartile	0.29633
50.0%	median	-6.5834
25.0%	quartile	-23.454
10.0%		-34.276
2.5%		-62.602
0.5%		-62.602
0.0%	minimum	-62.602

Moments

Mean	-11.72613
Std Dev	67.837957
Std Err Mean	3.503137
Upper 95% Mean	-4.496011
Lower 95% Mean	-18.95625
N	25

Test Mean=value

Hypothesized Value	0
Actual Estimate	10.4699
DF	24
Std Dev	67.1647

	t Test
Test Statistic	3.0187
Prob > |t|	0.0059*
Prob > t	0.0030*
Prob < t	0.9970

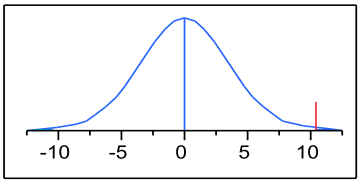

Test Mean=value

Hypothesized Value	0
Actual Estimate	-11.726
DF	24
Std Dev	67.838

	t Test
Test Statistic	-3.3473
Prob > |t|	0.0027*
Prob > t	0.9987
Prob < t	0.0013*

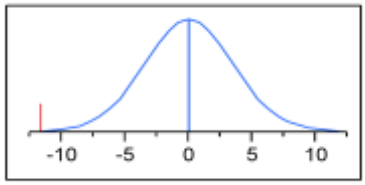

C.16 Distributions @48hours

Difference of maximum temperature

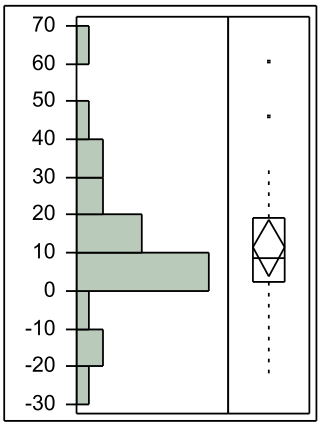

Quantiles

100.0%	maximum	60.2
99.5%		60.2
97.5%		60.2
90.0%		37.522
75.0%	quartile	19.4048
50.0%	median	8.86618
25.0%	quartile	2.36023
10.0%		-14.753
2.5%		-22.018
0.5%		-22.018
0.0%	minimum	-22.018

Moments

Mean	11.460153
Std Dev	72.711566
Std Err Mean	3.6355783
Upper 95% Mean	18.963618
Lower 95% Mean	3.9566882
N	25

Difference of maximum temperature difference

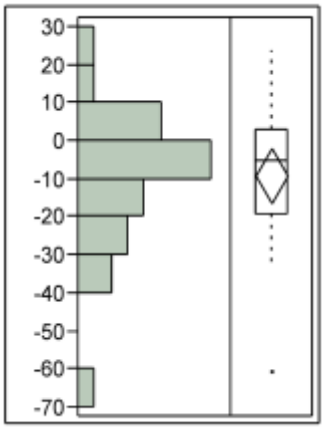

Quantiles

100.0%	maximum	23.5
99.5%		23.5
97.5%		23.5
90.0%		9.35417
75.0%	quartile	2.85534
50.0%	median	-5.1438
25.0%	quartile	-19.078
10.0%		-32.011
2.5%		-60.612
0.5%		-60.612
0.0%	minimum	-60.612

Moments

Mean	-9.267744
Std Dev	69.231714
Std Err Mean	3.4615857
Upper 95% Mean	-2.123382
Lower 95% Mean	-16.41211
N	25

Test Mean=value

Hypothesized Value	0
Actual Estimate	11.4602
DF	24
Std Dev	72.7116

	t Test
Test Statistic	3.1522
Prob > |t|	0.0043*
Prob > t	0.0022*
Prob < t	0.9978

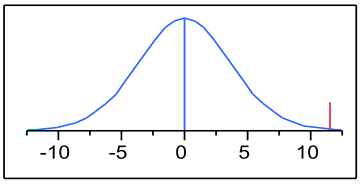

Test Mean=value

Hypothesized Value	0
Actual Estimate	-9.2677
DF	24
Std Dev	69.2317

	t Test
Test Statistic	-2.6773
Prob > |t|	0.0132*
Prob > t	0.9934
Prob < t	0.0066*

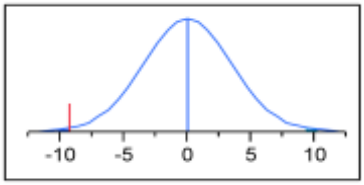

C.17 Distributions @ 51 hours

Difference of maximum temperature

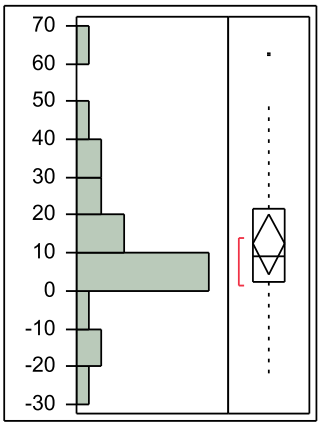

Quantiles

100.0%	maximum	62.18
99.5%		62.18
97.5%		62.18
90.0%		40.516
75.0%	quartile	21.4653
50.0%	median	9.10948
25.0%	quartile	2.504
10.0%		-14.634
2.5%		-22.644
0.5%		-22.644
0.0%	minimum	-22.644

Moments

Mean	12.273917
Std Dev	19.034465
Std Err Mean	3.806893
Upper 95% Mean	20.130958
Lower 95% Mean	4.4168757
N	25

Difference of maximum temperature difference

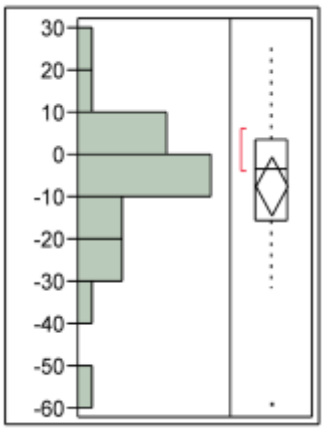

Quantiles

100.0%	maximum	25.95
99.5%		25.95
97.5%		25.95
90.0%		8.02444
75.0%	quartile	3.36245
50.0%	median	-3.6387
25.0%	quartile	-15.631
10.0%		-30.356
2.5%		-59.306
0.5%		-59.306
0.0%	minimum	-59.306

Moments

Mean	-7.45303
Std Dev	17.013448
Std Err Mean	3.4026897
Upper 95% Mean	-0.430224
Lower 95% Mean	-14.47584
N	25

Test Mean=value

Hypothesized Value	0
Actual Estimate	12.2739
DF	24
Std Dev	19.0345

	t Test
Test Statistic	3.2241
Prob > |t|	0.0036*
Prob > t	0.0018*
Prob < t	0.9982

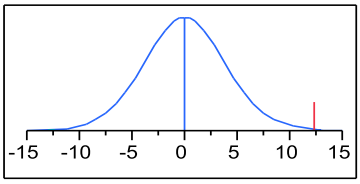

Test Mean=value

Hypothesized Value	0
Actual Estimate	-7.453
DF	24
Std Dev	17.0134

	t Test
Test Statistic	-2.1903
Prob > |t|	0.0385*
Prob > t	0.9808
Prob < t	0.0192*

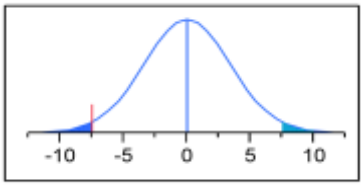

C.18 Distributions @ 57 hours

Difference of maximum temperature

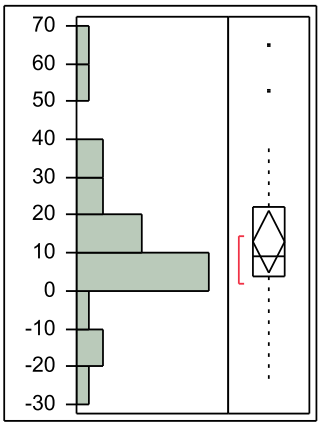

Quantiles

100.0%	maximum	64.46
99.5%		64.46
97.5%		64.46
90.0%		44.344
75.0%	quartile	22.3991
50.0%	median	9.08422
25.0%	quartile	3.6572
10.0%		-15.252
2.5%		-23.343
0.5%		-23.343
0.0%	minimum	-23.343

Moments

Mean	13.015798
Std Dev	19.938772
Std Err Mean	3.9877543
Upper 95% Mean	21.246118
Lower 95% Mean	4.7854776
N	25

Difference of maximum temperature difference

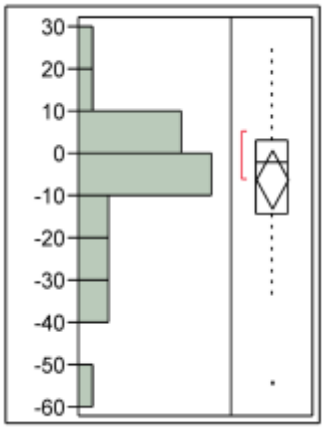

Quantiles

100.0%	maximum	26.35
99.5%		26.35
97.5%		26.35
90.0%		12.2787
75.0%	quartile	3.2026
50.0%	median	-2.2677
25.0%	quartile	-14.259
10.0%		-32.545
2.5%		-54.377
0.5%		-54.377
0.0%	minimum	-54.377

Moments

Mean	-6.145271
Std Dev	17.020201
Std Err Mean	3.4040401
Upper 95% Mean	0.8803227
Lower 95% Mean	-13.17086
N	25

Test Mean=value

Hypothesized Value	0
Actual Estimate	13.0158
DF	24
Std Dev	19.9388

	t Test
Test Statistic	3.2639
Prob > |t|	0.0033*
Prob > t	0.0016*
Prob < t	0.9984

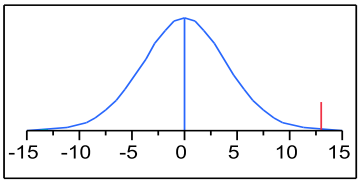

Test Mean=value

Hypothesized Value	0
Actual Estimate	-6.1453
DF	24
Std Dev	17.0202

	t Test
Test Statistic	-1.8053
Prob > |t|	0.0836
Prob > t	0.9582
Prob < t	0.0418*

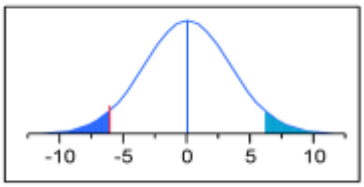

C.19 Distribution @ 60hours

Difference of maximum temperature

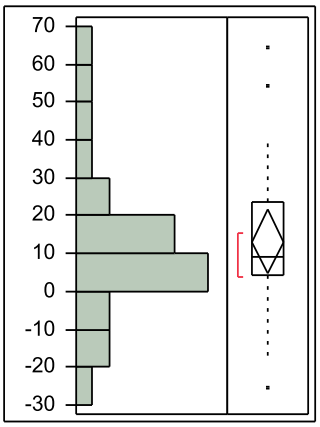

Quantiles

100.0%	maximum	64.41
99.5%		64.41
97.5%		64.41
90.0%		46.08
75.0%	quartile	23.7243
50.0%	median	9.19779
25.0%	quartile	4.39924
10.0%		-14.997
2.5%		-25.599
0.5%		-25.599
0.0%	minimum	-25.599

Moments

Mean	13.225147
Std Dev	20.38704
Std Err Mean	4.0774079
Upper 95% Mean	21.640503
Lower 95% Mean	4.8097906
N	25

Test Mean=value

Hypothesized Value	0
Actual Estimate	13.2251
DF	24
Std Dev	20.387

Difference of maximum temperature difference

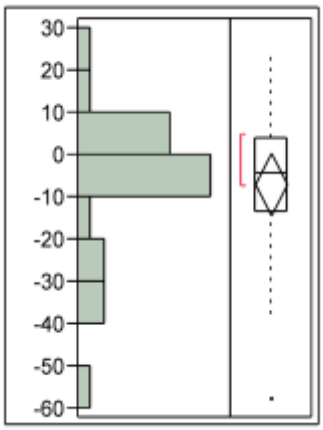

Quantiles

100.0%	maximum	23.72
99.5%		23.72
97.5%		23.72
90.0%		13.1697
75.0%	quartile	3.77453
50.0%	median	-4.3533
25.0%	quartile	-13.418
10.0%		-36.339
2.5%		-57.721
0.5%		-57.721
0.0%	minimum	-57.721

Moments

Mean	-6.842678
Std Dev	17.783313
Std Err Mean	3.5566626
Upper 95% Mean	0.4979132
Lower 95% Mean	-14.18327
N	25

Test Mean=value

Hypothesized Value	0
Actual Estimate	-6.8427
DF	24
Std Dev	17.7833

	t Test
Test Statistic	3.2435
Prob > |t|	0.0035*
Prob > t	0.0017*
Prob < t	0.9983

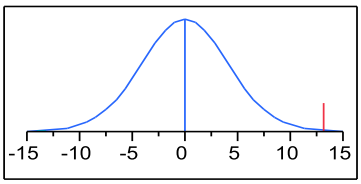

	t Test
Test Statistic	-1.9239
Prob > |t|	0.0663
Prob > t	0.9668
Prob < t	0.0332*

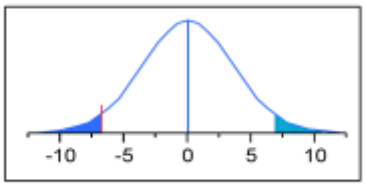

C.20 Distribution @63hours

Difference of maximum temperature

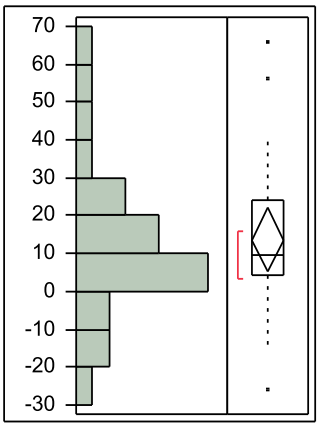

Quantiles

100.0%	maximum	65.64
99.5%		65.64
97.5%		65.64
90.0%		47.164
75.0%	quartile	24.1061
50.0%	median	9.85009
25.0%	quartile	4.06593
10.0%		-14.461
2.5%		-26.022
0.5%		-26.022
0.0%	minimum	-26.022

Moments

Mean	13.577414
Std Dev	20.69806
Std Err Mean	4.139612
Upper 95% Mean	22.121153
Lower 95% Mean	5.0336745
N	25

Test Mean=value

Hypothesized Value	0
Actual Estimate	13.5774
DF	24
Std Dev	20.6981

Difference of maximum temperature difference

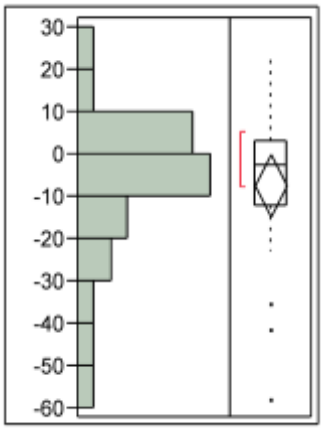

Quantiles

100.0%	maximum	22.17
99.5%		22.17
97.5%		22.17
90.0%		12.7371
75.0%	quartile	3.13653
50.0%	median	-2.5968
25.0%	quartile	-12.296
10.0%		-38.051
2.5%		-58.195
0.5%		-58.195
0.0%	minimum	-58.195

Moments

Mean	-7.438596
Std Dev	17.887155
Std Err Mean	3.577431
Upper 95% Mean	-0.055141
Lower 95% Mean	-14.82205
N	25

Test Mean=value

Hypothesized Value	0
Actual Estimate	-7.4386
DF	24
Std Dev	17.8872

	t Test
Test Statistic	3.2799
Prob > |t|	0.0032*
Prob > t	0.0016*
Prob < t	0.9984

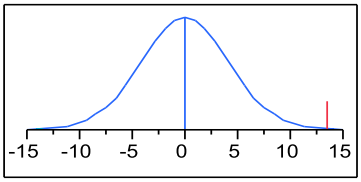

	t Test
Test Statistic	-2.0793
Prob > |t|	0.0484*
Prob > t	0.9758
Prob < t	0.0242*

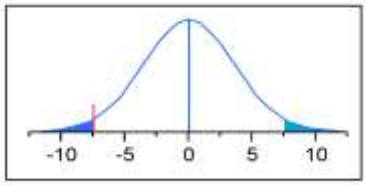

C.21 Distribution @66hours

Difference of maximum temperature

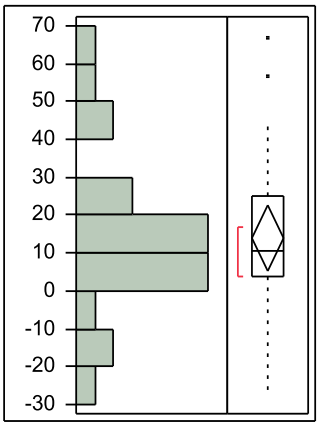

Quantiles

100.0%	maximum	66.67
99.5%		66.67
97.5%		66.67
90.0%		48.64
75.0%	quartile	24.8416
50.0%	median	10.5507
25.0%	quartile	3.93033
10.0%		-14.292
2.5%		-26.144
0.5%		-26.144
0.0%	minimum	-26.144

Moments

Mean	14.141324
Std Dev	21.090183
Std Err Mean	4.2180366
Upper 95% Mean	22.846923
Lower 95% Mean	5.435724
N	25

Test Mean=value

Hypothesized Value	0
Actual Estimate	14.1413
DF	24
Std Dev	21.0902

Difference of maximum temperature difference

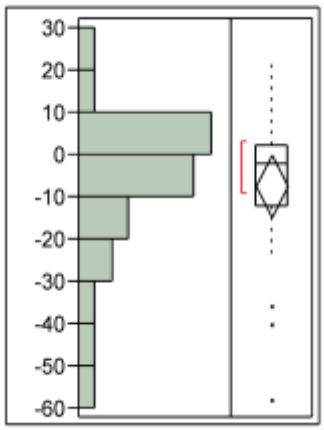

Quantiles

100.0%	maximum	21.21
99.5%		21.21
97.5%		21.21
90.0%		11.371
75.0%	quartile	2.32693
50.0%	median	-2.0633
25.0%	quartile	-12.16
10.0%		-37.72
2.5%		-58.177
0.5%		-58.177
0.0%	minimum	-58.177

Moments

Mean	-7.4794
Std Dev	17.655142
Std Err Mean	3.5310285
Upper 95% Mean	-0.191716
Lower 95% Mean	-14.76708
N	25

Test Mean=value

Hypothesized Value	0
Actual Estimate	-7.4794
DF	24
Std Dev	17.6551

	t Test
Test Statistic	3.3526
Prob > |t|	0.0026*
Prob > t	0.0013*
Prob < t	0.9987

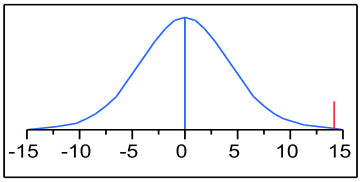

	t Test
Test Statistic	-2.1182
Prob > |t|	0.0447*
Prob > t	0.9776
Prob < t	0.0224*

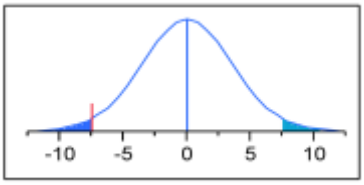

C.22 Distribution @69hours

Difference of maximum temperature

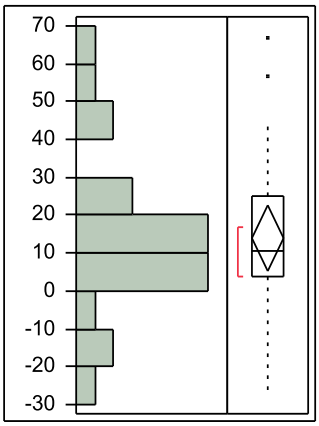

Quantiles

100.0%	maximum	66.67
99.5%		66.67
97.5%		66.67
90.0%		48.64
75.0%	quartile	24.8416
50.0%	median	10.5507
25.0%	quartile	3.93033
10.0%		-14.292
2.5%		-26.144
0.5%		-26.144
0.0%	minimum	-26.144

Moments

Mean	14.141324
Std Dev	21.090183
Std Err Mean	4.2180366
Upper 95% Mean	22.846923
Lower 95% Mean	5.435724
N	25

Test Mean=value

Hypothesized Value	0
Actual Estimate	14.1413
DF	24
Std Dev	21.0902

Difference of maximum temperature difference

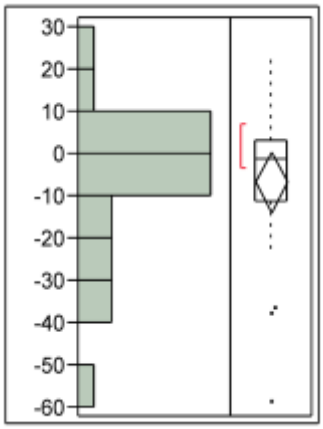

Quantiles

100.0%	maximum	22.69
99.5%		22.69
97.5%		22.69
90.0%		10.8172
75.0%	quartile	3.14299
50.0%	median	-1.3877
25.0%	quartile	-11.473
10.0%		-37.107
2.5%		-58.608
0.5%		-58.608
0.0%	minimum	-58.608

Moments

Mean	-6.694171
Std Dev	17.721343
Std Err Mean	3.5442686
Upper 95% Mean	0.6208393
Lower 95% Mean	-14.00918
N	25

Test Mean=value

Hypothesized Value	0
Actual Estimate	-6.6942
DF	24
Std Dev	17.7213

	t Test
Test Statistic	3.3526
Prob > |t|	0.0026*
Prob > t	0.0013*
Prob < t	0.9987

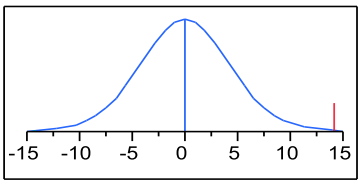

	t Test
Test Statistic	-1.8887
Prob > |t|	0.0711
Prob > t	0.9645
Prob < t	0.0355*

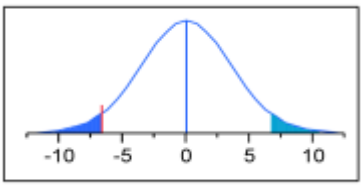

C.23 Distribution@72hours

Difference of maximum temperature

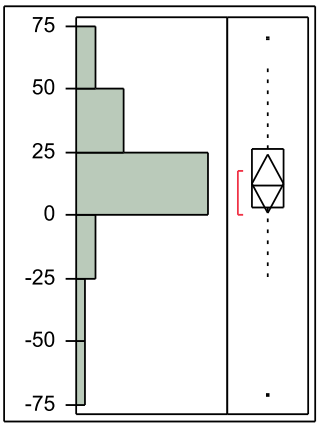

Quantiles

100.0%	maximum	69.71
99.5%		69.71
97.5%		69.71
90.0%		52.086
75.0%	quartile	26.6281
50.0%	median	11.8467
25.0%	quartile	3.61564
10.0%		-19.557
2.5%		-71.47
0.5%		-71.47
0.0%	minimum	-71.47

Moments

Mean	12.729776
Std Dev	28.062619
Std Err Mean	5.6125237
Upper 95% Mean	24.313456
Lower 95% Mean	1.1460962
N	25

Test Mean=value

Hypothesized Value	0
Actual Estimate	12.7298
DF	24
Std Dev	28.0626

Difference of maximum temperature difference

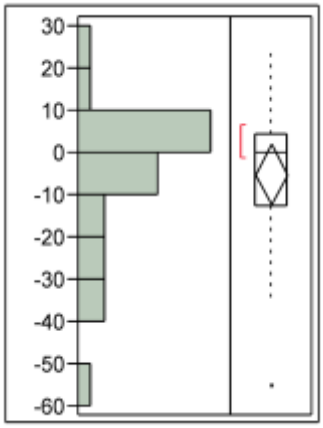

Quantiles

100.0%	maximum	24.44
99.5%		24.44
97.5%		24.44
90.0%		11.5374
75.0%	quartile	4.42417
50.0%	median	-0.1808
25.0%	quartile	-12.462
10.0%		-33.679
2.5%		-55.327
0.5%		-55.327
0.0%	minimum	-55.327

Moments

Mean	-5.163808
Std Dev	17.260886
Std Err Mean	3.4521771
Upper 95% Mean	1.9611356
Lower 95% Mean	-12.28875
N	25

Test Mean=value

Hypothesized Value	0
Actual Estimate	-5.1638
DF	24
Std Dev	17.2609

	t Test
Test Statistic	2.2681
Prob > |t|	0.0326*
Prob > t	0.0163*
Prob < t	0.9837

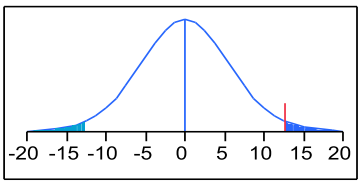

	t Test
Test Statistic	-1.4958
Prob > |t|	0.1477
Prob > t	0.9261
Prob < t	0.0739

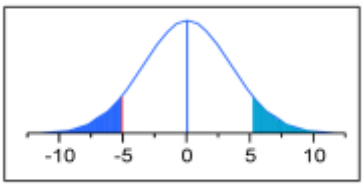

APPENDIX D ADDITIONAL SENSITIVITY STUDY TABLES AND FIGURES

Table D.1 Pier 3 footing sensitivity study summary

Group	Input	Dimensional Size	Fresh Placement Temp.	Top Insulation	Side Insulation	Form removal time	Placement Date	Mix Design
General	Material Type	Concrete	Concrete	Concrete	Concrete	Concrete	Concrete	Concrete
	Material Name	Pier 3 ftg	Pier 3 ftg	Pier 3 ftg	Pier 3 ftg	Pier 3 ftg	Pier 3 ftg	Pier 3 ftg
	Thickness	Varies	8.23m	8.23m	8.23m	8.23m	8.23m	8.23m
	Start Time	0	0	0	0	0	0	0
	Fresh Temperature	20.5°C	Varies	20.5°C	20.5°C	20.5°C	20.5°C	20.5°C
Dimensional Size	Width	Varies	2.2m	2.2m	2.2m	2.2m	2.2m	2.2m
	Length	Varies	13.1m	13.1m	13.1m	13.1m	13.1m	13.1m
Surface Boundary Condition	ambient temp.	min. :8 C, max. :20.5C, start time :11 hr					Varies	min. :8 C, max. :20.5C, start time :11 hr
	wind speed	5m/s	5m/s	5m/s	5m/s	5m/s	5m/s	5m/s
	top concrete insulation material	Plastic foil	Plastic foil	Varies	Plastic foil	Plastic foil	Plastic foil	Plastic foil
	top concrete insulation removal time	371 hr	371 hr	371 hr	371 hr	371 hr	371 hr	371 hr
	side concrete insulation material	Plywood formwork	Plywood formwork	Plywood formwork	Varies	Plywood formwork	Plywood formwork	Plywood formwork
	side concrete insulation removal	312 hr	312 hr	312 hr	312 hr	Varies	312 hr	312 hr
	bottom concrete insulation material	none	none	none	none	none	none	none
	bottom concrete insulation removal	none	none	none	none	none	none	none
	soil insulation material	none	none	none	none	none	none	none
	soil insulation removal	none	none	none	none	none	none	none
Material Properties		see table 14	see table 14	see table 14	see table 14	see table 14	see table 14	Varies

Concrete Properties	see table 14	see table 14	see table 14	see table 14	see table 14	see table 14	see table 14
Calculation parameters	see table 7	see table 7	see table 7	see table 7	see table 7	see table 7	see table 7
Subbase material	Soil	Soil	Soil	Soil	Soil	Soil	Soil

Table D.2 Variables summary for pier 3 footing sensitivity study

	Dimensions	**Placement Temp.**	**Top. Insulation**	**Side Insulation**	**Removal time**	**Placement Date**	**Mix Design**
Parameter (Width*Length*Depth)	27'*43'*5’ 27'*43'*6’ 27'*43'*7’ 27'*43'*5’ 27'*43'*10' 35'*43'*7.25' 40'*43'*7.25'	40-90° F 10°F Increment	see insulation material table	Insulation-mat. table	48-336 hr 24 hour increments	11/19/2008 7/30/2008 Placement Temp. 40-90° F 10°F Increments	427-727Pcy 100pcy Increments **CTE value** 7.36,9,11,13 *10^{-6}/°C **Thermal Cond.** 5.39,8.4,10,13,18 **GGBFS** 10-50% 10% Increment **Fly Ash** 10-50% 10% Increment

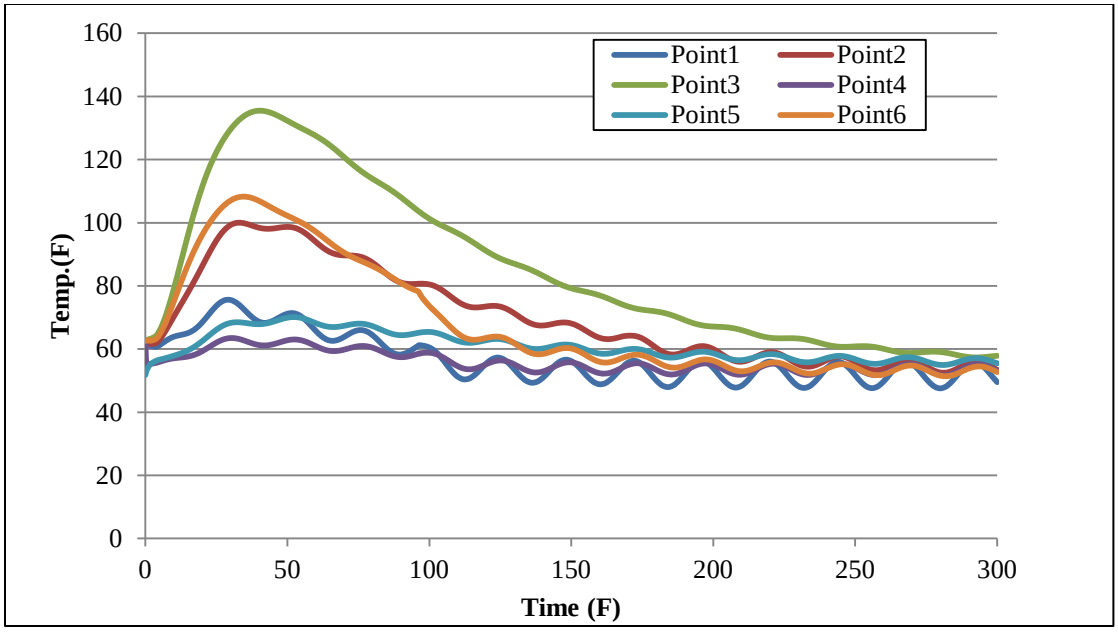

Figure D.1 Temperature development results for pier 1 footing sensor location study

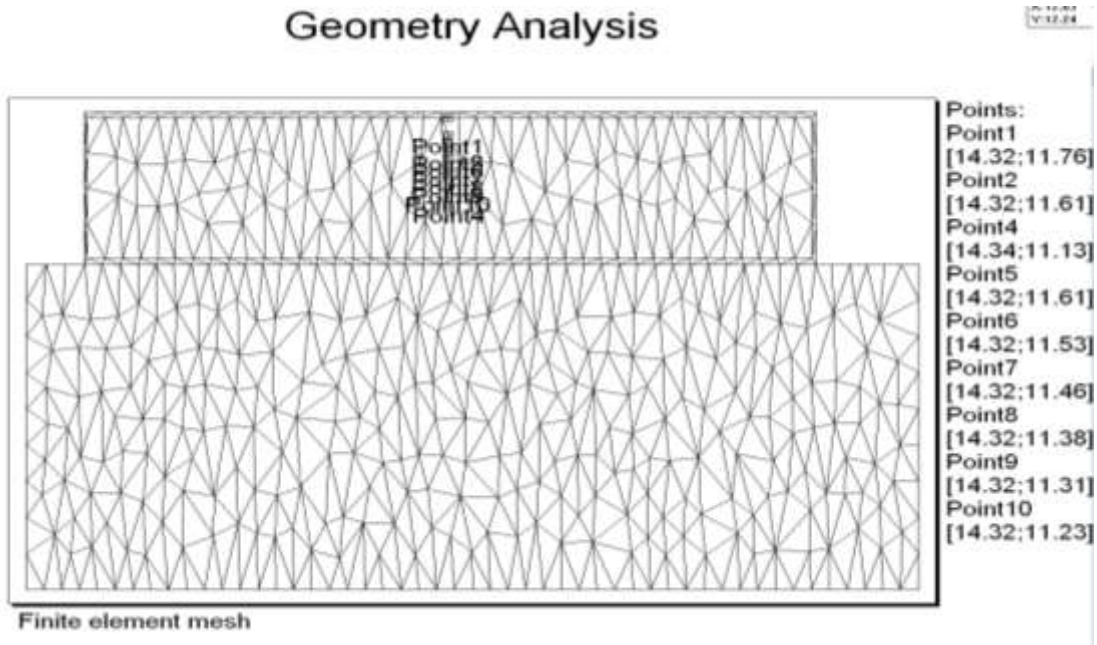

Figure D.2 Cross section of sensor location study at longitudinal direction

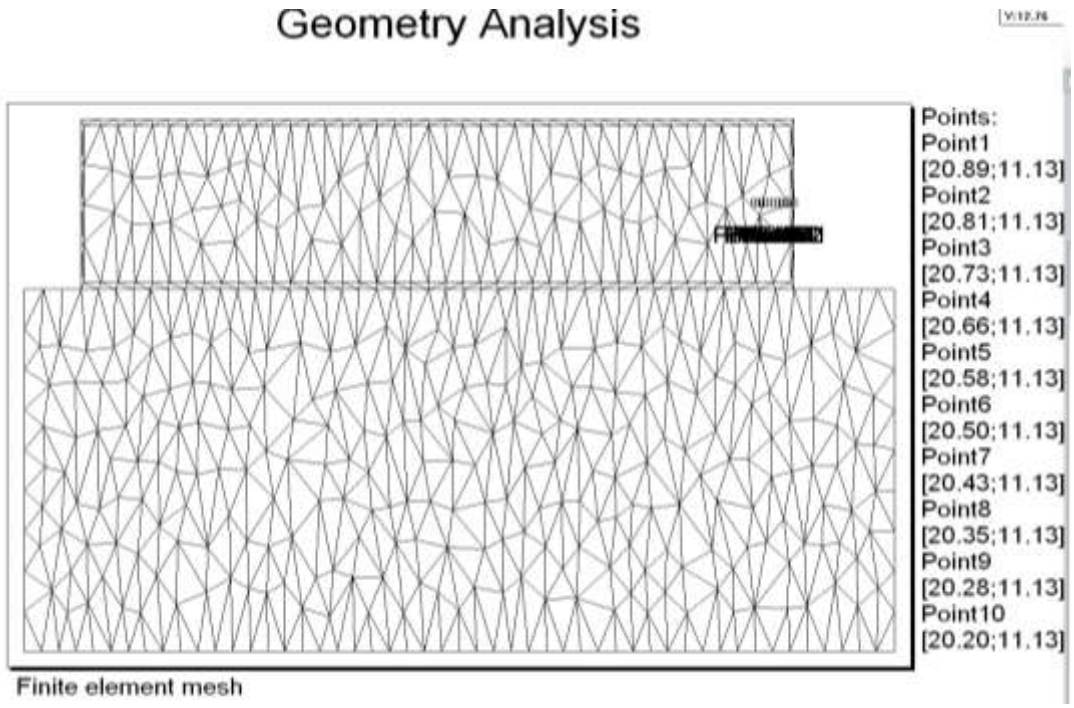

Figure D.3 Temperature development at difference location (3in interval in lateral direction)

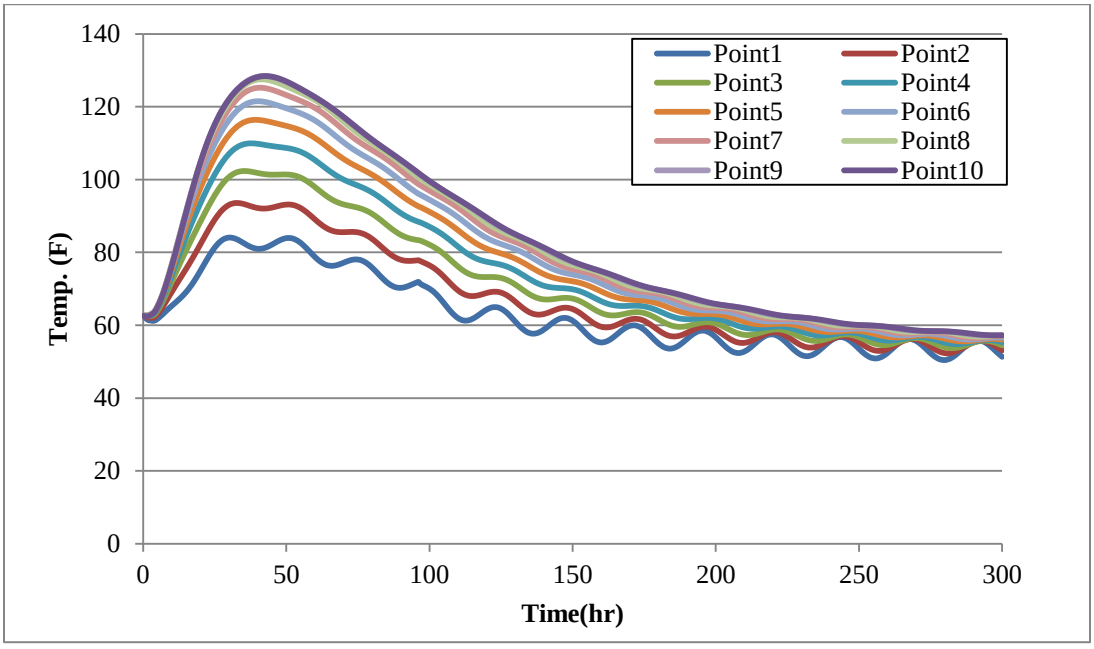

Figure D.4 Pier 1footing temperature development different location (from top surface to inside)

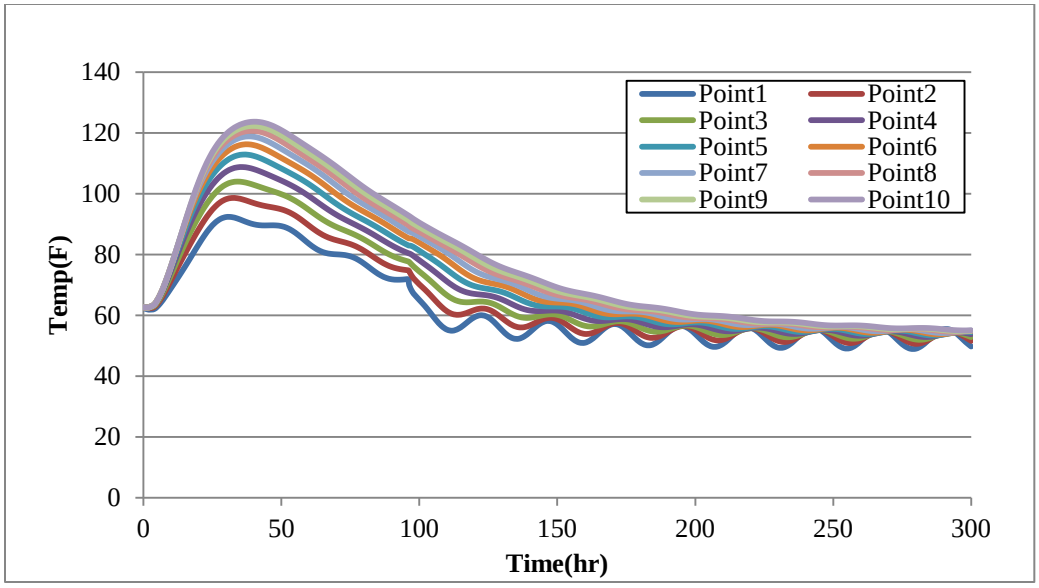

Figure D.5 Pier 1footing temperature development different location (from side surface to inside)

Table D.3 Sensitivity study summary on dimensional size for pier 1 footing

Dimensions(ft)			Dimensions(mm)			Max. Temp(F)	Max. Temp. Diff(F)	Stress/ Strength Ratio			
								Soil		concrete	
Width	Length	Depth	Width	Length	Depth			Before removed	After removed	Before removed	After removed
12	43	4.5	3700	13110	1372	129	46	0.62	0.25	0.52	0.67
12	43	5	3700	13110	1524	141	42	1.09	0.33	0.52	0.7
12	43	6	3700	13110	1829	150	53	1.17	0.47	0.52	1
12	43	7	3700	13110	2134	159	62	1.2	0.6	0.49	1.4
12	43	9	3700	13110	2744	170	78	1.28	0.7	0.32	2.3
12	43	4.5	3700	13110	1372	129	46	0.62	0.25	0.52	0.67
15	43	4.5	4573	13110	1372	129	58	1.09	0.33	0.52	0.67
25	43	4.5	7622	13110	1372	129	69	1.17	0.47	0.52	0.67
30	43	4.5	9146	13110	1372	129	82	1.2	0.6	0.52	0.67
35	43	4.5	10671	13110	1372	129	95	1.28	0.7	0.52	0.67
12	30	4.5	3700	9146	1372	129	46	0.62	0.25	0.52	0.67
12	43	4.5	3700	13110	1372	129	46	0.62	0.25	0.52	0.67
12	50	4.5	3700	15244	1372	129	46	0.62	0.25	0.52	0.67
12	60	4.5	3700	18293	1372	129	46	0.62	0.25	0.52	0.67
12	70	4.5	3700	21341	1372	129	46	0.62	0.25	0.52	0.67
12	77	4.5	3700	23476	1372	129	46	0.62	0.25	0.52	0.67

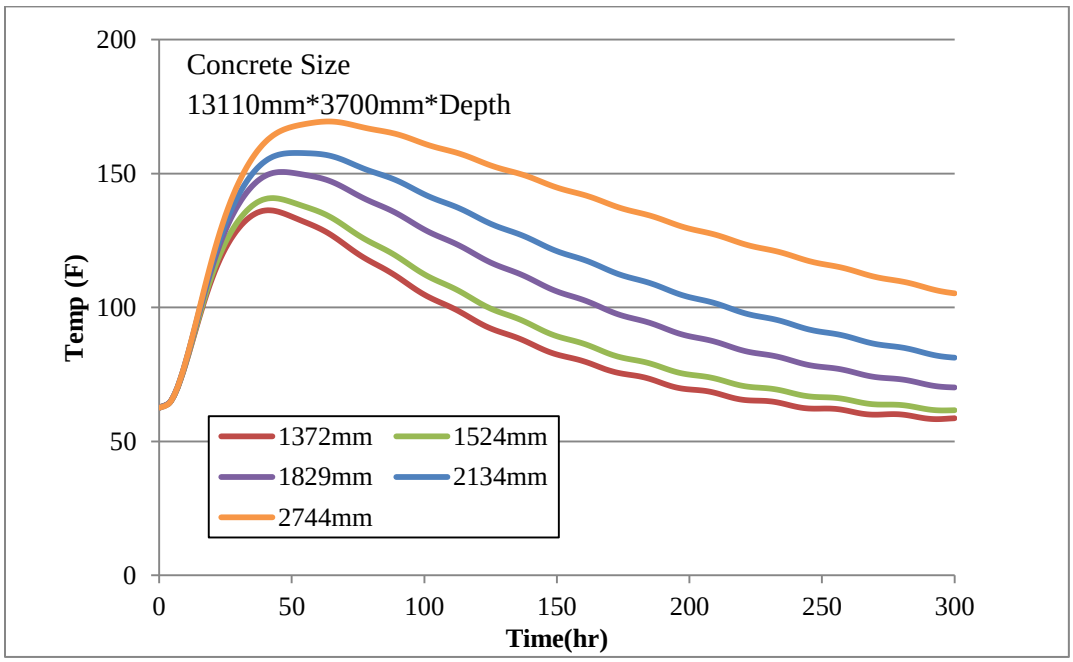

Figure D.6 Pier 1 footing maximum temperature results when depth varies (soil/concrete)

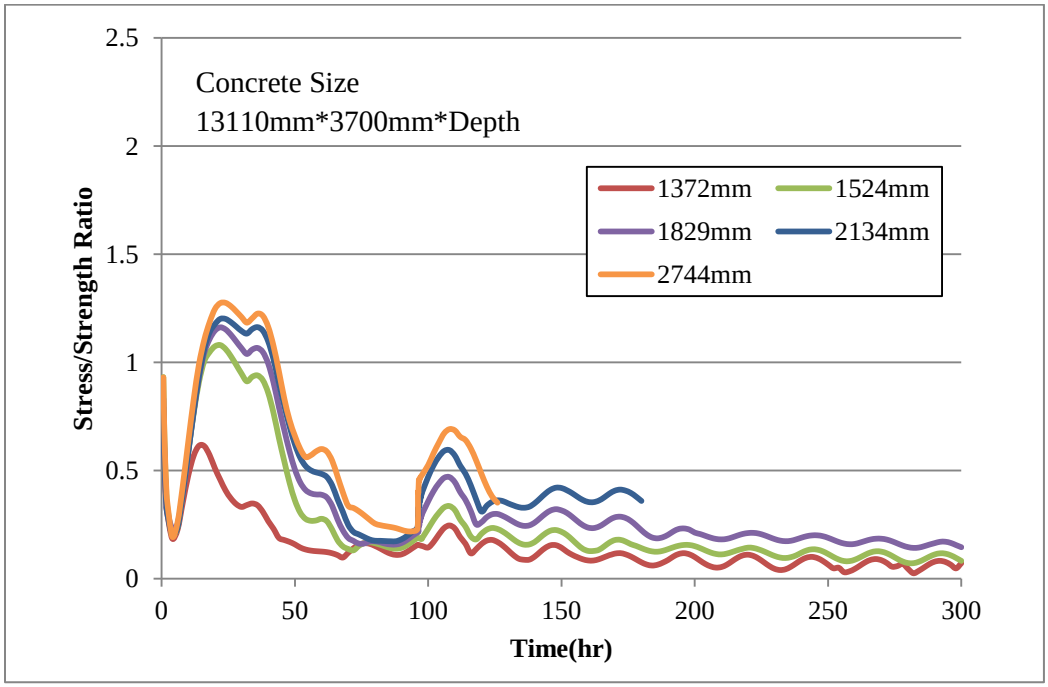

Figure D.7 Pier 1 footing stress/strength ratio results when depth varies (soil)

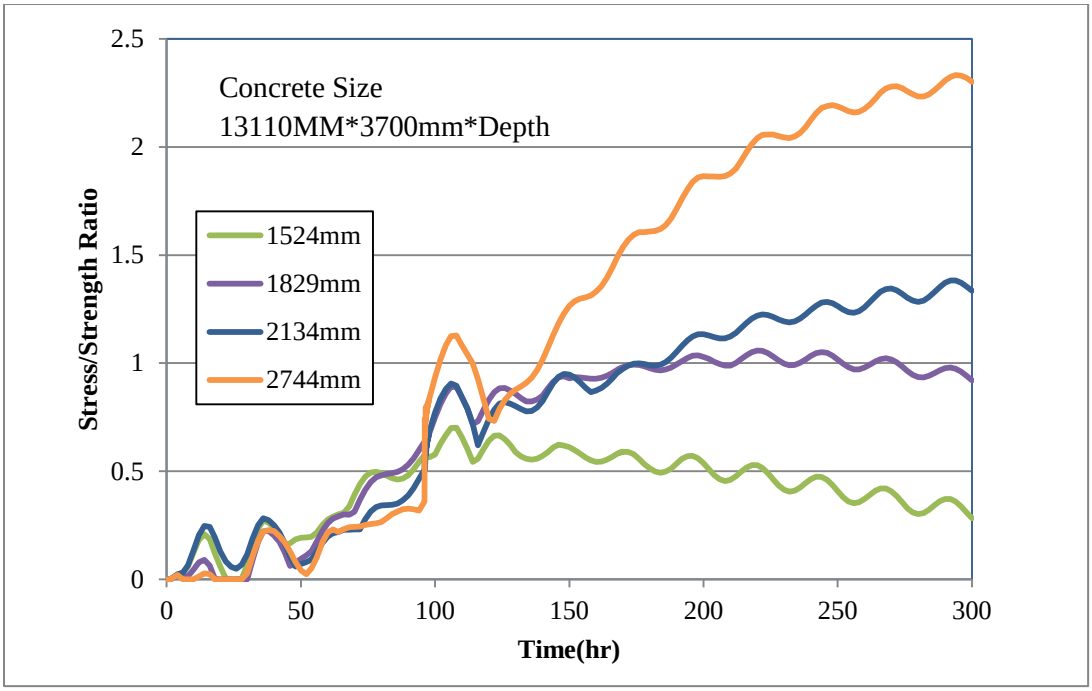

Figure D.8 Pier 1 footing stress/strength ratio results when depth varies (concrete)

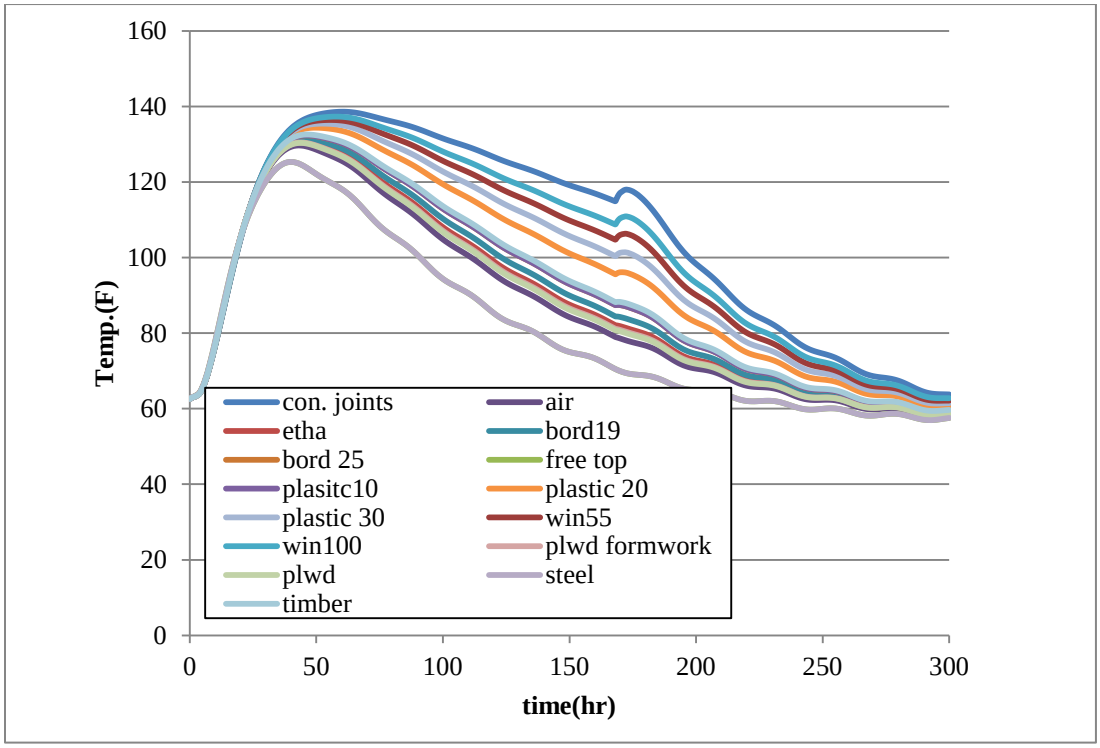

Figure D.9 Pier 1 footing maximum temperature with top insulation varies (soil/concrete)

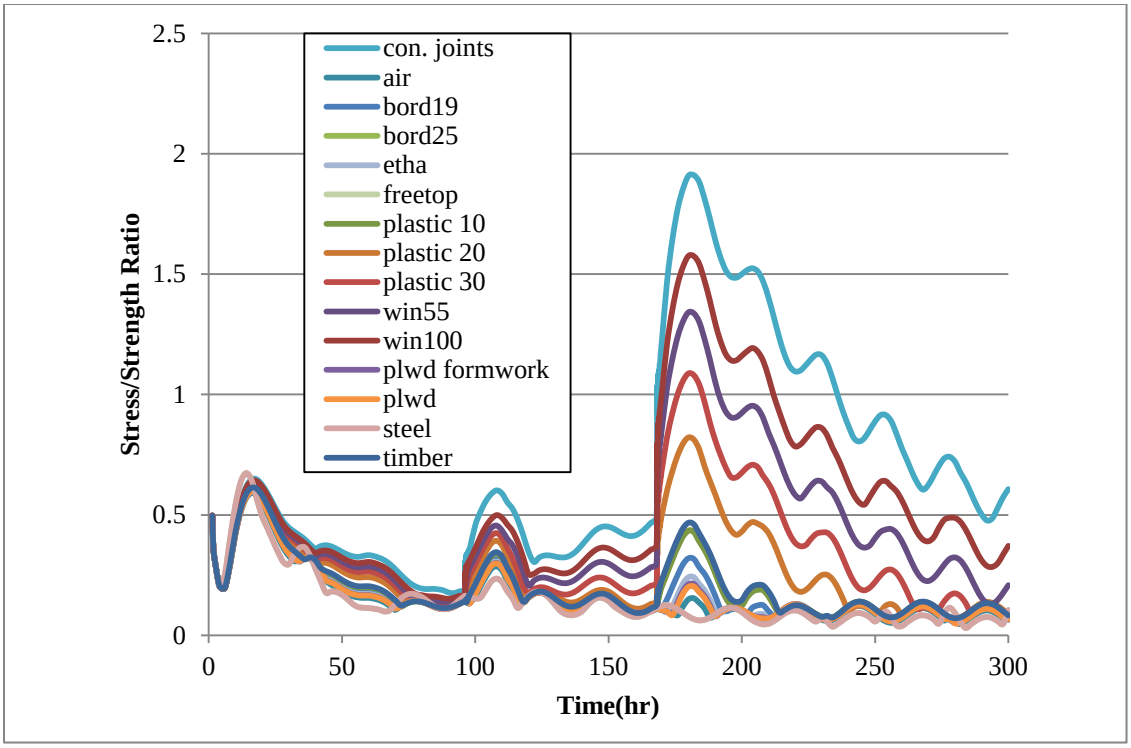

Figure D.105 Pier 1 footing stress/strength ratio with top insulation varies (soil)

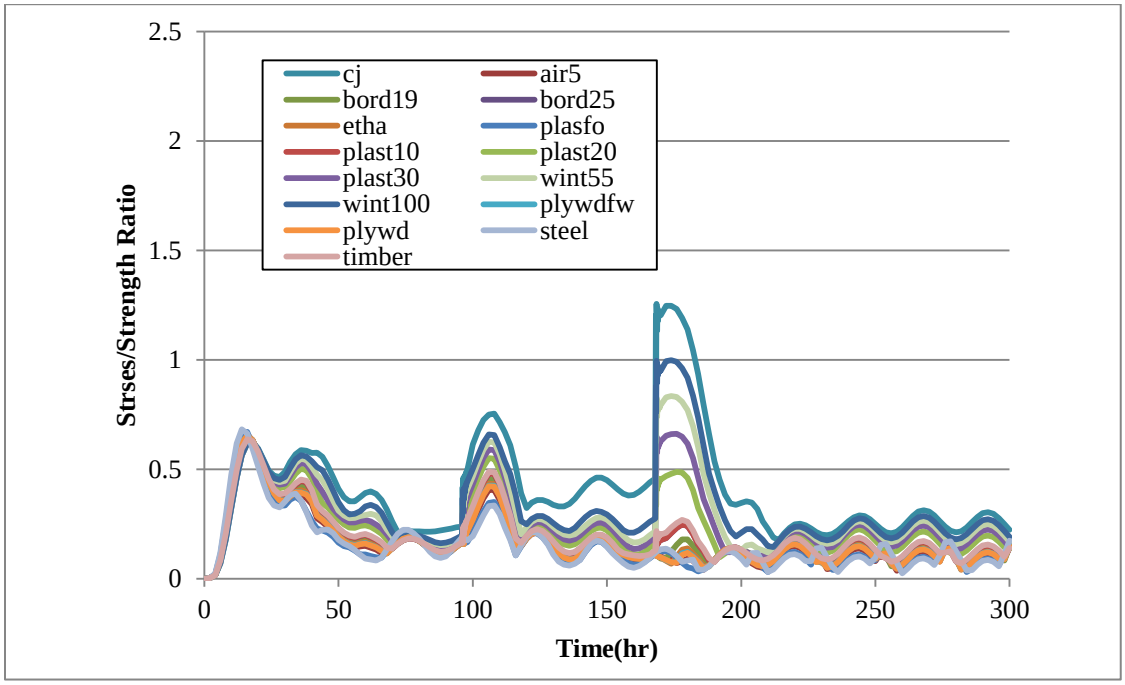

Figure D.106 Pier 1 footing stress/strength ratio with top insulation varies (concrete)

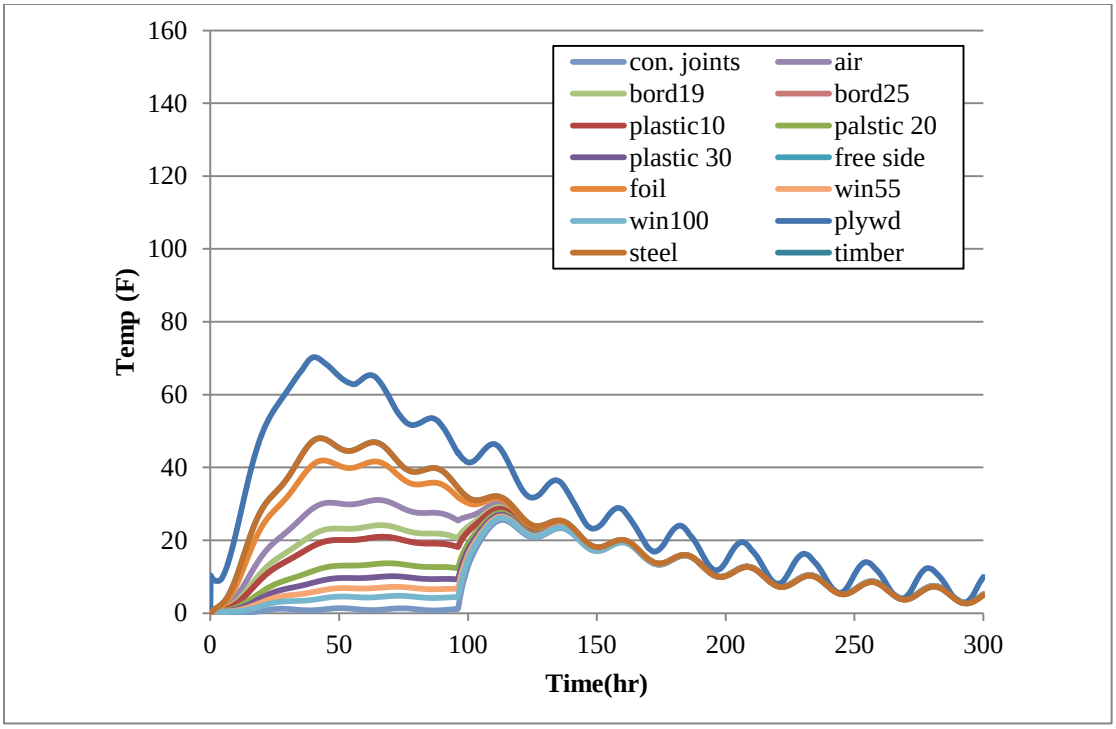

Figure D.107 Pier 1 footing maximum temperature difference with side insulation varies (soil/concrete)

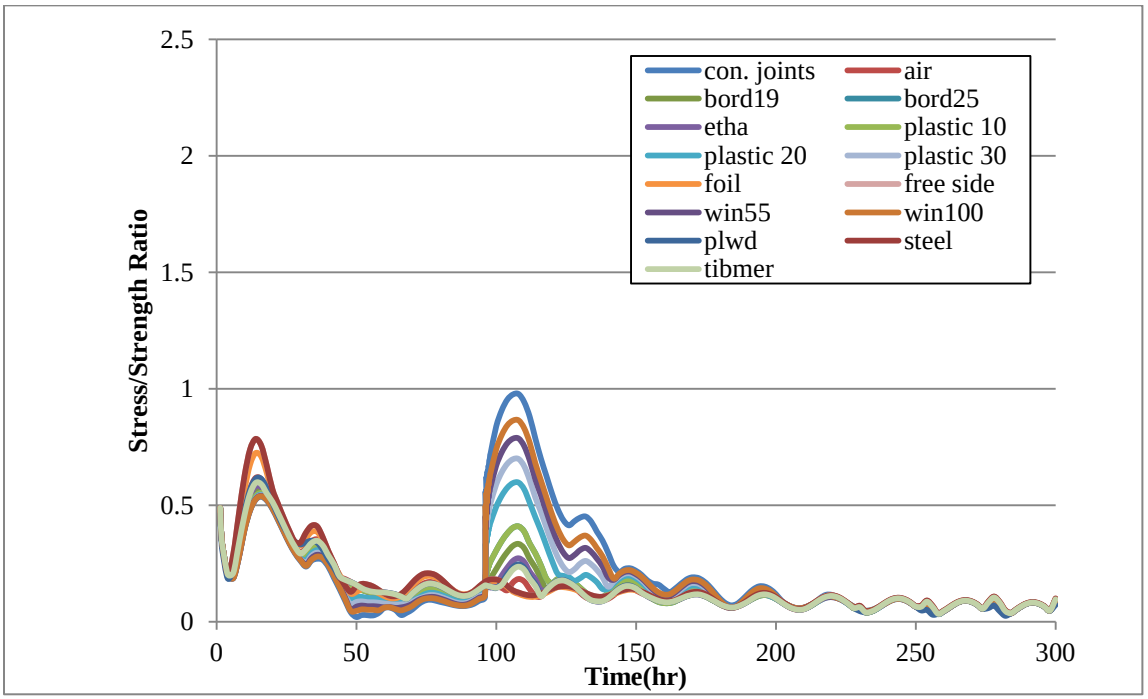

Figure D.108 Pier 1 footing stress/strength ratio with side insulation varies (soil)

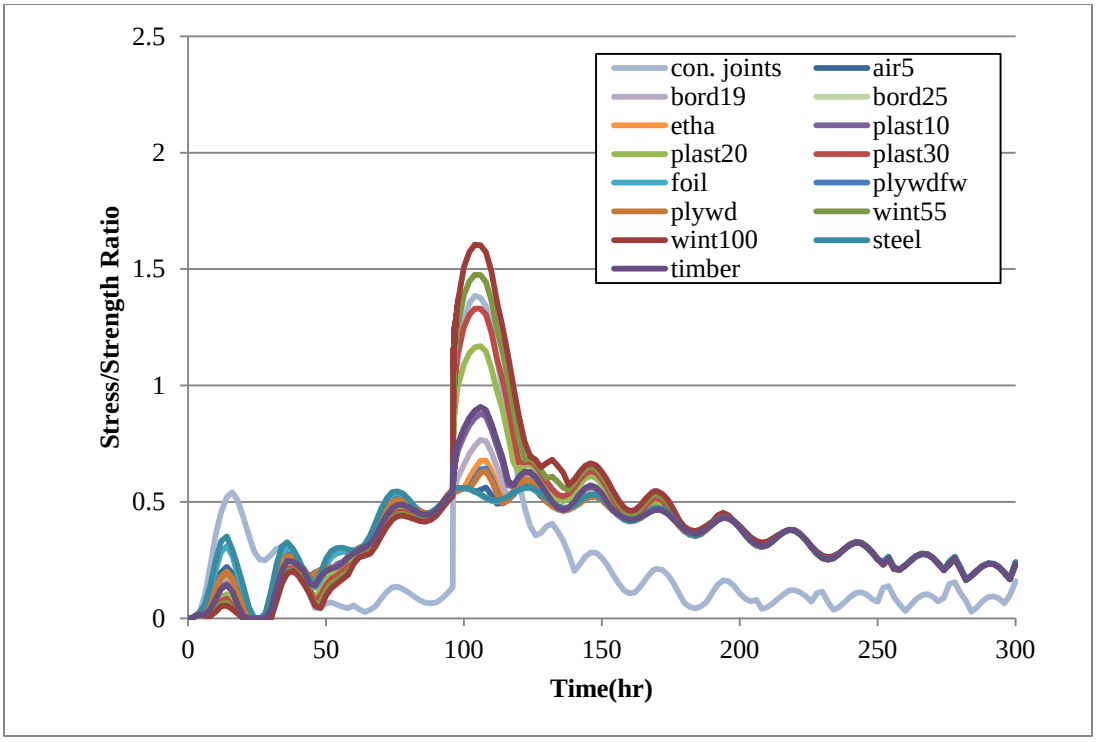

Figure D.109 Pier 1 footing stress/strength ratio with side insulation varies (concrete)

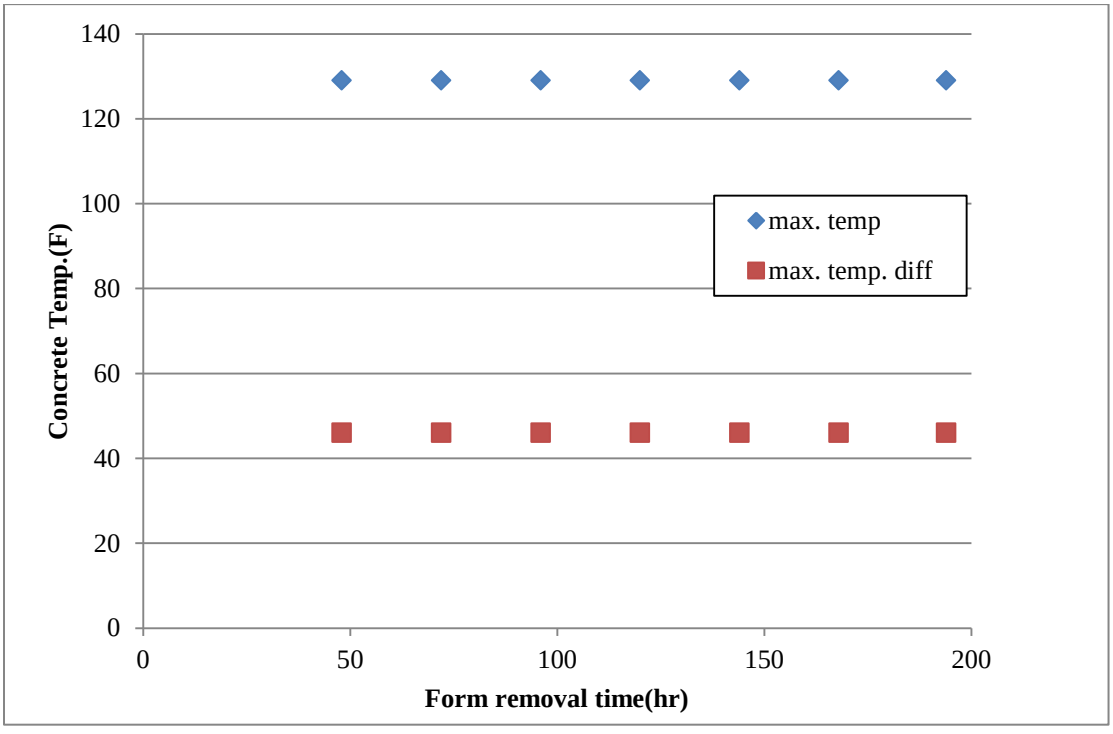

Figure D.110 Relationship of temperature to form removal time for pier 1 footing

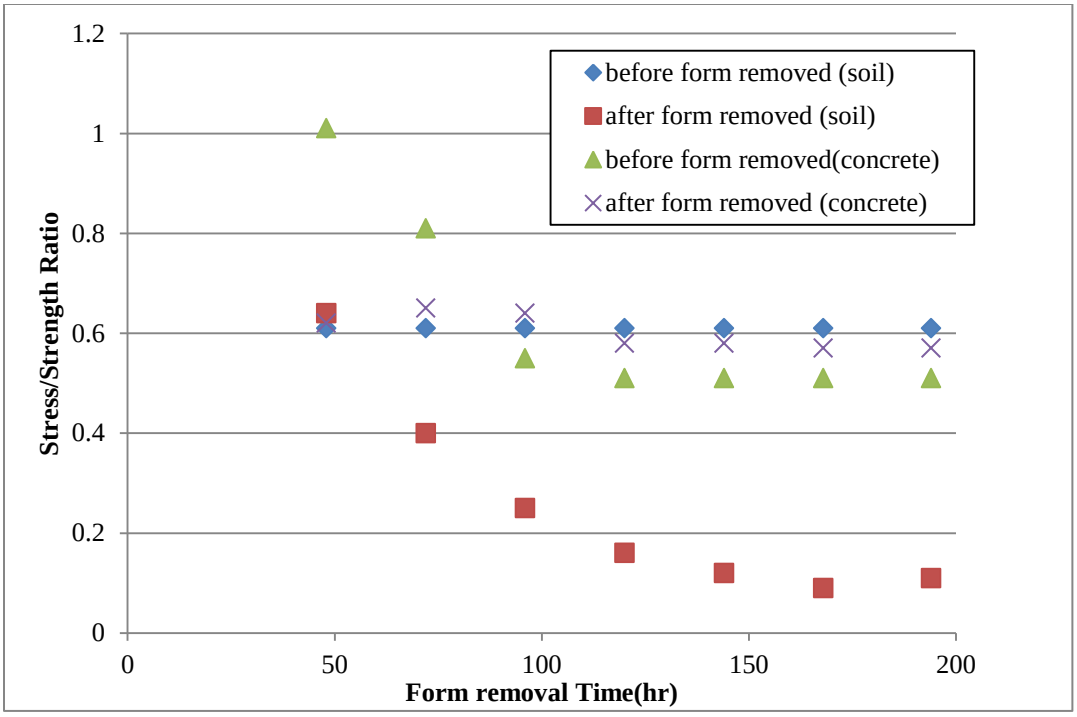

Figure D.111 Relationship of stress/strength ratio to form removal time for pier 1 footing

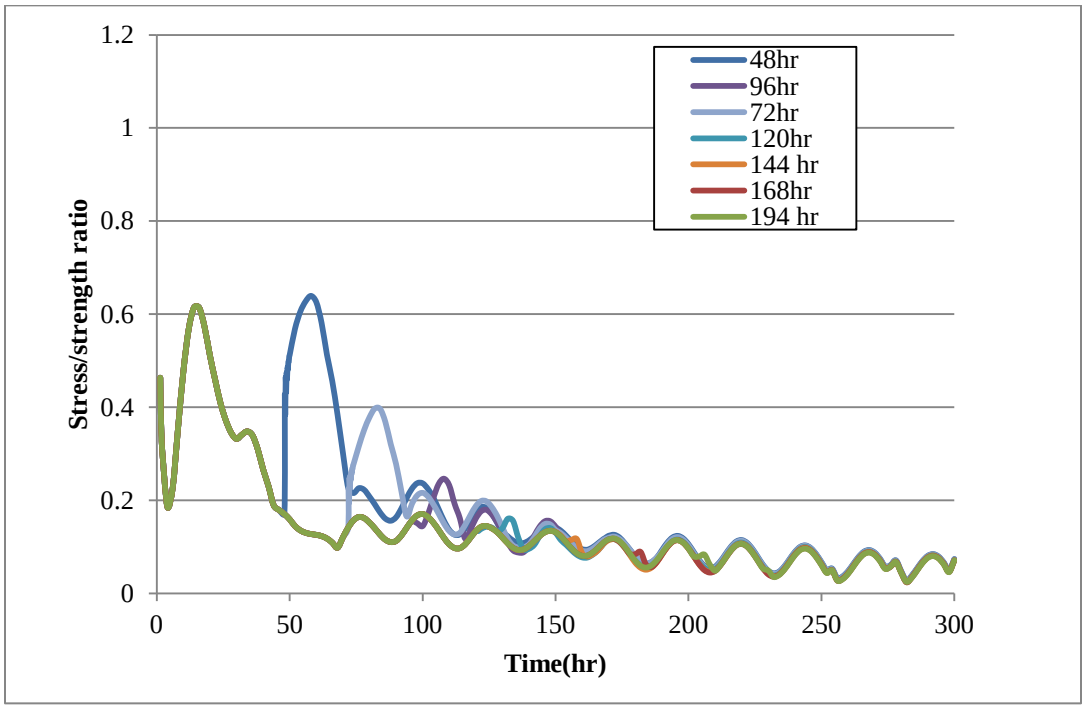

Figure D.112 Pier 1 footing stress/strength ratio with form removal time varies (soil)

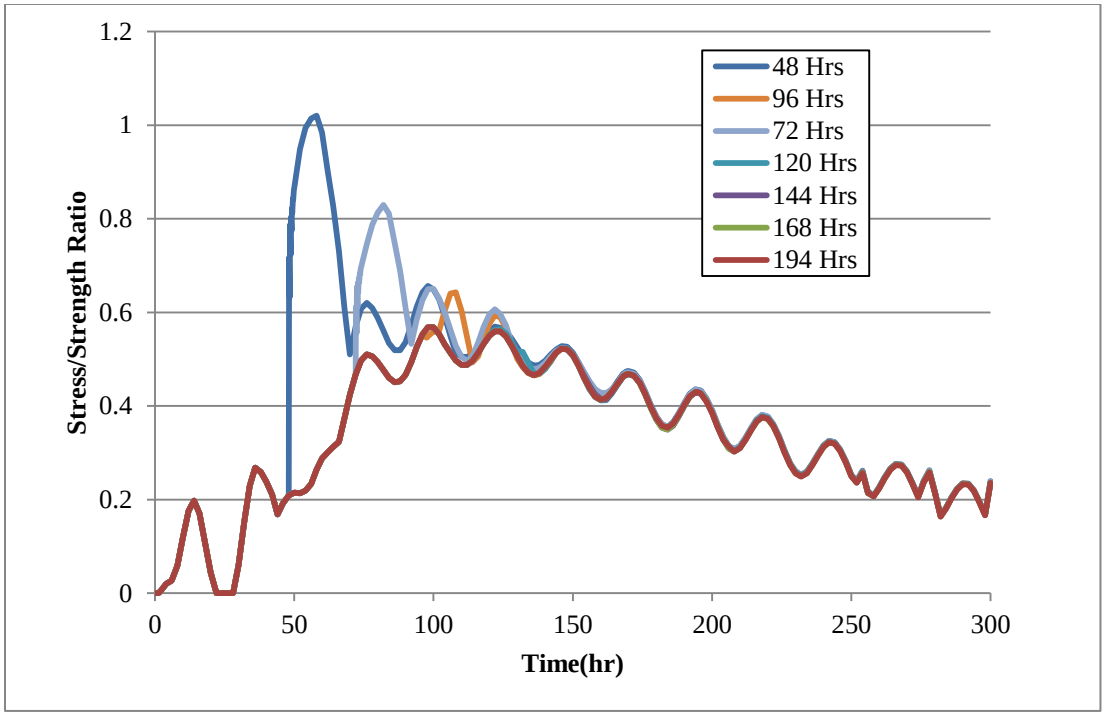

Figure D.113 Pier 1 footing stress/strength ratio with form removal time varies (concrete)

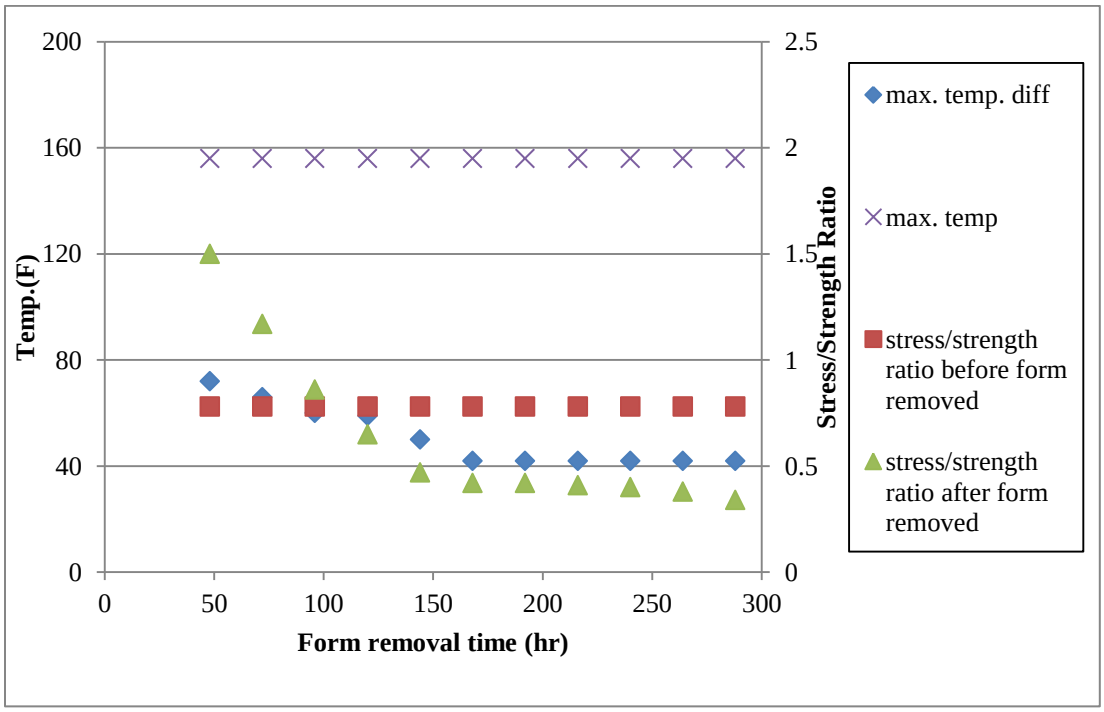

Figure D.114 Relationship of temperature and stress/strength ratio to form removal time for pier 3 footing

Table D.4 Sensitivity study summary on placement date and time for pier 3 footing

Placement Date&Time	Placement Temp.(F)	Max. temperature(F)	Maximum temperature difference(F)	tensile stress/strength ratio(F)	
				Before removed	After removed
Jul.20,2008	40	121	37	0.71	0.3
	50	132	40	0.81	0.3
	60	142	41	0.8	0.3
	70	158	44	0.82	0.3
	80	168	50	1.16	0.3
	90	181	58	1.44	0.4
Oct.20, 2008	40	140	26	1.36	0.39
	50	142	30	1.19	0.39
	60	158	34	1.2	0.4
	70	162	40	1.15	0.43
	80	178	40	1.1	0.55
	90	185	40	1.2	0.6

Table D.5 Sensitivity study summary on placement date and time for pier 1 footing

Placement Date&Time	Placement Temp.(F)	Max. temperature (F)	Maximum temperature difference(F)	tensile stress/strength ratio(F)			
				Soil		Concrete	
				Before removed	After removed	Before removed	After removed
Jul.20,2008	40	119	57	0.64	0.32	0.35	0.65
	50	123	61	0.65	0.26	0.48	0.67
	60	130	68	0.58	0.22	0.59	0.69
	70	141	81	0.68	0.21	0.7	0.85
	80	152	88	0.8	0.22	1.01	1.09
	90	163	101	1.2	0.25	1.21	1.49
Oct.20, 2008	40	107.3	27.3	0.9	0.37	0.35	0.8
	50	114.2	29.2	0.43	0.3	0.45	0.8
	60	124.2	34.3	0.56	0.26	0.59	0.8
	70	129.8	34.5	0.6	0.2	0.69	0.8
	80	147.2	42	0.86	0.22	0.92	1.01
	90	161	48	1.1	0.27	1.22	1.4

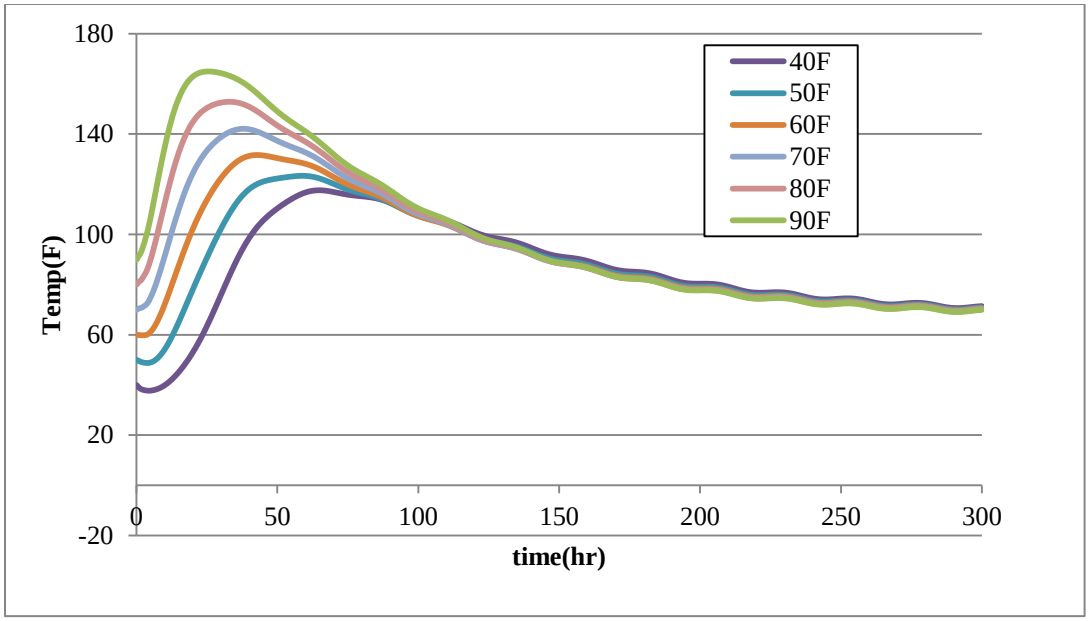

Figure D.20 Pier 1 footing maximum temperature for summer placement with fresh placement temperature time varies

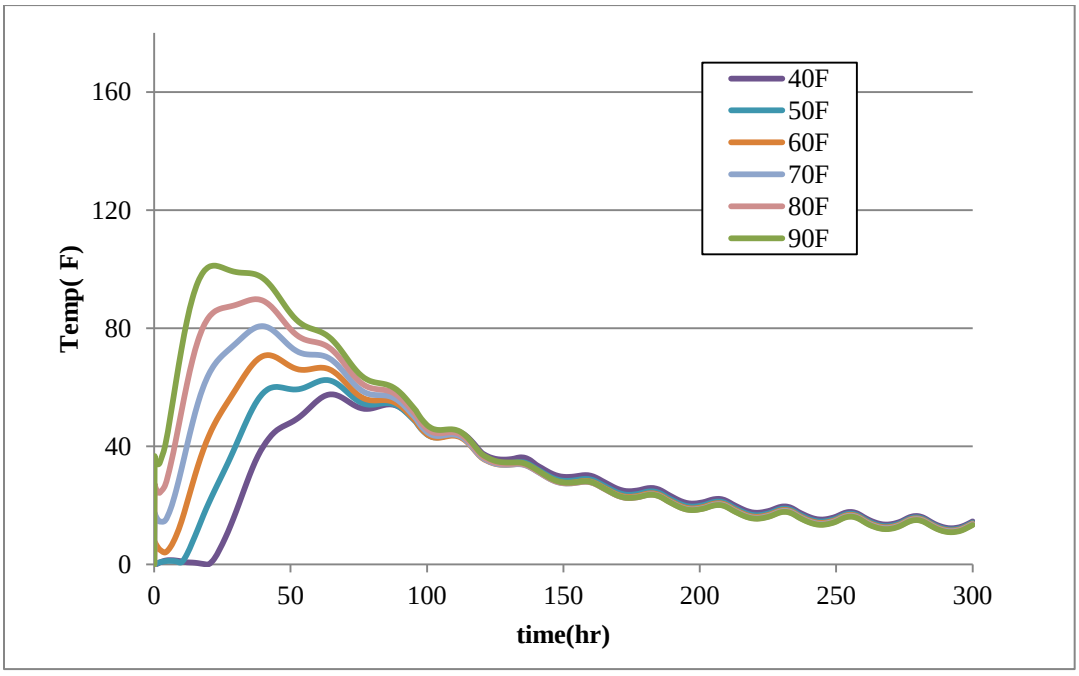

Figure D.21 Pier 1 footing maximum temperature difference for summer placement with fresh placement temperature time varies

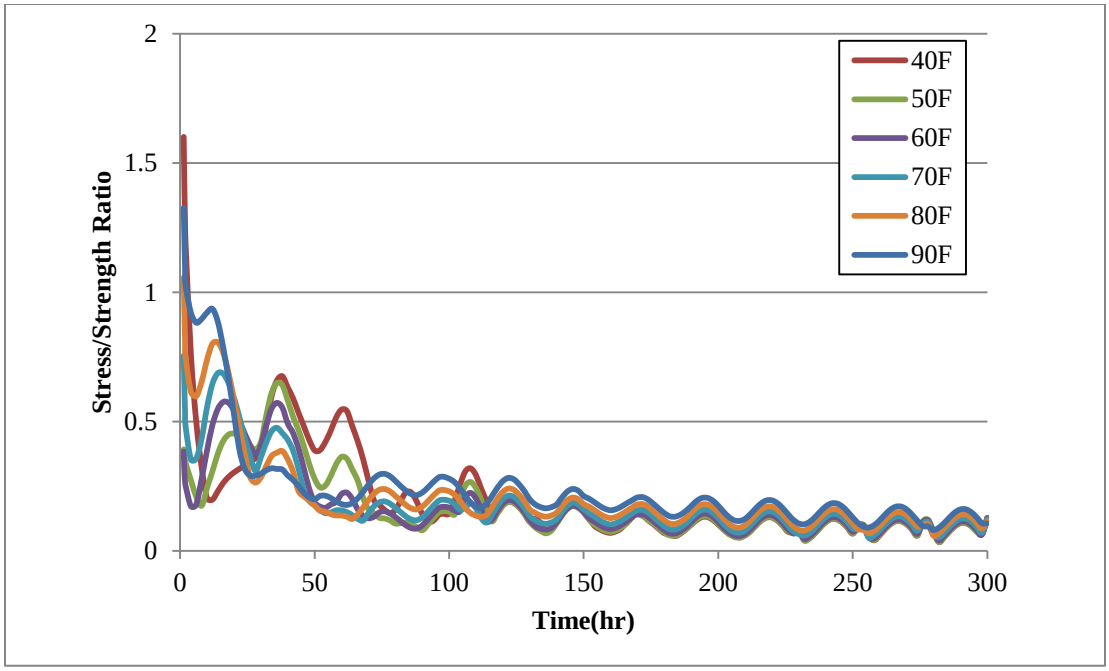

Figure D.22 Pier 1 footing stress/strength for summer placement with fresh placement temperature time varies (soil)

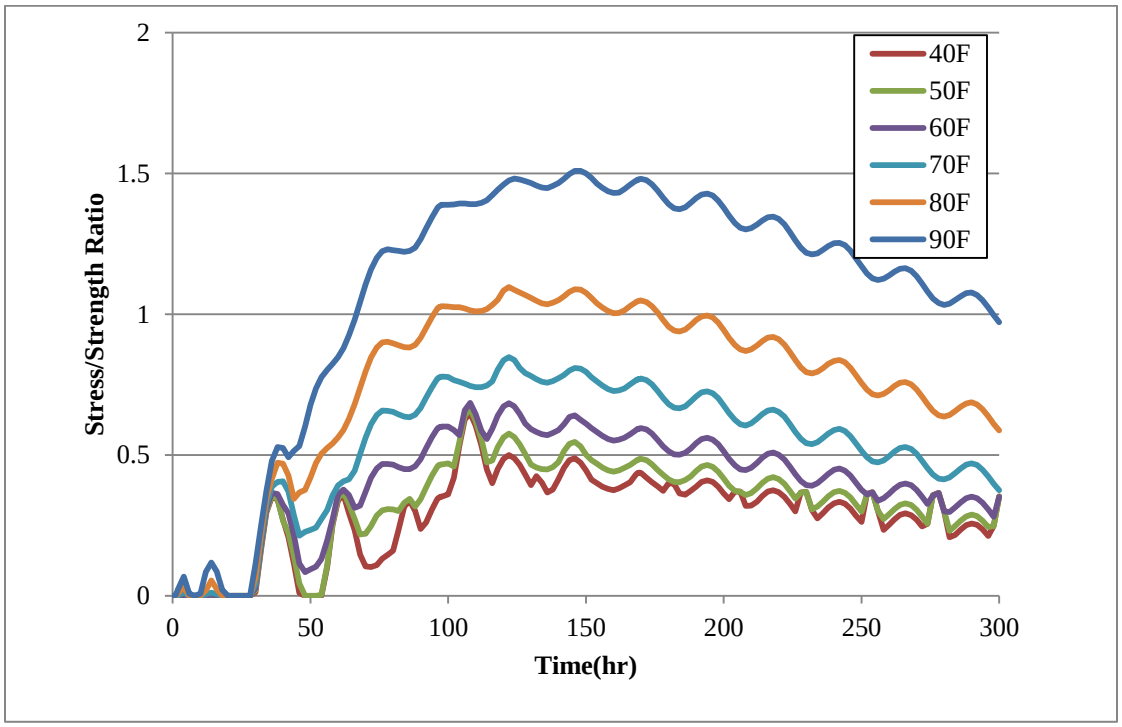

Figure D.23 Pier 1 footing stress/strength for summer placement with fresh placement temperature time varies (concrete)

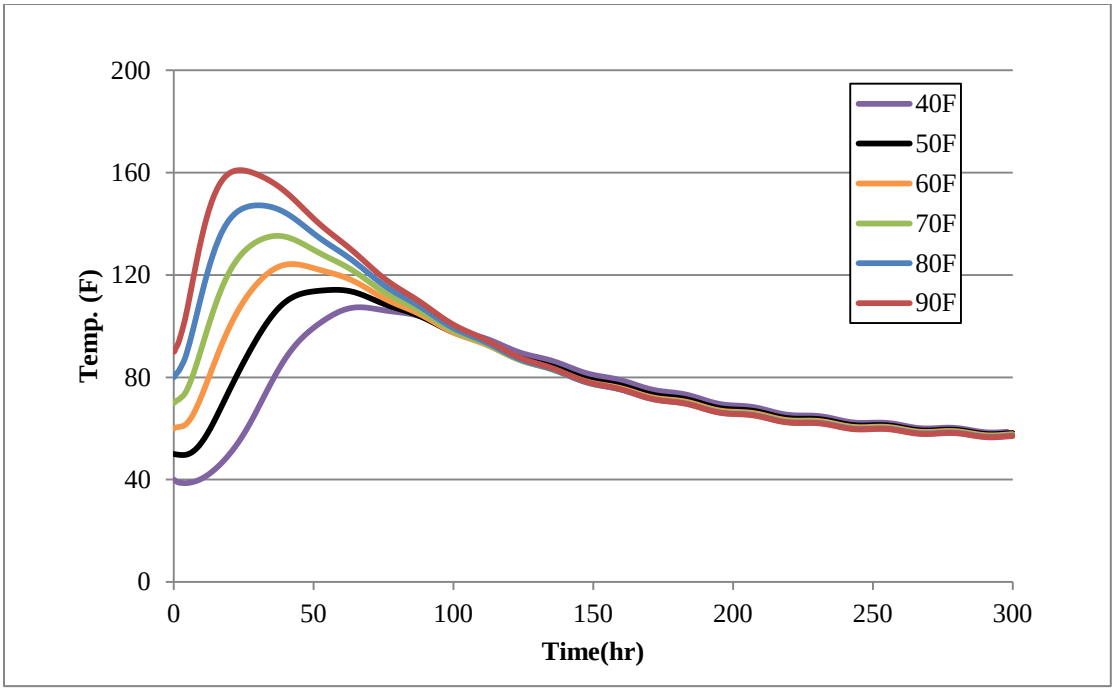

Figure D.115 Pier 1 footing maximum temperature for winter placement with fresh placement temperature time varies

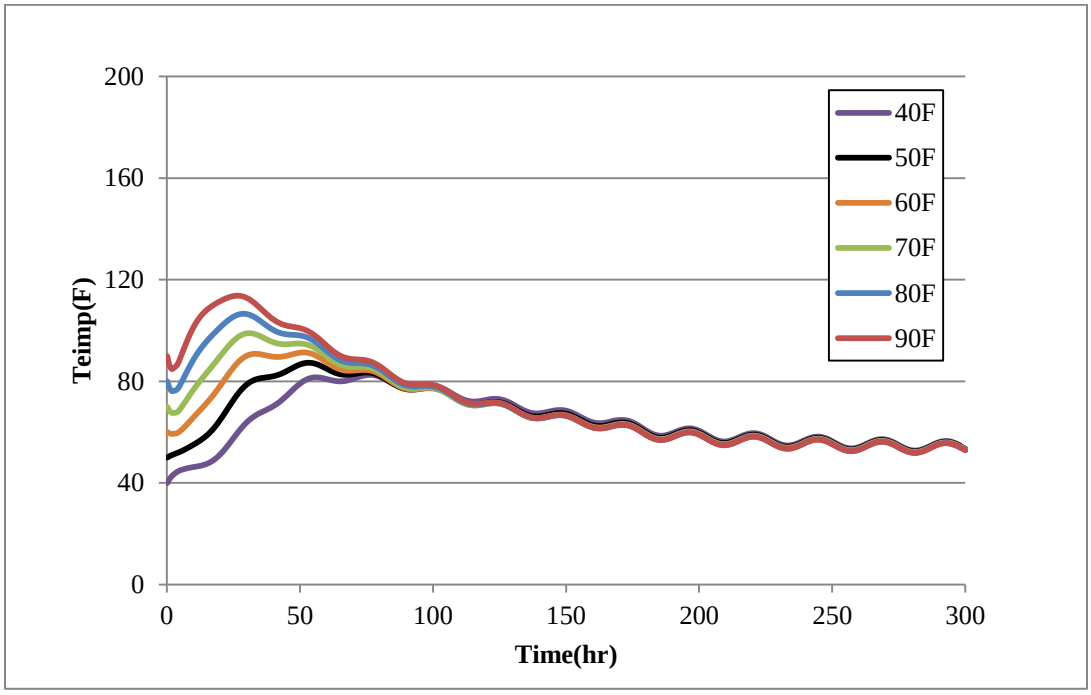

Figure D.25 Pier 1 footing maximum temperature for winter placement with fresh placement temperature time varies

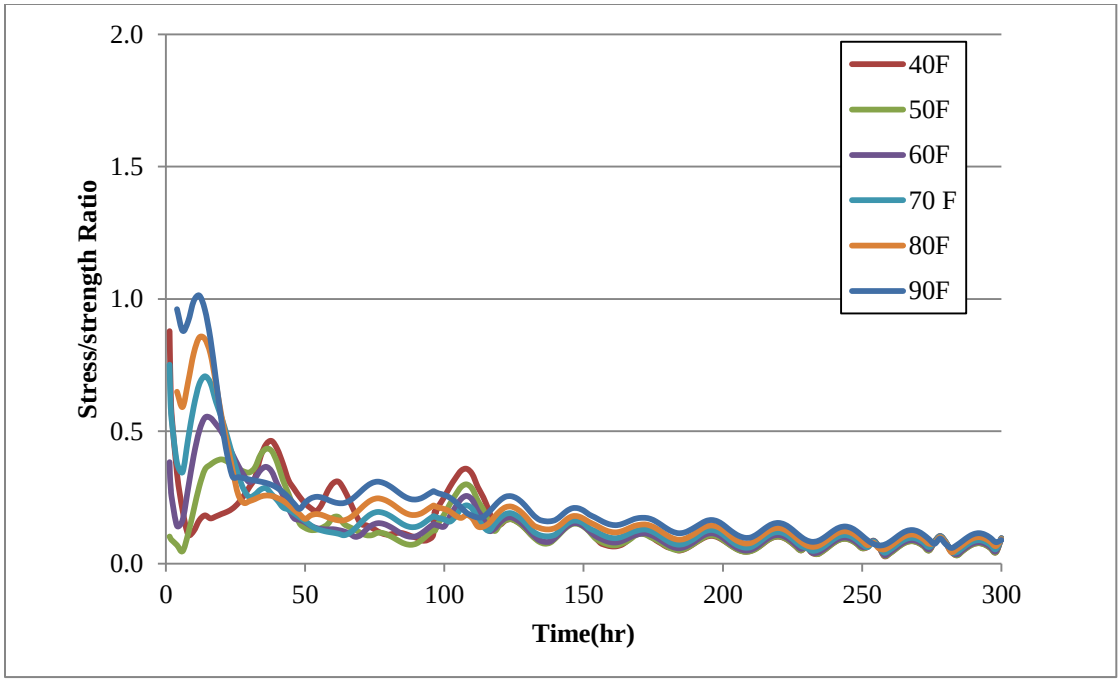

Figure D.26 Pier 1 footing stress/strength ratio for winter placement with fresh placement temperature time varies (soil)

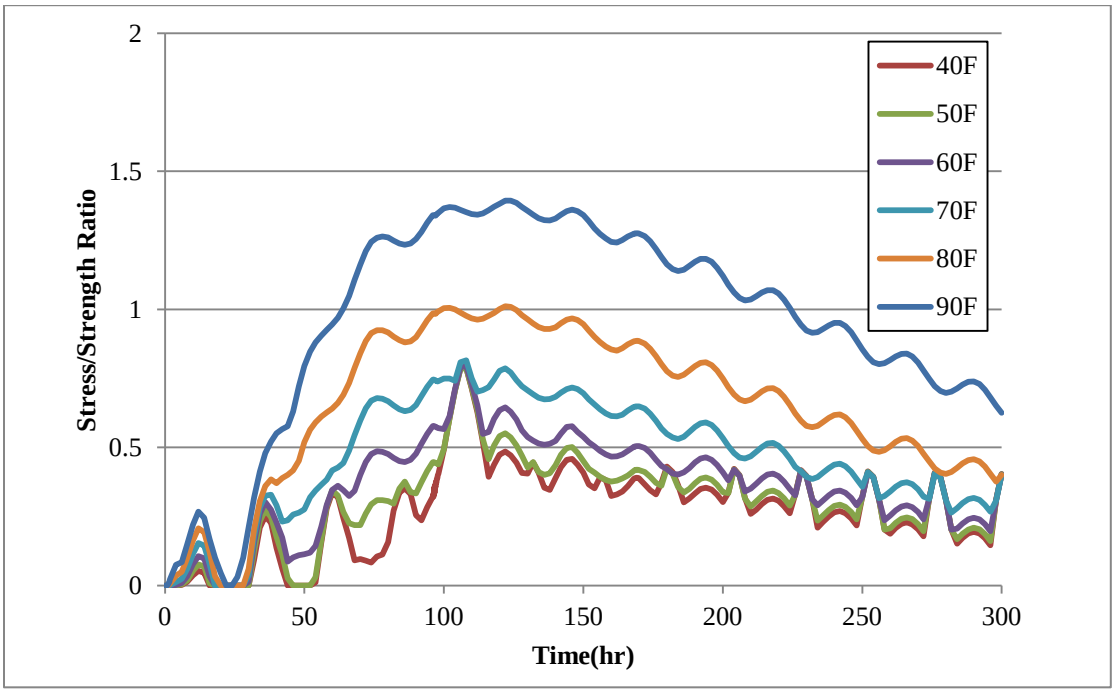

Figure D.27 Pier 1 footing stress/strength ratio for winter placement with fresh placement temperature time varies (concrete)

Table D.6 Sensitivity study summary on cement content for pier 1 footing

cement pcy	max. temp(F)	max. temp. diff(F)	stress/strength ratio			
			soil		concrete	
			before form removed	after form removed	before form removed	after form removed
560	168	52	1	0.35	1.9	2.6
660	205	63	1.5	0.51	2.9	3.9
760	238	73	2.1	0.65	3.4	4.6

Table D.7 Sensitivity study summary on cement content for pier 3 footing

Cement pcy	max. temp(F)	max. temp. diff(F)	stress/strength ratio	
			before form removed	after form removed
427	178	58	1.1	0.4
527	210	70	1.59	0.6
627	248	80	2.38	0.75
727	276	88	3.45	1

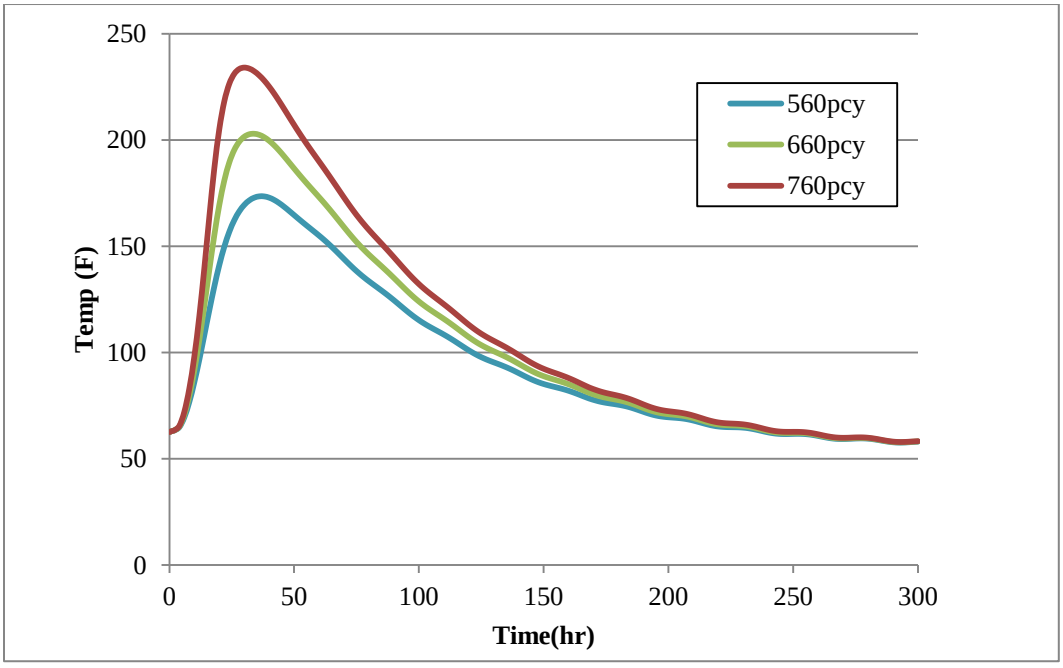

Figure D.28 Pier 1 footing maximum temperature with cement content varies (soil/concrete)

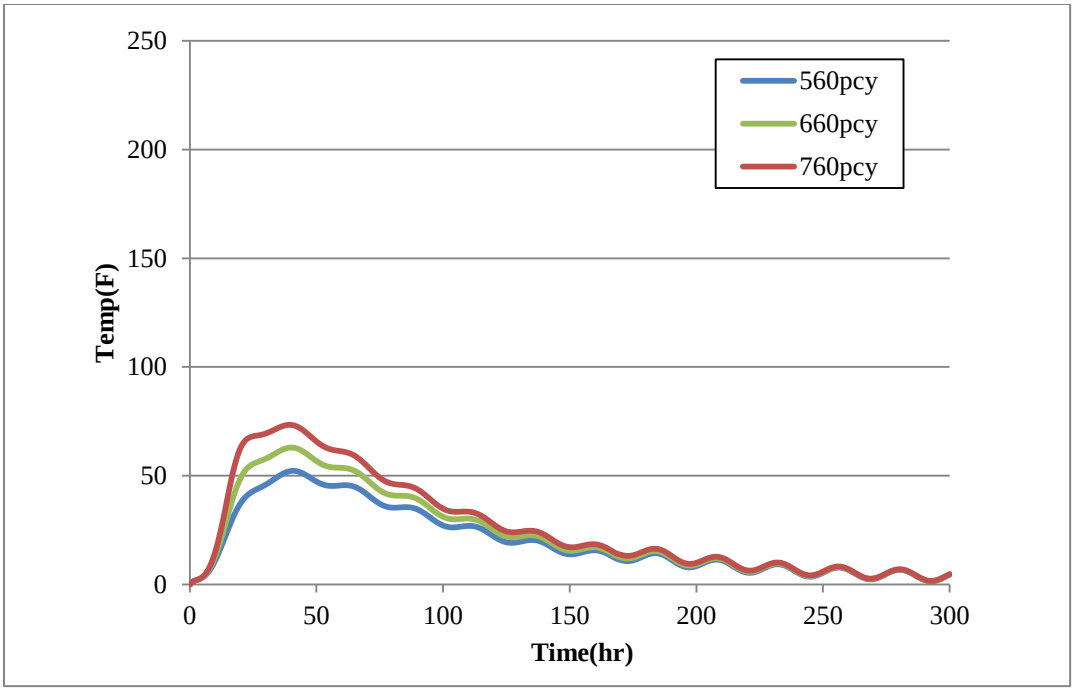

Figure D.29 Pier 1 footing maximum temperature difference with cement content varies (soil/concrete)

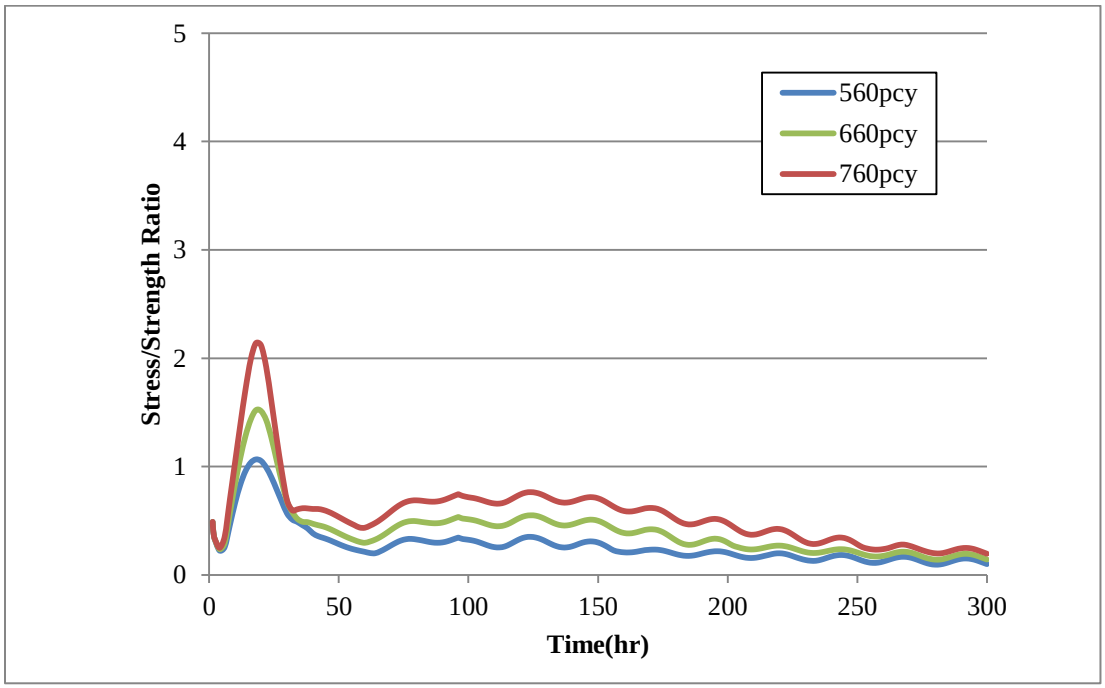

Figure D. 30 Pier 1 footing stress/strength ratio with cement content varies (soil)

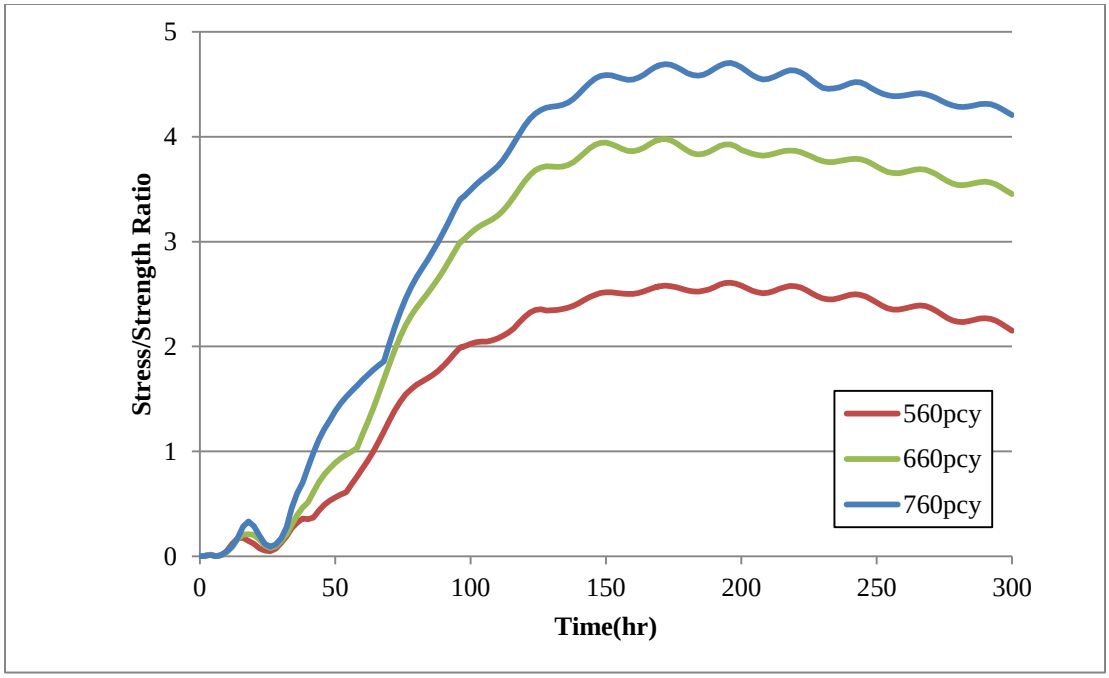

Figure D.31 Pier 1 footing stress/strength ratio with cement content varies (concrete)

Table D.8 Sensitivity study summary thermal conductivity for pier 1 footing

Thermal Conductivity (KJ/kg/°C)	Max. Temp(F)	Max. Temp. Diff(F)	Stress/ strength ratio			
			Soil		Concrete	
			before form removed	after form removed	before form removed	after form removed
5.39	133	31	0.68	0.2	0.61	0.8
8	129	46	0.61	0.25	0.52	0.67
10	121	21	0.6	0.1	0.52	0.6
13	113	18	0.49	0.1	0.49	0.52
18	109	16	0.45	0.1	0.44	0.44

Table D.8 Sensitivity study summary thermal conductivity for pier 3 footing

Thermal Conductivity (KJ/kg/°C)	Max. Temp(F)	Max. Temp. Diff(F)	Stress/ strength ratio	
			before form removed	after form removed
5.39	164	52	0.82	0.45
8	156	42	0.8	0.28
10	152	40	0.79	0.3
13	147	34	0.75	0.31
18	140	25	0.71	0.34

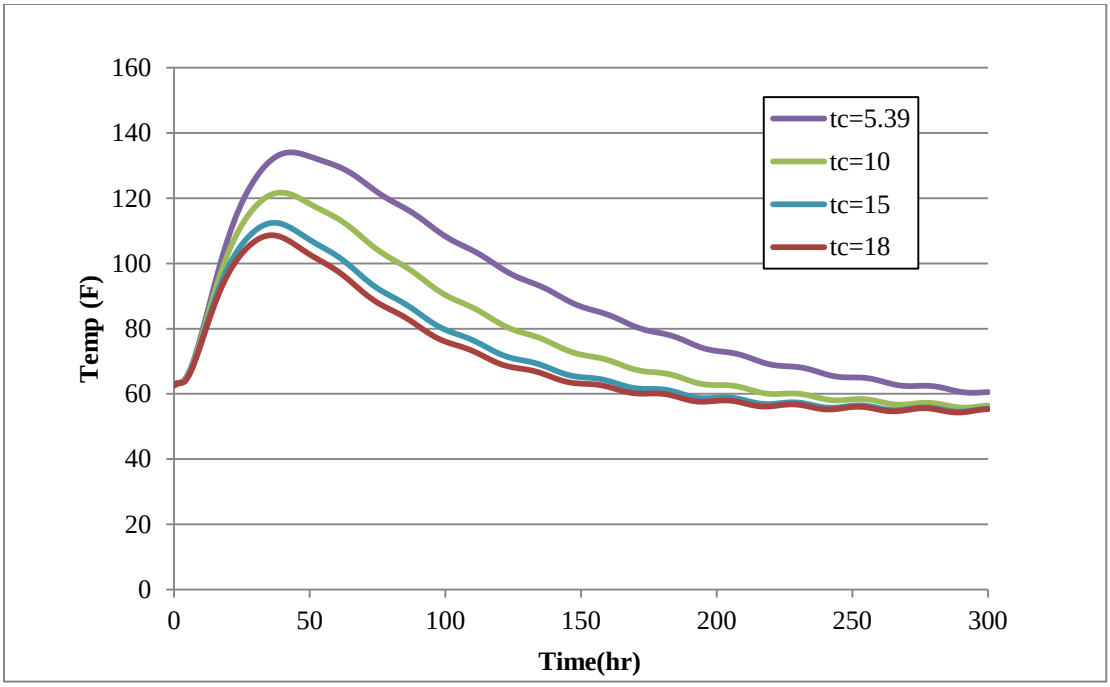

Figure D.32 Pier 1 footing maximum temperature with thermal conductivity (KJ/Kg/°C) varies (soil/concrete)

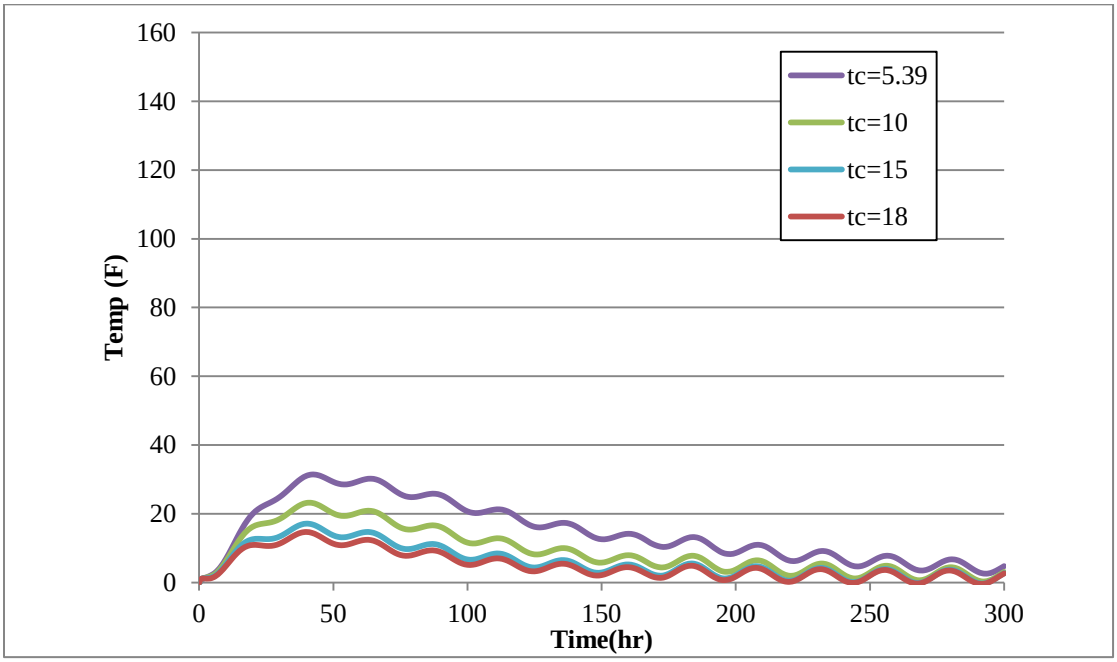

Figure D.33 Pier 1 footing maximum temperature difference with thermal conductivity (KJ/Kg/°C) varies (soil/concrete)

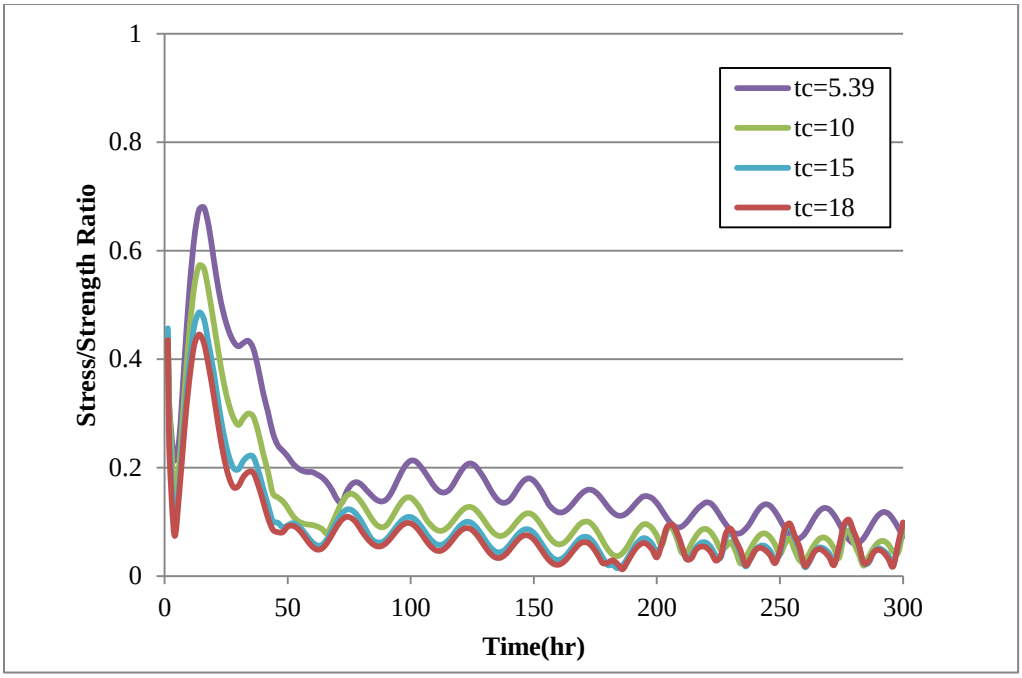

Figure D.34 Pier 1 footing stress/strength ratio with thermal conductivity (KJ/Kg/°C) varies (soil)

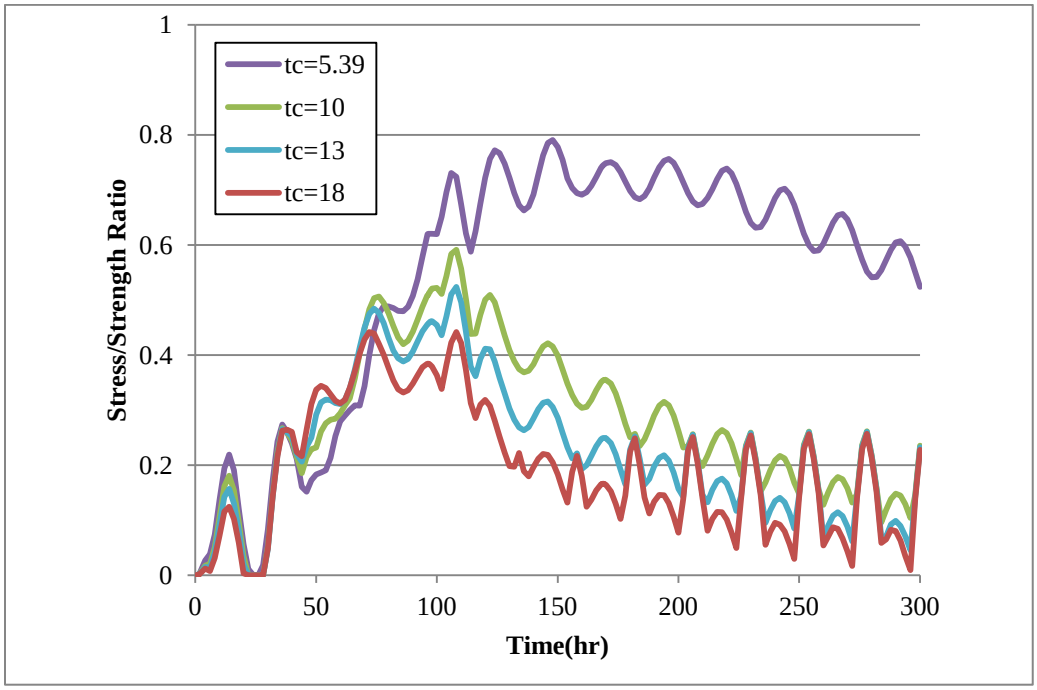

Figure D.35 Pier 1 footing stress/strength ratio with thermal conductivity (KJ/Kg/°C) varies (concrete)

Table D.9 Sensitivity study summary coefficient of thermal expansion for pier 1 footing

CTE (*10-6/°C)	Max. Temp (F)	Max. Temp. Diff(F)	Stress/ strength ratio			
			Soil		Concrete	
			before form removed	after form removed	before form removed	after form removed
7.36	129	46	0.61	0.25	0.52	0.67
9	129	46	0.75	0.2	0.62	0.8
11	129	46	0.91	0.25	0.78	1
13	129	46	1.1	0.3	0.9	1.19

Table D.10 Sensitivity study summary coefficient of thermal expansion for pier 3 footing

CTE (*10-6/°C)	Max. Temp (F)	Max. Temp. Diff(F)	Stress/ strength ratio	
			before form removed	after form removed
7.36	156	42	0.8	0.28
9	156	42	1	0.38
11	156	42	1.21	0.43
13	156	42	1.42	0.5

Table D.11 Cooling Pipes Layout Summary

Description	Distance from Top surface(ft)	Distance from Side surface(ft)	Vertical Spacing(ft)	Horizontal Spacing(ft)
Pier 3 footing	1.25	2.5	2	3
Larger Vertical Spacing	0.5	2.5	2.6	3
Pier close to top	0.59	2.5	2	3

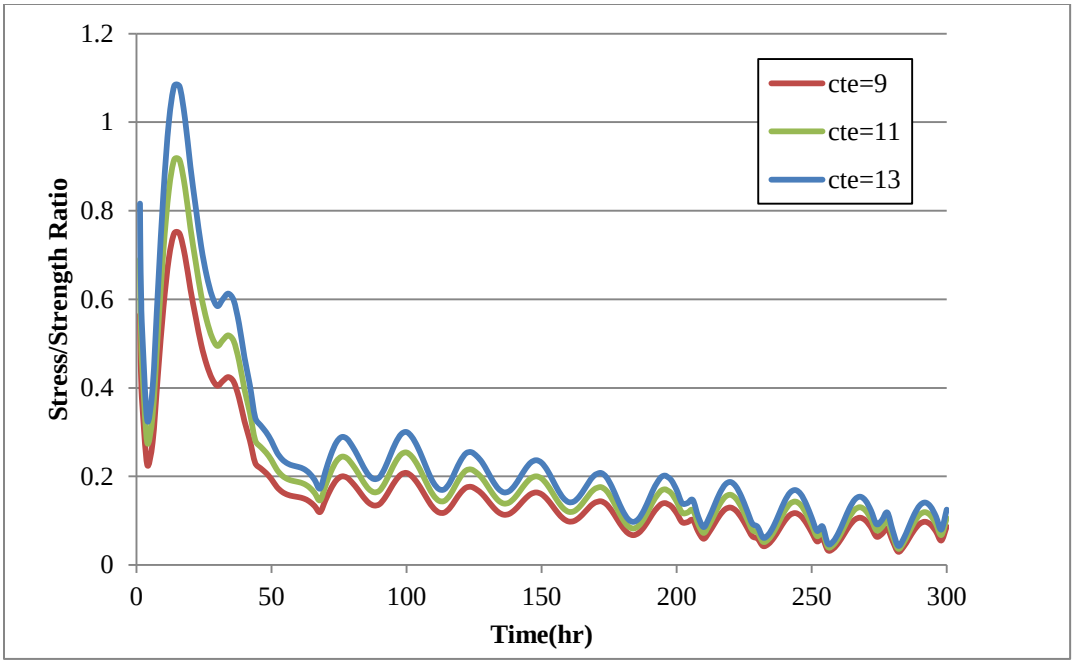

Figure D.36 Pier 1 footing stress/strength ratio with CTE(*10^{-6}/°C) varies (soil)

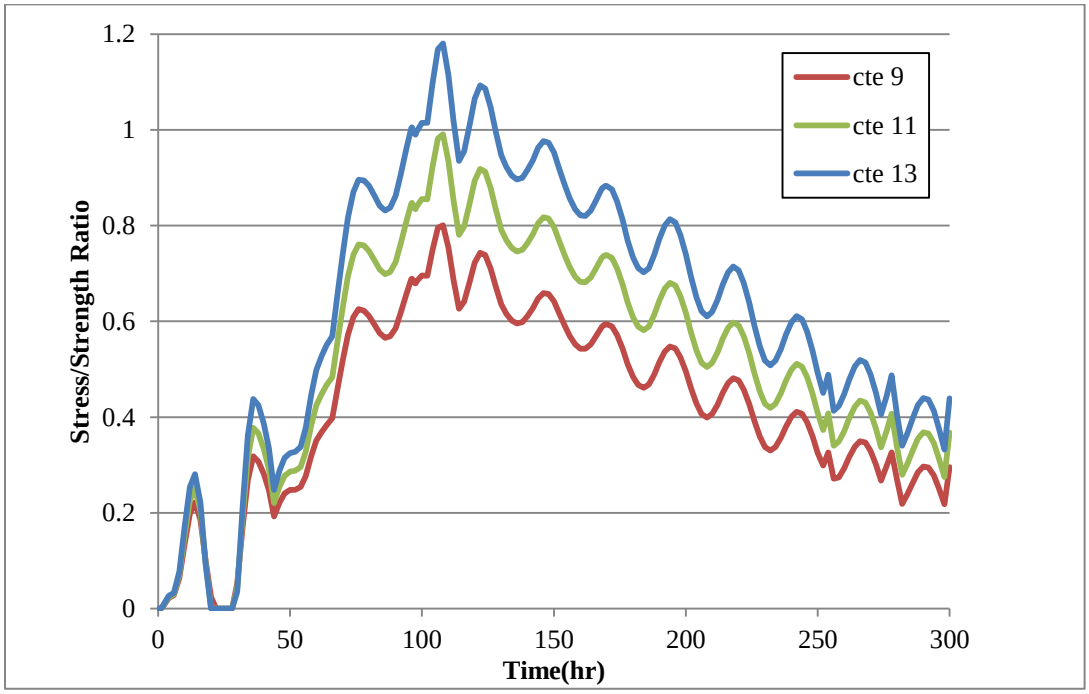

Figure D.37 Pier 1 footing stress/strength ratio with CTE (*10^{-6}/°C) varies (concrete)

APPENDIX E EXAMPLES OF ISO-CURVE RESULTS FROM 4C PROGRAM

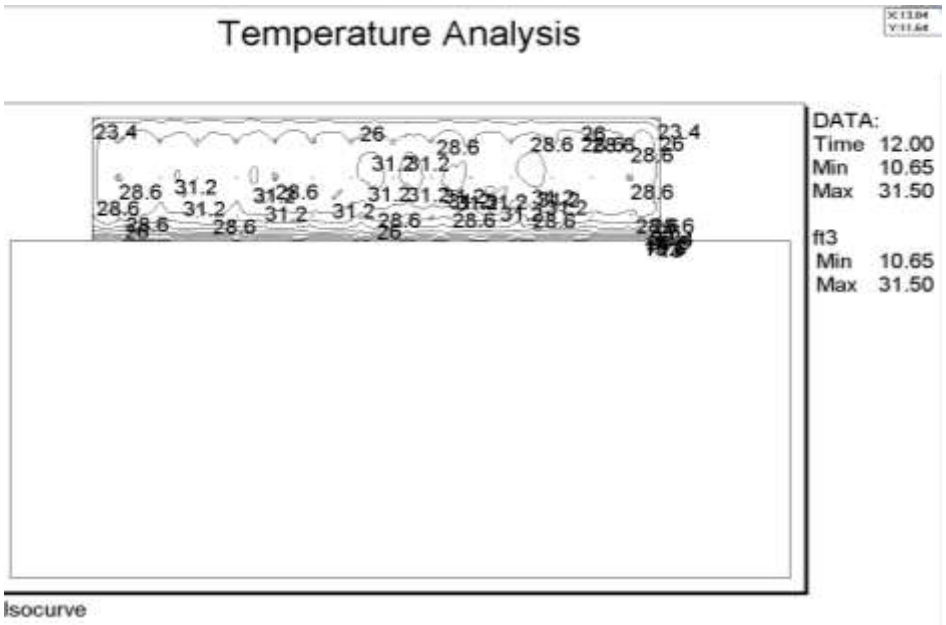

Figure E.1 Example temperature development isocurve results for right-half cross section of pier 3 footing with cooling pipe applied at 12 hours (not in scale)

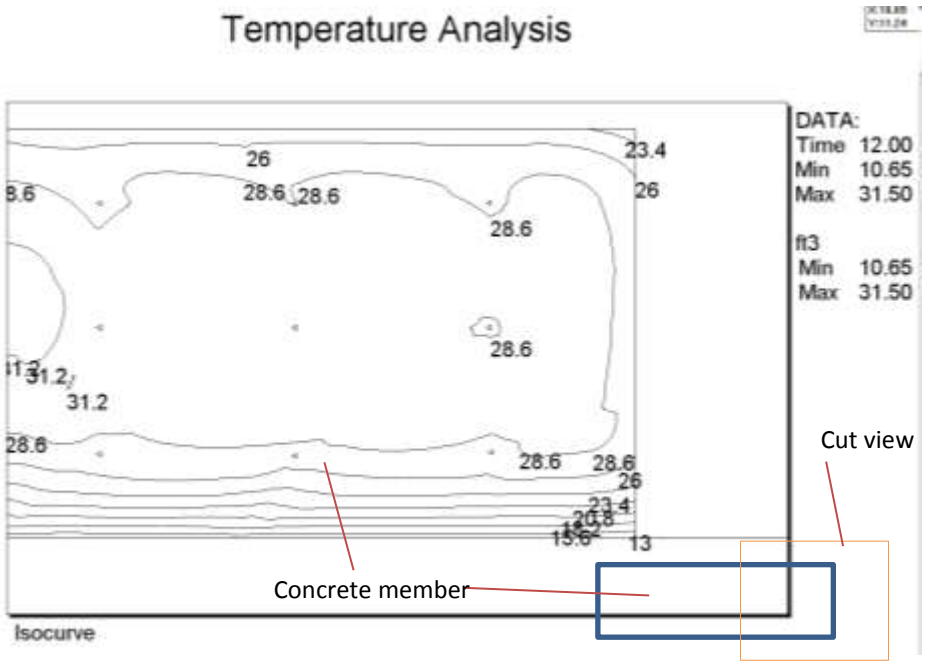

Figure E.2 Example temperature development isocurve results for right-half cross section of pier 3 footing with cooling pipe applied at 12 hours (not in scale)

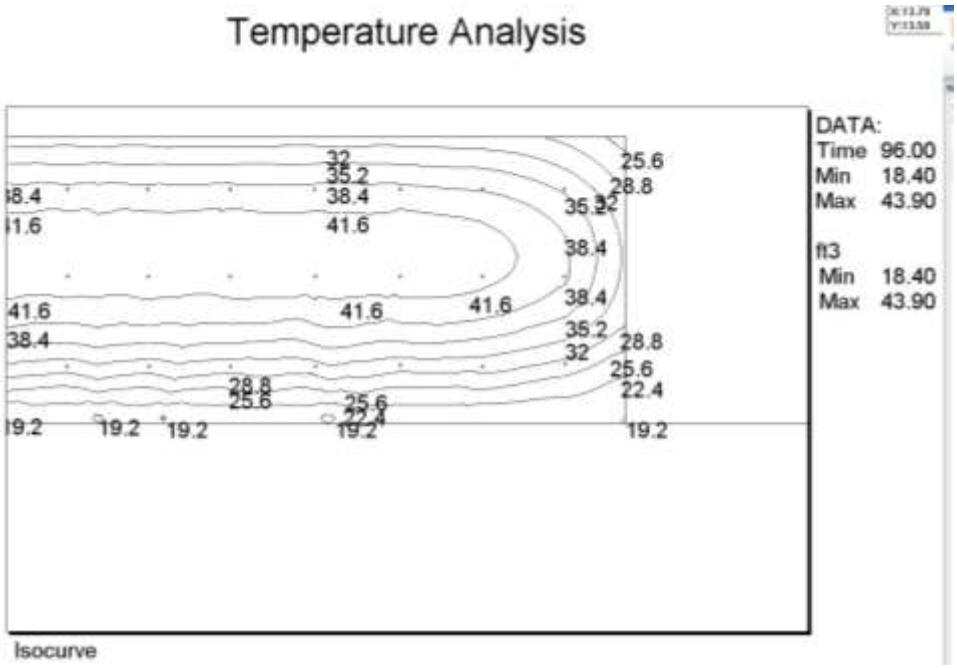

Figure E.3 Example temperature development isocurve results for right-half cross section of pier 3 footing with cooling pipe applied at 96 hours (not in scale)

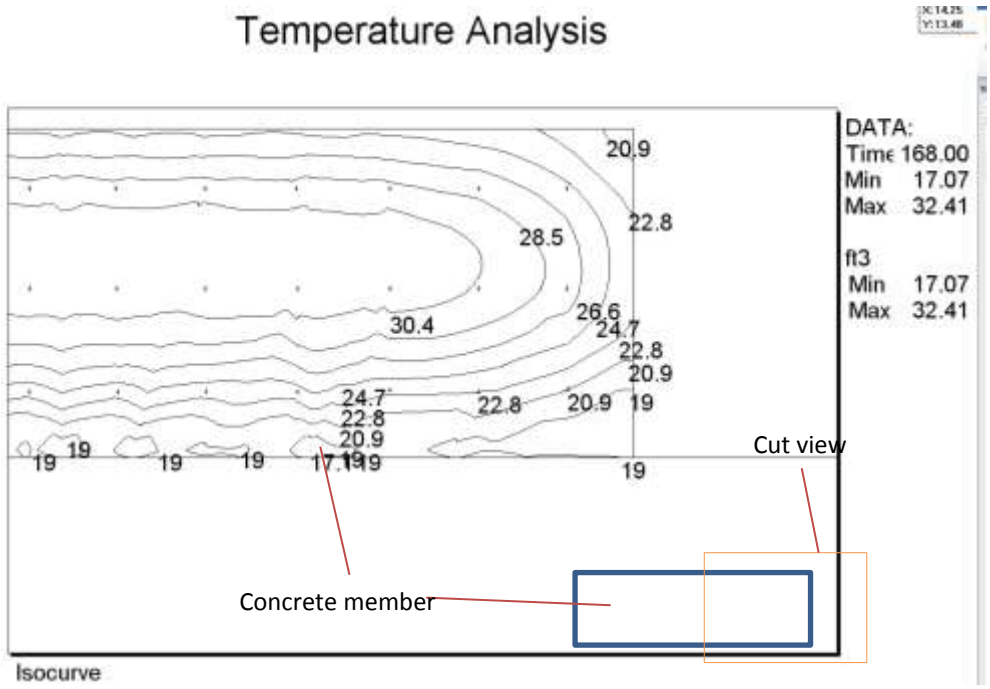

Figure E.4 Example temperature development isocurve results for right-half cross section of pier 3 footing with cooling pipe applied at 168 hours (not in scale)

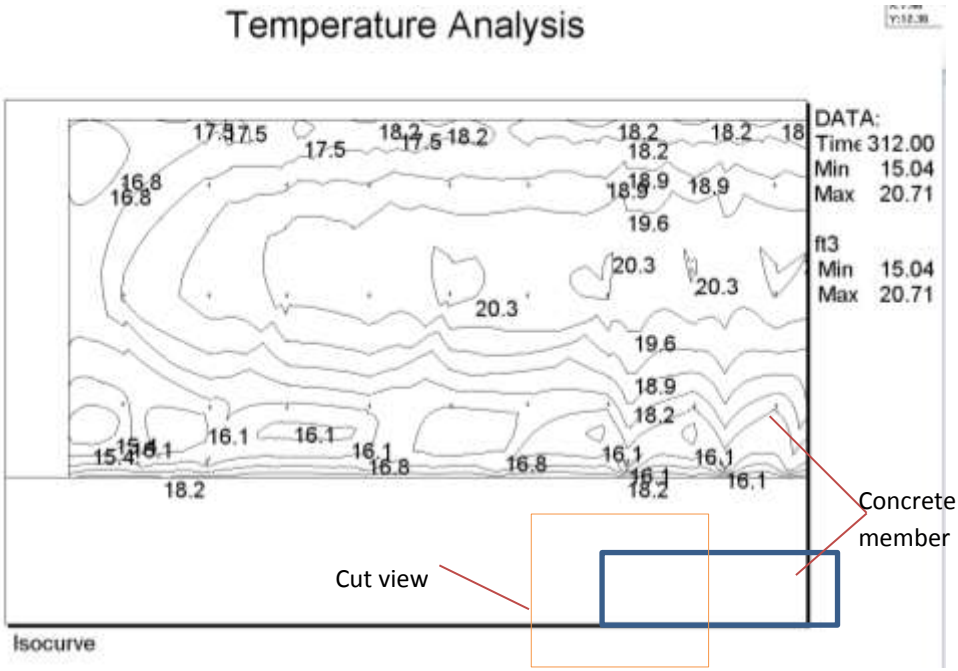

Figure E.5 Example temperature development isocurve results for right-half cross section of pier 3 footing with cooling pipe applied at 312 hours (not in scale)

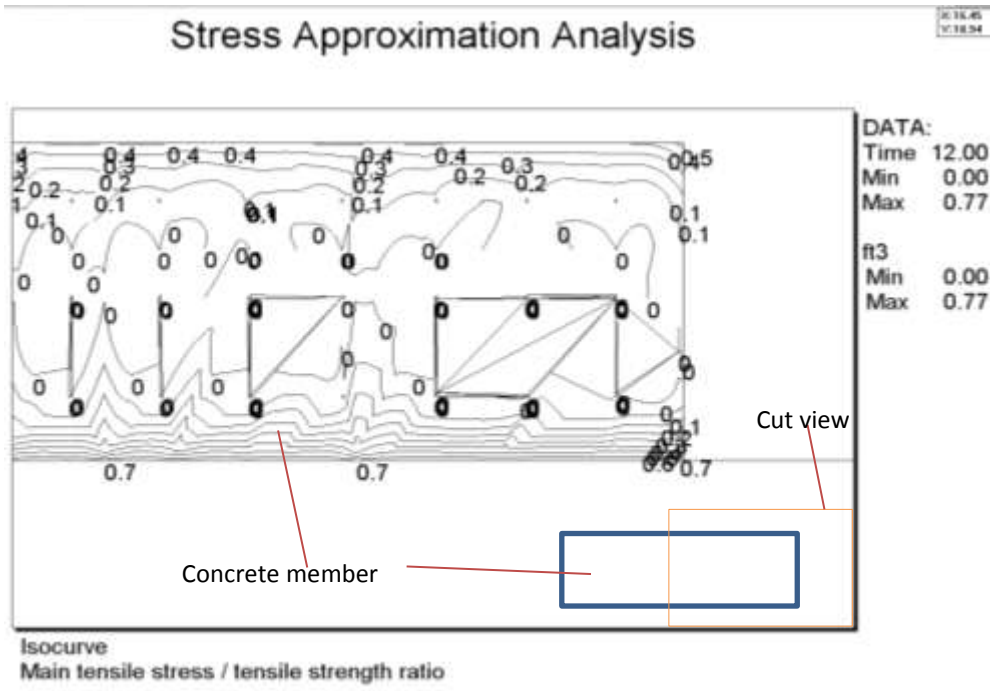

Figure E.6 Example stress/strength ratio development isocurve results for right-half cross section of pier 3 footing with cooling pipe applied at 12 hours (not in scale)

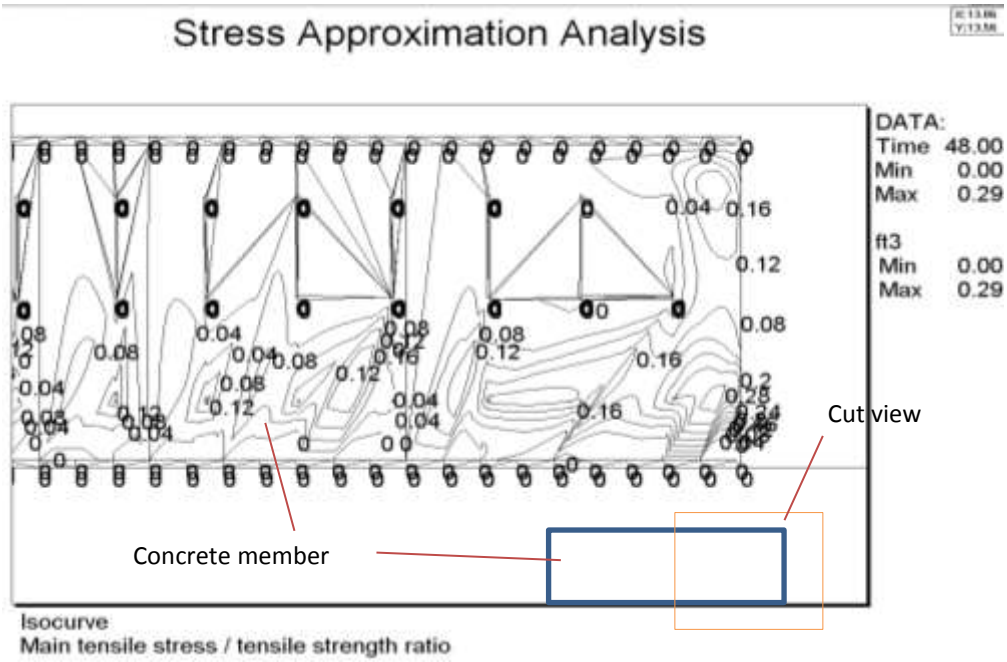

Figure E.7 Example stress/strength ratio development isocurve results for right-half cross section of pier 3 footing with cooling pipe applied at 48 hours(not in scale)

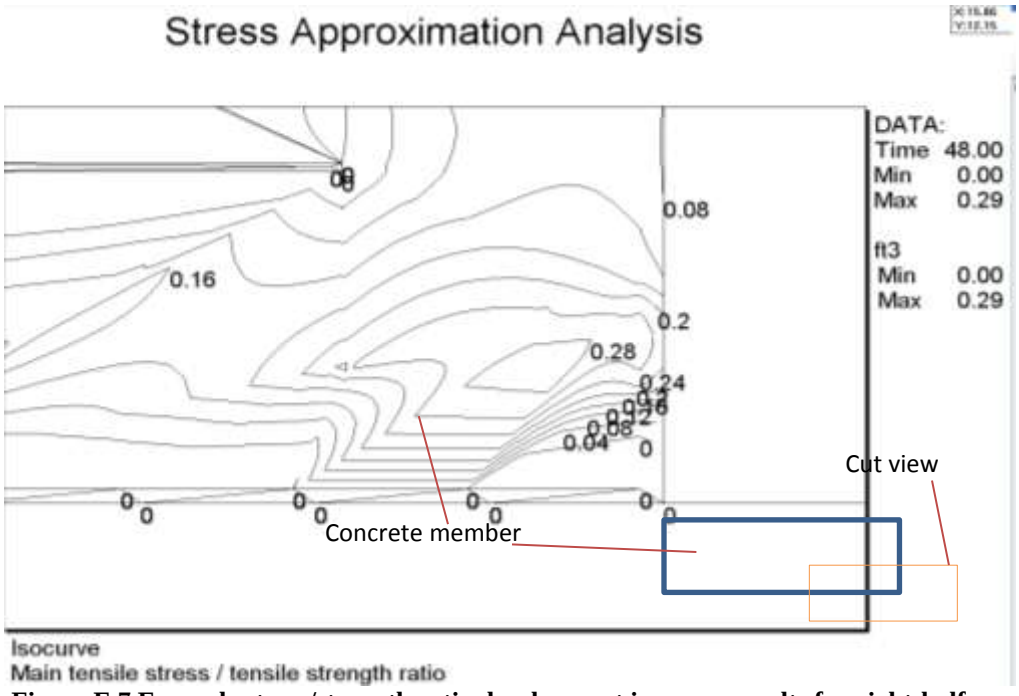

Figure E.7 Example stress/strength ratio development isocurve results for right-half cross section of pier 3 footing with cooling pipe applied at 48 hours (not in scale)

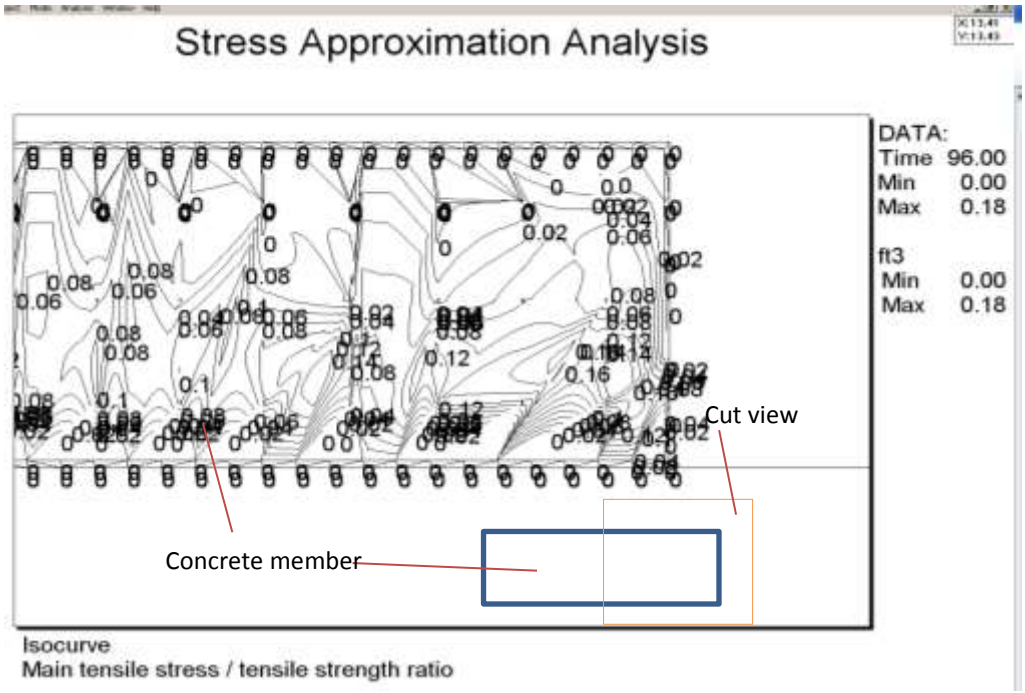

Figure E.8 Example stress/strength ratio development isocurve results for right-half cross section of pier 3 footing with cooling pipe applied at 96 hours(not in scale)

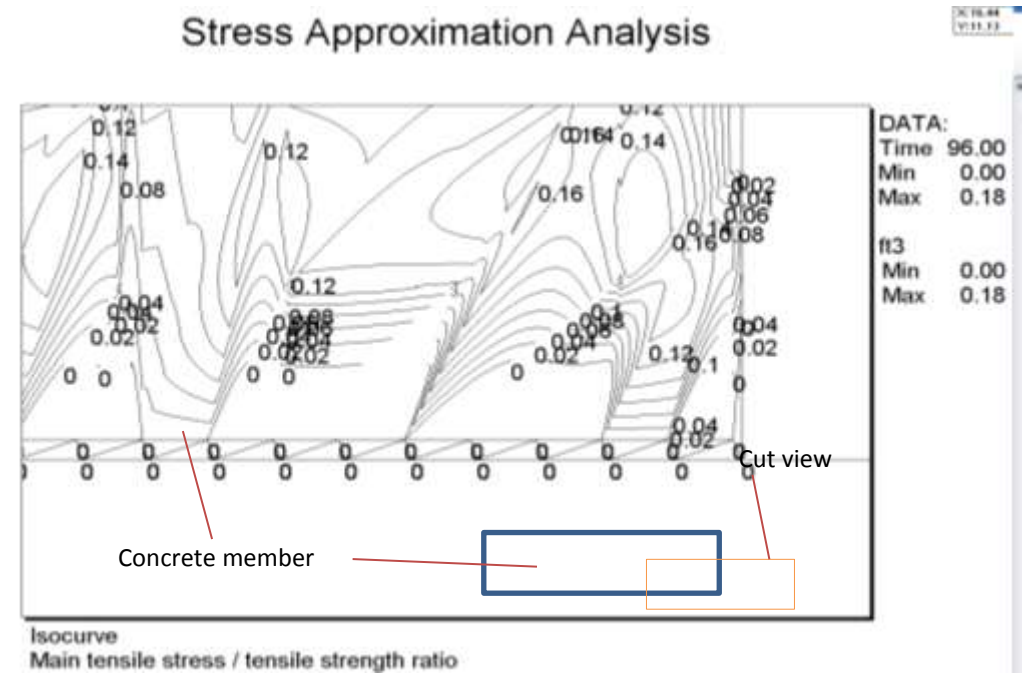

Figure E.9 Example stress/strength ratio development isocurve results for right-half cross section of pier 3 footing with cooling pipe applied at 96 hours(not in scale)

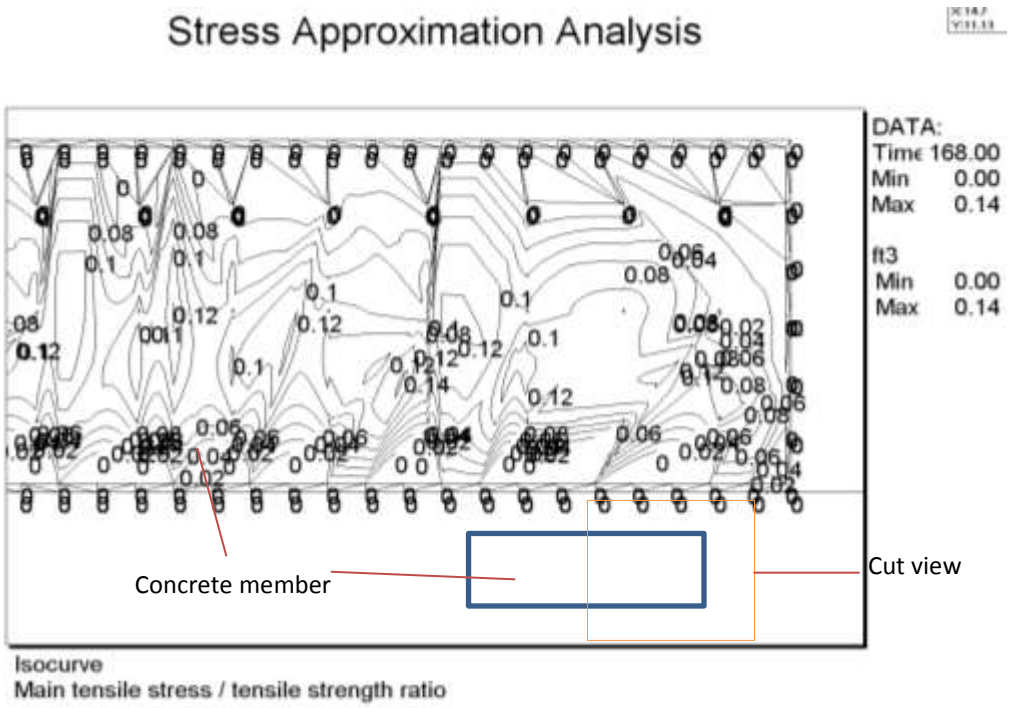

Figure E.10 Example stress/strength ratio development isocurve results for right-half cross section of pier 3 footing with cooling pipe applied at 168 hours(not in scale)

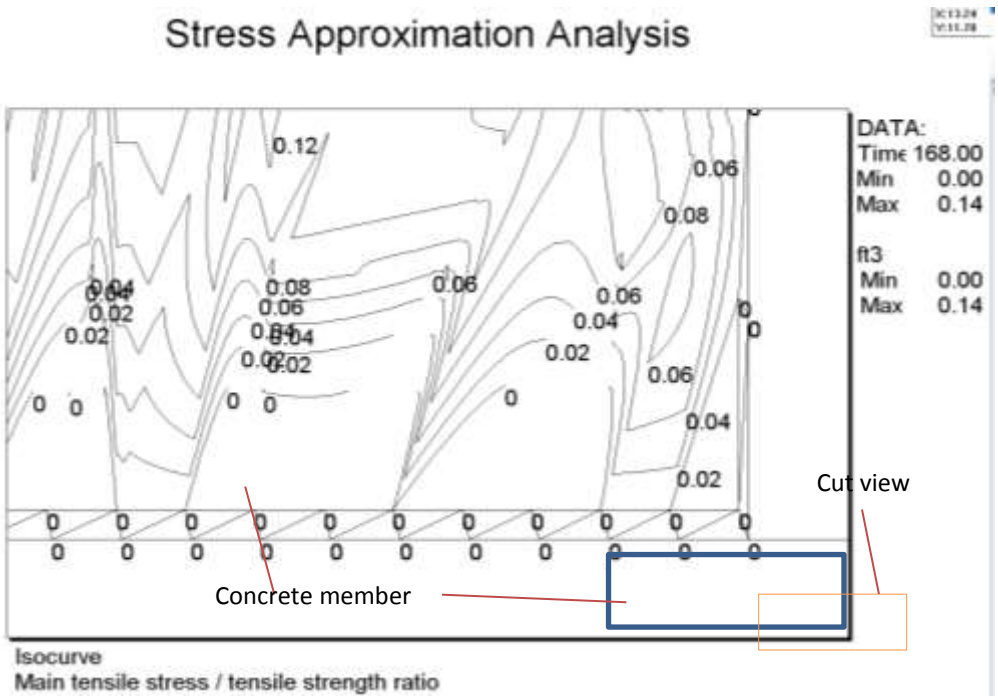

Figure E.11 Example stress/strength ratio development isocurve results for right-half cross section of pier 3 footing with cooling pipe applied at 168 hours(not in scale)

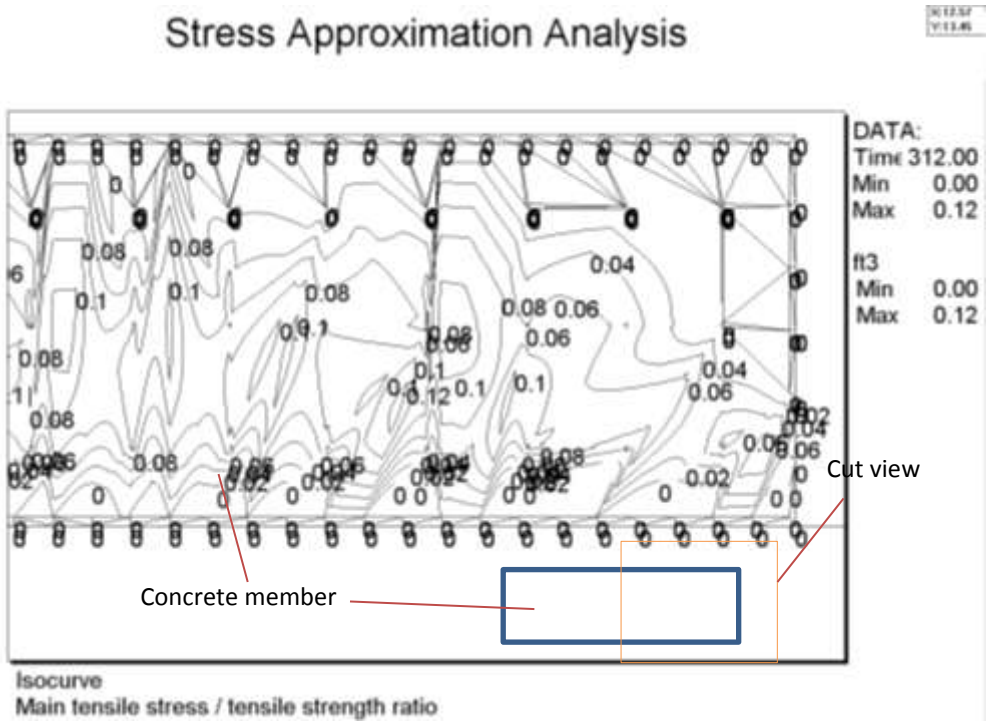

Figure E.12 Example stress/strength ratio development isocurve results for right-half cross section of pier 3 footing with cooling pipe applied at 312 hours(not in scale)

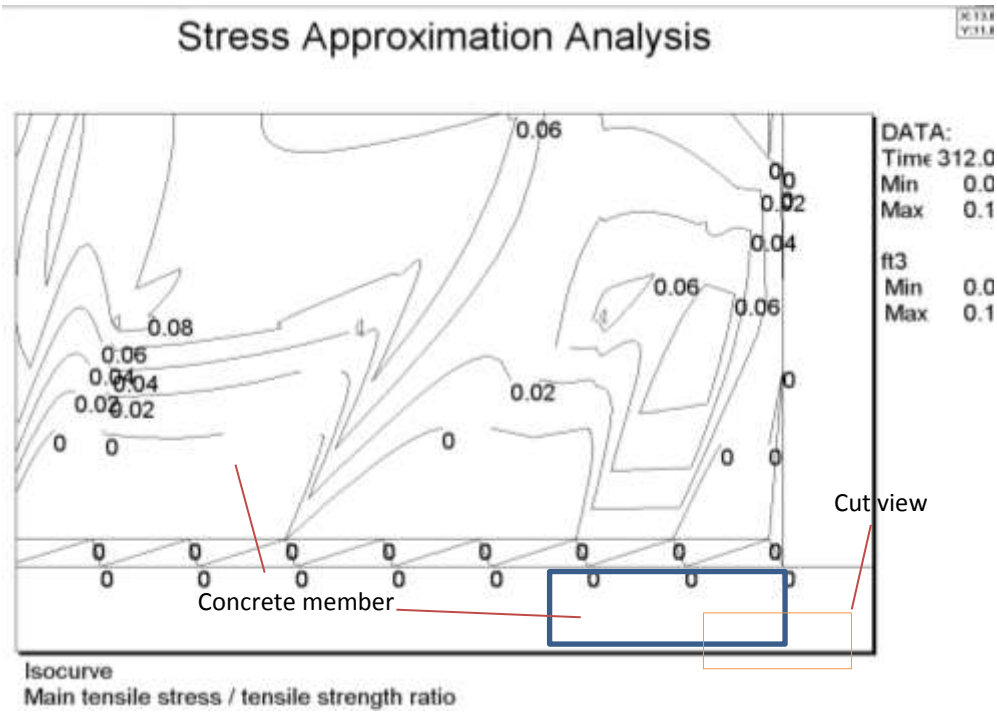

Figure E.13 Example stress/strength ratio development isocurve results for right-half cross section of pier 3 footing with cooling pipe applied at 312 hours(not in scale)

APPENDIX F I-80 BRIDGE CASE STUDY RESULTS

Table F.1 Ambient temperature of Footings and Columns

Concrete Member	Ambient. Temp(C)			Ambient. Temp(F)		
	min	max	ave	min	max	ave
Pier 1 Footing	7.5	14	10.75	45.5	57.2	51.35
Pier 2 Footing	-5	13	4	23	55.4	39.2
Pier 3 Footing	8	20.5	14.25	46.4	68.9	57.65
Pier 4 Footing	8	15	11.5	46.4	59	52.7
Pier 5 Footing	-10	5	-2.5	14	41	27.5
Pier 6 Footing	-4	12	4	24.8	53.6	39.2
Pier 1 Column	-11	-4	-7.5	12.2	24.8	18.5
Pier 2 Column	-10	2	-4	14	35.6	24.8
Pier 3 Column	-14	-8	-11	6.8	17.6	12.2
Pier 4 Column	4	13	8.5	39.2	55.4	47.3
Pier 5 Column	6	13	9.5	42.8	55.4	49.1
Pier 6 Column	-4	12	4	24.8	53.6	39.2
Pier 7 Column	3	20	11.5	37.4	68	52.7
Pier 10 Column	18.3	36	27.15	64.94	96.8	80.87

Table F.2 Case study on stress/strength ratio summary (Soil)

Concrete Member	Size(ft)	Max. Temp(F)		Temp Diff(F)			Stress/Strength Ratio				Stress/Strength Ratio			
		ACTUAL	4C	ACTUAL	4C (surface)	4C (sensor)	0-24hr	24-48hr	48-72hr	>72hr	0-24hr	24-48hr	48-72hr	>72hr
Pier 1 Footing	43*12*4.5	131	128	34.2	46	27	0.61	0.35	0.16	0.16	0.11	0.26	0.44	0.62
Pier 2 Footing	43*15*5	134.6	123	34.2	58	44	1.1	0.6	0.19	0.33	0.47	0.50	0.60	0.72
Pier 3 Footing	43*27*7.25	153.5	146	56.5	67	50	0.65	0.6	0.36	0.28	0.03	0.28	0.35	1.58
Pier 4 Footing	43*15*5	142	137	51	54	42	0.75	0.32	0.21	0.22	0.09	0.34	0.58	0.80
Pier 5 Footing	46*19*6.5	136.4	120	50.4	69	58	1.8	1.23	0.51	0.36	0.11	0.28	0.34	0.64
Pier 6 Footing	46*18*5.75	156.2	142	50.4	72	60	1.4	1.21	0.2	0.35	0.38	0.43	0.76	1.10
Pier 1 Column	43*12*4	131	87	15.3	36	27	1.85	0.77	0.11	0.2	0.35	0.17	0.45	0.50
Pier 2 Column	43*15*5	126.5	128	38.7	67	53	1.77	0.78	0.18	0.3	0.35	0.29	0.55	0.78
Pier 3 Column	43*27*6	128.3	121	28.7	78	64	3.19	2.5	0.43	0.26	0.55	0.27	0.34	0.74
Pier 4 Column	43*15*5	140.9	132	34	58	43	0.78	0.55	0.2	0.22	0.18	0.27	0.49	0.70
Pier 5 Column	46*19*5	142	137	39.5	55	42	0.78	0.57	0.36	0.32	0.10	0.22	0.54	0.76
Pier 7 Column	46*18*8.33	149	152	50.4	101	88	2.38	1.19	0.45	0.35	0.30	0.30	0.35	1.90
Pier 10 Column	43*19*8.33	159.8	179	52.2	77	66	0.9	0.6	0.42	0.31	0.21	0.38	0.29	1.8

Table F.3 Summary of maxium temperature difference & difference between computer calculated (4C)and actual(CTL) in centigrade

Concrete Member	Temp Diff(°C)			Temp. Diff between Actual measured (CTL) and 4C prediction (°C)	
	ACTUAL	4C(surface)	4C(sensor)	Temp. Diff between Actual to 4C (surface)	Temp. Diff between surface and 3 in below surface (sensor)
Pier 1 Footing	19	25.6	15	4	10.6
Pier 2 Footing	19	32.2	24.4	-5.4	7.8
Pier 3 Footing	31.4	37.2	27.8	3.6	9.4
Pier 4 Footing	28.3	30	23.3	5	6.7
Pier 5 Footing	28	38.3	32.2	-4.2	6.1
Pier 6 Footing	28	40	33.3	-5.3	6.7
Pier 1 Column	8.5	27.8	14.4	-5.9	13.4
Pier 2 Column	21.5	45	27.2	-5.7	17.8
Pier 3 Column	15.9	34.4	53.9	-37.9	-19.4
Pier 4 Column	18.9	27.8	22.8	-3.9	5
Pier 5 Column	21.9	37.8	23.3	-1.4	14.4
Pier 10Column	28	61.1	45.6	-17.6	15.6
ave				-6.225	7.842

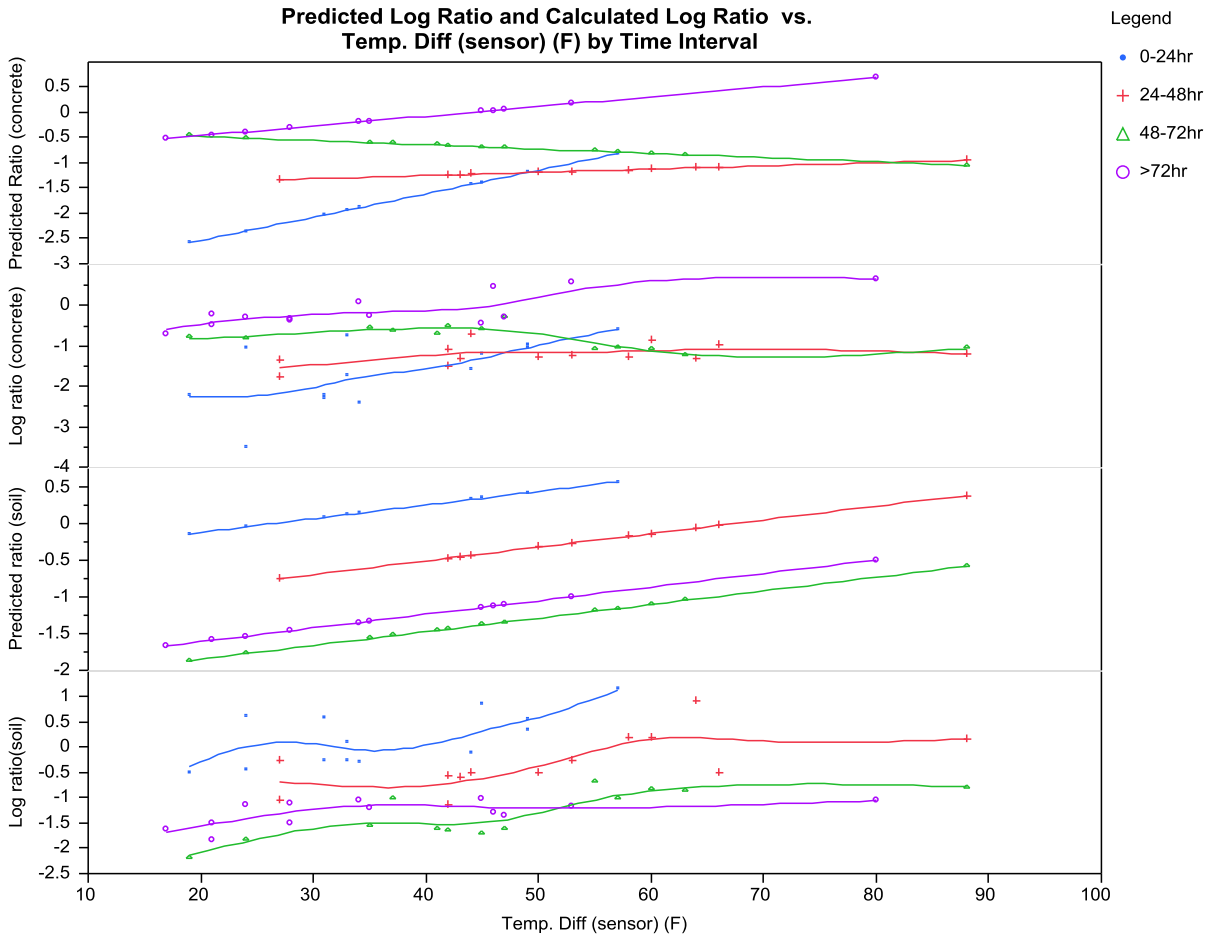

Figure F.1 Comparison of established model and observations

F.1 Statistical analysis results on unequal variance of case study 6.1.2

Oneway Analysis of Log ratio (concrete) By Time Interval

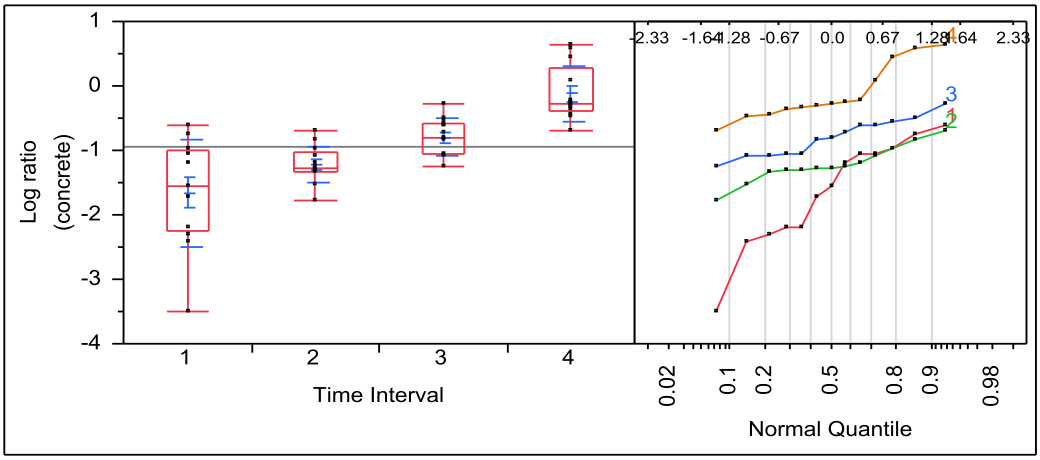

Means and Std Deviations

Level	Number	Mean	Std Dev	Std Err Mean	Lower 95%	Upper 95%
1	13	-1.6562	0.835316	0.23167	-2.161	-1.151
2	13	-1.2172	0.278684	0.07729	-1.386	-1.049
3	13	-0.7978	0.285712	0.07924	-0.970	-0.625
4	13	-0.1206	0.428912	0.11896	-0.380	0.139

Tests that the Variances are Equal

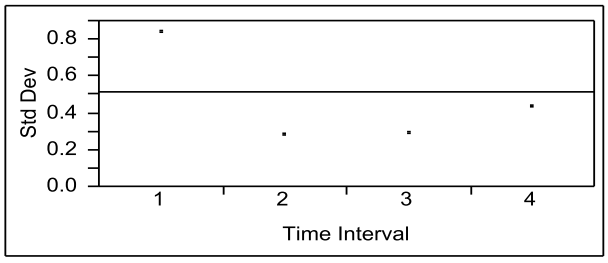

Level	Count	Std Dev	MeanAbsDif to Mean	MeanAbsDif to Median
1	13	0.8353160	0.6783054	0.6828098
2	13	0.2786843	0.1997430	0.1922640
3	13	0.2857120	0.2353399	0.2370176
4	13	0.4289121	0.3484090	0.3031154

Test	F Ratio	DFNum	DFDen	Prob > F

Test	F Ratio	DFNum	DFDen	Prob > F
O'Brien[.5]	4.1984	3	48	0.0102*
Brown-Forsythe	6.9311	3	48	0.0006*
Levene	8.0266	3	48	0.0002*
Bartlett	6.6855	3	.	0.0002*

Oneway Analysis of Log ratio(soil) By Time Interval

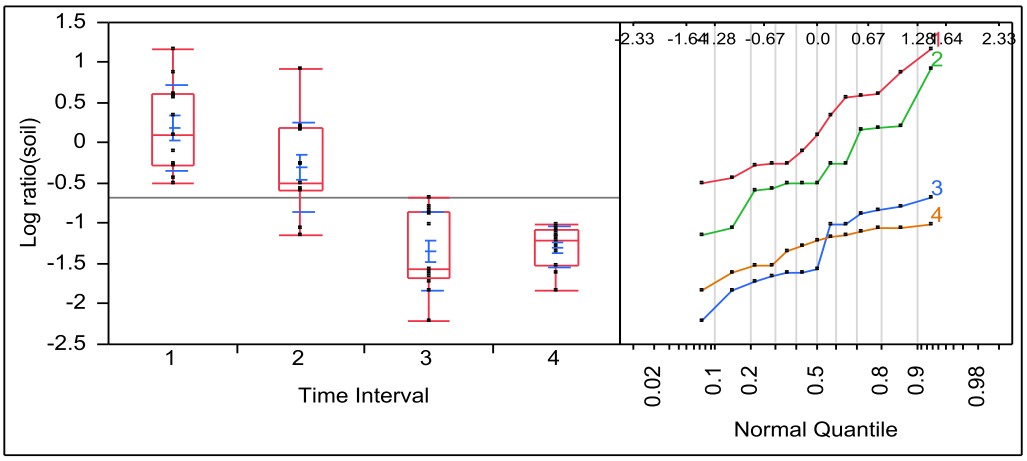

Means and Std Deviations

Level	Number	Mean	Std Dev	Std Err Mean	Lower 95%	Upper 95%
1	13	0.1860	0.537535	0.14909	-0.139	0.511
2	13	-0.3003	0.560026	0.15532	-0.639	0.038
3	13	-1.3401	0.486626	0.13497	-1.634	-1.046
4	13	-1.2950	0.252418	0.07001	-1.448	-1.142

Tests that the Variances are Equal

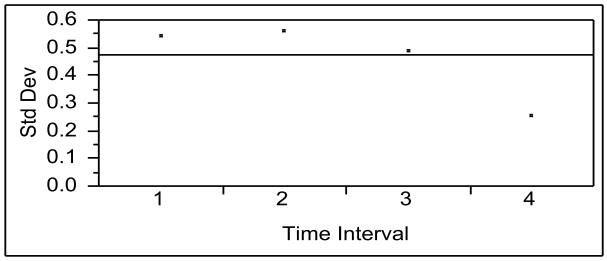

Level	Count	Std Dev	MeanAbsDif to Mean	MeanAbsDif to Median
1	13	0.5375350	0.4648666	0.4733277
2	13	0.5600263	0.4276509	0.4114551
3	13	0.4866262	0.4329359	0.4197251
4	13	0.2524181	0.2065233	0.1986560

Test	F Ratio	DFNum	DFDen	Prob > F
O'Brien[.5]	1.8192	3	48	0.1562
Brown-Forsythe	2.0904	3	48	0.1139
Levene	3.3113	3	48	0.0277*
Bartlett	2.4819	3	.	0.0590

F.2 Statistical analysis results on fit model with unequal slope of case study 6.1.2

Response Log ratio (concrete)
Regression Plot

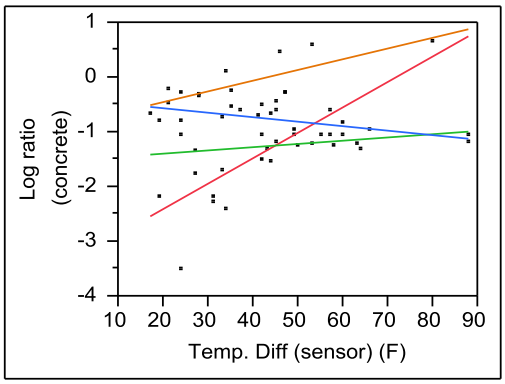

Summary of Fit

RSquare	0.747818
RSquare Adj	0.707699
Root Mean Square Error	0.40873
Mean of Response	-0.94796
Observations (or Sum Wgts)	52

Analysis of Variance

Source	DF	Sum of Squares	Mean Square	F Ratio
Model	7	21.797642	3.11395	18.6396
Error	44	7.350663	0.16706	**Prob > F**
C. Total	51	29.148305		<.0001*

Lack Of Fit

Source	DF	Sum of Squares	Mean Square	F Ratio
Lack Of Fit	36	3.6464840	0.101291	0.2188
Pure Error	8	3.7041793	0.463022	**Prob > F**
Total Error	44	7.3506633		0.9993
				Max RSq
				0.8729

Effect Tests

Source	Nparm	DF	Sum of Squares	F Ratio	Prob > F
Time Interval	3	3	12.508067	24.9572	<.0001*
Temp. Diff (sensor) (F)	1	1	2.762130	16.5337	0.0002*
Time Interval*Temp. Diff (sensor) (F)	3	3	3.757061	7.4964	0.0004*

Prediction Expression

-1.5307937436689

$$+\text{Match}\left(\text{Time Interval}\right)\begin{cases}1 \Rightarrow -0.5068991814759\\ 2 \Rightarrow -0.4213143237971\\ 3 \Rightarrow 0.08547639789956\\ 4 \Rightarrow 0.84273710737347\\ \text{else} \Rightarrow .\end{cases}$$

$$+0.01593864307519*\text{Temp. Diff (sensor) (F)}$$

$$+\text{Match}\left(\text{Time Interval}\right)\begin{cases}1 \Rightarrow \left(\text{Temp. Diff (sensor) (F)}-42.8653846153846\right)*0.03062451529972\\ 2 \Rightarrow \left(\text{Temp. Diff (sensor) (F)}-42.8653846153846\right)*-0.0096390485977\\ 3 \Rightarrow \left(\text{Temp. Diff (sensor) (F)}-42.8653846153846\right)*-0.0242735705665\\ 4 \Rightarrow \left(\text{Temp. Diff (sensor) (F)}-42.8653846153846\right)*0.00328810386449\\ \text{else} \Rightarrow .\end{cases}$$

Response Log ratio(soil)
Regression Plot

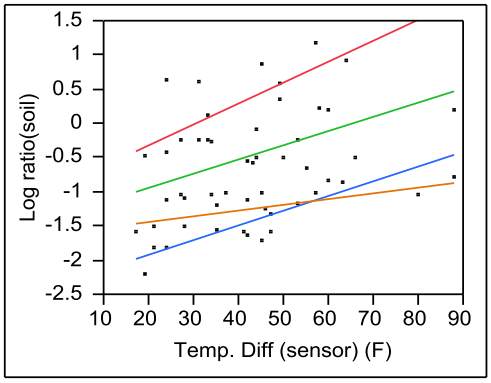

Summary of Fit

RSquare	0.82179
RSquare Adj	0.793438
Root Mean Square Error	0.365811
Mean of Response	-0.68735
Observations (or Sum Wgts)	52

Analysis of Variance

Source	**DF**	**Sum of Squares**	**Mean Square**	**F Ratio**
Model	7	27.151456	3.87878	28.9856
Error	44	5.887973	0.13382	**Prob > F**
C. Total	51	33.039429		<.0001*

Lack Of Fit

Source	**DF**	**Sum of Squares**	**Mean Square**	**F Ratio**
Lack Of Fit	36	4.2943198	0.119287	0.5988
Pure Error	8	1.5936531	0.199207	**Prob > F**
Total Error	44	5.8879730		0.8602
				Max RSq
				0.9518

Effect Tests

Source	Nparm	DF	Sum of Squares	F Ratio	Prob > F
Time Interval	3	3	21.694426	54.0398	<.0001*
Temp. Diff (sensor) (F)	1	1	4.469699	33.4014	<.0001*
Time Interval*Temp. Diff (sensor) (F)	3	3	0.645949	1.6090	0.2009

Prediction Expression

-1.5605437298211

$$+\text{Match}\left(\text{Time Interval}\right)\begin{cases}1 \Rightarrow 1.07425257437439\\ 2 \Rightarrow 0.21998998825247\\ 3 \Rightarrow -0.7409998585688\\ 4 \Rightarrow -0.5532427040581\\ \text{else} \Rightarrow .\end{cases}$$

$$+0.02027535215612*\text{Temp. Diff (sensor) (F)}$$

$$+\text{Match}\left(\text{Time Interval}\right)\begin{cases}1 \Rightarrow \left(\text{Temp. Diff (sensor) (F)}-42.8653846153846\right)*0.01009668156876\\ 2 \Rightarrow \left(\text{Temp. Diff (sensor) (F)}-42.8653846153846\right)*0.00056888108095\\ 3 \Rightarrow \left(\text{Temp. Diff (sensor) (F)}-42.8653846153846\right)*0.00125095623026\\ 4 \Rightarrow \left(\text{Temp. Diff (sensor) (F)}-42.8653846153846\right)*-0.01191651888\\ \text{else} \Rightarrow .\end{cases}$$

F.3 Statistical analysis results fit the model with equal slope of case study 6.1.2

Response Log ratio (concrete)

Regression Plot

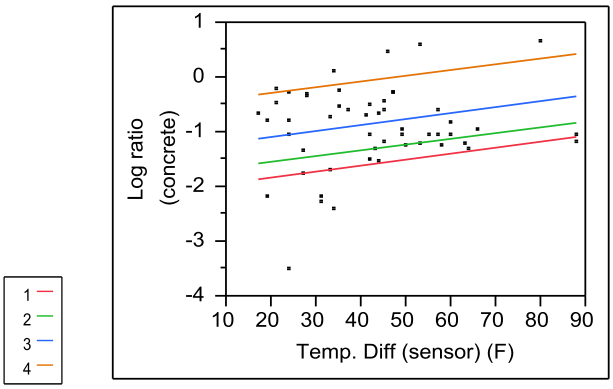

Summary of Fit

RSquare	0.618924
RSquare Adj	0.586492
Root Mean Square Error	0.486143
Mean of Response	-0.94796
Observations (or Sum Wgts)	52

Analysis of Variance

Source	DF	Sum of Squares	Mean Square	F Ratio
Model	4	18.040581	4.51015	19.0837
Error	47	11.107724	0.23633	**Prob > F**
C. Total	51	29.148305		<.0001*

Lack Of Fit

Source	DF	Sum of Squares	Mean Square	F Ratio
Lack Of Fit	39	7.403545	0.189834	0.4100
Pure Error	8	3.704179	0.463022	**Prob > F**
Total Error	47	11.107724		0.9696
				Max RSq
				0.8729

Effect Tests

Source	Nparm	DF	Sum of Squares	F Ratio	Prob > F

Source	Nparm	DF	Sum of Squares	F Ratio	Prob > F
Time Interval	3	3	17.273631	24.3632	<.0001*
Temp. Diff (sensor) (F)	1	1	1.384452	5.8580	0.0194*

Prediction Expression

-1.4010099647299

$$+\text{Match}\left(\text{Time Interval},\ 1 \Rightarrow -0.6397899300604,\ 2 \Rightarrow -0.3559972405087,\ 3 \Rightarrow 0.10478406801425,\ 4 \Rightarrow 0.89100310255478,\ \text{else} \Rightarrow .\right)$$

+0.01056924601681*Temp. Diff (sensor) (F)

Response Log ratio(soil)
Regression Plot

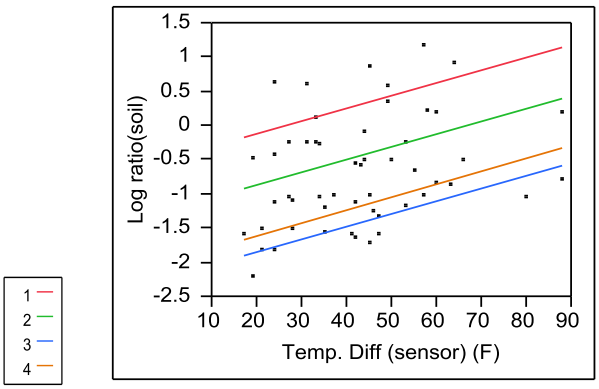

Summary of Fit

RSquare	0.802239
RSquare Adj	0.785408
Root Mean Square Error	0.372853
Mean of Response	-0.68735
Observations (or Sum Wgts)	52

Analysis of Variance

Source	DF	Sum of Squares	Mean Square	F Ratio
Model	4	26.505507	6.62638	47.6650
Error	47	6.533922	0.13902	**Prob > F**
C. Total	51	33.039429		<.0001*

Lack Of Fit

Source	DF	Sum of Squares	Mean Square	F Ratio
Lack Of Fit	39	4.9402691	0.126674	0.6359
Pure Error	8	1.5936531	0.199207	**Prob > F**
Total Error	47	6.5339222		0.8352
				Max RSq
				0.9518

Effect Tests

Source	Nparm	DF	Sum of Squares	F Ratio	Prob > F

Source	Nparm	DF	Sum of Squares	F Ratio	Prob > F
Time Interval	3	3	23.474421	56.2856	<.0001*
Temp. Diff (sensor) (F)	1	1	4.303197	30.9539	<.0001*

Prediction Expression

-1.4860939674772

$$+\text{Match}\left(\text{Time Interval},\ 1 \Rightarrow 0.99409704691041,\ 2 \Rightarrow 0.23405880876807,\ 3 \Rightarrow -0.7326778198719,\ 4 \Rightarrow -0.4954780358066,\ \text{else} \Rightarrow .\right)$$

+0.01863376552693*Temp. Diff (sensor) (F)

F.4 Statistical analysis results on maximum temperature of case study 6.2

Actual by Predicted Plot

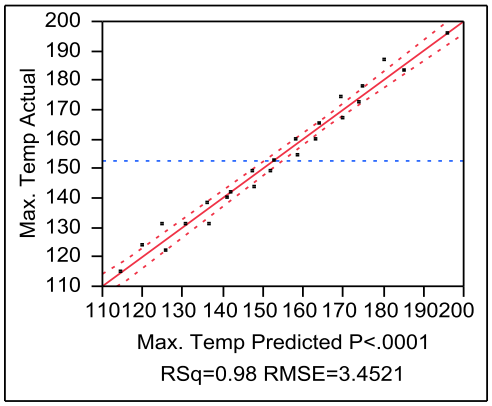

Summary of Fit

RSquare	0.9775
RSquare Adj	0.975357
Root Mean Square Error	3.452116
Mean of Response	152.675
Observations (or Sum Wgts)	24

Analysis of Variance

Source	DF	Su Sq
Model	2	1087
Error	21	25
C. Total	23	1112

Parameter Estimates

Term	Estimate
Intercept	43.987143
Depth	5.2714286
Fresh Temp.	1.1044286

Effect Tests

Effect Tests

Source	Nparm	DF	Sum of Squares	F Ratio	Prob > F
Depth	1	1	2334.1886	195.8688	<.0001*
Fresh Temp.	1	1	8538.3373	716.4777	<.0001*

Source	Nparm	DF	Sum of Squares	F Ratio	Prob > F

Prediction Expression

43.9871428571429
+5.27142857142857*Depth
+1.10442857142857*Fresh Tem

Contour Plot for Max. Temp

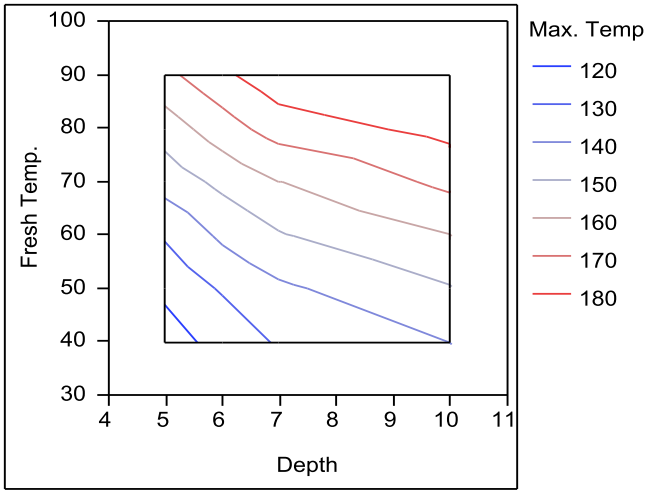

F.5 Statistical analysis results on maximum temperature difference of case study 6.2

Max. Temp. Diff

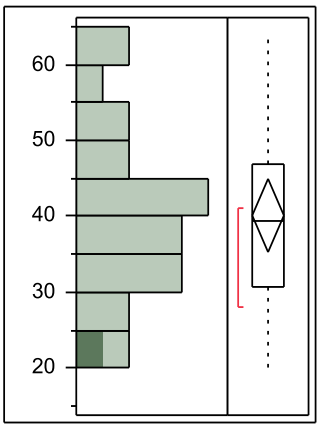

Quantiles

100.0%	maximum	64
99.5%		64
97.5%		64
90.0%		59
75.0%	quartile	47
50.0%	median	39.5
25.0%	quartile	30.75
10.0%		25
2.5%		20
0.5%		20
0.0%	minimum	20

Moments

Mean	40.125
Std Dev	11.357099
Std Err Mean	2.3182581
Upper 95% Mean	44.920682
Lower 95% Mean	35.329318
N	24

Actual by Predicted Plot

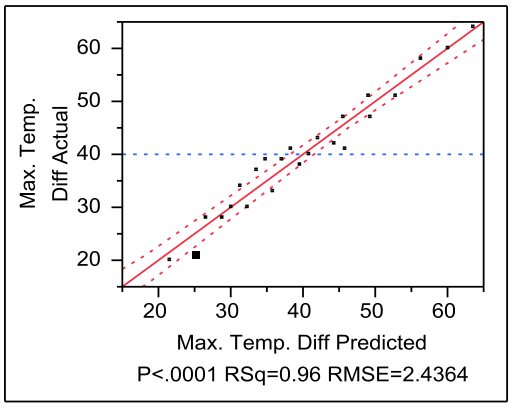

Summary of Fit

RSquare	0.95798
RSquare Adj	0.953978
Root Mean Square Error	2.436402
Mean of Response	40.125
Observations (or Sum Wgts)	24

Analysis of Variance

Source	DF	Sum of Squares	Mean Square	F Ratio
Model	2	2841.9679	1420.98	239.3819
Error	21	124.6571	5.94	**Prob > F**
C. Total	23	2966.6250		<.0001*

Parameter Estimates

Term	Estimate	Std Error	t Ratio	Prob>|t|
Intercept	-16.79286	2.700531	-6.22	<.0001*
Depth	4.8214286	0.265833	18.14	<.0001*
Fresh Temp.	0.3564286	0.029121	12.24	<.0001*

Prediction Expression

-16.792857142857
+4.82142857142857*Depth
+0.35642857142857*Fresh Temp.

Contour Plot for Max. Temp. Diff

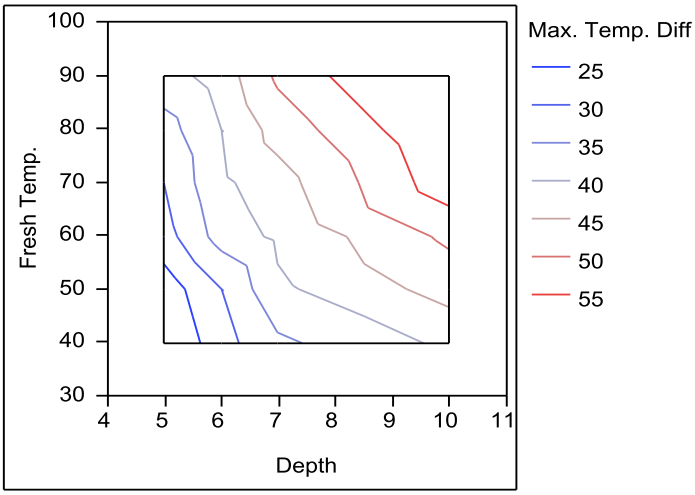

F.6 Statistical analysis results on stress/strength ratio before form removed of case study 6.2

Distributions
Stress/Strength Ratio before form removed

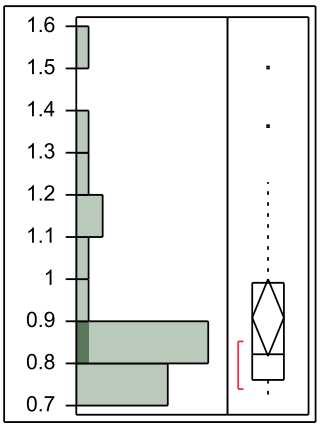

Quantiles

100.0%	maximum	1.5
99.5%		1.5
97.5%		1.5
90.0%		1.295
75.0%	quartile	0.9925
50.0%	median	0.82
25.0%	quartile	0.76
10.0%		0.73
2.5%		0.71
0.5%		0.71
0.0%	minimum	0.71

Moments

Mean	0.9079167
Std Dev	0.2148605
Std Err Mean	0.0438582
Upper 95% Mean	0.9986443
Lower 95% Mean	0.817189
N	24

Actual by Predicted Plot

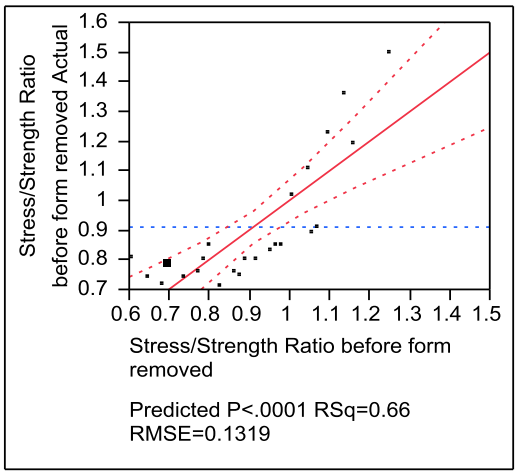

Summary of Fit

RSquare	0.655946
RSquare Adj	0.623179
Root Mean Square Error	0.131894
Mean of Response	0.907917
Observations (or Sum Wgts)	24

Analysis of Variance

Source	DF	Sum of Squares	Mean Square	F Ratio
Model	2	0.6964804	0.348240	20.0184
Error	21	0.3653155	0.017396	**Prob > F**
C. Total	23	1.0617958		<.0001*

Parameter Estimates

Term	Estimate	Std Error	t Ratio	Prob>|t|
Intercept	0.0505952	0.146192	0.35	0.7327
Depth	0.0385714	0.014391	2.68	0.0140*
Fresh Temp.	0.0090357	0.001576	5.73	<.0001*

F.7 Statistical analysis results on stress/strength ratio after form removed of case study 6.2

Distributions
Stress/Strength Ratio after form removed

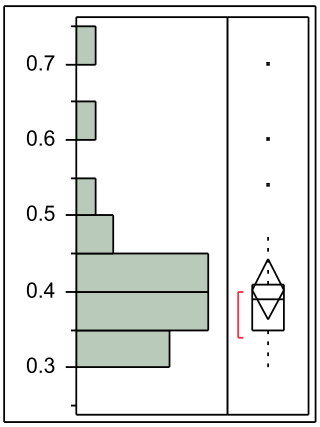

Quantiles

100.0%	maximum	0.7
99.5%		0.7
97.5%		0.7
90.0%		0.57
75.0%	quartile	0.41
50.0%	median	0.39
25.0%	quartile	0.35
10.0%		0.305
2.5%		0.3
0.5%		0.3
0.0%	minimum	0.3

Moments

Mean	0.4033333
Std Dev	0.0954471
Std Err Mean	0.0194831
Upper 95% Mean	0.4436371
Lower 95% Mean	0.3630296
N	24

Actual by Predicted Plot

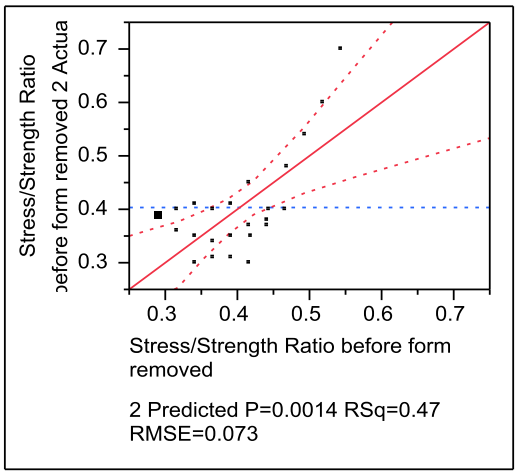

Summary of Fit

RSquare	0.466564
RSquare Adj	0.415761
Root Mean Square Error	0.072956
Mean of Response	0.403333
Observations (or Sum Wgts)	24

Analysis of Variance

Source	DF	Sum of Squares	Mean Square	F Ratio
Model	2	0.09776071	0.048880	9.1837
Error	21	0.11177262	0.005323	**Prob > F**
C. Total	23	0.20953333		0.0014*

Parameter Estimates

Term	Estimate	Std Error	t Ratio	Prob>|t|
Intercept	0.0633333	0.080865	0.78	0.4423
Depth	0.0253571	0.00796	3.19	0.0045*
Fresh Temp.	0.0025	0.000872	2.87	0.0092*

APPENDIX G AN EXAMPLE OF US 34 CASE STUDY USING 4C PROGRAM

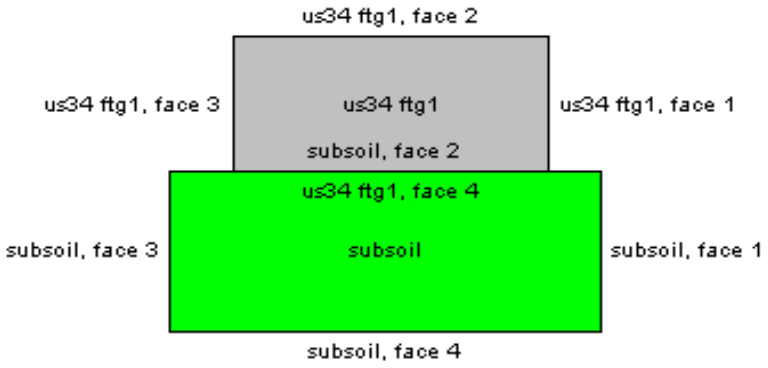

Figure G.1 US34 pier 1 footing layout (not in scale)

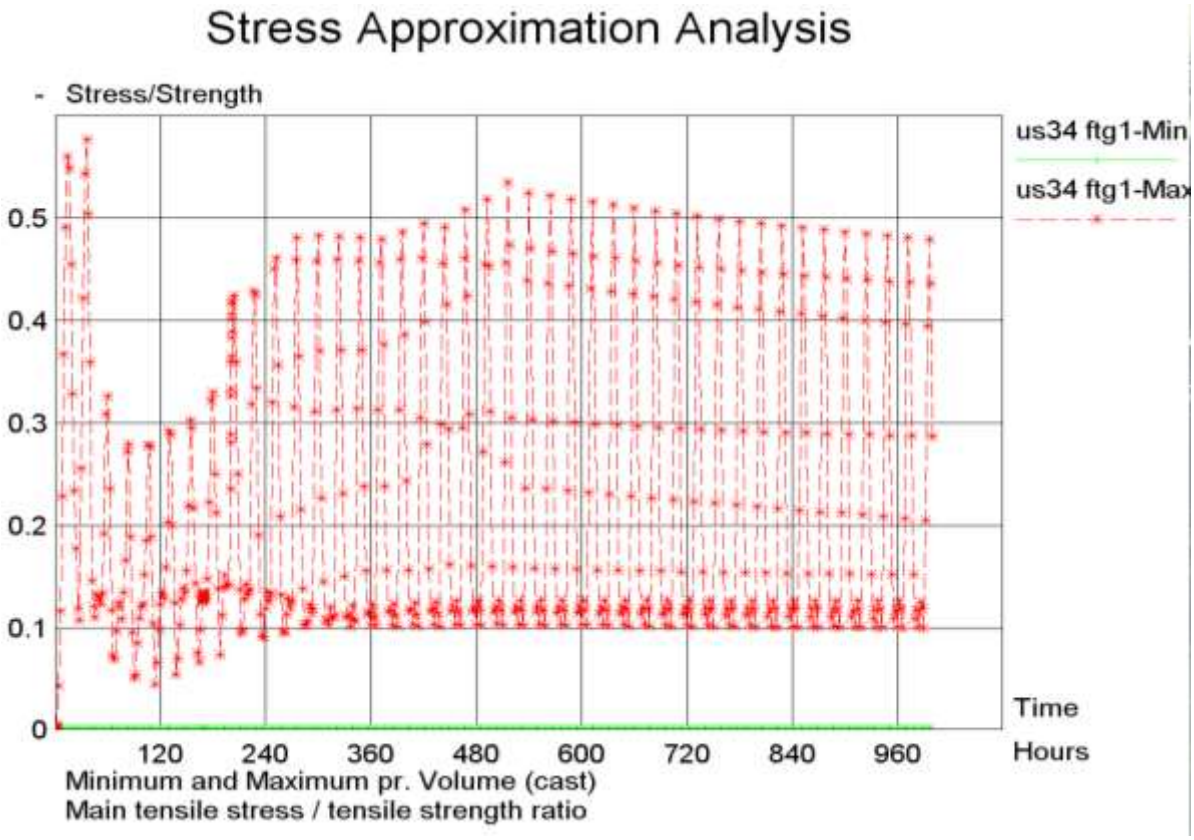

Figure G.2 Stress/strength ratio development for pier 1 footing during 1000hours.

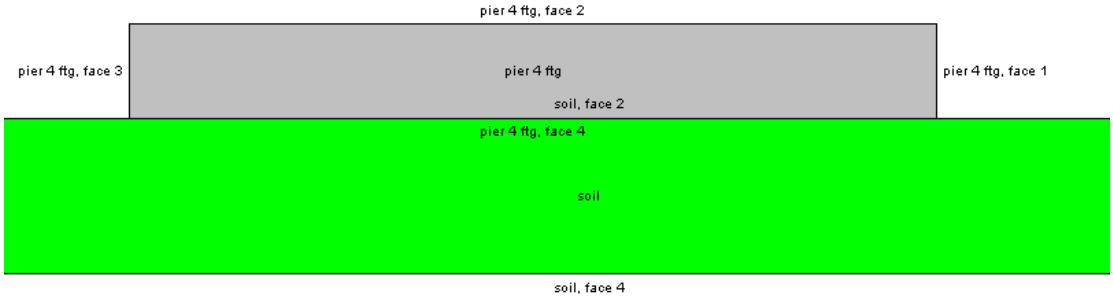

Figure G.3 US34 pier 4 footing layout without cooling pipes (not in scale)

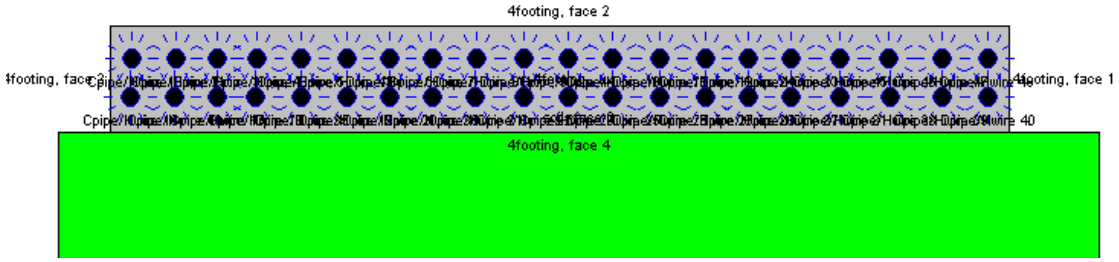

Figure G.4 US34 pier 4 footing layout with cooling pipes (not in scale)

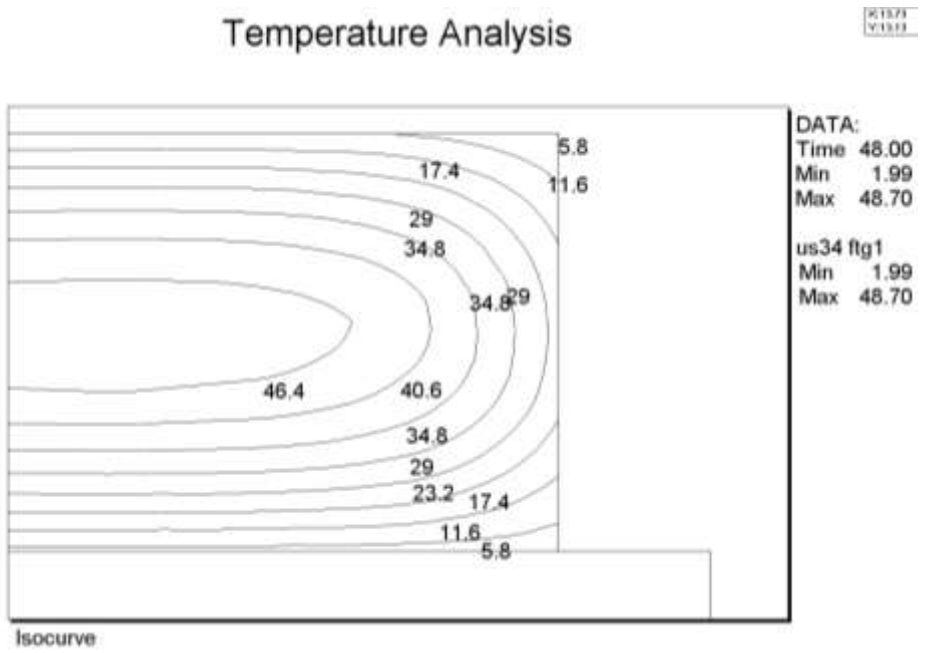

Figure G.5 US34 pier 1 footing temperature iso-curve development on cross section (symmetrical right half)

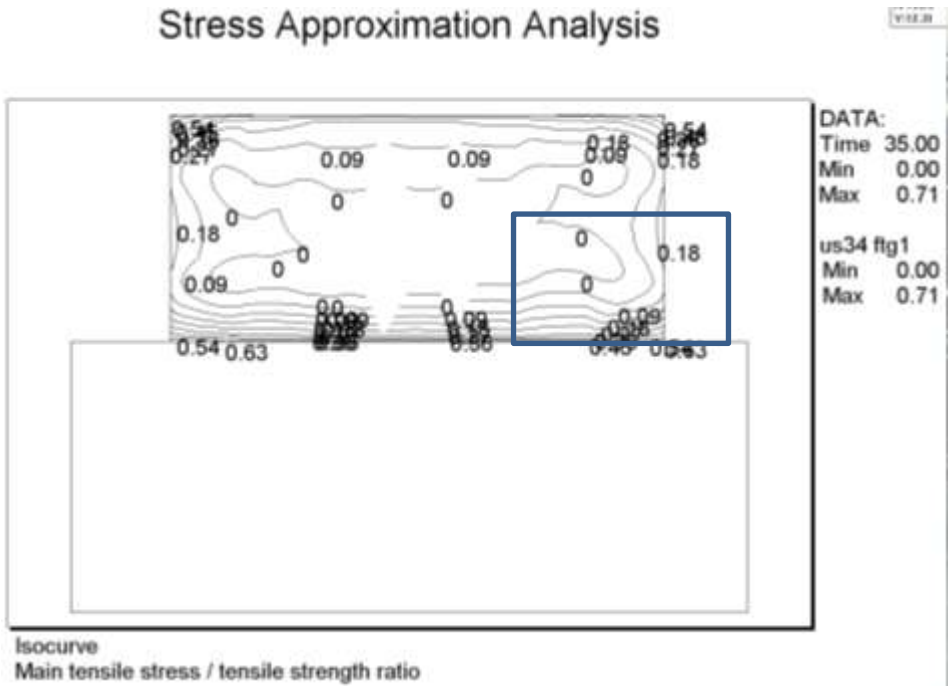

Figure G.6 US34 pier 1 footing stress/strength ratio iso-curve on cross section

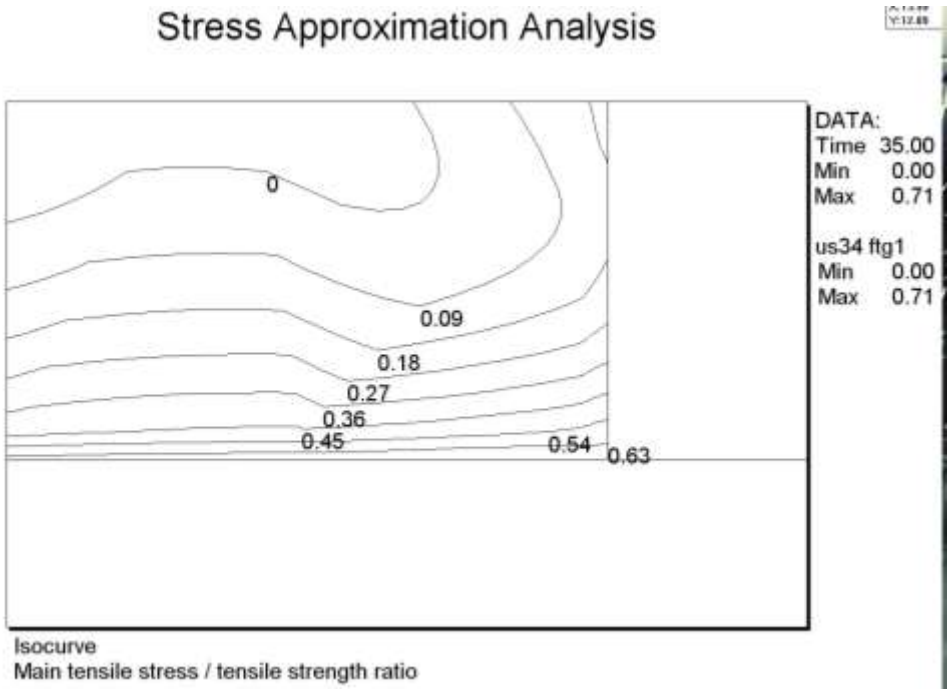

Figure G.7 US34 pier 1 footing stress/strength ratio iso-curve on cross section (right bottom corner)

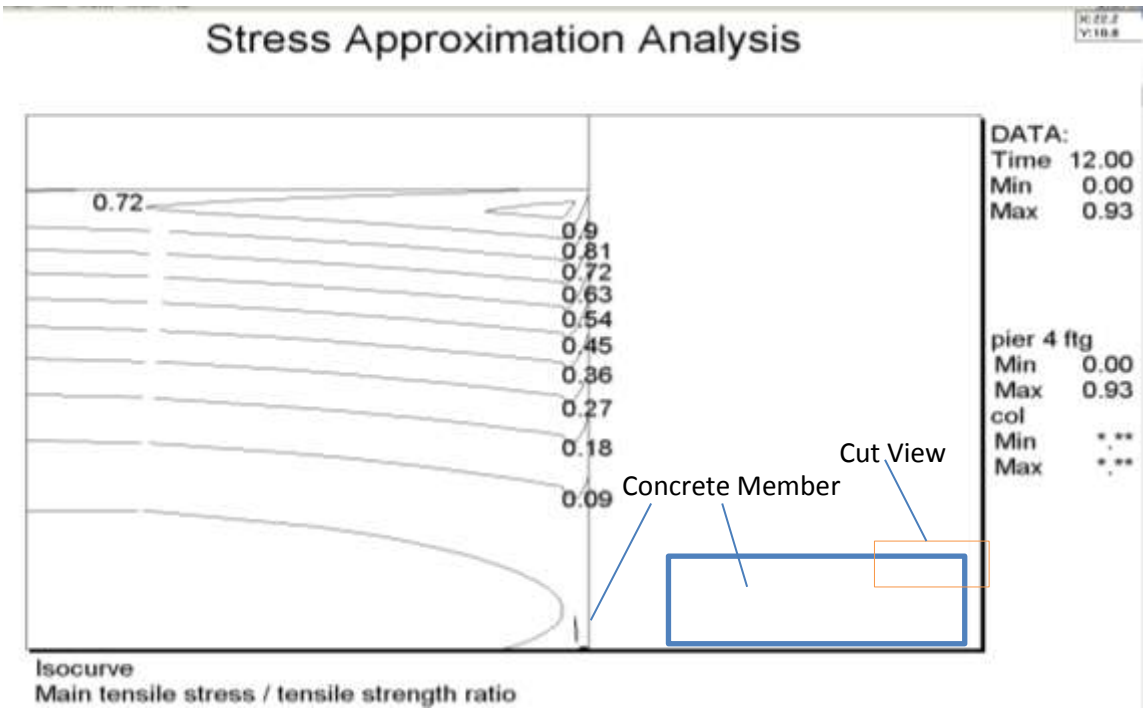

Figure G.8 US34 pier 4 footing stress/strength ratio iso-curve on cross section (without cooling pipes)

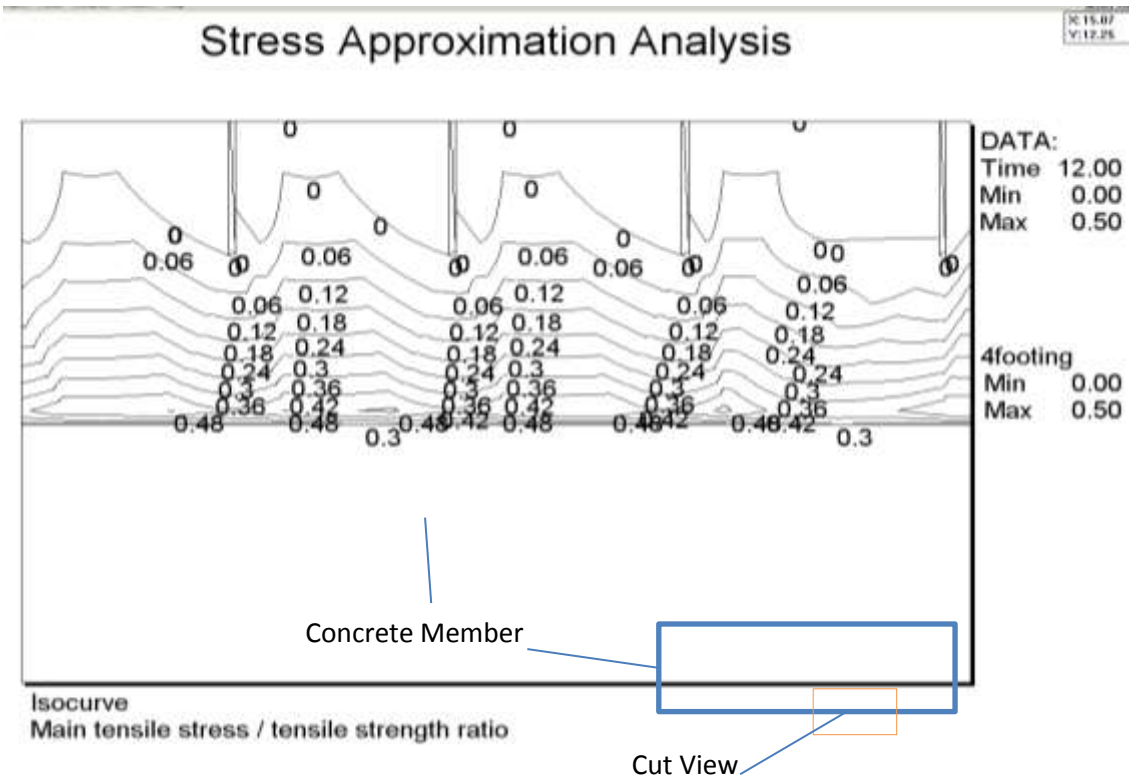

Figure G.9 US34 pier 4 footing stress/strength ratio iso-curve on cross section (with cooling pipes)